DEVELOPMENT OF THE SELECTIVE-SHEAR COAGULATION PROCESS FOR ULTRAFINE COAL CLEANING

by

Ricky Quay Honaker

Thesis submitted to the Faculty of the
Virginia Polytechnic Institute and State University
in partial fulfillment of the requirements for the degree of

MASTER OF SCIENCE

in

Mining and Minerals Engineering

APPROVED:

G. H. Luttrell, Co-chairman

R. H. Yoon, Co-chairman

M. E. Karmis, Dept. Head

G. T. Adel

September, 1988
Blacksburg, Virginia

DEVELOPMENT OF THE SELECTIVE-SHEAR COAGULATION PROCESS FOR ULTRAFINE COAL CLEANING

by

RICKY QUAY HONAKER

Committee Co-chairmen: Dr. Gerald Luttrell
Dr. Roe-Hoan Yoon
Mining and Minerals Engineering

(ABSTRACT)

In order to produce coal containing less than 2% ash using a physical cleaning process, the coal must initially be ground to liberate the mineral matter. The result is a micronized feed material that cannot be efficiently treated using the commercial methods currently available. Therefore, an advanced physical cleaning technique for ultrafine coal, called "selective-shear coagulation", is presently being investigated. The process utilizes high shear conditions to overcome the strong electrostatic repulsive force between particles. The attractive hydrophobic interaction and van der Waals forces control the coagulation of the coal particles.

The effects of various chemical parameters, such as pH and ion concentration, were studied. An optimum pH range was established for tap water and distilled water media. The presence of multivalent cations in the system increased

coal recovery, but decreased selectivity.

Physical parameters of the selective coagulation process, such as particle size, percent solids, and specific energy input, were studied. It was found that separation efficiency improved with decreasing particle size. An optimum feed percent solids was found by maximizing separation efficiency. In the case of distilled water, test results revealed that additional specific energy provided by mechanical agitation was required to induce coagulation after grinding. However, additional mixing was found unnecessary in the case of tap water.

A continuous selective-shear coagulation process using an elutriation column as the separator was designed and characterized. A steady-state population balance model of the elutriation column was developed. The predictions were found to be in good agreement with experimental results.

ACKNOWLEGDMENTS

The author wishes to express his gratitude and appreciation to Dr. Gerald Luttrell and Dr. Roe-Hoan Yoon for their guidance and support throughout the course of this investigation. He is also very grateful to Dr. Greg Adel for his advice during this project. He also extends gratitude to Dr. Michael Karmis, the Mining and Minerals Engineering Department, and the U.S. Department of Energy for the financial support which made this work possible.

Appreciation is also extended to Beth Dillinger and Wayne Slusser for their technical advice and assistance. Special thanks are given to the author's fellow graduate students for their support and friendship.

Special appreciation is given to Zhenghe Xu and Michael Mankosa for their assistance; The many long discussions and invaluable suggestions that they made contributed greatly to the completion of this investigation. Gratitude is also expressed to the rest of the Plantation Road crew for being such a great group of people to work with day to day.

Finally, the author would like to express his deepest appreciation to his wife, Lisa, for her constant encouragement, endless support, understanding, and love.

TABLE OF CONTENTS

Page

TITLE PAGE i

ABSTRACT ii

ACKNOWLEDGEMENTS iv

TABLE OF CONTENTS v

LIST OF FIGURES viii

LIST OF TABLES xv

1. INTRODUCTION 1

1.1 Preamble 1

1.2 Literature Review 4

1.2.1 Oil Agglomeration Process 5
1.2.2 Otisca-T Process 7
1.2.3 Selective Flocculation Process 8
1.2.4 Microbubble Column Flotation 11
1.2.5 Selective-Shear Coagulation Process . 13

1.3 Objectives 15

2. SURFACE CHEMISTRY EFFECTS ON THE SELECTIVE COAGULATION OF COAL 18

2.1 Introduction 18

2.2 Experimental 21

2.2.1 Sample Preparation 21
2.2.2 Experimental Procedure 21
2.2.3 Zeta Potential Measurements 26

2.3 Results 28

2.3.1 Effect of pH 28
2.3.2 Effect of Ions 42
2.3.3 Effect of the Grinding Environment . . 49

2.3.4 Effect of Kerosene Addition 56
2.3.5 Electrokinetic Study on Coal 59

2.4 Discussion 63

2.5 Summary and Conclusions 78

3. THE EFFECT OF THE ASSOCIATED PHYSICAL PARAMETERS ON THE SELECTIVE COAGULATION OF COAL 80

3.1 Introduction 80

3.2 Experimental 82

3.3 Results 82

3.3.1 Effect of Multi-Stage Treatment . . . 82
3.3.2 Effect of Percent Solids 90
3.3.3 Effect of Particle Size 93
3.3.4 Effect of Energy Parameters 95

3.4 Discussion 109

3.5 Summary and Conclusions 118

4. A CONTINUOUS ELUTRIATION COLUMN FOR THE SELECTIVE-SHEAR COAGULATION PROCESS 120

4.1 Introduction 120

4.2 Process Description 122

4.3 Experimental 126

4.4 Results 127

4.4.1 Effect of Elutriation Water Rate . . . 127
4.4.2 Effect of Feed Rate 129
4.4.3 Effect of Feed Percent Solids 133
4.4.4 Process Dynamics 133

4.5 Discussion 142

4.5.1 Operational Parameters 142
4.5.2 Mean Residence Time 149
4.5.3 Steady-State 151

4.6 Summary and Conclusions 154

5. A STEADY-STATE MODEL FOR AN ELUTRIATION COLUMN . . 156

5.1 Introduction 156

5.2 Process Description 158

5.3 Model Development 159

5.4 Program Capabilities 167

5.5 Experimental 169

5.6 Results 170

5.6.1 Model Predictions 170
5.6.2 Comparison of Experimental Data and Model Predictions 180

5.7 Discussion 186

5.8 Summary and Conclusions 191

6. SUMMARY AND RECOMMENDATIONS FOR FUTURE WORK . . . 193

6.1 Summary 193

6.2 Recommendations for Future Work 197

REFERENCES 200

APPENDIX I: Effect of Particle Size on Turbulent Collision Rate 207

APPENDIX II: Program and Simulation Examples 210

VITA 224

LIST OF FIGURES

		Page
Figure 2.1	The five-cell mixing device used for the batch-type experiments	24
Figure 2.2	Schematic representation of the steps used in the batch-type experiments	25
Figure 2.3	Schematic illustration of multiple cleaning stages.	27
Figure 2.4	The effect of pH on coal recovery and product ash percent for the Elkhorn No.3 coal seam containing 12% ash in tap water using 3 cleaning stages.	30
Figure 2.5	The effect of pH on coal recovery and product ash percent for the Elkhorn No.3 coal seam containing 6.0% ash in tap water using 3 cleaning stages.	32
Figure 2.6	The effect of pH on coal recovery and product ash percent for the Upper Cedar Grove coal seam containing 12.0% ash in tap water using 8 cleaning stages.	33
Figure 2.7	The effect of pH on coal recovery and product ash percent for the Upper Cedar Grove coal seam containing 24.0 % ash in distilled water using 8 cleaning stages. .	34
Figure 2.8	The effect of pH on coal recovery and product ash percent for the Upper Cedar Grove coal seam containing 12 % ash in tap water using 3 cleaning stages.	35
Figure 2.9	The effect of pH on coal recovery and product ash percent for the Upper Cedar Grove coal seam containing 3.4% ash in tap water using 8 cleaning stages.	36
Figure 2.10	The effect of pH on coal recovery and product ash percent for the Taggart coal seam containing 28.0% ash in tap water using 3 cleaning stages.	37

Figure 2.11 The effect of pH on coal recovery and product ash percent for the Splash Dam coal seam containing 3.5% ash in tap water using 3 cleaning stages. 38

Figure 2.12 The effect of pH on coal recovery and product ash percent for the Upper Freeport coal seam containing 13.0% ash in tap water using 3 cleaning stages. 39

Figure 2.13 The effect of pH on coal recovery and product ash percent for the Blair coal seam containing 38.0% ash in tap water using 3 cleaning stages. 40

Figure 2.14 The effect of pH on coal recovery and product ash percent for the Pittsburgh No.8 coal seam containing 8.28% ash in tap water using 3 cleaning stages. 41

Figure 2.15 The effect of pyritic sulfur content in the feed coal sample on separation efficiency 43

Figure 2.16 A comparison between using tap water and distilled water as the slurry medium over a range in pH for the Elkhorn No.3 coal seam using 3 cleaning stages 45

Figure 2.17 Effect of Ca^{2+} concentration on coal recovery and product ash percent using double distilled water at pH 9 48

Figure 2.18 Effect of a small Ca^{2+} concentration on coal recovery and product ash percent. . . 50

Figure 2.19 Effect of pH on coal recovery when using soft and hard grinding media 51

Figure 2.20 Effect of pH on product ash percent when using soft and hard grinding media 52

Figure 2.21 The effect of the grinding environment on recovery 53

Figure 2.22 The effect of the grinding environment on product ash percent. 54

Figure 2.23 The effect of kerosene addition on coal recovery and product ash percent for the Elkhorn No.3 coal seam 57

Figure 2.24 The effect of adding 1 lb/ton of kerosene on coal recovery and product ash percent for the Upper Freeport coal seam 58

Figure 2.25 Zeta potential measurements over a range in pH for Elkhorn No.3 coal and mineral matter in distilled water. 60

Figure 2.26 Zeta potential measurements over a range in pH for Upper Cedar Grove coal and mineral matter in distilled water. 61

Figure 2.27 Zeta potential measurements over a range in pH for Pittsburgh No.8 coal and mineral matter in tap water. 62

Figure 2.28 A comparison of zeta potentials of coal and mineral matter in distilled and tap water. 64

Figure 2.29 The effect of calcium additions on the zeta potentials of coal. 65

Figure 2.30 The effect of calcium additions on the zeta potentials of mineral matter. 66

Figure 2.31 A comparison of process performance and zeta potential measurements over a range in pH using distilled water. 68

Figure 2.32 The electrostatic potential energy of interaction versus 2 times the particle-particle separation distance 70

Figure 3.1 The effect of cleaning stages on recovery and product ash percent for the Elkhorn No.3 coal seam containing 12% ash. 85

Figure 3.2 The effect of cleaning stages on recovery and product ash percent for the Elkhorn No.3 coal seam containing 5.25% ash. . . . 86

Figure 3.3 The effect of cleaning stages on recovery and product ash percent for the Upper Cedar Grove coal seam containing 12% ash . 87

Figure 3.4 The effect of cleaning stages on recovery and product ash percent for the Upper Cedar Grove coal seam containing 3.4% ash. 88

Figure 3.5 The effect of cleaning stages on recovery and product ash percent for the RL-Consol coal sample containing 5.5% ash. 89

Figure 3.6 The effect of % solids on coal recovery product ash percent for the Upper Cedar Grove coal seam containing 24% ash 91

Figure 3.7 The effect of percent solids on coal recovery and product ash percent for the Elkhorn No.3 coal seam containing 5.25% ash. 92

Figure 3.8 The effect of particle size on coal recovery, product ash percent, and sulfur reduction for the Elkhorn No.3 coal seam containing 12% ash 94

Figure 3.9 Coal recovery versus product ash percent curves for two particle sizes using the Upper Cedar Grove coal seam containing 24% ash. 96

Figure 3.10 Coal recovery versus product ash percent curves for three particle sizes using an Elkhorn No.3 coal seam sample containing 5.25% ash. 97

Figure 3.11 The effect of agitation time on coal recovery 98

Figure 3.12 The effect of agitation time on product ash percent. 99

Figure 3.13 The effect of rotational speed on coal recovery for three agitation times 101

Figure 3.14 The effect of rotational speed on product ash percent for three agitation times. . . 102

Figure 3.15 Coal recovery versus rotational speed curves for three different media conditions 104

Figure 3.16 Product ash percent versus rotational speed curves for three different media conditions 105

Figure 3.17 The effect of specific energy input on recovery for 3 media conditions; specific energy accumulated over 3 cleaning stages. 107

Figure 3.18 The effect of specific energy input on product ash percent for 3 media conditions; specific energy accumulated over 3 cleaning stages 108

Figure 3.19 The effect of specific energy input on separation efficiency for 3 media conditions; specific energy accumulated over 3 cleaning stages 110

Figure 3.20 Shear coagulation domain for 1 micron particles as a function of shear rate and zeta potential 114

Figure 3.21 Total potential energy of interaction between particles of 1 micron diameter in 0.001 M electrolyte, as calculated by DLVO theory - constant potential assumption . . 117

Figure 4.1 Flowsheet for the continuous selective coagulation/elutriation process. 123

Figure 4.2 Diagram of the continuous elutriation column 125

Figure 4.3 The effect of elutriation water rate on coal recovery, sulfur reduction, and product ash percent. 128

Figure 4.4 The effect of feed rate on coal recovery, sulfur reduction, and product ash percent. 130

Figure 4.5 Coal recovery versus elutriation water rate curves for 2 feed rates 131

Figure 4.6 Product ash percent versus elutriation water rate curves for 2 feed rates 132

Figure 4.7 Coal recovery versus elutriation water rate curves for 2 percent solids 134

Figure 4.8 Product ash percent versus elutriation water rate curves for 2 percent solids . . 135

Figure 4.9 Coal recovery and product ash percent versus accumulated operation time for Elkhorn No.3 coal seam containing 12% ash. 136

Figure 4.10 Coal recovery and product ash percent versus accumulated operation time for Elkhorn No.3 coal seam containing 1.6% ash. 138

Figure 4.11 Coal recovery and product ash percent versus mean residence time in the column . 139

Figure 4.12 The effect of particle diameter and solid density on particle settling velocity according to Stoke's equation. 144

Figure 4.13 Particulate residence time versus column length for 75 micron agglomerates and 5 micron particles 153

Figure 5.1 Schematic of a simple elutriation column . 160

Figure 5.2 Schematic representation of the sections in an elutriation column 161

Figure 5.3 Schematic representation of the mass and volumetric flow balances for the column. . 163

Figure 5.4 Model predictions showing the effect of elutriation water rate on coal recovery over a range of coagulum sizes 171

Figure 5.5 Model predictions showing the effect of feed rate on coal recovery over a range of coagulum sizes 173

Figure 5.6 Model predictions showing the effect of feed solids concentration on coal recovery 174

Figure 5.7 Model predictions showing coal recovery versus elutriation water rate for various feed percent solids values 176

Figure 5.8 Model predictions showing the effect of feed height on coal recovery over a range of elutriation water rates 177

Figure 5.9 Model predictions showing the effect of upper cell diameter on coal recovery for three elutriation water rates. 178

Figure 5.10 Model predictions showing the effect of both the upper and lower cell diameters on coal recovery 179

Figure 5.11 A comparison between model predictions and experimental results showing the effect of elutriation water rate on coal recovery. . 181

Figure 5.12 A comparison between model predictions and experimental results showing the effect of elutriation water rate on product ash percent 182

Figure 5.13 A comparison between model predictions and experimental results showing the effect of feed rate on coal recovery 184

Figure 5.14 A comparison between model predictions and experimental results showing the effect of feed rate on product ash percent 185

Figure 5.15 A comparison between model predictions and experimental results showing the effect of feed percent solids on coal recovery over a range of elutriation water rates 187

LIST OF TABLES

		Page
Table 2.1	Various Coal Seam Samples Studied	22
Table 2.2	Tabulated Results for Various Coal Seam Samples	44
Table 2.3	Effect of Multivalent Cations	47
Table 3.1	Various Coal Seam Samples Studied	83
Table 4.1	Selective Coagulation/Elutriation Process Results	141
Table 5.1	Nomenclature	164

CHAPTER 1

INTRODUCTION

1.1 Preamble

The growing national need for energy independence and the concern over the depletion of petroleum resources has generated a great deal of interest in using America's large coal reserves to produce a fuel in the form of coal-water mixtures. Recent studies by the U.S. Energy Information Administration indicate that the United States possesses 483 billion tons of economically recoverable coal, which accounts for 82% of the total energy resources (Hutton and Gould, 1982). Coal-water mixtures appear to have the ability to replace the petroleum products used to operate turbines in power plants and industrial boilers. However, compared to petroleum-type products, coal is an extremely "dirty" fuel. Therefore, in order for coal to be a commercially suitable replacement for petroleum, a vast amount of research has been undertaken in search of beneficiation techniques which will produce a superclean (< 2% ash) or ultraclean (< 1% ash) coal product.

Physical cleaning methods require liberation of the mineral matter in order to produce a product containing less than 2% ash by weight. This normally requires a

substantial amount of grinding which can account for 40-60% of the total processing cost (Leja, 1982). The liberation size of the mineral matter is a characteristic of the coal seam. Pyritic sulfur is normally the hardest type of mineral matter to remove due to its fine liberation size. However, it is very beneficial to remove the coal pyrite since the result is a decrease in both the product ash and the product sulfur content. Experimental investigations by Mathieu and Mainwaring (1986) have indicated an increase in pyritic sulfur reduction with increasing grinding time. In fact, their results show that particle sizes of less than approximately 10 microns are needed for complete pyritic sulfur rejection. Further results reported by McCartney et al. (1969) on 61 U.S. coal seam samples indicated that the mean coal pyrite particle size was in the range of 20 to 95 microns. Kneller and Maxwell (1985) reported a mean size of 4 microns for several Ohio seam coal samples. Since an ash level between 1 and 4% and a sulfur level of less than 1% is required in order to meet existing emmision standards and fulfill boiler requirements (Bethell and Sell, 1983), fine grinding is a necessary step for the physical treatment of coal intended for coal-water mixtures.

Chemical cleaning techniques, which do not require grinding of the coal to the extent that physical techniques do, have been studied as a means of producing coal

containing a low level of impurities. While the chemical processes have shown great potential, especially in the reduction of sulfur, the expense and environmental problems associated with the processes have hindered their development. The cost of producing clean coal by chemical means has been estimated to be around $25-30 per ton (Boron and Kollrack, 1983). Physical coal cleaning methods, on the other hand, are considered to be less costly and more environmentally acceptable. For this reason, a great deal of attention is currently being given to the development of advanced physical coal cleaning techniques for the recovery of fine coal.

Froth flotation is the most common commercially available process for fine coal (-28 mesh) cleaning today. According to one estimate, nearly 3 million tons of clean coal are produced each year by this method (Wright, 1985). The process is based on the hydrophobic nature of the coal particles and the associated hydrophilic impurities. Separation is achieved by passing fine air bubbles through a coal-water slurry. The hydrophobic coal particles collide and attach to the air bubbles, which are stabilized by an addition of a frother solution. The attached coal particles float to the top of the cell where they are collected as a concentrate. The hydrophilic gangue material settles to the bottom of the cell, where it is

withdrawn and sent to a thickener for dewatering. The hydrophobicity of a coal sample can be enhanced by the addition of a collector, such as kerosene.

There are three basic problems with the froth flotation process. First, as the particle size of the coal particles is reduced, recovery drops due to a decrease in the number of particle-bubble collisions. Therefore, in conventional froth flotation applications using miconized coal (< 10 microns), coal recovery is very inadequate. Secondly, micronized mineral matter, especially clays, tends to be easily entrained in the water flowing with the coal concentrate and entrapped inside coal coagulums. Hence, the separation efficiency is fairly low when processing a micronized coal suspension. Thirdly, due to the hydrophobic nature of the coal pyrite, inorganic sulfur removal is very difficult. For these reasons, multiple cleaning stages and low throughputs are needed in order to produce the clean coal products which are desired for coal-water mixtures.

1.2 Literature Review

The desire to produce superclean coal more efficiently and economically is spurring research groups and other organizations into development of new advanced physical cleaning techniques. The result is a host of potential

processes. Some of the more prominent processes include oil agglomeration (National Research Council of Canada, Consolidated Coal), the Otisca-T process (Otisca Industries), selective flocculation (Battelle Laboratories), and microbubble column flotation (Virginia Tech). Another advanced physical cleaning technique for ultrafine coal cleaning has been discovered at Virginia Tech. It involves the selective coagulation of coal/mineral matter suspensions. A brief description of the aforementioned advanced physical cleaning techniques is presented in the following pages.

1.2.1 Oil Agglomeration Process

The oil agglomeration process is not a new technique for fine coal cleaning. Since its introduction in 1921, the use of oil agglomeration has been investigated in laboratories and pilot plants. The largest oil agglomeration plant built to date treated 600 tons per day in 1926 and processed a total of 36,000 tons of clean coal before closing down due to economic problems (Mehrotra et al., 1983). Several variations of oil agglomeration have been developed over the years. Some of the more recognized processes include the Trent Process (1921), the Convertol Process (1952), the Spherical Agglomeration Process (1961), the Shell Pelletizing Separator Process (1968), the Olifloc

Process (1977), the CFRI Process (1976), and the Broken Hill Proprietary Process (1977).

The fundamental basis of the process involves the preferential wetting of the hydrophobic coal particles by oil. In the presence of a sufficient amount of oil and mechanical agitation, the oil-coated coal particles collide with each other and form agglomerates. The hydrophilic gangue particles resist wetting by the oil and remain in the aqueous solution. Hence, a separation can be made. There are normally five steps in an oil agglomeration process which are listed below (Steedman and Krishman, 1987):

1. Slurry conditioning
2. Oil heating and emulsification
3. Slurry-oil contact and oil agglomeration
4. Agglomerate recovery
5. Dewatering and/or pelletization.

Light oils are generally required to obtain a high level of rejection of impurities. Heavy oils are important for agglomerate size and dewatering.

In comparison to froth flotation, oil agglomeration normally achieves a higher coal recovery and product ash percent value. This is due to the fact that a coal-oil bond is stronger than a coal-air bond. Also, the separation efficiency of an oil agglomeration process does

not decrease with particle size as in froth flotation (Steedman and Krishnan, 1987). However, both processes suffer from the inability to reject coal pyrite. The major problem with the oil agglomeration technique, which has hampered its commercial development, is oil consumption. One estimate indicated that the cost of treating one ton of clean coal is $19.42 (July 1980 dollars), where 58% of the per ton cost is attributable to the cost of the oil (Mezey et al., 1985). Several research groups are presently investigating methods to reduce the oil consumption to an economical level.

1.2.2 Otisca-T Process

The Otisca process is presently under development by Otisca Industries. Its principles are similar to the oil agglomeration processes, except that it uses a heavy organic liquid, trichloroflouromethane (CCl_3F), to selectively extract coal from aqueous suspensions. The mineral matter and pyritic sulfur are removed by gravity separation in a static bath of the cleaning medium to produce a clean coal product. The moisture on the hydrophobic surface is removed prior to the gravity separation by the addition of certain chemical compounds. The clean coal and the reject are heated to $100^{o}F$ to evaporate the organic liquid present on the surface of the

particles. The cleaning medium vapors are then condensed and recycled (Hutton and Gould, 1982).

The major advantage of this process is the ability to treat coarse and fine coal fractions, the most attractive being the 200 x 0 mesh fraction. Also, the process rejects both the pyritic sulfur and the ash material very efficiently. Another very important advantage is the elimination of the clean coal dewatering circuit due to the low surface moisture present on the coal particles after the cleaning treatment. Environmental hazards and large capital costs, due to the large reaction vessels and numerous safety features, are the main disadvantages of the Otisca-T process (Steedman and Krishnan, 1987).

1.2.3 Selective Flocculation Process

Selective flocculation is a process that is well established in the mineral industry for the treatment of ultrafine particles. The process has been thoroughly studied and applied on systems of potash (Banks, 1979), iron ore (Villar and Dawe, 1975), galena and calcite (Yarar and Kitchener, 1970), cassiterite (Appleton et al., 1975), hematite (Read, 1971; Bagster, 1984), calcite, rutile, alumina, and quartz (Friend et al., 1973; Friend and Kitchener, 1972), and scheelite (Warren, 1975). Warren (1981) published an article completely describing the shear

flocculation process. The application of selective flocculation for treating coal fines was introduced in the late 70's. A large amount of the research and development for the process was performed by Attia and Krishnan at Battelle's Columbus Laboratories (1983, 1984, 1985, 1986). At the Battelle laboratories, a pilot plant treating 1 ton per day was designed based on batch test results (Conkle et al., 1986). Data produced by the pilot plant are currently proprietary.

The selective flocculation process utilizes the differences in the physical-chemical properties between the coal and gangue particles in a suspension. The coal is selectively agglomerated by the addition of an organic flocculant which adsorbs preferentially on the coal surface and by applying a sufficient amount of mechanical energy. It was recognized early from laboratory tests that commercially available flocculants used for dewatering were not effective as a selective flocculant for coal. Therefore, water-dispersible flocculants that contain hydrophobic functional groups were designed through a cooperative effort between Battelle Columbus Division and Dai-Ichi Kogyu Seiyaku Co. Ltd. specifically for the selective flocculation of coal (Ishizuka et al., 1984). The steps involved in using the process are:

1. Dispersion of the coal suspension

2. Flocculant adsorption and floc formation
3. Floc conditioning
4. Floc separation.

Reported applications of the process include a) producing very low ash coals for coal-water mixtures with high BTU recovery, b) recovering coal from fines rejected from wash plants, c) providing alternatives to flotation in conventional coal cleaning, and d) recovering coal from tailing ponds (Krishnan, 1987).

The selective flocculation process has the ability to effectively treat both fine (-100 mesh) and ultrafine (-325 mesh) coals. Compared to froth flotation, the selective flocculation process can effectively treat smaller material, therefore, more of the mineral matter can be liberated and rejected. The liberated coal pyrite, which is floated in froth flotation, is dispersed and removed with the mineral matter when the flocculation technique is used (Attia et al., 1984). Hence, the process is very effective in the removal of inorganic sulfur. Also, Attia et al. (1984) reported an economical advantage over conventional froth flotation when producing a clean coal product containing 2% mineral matter. They reported that, based on laboratory test results, the cost of producing 1 ton of clean coal using the selective flocculation process is expected to be around $0.5-2.0, assuming an 85 % recycle

of dispersants and pH modifiers. In multi-stage flotation, they estimated the cost to be around $3-6 per ton. On the other hand, Hucko (1977) concluded that although the selective flocculation process was feasible for the treatment of coal slurries, the high cost of reagents, especially dispersants, would make the process prohibitively expensive.

1.2.4 Microbubble Column Flotation

The microbubble flotation process was developed at Virginia Tech in the early 1980's in an attempt to overcome some of the deficiencies of conventional flotation (Yoon, 1982). Initial indications showing that the use of microbubbles could increase the recovery of ultrafine coal were obtained through hydrodynamic studies (Flint and Howarth, 1971; Reay and Ratcliff, 1973; Collins and Jameson, 1976; Anfruns and Kitchener, 1977). The use of a column having a countercurrent feeding arrangement was later found to enhance bubble-particle collision (Luttrell et al., 1988). Also, the addition of countercurrent wash water to the column provided a means of minimizing the hydraulic entrainment problem encountered in conventional froth flotation. Therefore, the combination of microbubbles and column flotation was investigated and found to be a very efficient physical cleaning technique

for ultrafine coal.

The fundamental basics of the two flotation processes, conventional and microbubble column, are the same. A coal slurry is fed downward into the column against a rising suspension of fine bubbles. The hydrophobic coal particles attach to the bubbles and report to the top of the cell as concentrate. The bubble size produced in the microbubble column is approximately 70-250 microns in diameter, which is at least an order of magnitude smaller than that generated by sparging mechanisms (Luttrell et al., 1988). The hydrophilic mineral matter is collected at the bottom of the column. Countercurrent wash water is added in the froth to minimize entrainment of gangue material, especially micronized clay particles. Characterization of the column parameters was reported by Luttrell et al. (1988). A 1/4 ton per hour pilot plant has been constructed to test the microbubble process at Virginia Tech. Results from the pilot plant have not yet been published.

Advantages of the microbubble flotation column over conventional froth flotation are:

1) Enhanced coal recovery due to an increased probabilty of collision. The increase is a result of better hydrodynamics in the column because of the use of smaller bubbles.

2) Increased selectivity due to the use of countercurrent wash water.
3) The ability to produce superclean and ultraclean coal while maintaining high recoveries (Yoon et al., 1987).
4) Smaller particle size fractions can be more efficiently treated.

1.2.5 Selective-Shear Coagulation Process

The use of selective coagulation as a physical cleaning technique was initially reported by Maynard et al. (1969) for kaolin slurries. In this case, weakly hydrophobic titanium particles were selectively coagulated and separated using a sedimentation technique. Pugh and Kitchener (1970) referred to this application when discussing the theory of selective coagulation in mixed colloidal suspensions using the classical Derjaguin-Landau-Verwey-Overbeek (DLVO) theory of colloid stability. They stated that selective coagulation of initially dispersed mixed colloidal systems was possible due to a difference in the coagulation rate between the various species. They reported that for a system having two colloidal components (1 and 2), the coagulation rate resulting from the 1-1 interaction must be more than 100 times greater than the coagulation rate for the interactions of 1-2 and 2-2 before a separation is possible. The controlling factors

affecting the coagulation rate between the components have been identified as the colloidal surface forces (i.e., electrostatic, van der Waals, hydrophobic interactions, and hydration forces) and the collision frequency (Warren, 1977). Shear rate was also found to be an important parameter for coagulation. Van de Ven and Mason (1976, 1977) defined shear coagulation or orthokinetic coagulation by measuring the stability of a suspension over a range of zeta potentials and shear rates. They concluded that selective coagulation can be induced in a mixed colloid suspension by carefully controlling the zeta potentials and shear rate.

Following their investigation into the theory of selective coagulation, Pugh and Kitchener (1972) reported results on the selective coagulation of a rutile/quartz colloid suspension. They investigated the effect of pH and electrolyte to determine the regions of instability for both components. Next, they selectively coagulated rutile in a slurry containing 1.1% by weight of rutile and 1.1% quartz at the appropriate pH and electrolyte concentration. At pH 9.5, an analysis of both the sediment and the supernatant found 93% and 2% rutile, respectively. The selective coagulation technique was also applied to a mixed suspension of hematite and quartz (Pugh, 1973). After selectively coagulating a 50/50 mixture of the two

components, the sediment analysis found 92% hematite and 8% quartz, while the supernatant was 1% hematite and 99% quartz at pH 9.

One advantage that the selective-shear coagulation process has over the other advanced physical cleaning techniques is very apparent. The selective-shear coagulation process requires pH modifiers and/or electrolytes, whereas the other processes require more expensive and complex chemical packages. This fact also makes the selective-shear coagulation process more environmentally acceptable. Another advantage is that the separation efficiency of the process should improve with a decrease in particle size due to the reduction of inertia effects. Therefore, the gangue material can be completely liberated from the valuable mineral while at the same time improving the separation efficiency. For this reason, the product quality should be better when using the selective coagulation process than when using any of the aforementioned physical cleaning techniques.

1.3 Objectives

The selective-shear coagulation (SSC) process for ultrafine coal treatment is a technique recently discovered at Virginia Tech. Its research and development will be the topic of this thesis. The objectives of this investigation

will be: 1) to identify and determine the effect of chemical and physical parameters of the SSC process, and 2) to design and test a continuous device in order to realistically utilize the selective-shear coagulation technique for cleaning ultrafine coal. In order to meet these objectives, the investigation will be separated into four separate tasks.

The first task involves the identification and study of the effect of various chemical parameters. This will require that the physical parameters be held constant while making chemical adjustments to the coal slurry suspension, i.e., by changing the pH or ion concentration. Also, the effect of enhancing the hydrophobicity of the coal particles by adding a small amount of fuel oil will be analyzed.

The second task will be concerned with characterizing the effect of the physical parameters, such as particle size, percent solids, agitation time, agitation speed, and specific energy input. This will be done at the optimum pH determined in Task 1 for a distilled water medium.

Design and characterization of a continuous selective-shear coagulation process is the goal for the third task. The separation device selected for the process is an elutriation column. The fourth task involves the development of a population balance model for the

elutriator, which will enhance the understanding of the operation and provide scale-up information.

CHAPTER 2

SURFACE CHEMISTRY EFFECTS ON THE SELECTIVE COAGULATION OF COAL

2.1 Introduction

In the past, research in the area of slurry stability has involved the de-stabilization of the entire particulate system, which required heterocoagulation for multiple materials or homocoagulation for systems containing a single material. Recent research at Virginia Tech on mixed colloidal suspensions (i.e., coal/ash systems) has shown that the desired minerals can be separated from slurries using selective-shear coagulation. The basis behind selective coagulation is the utilization of the difference in surface electrostatic repulsive forces and van der Waals forces between the various particulate components of a slurry. Another force important for hydrophobic materials, such as coal, is the hydrophobic interaction, which is an attractive force reportedly 1-2 orders of magnitude greater than the van der Waals force (Warren, 1981; Rabinovich and Deryaguin, 1988). This force is presently under extensive investigation to elucidate the origin of hydrophobic interactions (Churaev and Derjaguin, 1984; Rabinovich and Deryaguin, 1988; Xu and Yoon, 1988). A theoretical description of the selective coagulation process using the

DLVO theory was initially reported by Pugh and Kitchener (1970).

One example of selective coagulation, initially discovered in a laboratory, is the removal of colored impurity minerals from kaolin slurries (Maynard, 1969). The process consisted of dispersing china clay at about 30% solids in a solution containing about twice the amount of sodium hexametaphosphate that would be needed for optimum dispersion. After being held for 14 hours or more undisturbed, yellow streaks were observed which eventually settled to the bottom. The yellow streaks contained particles of titanium minerals which selectively coagulated and settled out. Other studied cases of selective coagulation involved mixed suspensions of rutile/quartz (Pugh and Kitchener, 1972) and hematite/quartz (Pugh, 1973).

In this investigation, coal slurry was cleaned by selectively coagulating the coal particles from a coal/ash suspension. This was accomplished by first adjusting the pH of the slurry so that the surface potentials of both the coal and the ash particles were relatively high. This adjustment minimized the amount of heterocoagulation, hence enhancing the selectivity of the process. The possible mechanisms which induced the coagulation of the coal particles in the presence of a high surface potential

include the van der Waals attractive force and hydrophobic interaction. High shear conditions were applied to overcome the repulsive particle interaction forces and to provide a high probability of particle-particle collisions which enhanced the coagulation rate. The coal coagula were separated from the mineral matter using a sedimentation technique which required only 3-5 minutes instead of the 14 hours needed for the clay suspension.

This chapter presents results of a study of the selective coagulation process on a coal-ash system and discusses the effect that surface chemistry has on the technique. Experiments were carried out over a range of pH values using several coal samples. These results were analyzed and discussed using zeta potential versus pH plots obtained in the laboratory. Also, the effect of ions that were present in the tap water or in the grinding environment or were artificially added was investigated. Enhancement of surface hydrophobicity through the addition of small amounts of a fuel oil was studied to determine its effect on coal recovery and selectivity. This treatment could prove to be beneficial for improving the selective coagulation process when treating partially oxidized coal samples.

2.2 Experimental

2.2.1 Sample Preparation

The coal samples used in this study are listed in Table 2.1, along with their respective ash values and place of origin. Upon arrival, each sample was crushed to -1/4 inch using a laboratory jaw crusher. The coal was then riffled into representative lots of approximately 1000 grams each, placed into air-tight containers, and stored in a freezer at -20^{o}C to minimize oxidation.

Prior to performing an experiment, a 160-gram coal sample was pulverized in a laboratory hammer mill to approximately 75 microns. This procedure was followed by wet-grinding for 30 minutes at 30% solids in a 5-1/4- inch diameter stirred ball mill using 1/16-inch stainless steel balls as the grinding media. This resulted in a mean particle size of approximately 5 microns as determined by an Elzone 80-XY particle size analyzer. Afterward, the sample was split into 8 smaller samples containing 20 grams each.

2.2.2 Experimental Procedure

Twenty grams of a 5-micron coal sample was placed in a 6-inch diameter mixing container. Four 1/2-inch baffles were placed vertically along the walls of the container equal distances apart. A 3-inch diameter serrated disk

Table 2.1 : Various Coal Seam Samples Studied

COAL SAMPLE	TYPE	FEED ASH (%)
Upper Cedar Grove	ROM	24.0
Upper Cedar Grove	ROM	12.0
Upper Cedar Grove	Processed	3.40
Lower Cedar Grove	ROM	1.44
Elkhorn No.3	ROM	12.0
Elkhorn No.3	Processed	6.00
Taggart	ROM	28.0
Splash Dam	ROM	3.50
Blair	ROM	38.0
Upper Freeport	ROM	13.0
Pittsburgh No.8	ROM	8.28

impeller was used for the agitation of the coal slurry. A multiple mixing device consisting of 5 such cells and impellers (Figure 2.1) was used for tests involving various slurry conditions. By using this type of mixing device, the agitation environment was kept constant for each condition.

After a 20-gram coal sample was added to a mixing cell, tap or distilled water was added to adjust the percent solids to 2% by weight. The pH was regulated by adding sodium hydroxide or hydrochloric acid to increase or decrease the pH.

The batch selective coagulation tests were carried out in three steps as schematically illustrated in Figure 2.2. Initially, the coal slurry was agitated for 5 minutes using the apparatus in the above discussion. Afterward, an additional 5 minutes was allowed for coagulum growth and sedimentation. Next, the supernatant containing a stable suspension of solids was siphoned from the container, thereby leaving the coagulated sediment in the container. The coagulated material was considered to be the product of the selective-shear coagulation process, whereas the supernatant was the reject.

Multiple cleaning stages were found to be needed to release particles of mineral matter entrapped in the coal coagula. This was accomplished by adjusting the percent

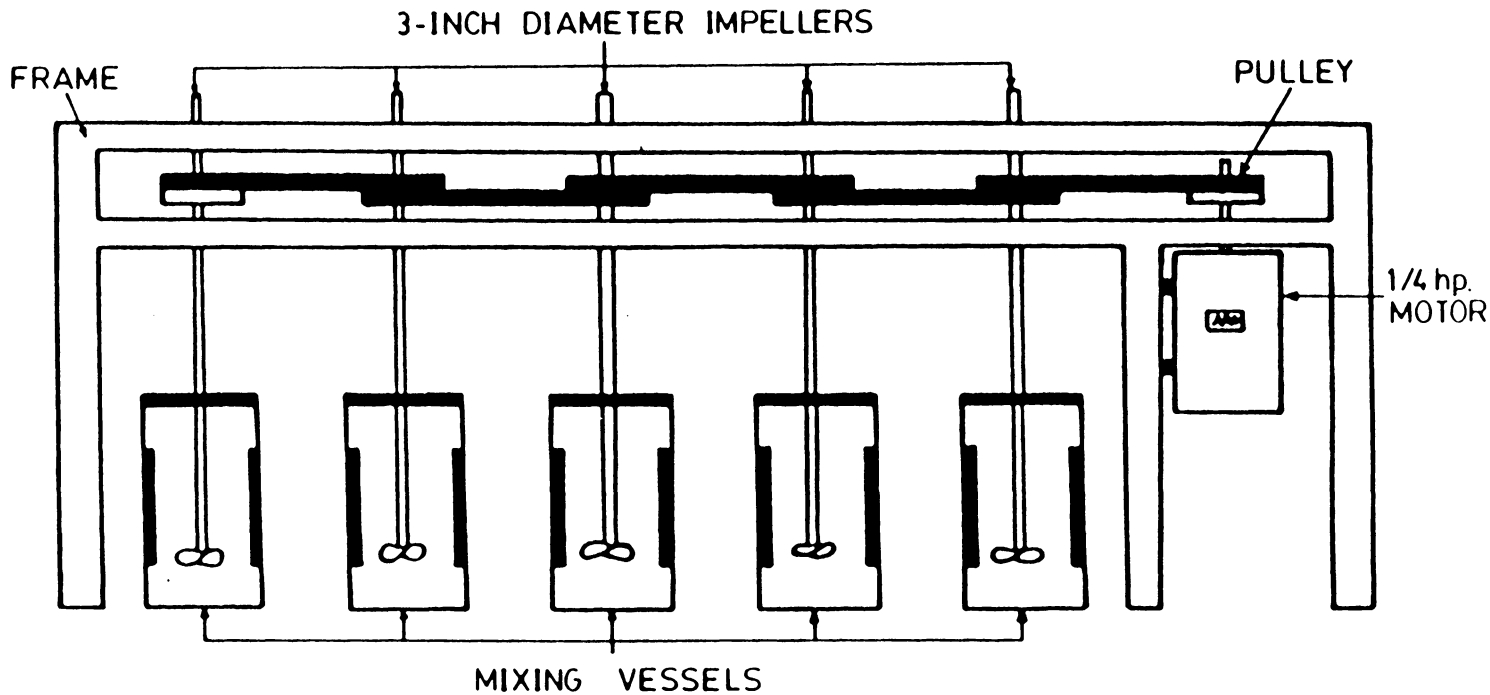

Figure 2.1 The five-cell mixing device used for the batch-type experiments .

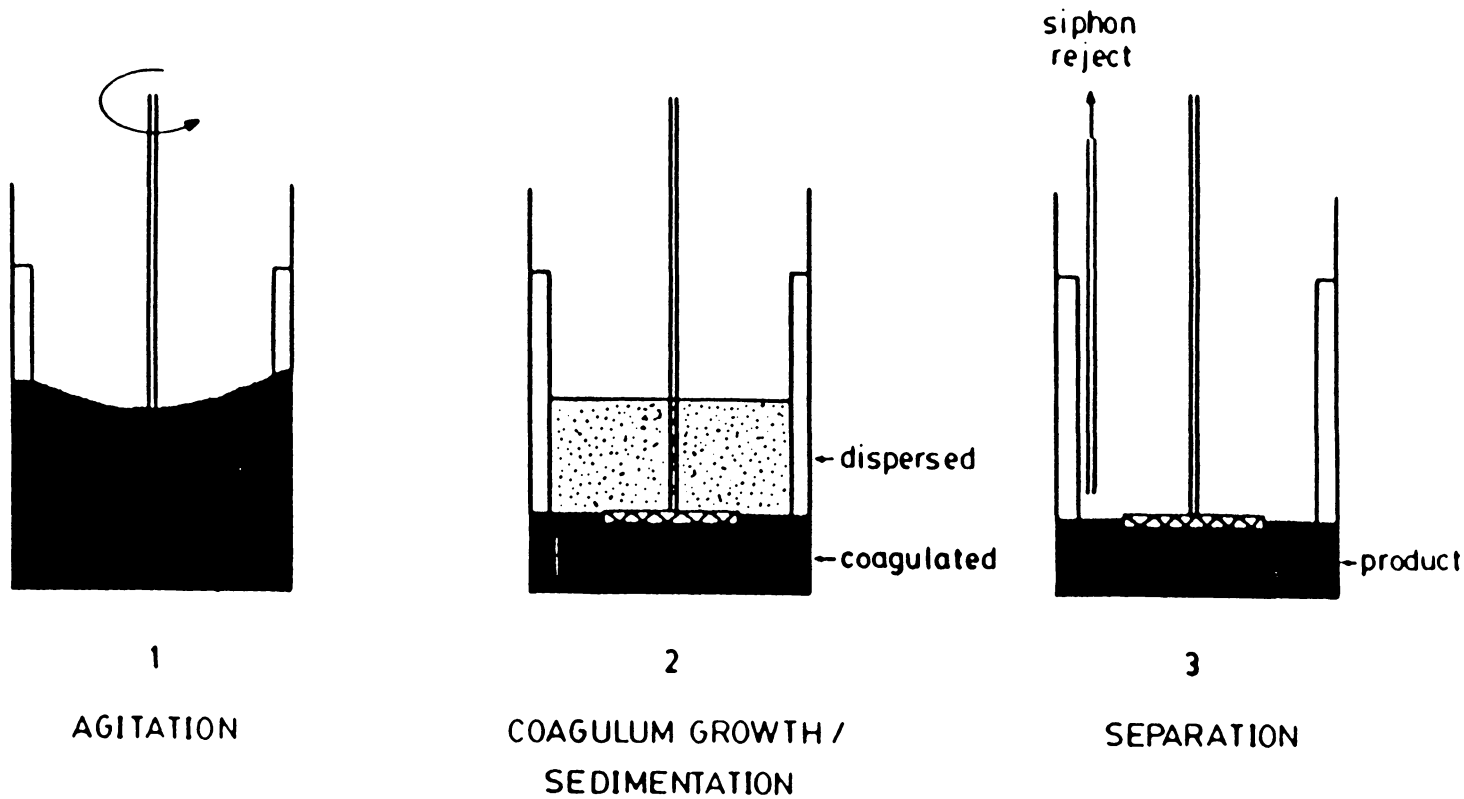

Figure 2.2 Schematic representation of the steps used in the batch-type experiments .

solids and pH of the product slurry from the previous stage of treatment to their respective levels and proceeding with agitation, sedimentation, and separation. The multiple stage cleaning technique is illustrated in Figure 2.3.

2.2.3 Zeta Potential Measurements

The clean coal sample for the zeta potential measurements was obtained by performing a heavy media separation at a specific gravity of 1.3 using magnetite. This separation resulted in a sample with an ash content of 2.2%. Samples of mineral matter were collected by hand-picking gangue particles from a fresh coal sample. The resulting ash content was 88.9%.

Prior to measuring zeta potentials, the samples were ground to -500 mesh. Approximately 0.20 grams of sample was withdrawn and combined with 500 ml of double-distilled water unless otherwise indicated. Potassium chloride was added to the suspension as a supporting electrolyte in the amount of 10^{-3} M. The pH was adjusted appropriately by adding hydrochloric acid to decrease the pH or sodium hydroxide to increase it. This system was agitated for 5 minutes prior to proceeding with the electrokinetic measurements.

All the electrokinetic measurements were performed

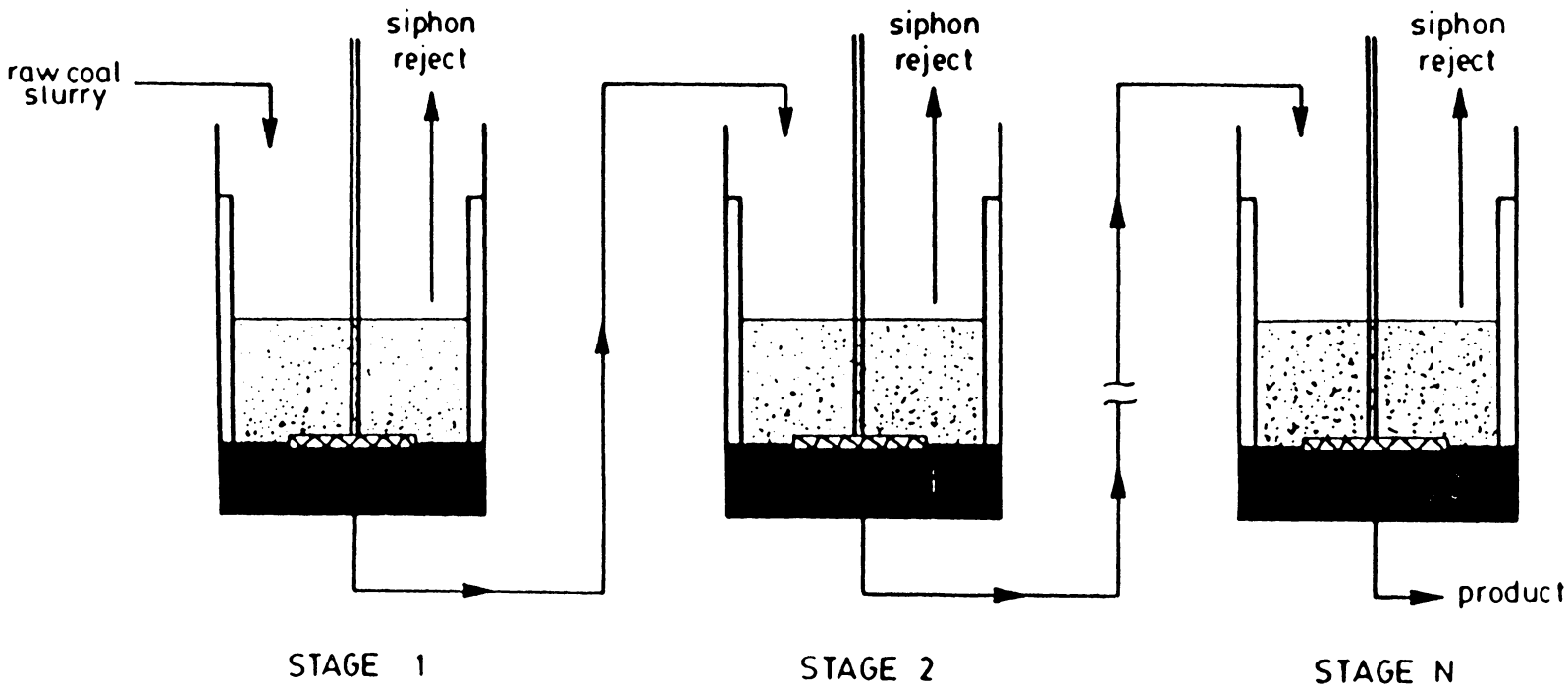

Figure 2.3 Schematic illustration of multiple cleaning stages.

using a zeta meter developed by Zeta Meter, Inc. of New York. The apparatus used a Riddick cell with a molybdenum anode and a platinum-iridium cathode. The electrophoretic mobility was converted to zeta potential by using the Helmholtz-Smoluchowski equation.

2.3 Results

2.3.1 Effect of pH

As mentioned earlier, the surface forces which control the coagulation behavior of colloids are electrostatic, van der Waals, and hydrophobic interactions. The electrostatic force is repulsive between particles of the same type except at their point of zero charge (pzc). At the pzc, coagulation normally occurs due to the attractive nature of the other surface forces (Pugh and Kitchener, 1970; Xu and Yoon, 1988). For particles of coal and mineral matter, the surface charge can be controlled by the addition of hydroxyl and hydronium ions (Campbell and Sun, 1970). Reported data in the literature have shown that coal particles tend to have higher pzc values than particles of mineral matter (Campbell and Sun, 1970; Wen and Sun, 1977; Arnold and Aplan, 1986). Therefore, selective coagulation of coal should be possible by controlling the pH of the slurry.

In order to study the effect of surface potential, coagulation behavior was investigated over a pH range of 3 to 11 using the mixing apparatus described earlier. Figure 2.4 is a typical plot of coal recovery and product ash percent versus pH for an Elkhorn No. 3 seam coal sample. Between pH values of 3 and 5, the coal recovery was very high (99%), but the ash content was also very high (11.7%). The high ash content in the clean coal product was probably due to the fact that the mineral matter coagulates along with the coal. Due to the low zeta potentials and the opposite charges of the coal and mineral matter in this pH range, both homocoagulation and heterocoagulation were possible.

Between pH 5 and 7, the product ash percent dropped significantly to 2.8%, while the coal recovery remained above 97%. The decrease in the ash content may be explained by a change in the surface charge of the coal particles from positive to negative and an increase in zeta potential which prevented the mineral matter particles from coagulating as the pH was increased.

Recovery declined slightly to 97% at pH 9 before sharply decreasing to 50% at pH 11. The product ash percent, on the other hand, increased from 3.0 at pH 9 to 14.5 at pH 11. The decrease in coal recovery may be attributed to an increase in the zeta potential of coal at

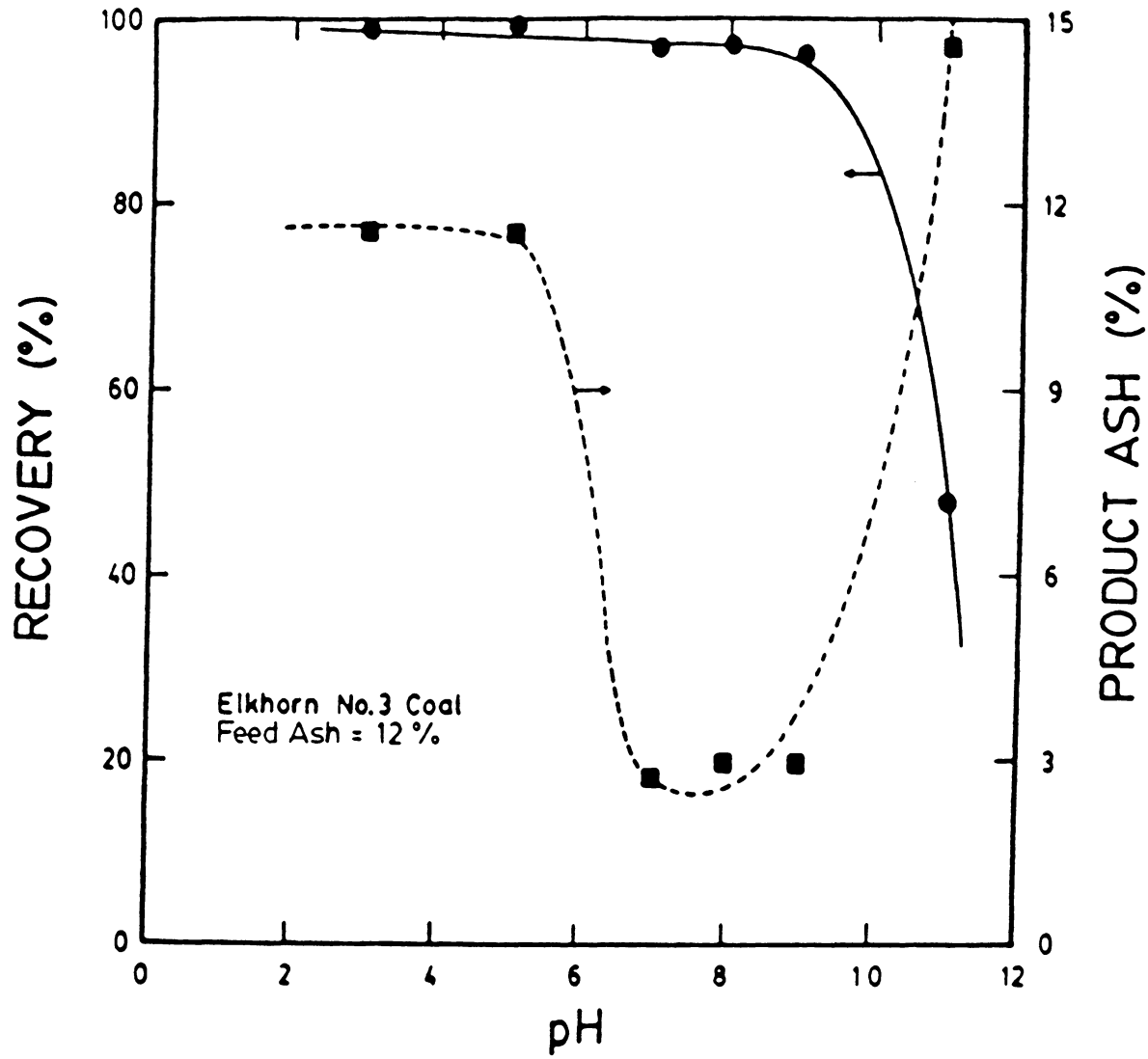

Figure 2.4 The effect of pH on coal recovery and product ash percent for the Elkhorn No.3 coal seam containing 12% ash in tap water using 3 cleaning stages.

high pH values, which would prevent the coal from coagulating. The increase in the ash content to a value greater than that found in the feed may be explained by the coagulation of mineral matter by a bridging mechanism. It may be possible that hydoxides, such as $Ca(OH)_2$, form on the surface of the mineral matter to induce coagulation. Thus, the optimum pH range for selective coagulation of the Elkhorn No. 3 coal sample was 7 to 9.

Similar curves were generated for the other coal samples studied, and these are illustrated in Figures 2.5-2.14. Some coal seam samples, such as the Upper Freeport, Blair, and Pittsburgh No. 8, did not perform well throughout the entire pH range. Reasons may include:

a) Surface oxidation of the coal particles.

b) Electrical conditions of both the coal and ash were not favorable for selective coagulation.

c) Excessive release of multivalent ions from the coal sample during grinding. This effect may be important especially when using a coal containing a large amount of pyrite. A high concentration of coal pyrite could result in a high iron content in the medium (Celik and Somasundaran, 1986). The effect this would have on the selective coagulation of the coal would be increased recovery and decreased

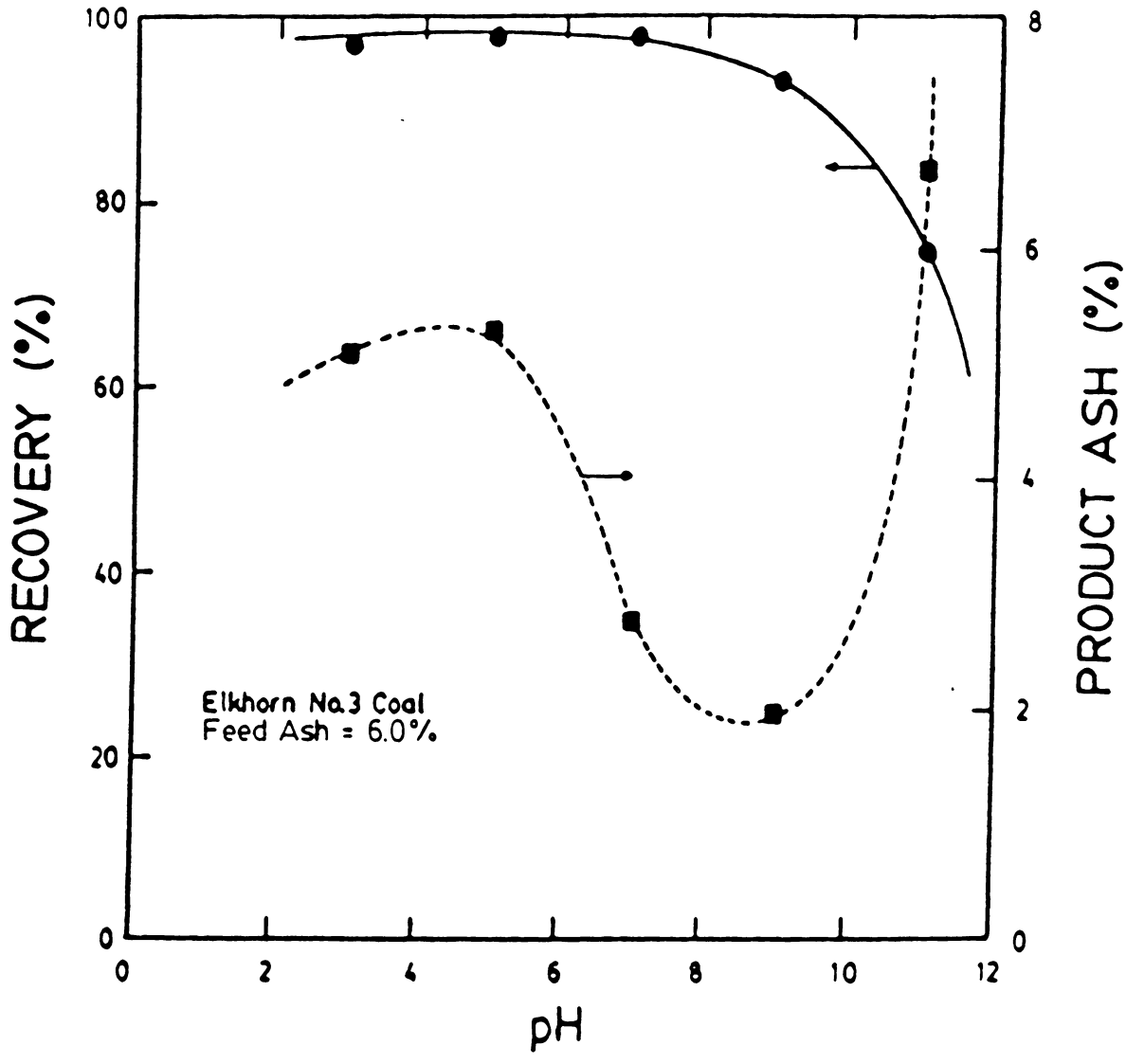

Figure 2.5 The effect of pH on coal recovery and product ash percent for the Elkhorn No.3 coal seam containing 6.0% ash in tap water using 3 cleaning stages.

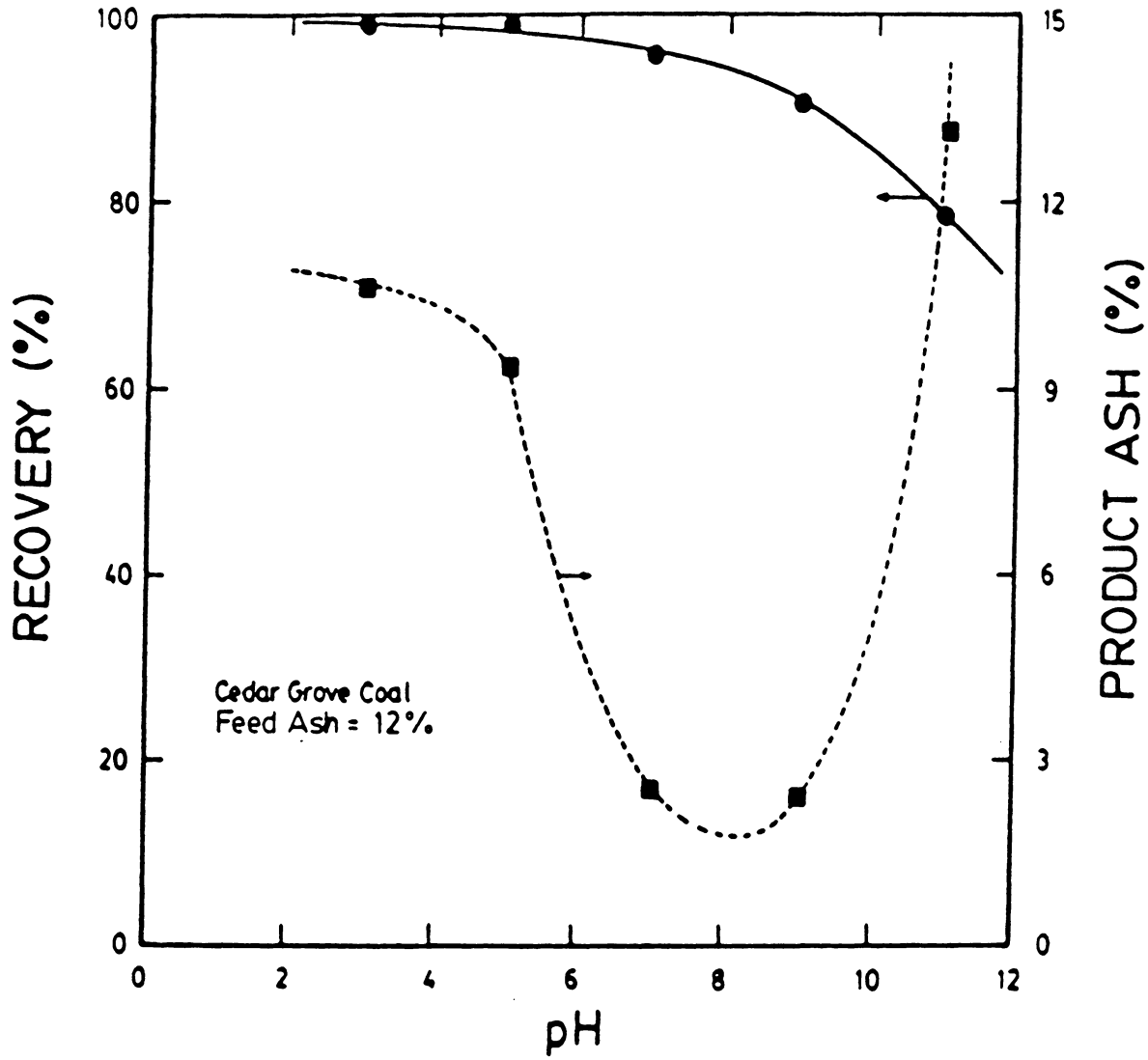

Figure 2.6 The effect of pH on coal recovery and product ash percent for the Upper Cedar Grove coal seam containing 12.0% ash in tap water using 8 cleaning stages.

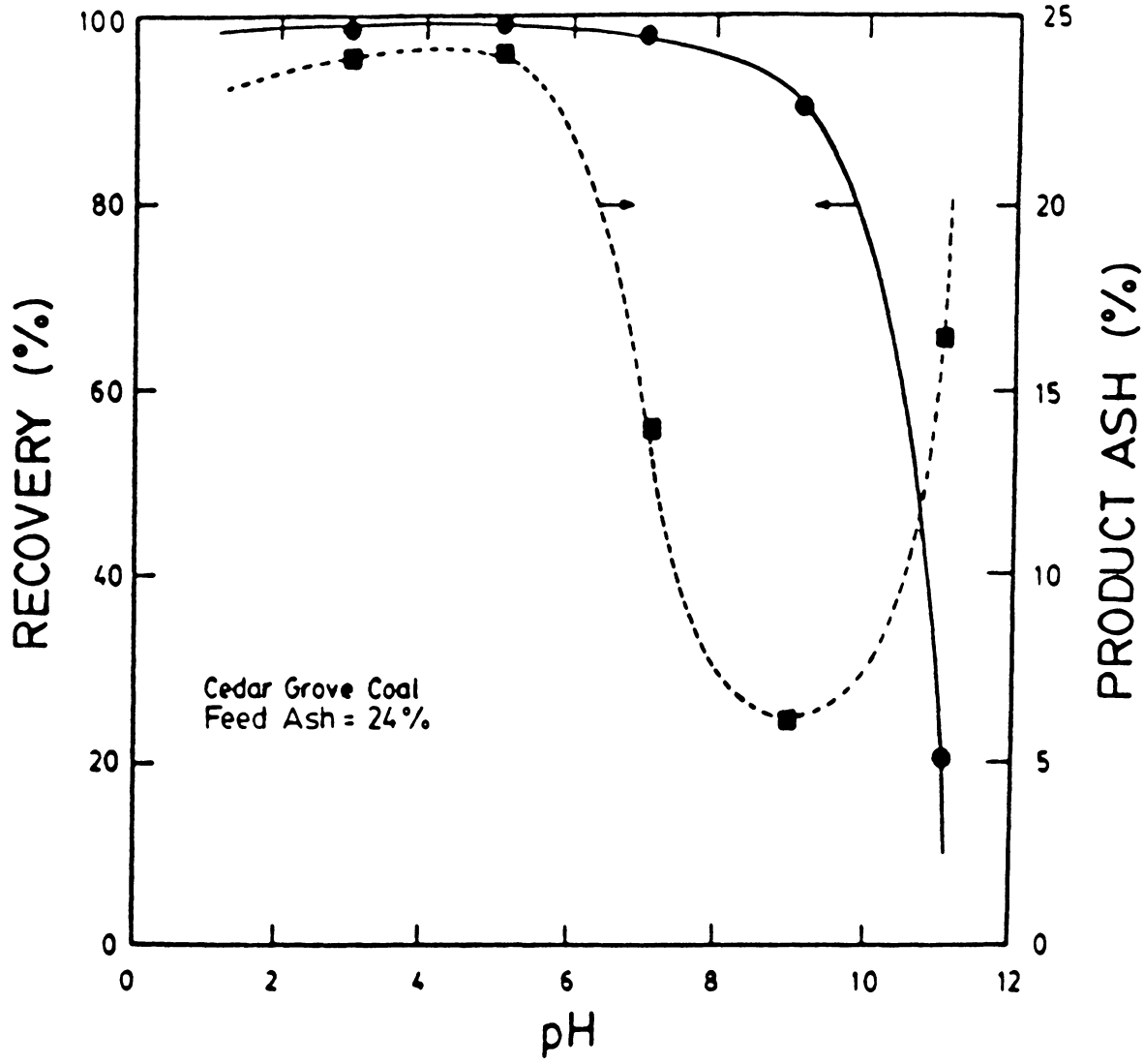

Figure 2.7 The effect of pH on coal recovery and product ash percent for the Upper Cedar Grove coal seam containing 24.0 % ash in distilled water using 8 cleaning stages.

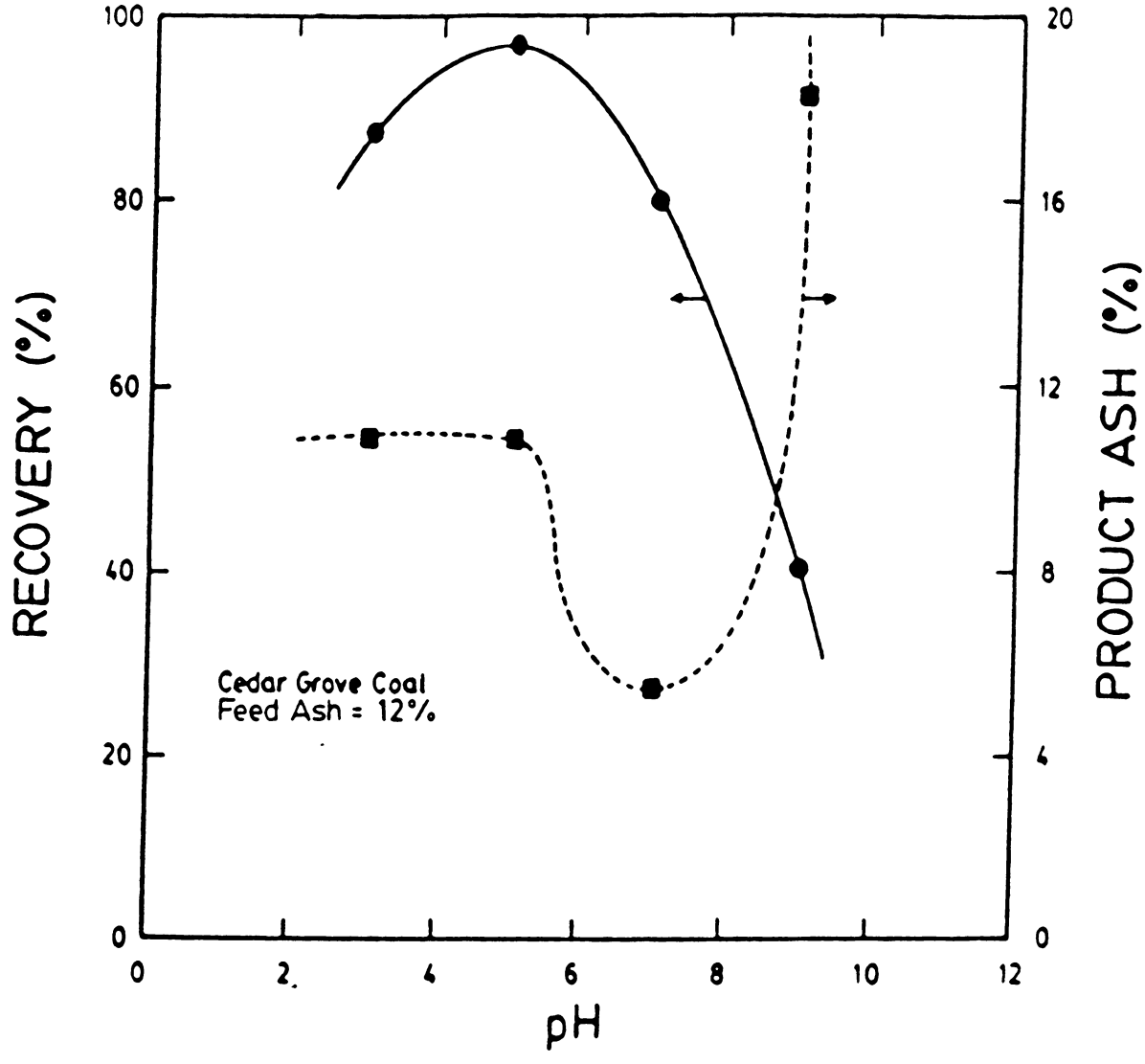

Figure 2.8 The effect of pH on coal recovery and product ash percent for the Upper Cedar Grove coal seam containing 12 % ash in tap water using 3 cleaning stages.

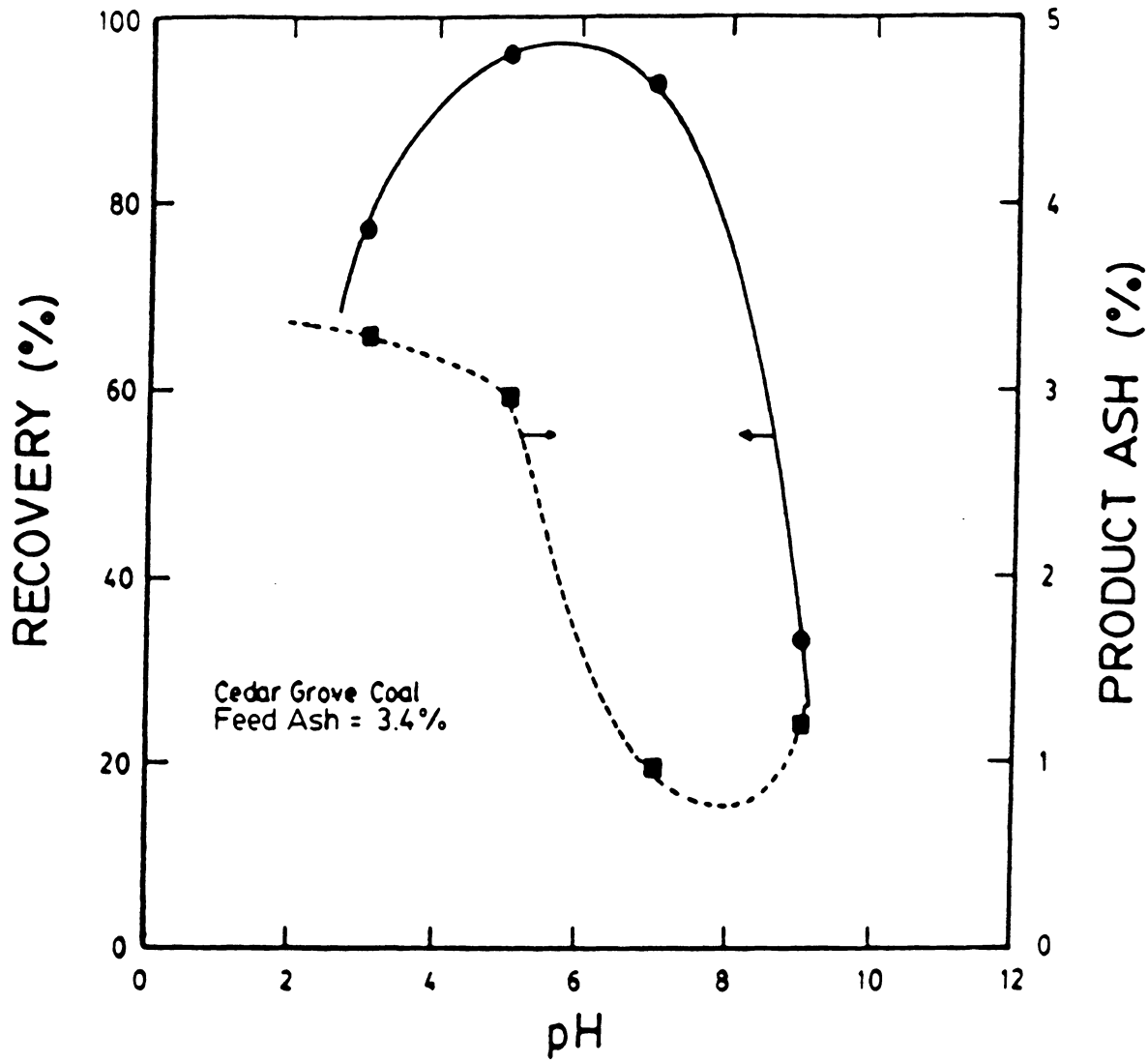

Figure 2.9 The effect of pH on coal recovery and product ash percent for the Upper Cedar Grove coal seam containing 3.4% ash in tap water using 8 cleaning stages.

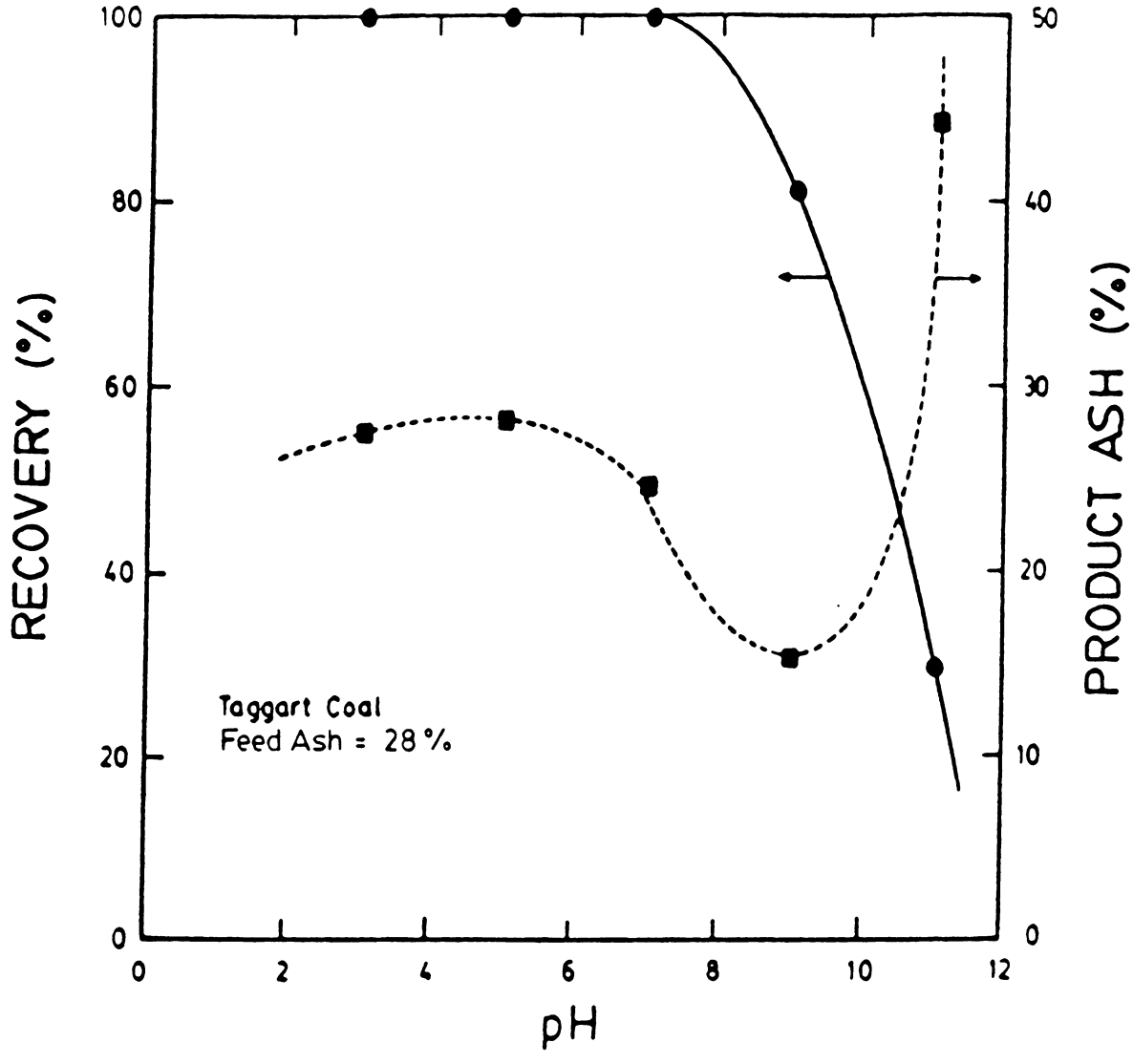

Figure 2.10 The effect of pH on coal recovery and product ash percent for the Taggart coal seam containing 28.0% ash in tap water using 3 cleaning stages.

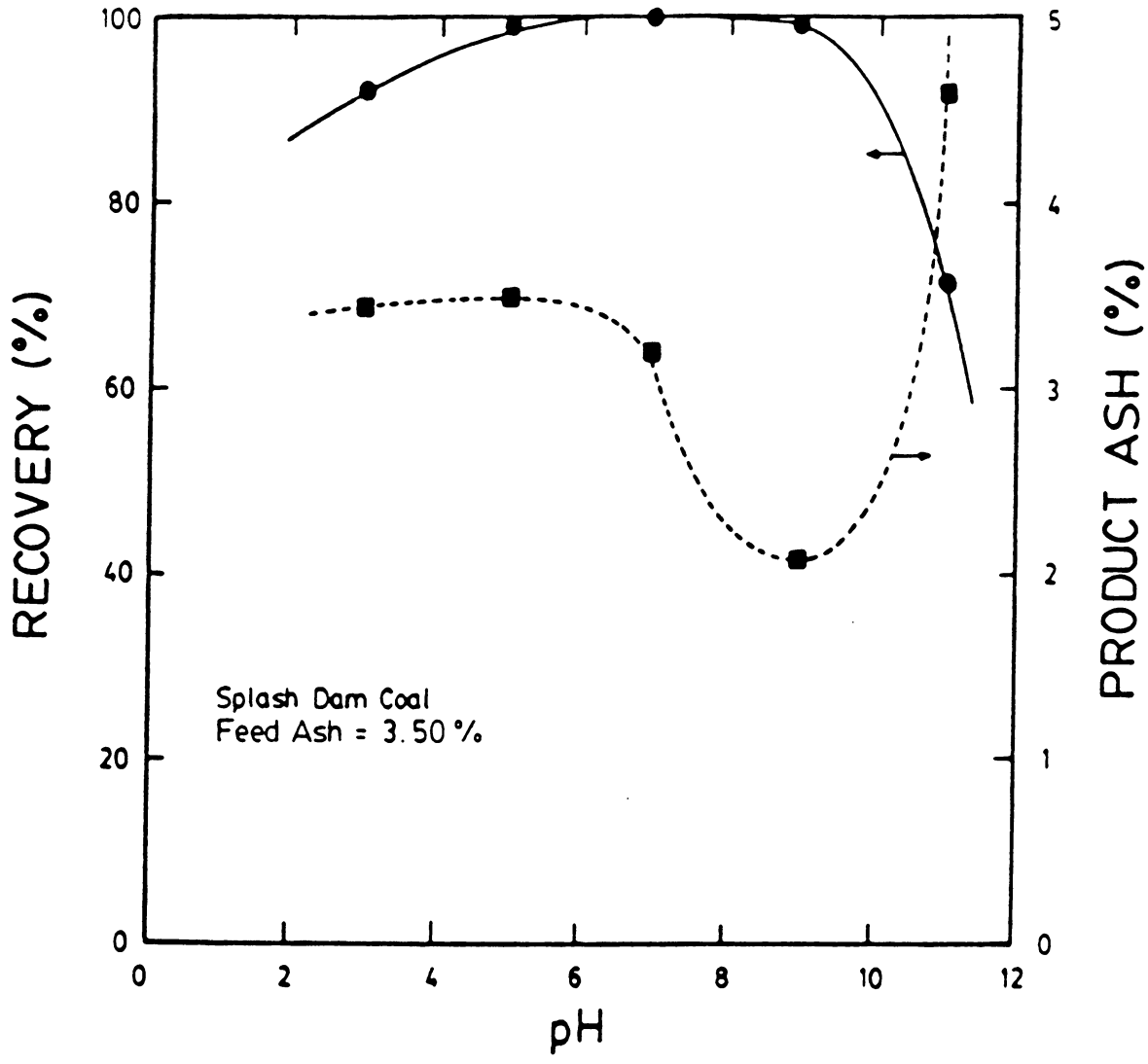

Figure 2.11 The effect of pH on coal recovery and product ash percent for the Splash Dam coal seam containing 3.5% ash in tap water using 3 cleaning stages.

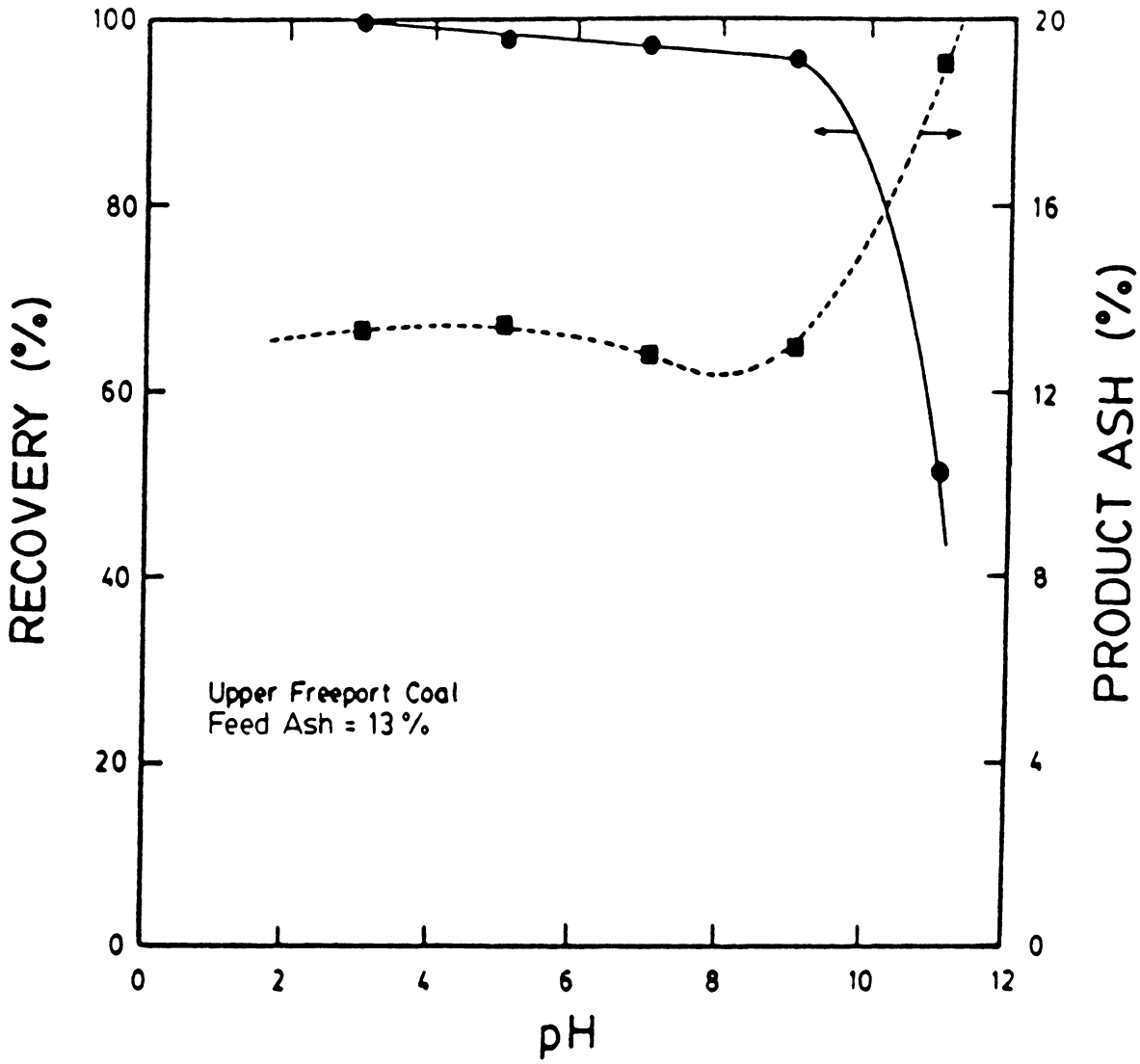

Figure 2.12 The effect of pH on coal recovery and product ash percent for the Upper Freeport coal seam containing 13.0% ash in tap water using 3 cleaning stages.

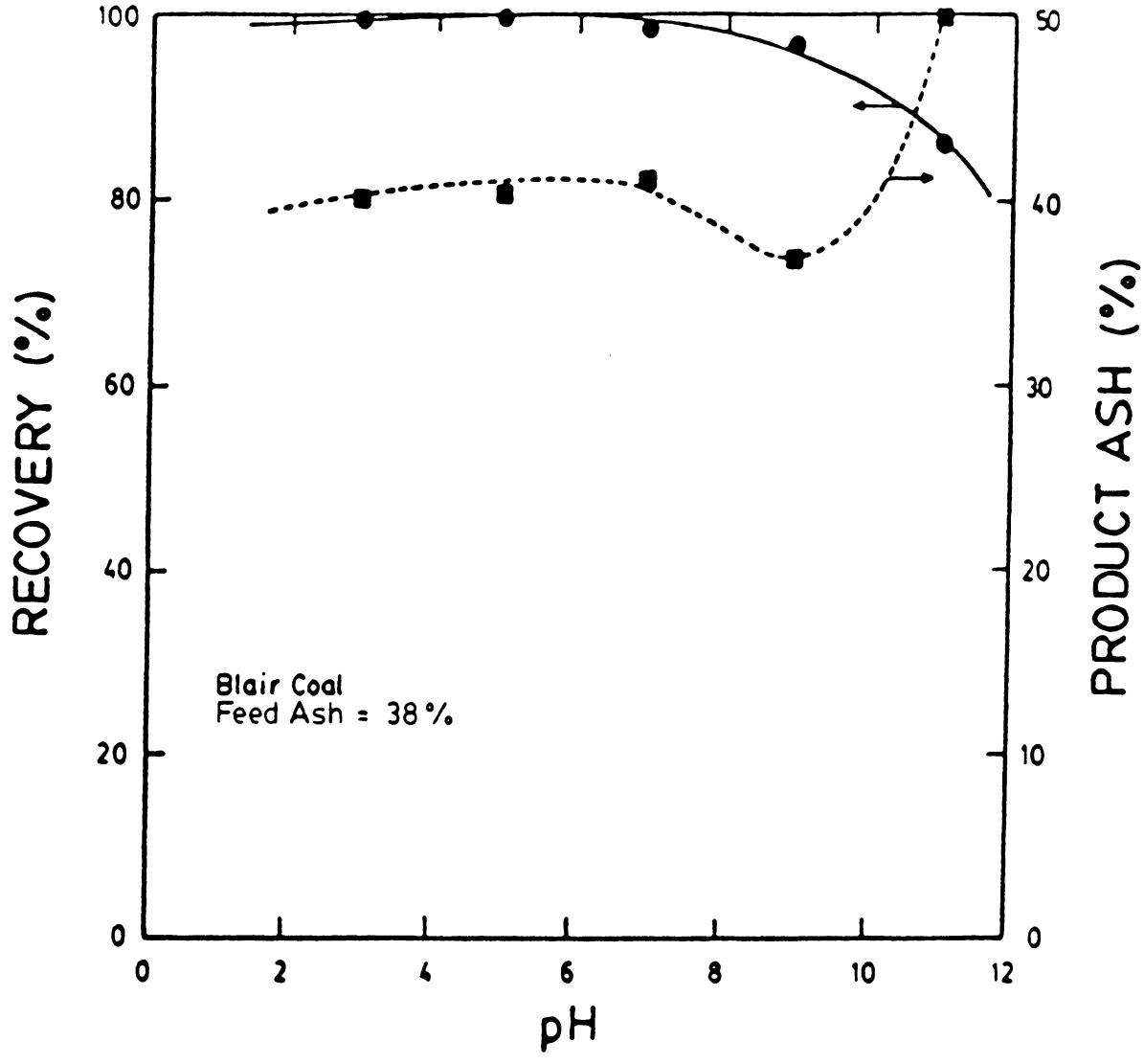

Figure 2.13 The effect of pH on coal recovery and product ash percent for the Blair coal seam containing 38.0% ash in tap water using 3 cleaning stages.

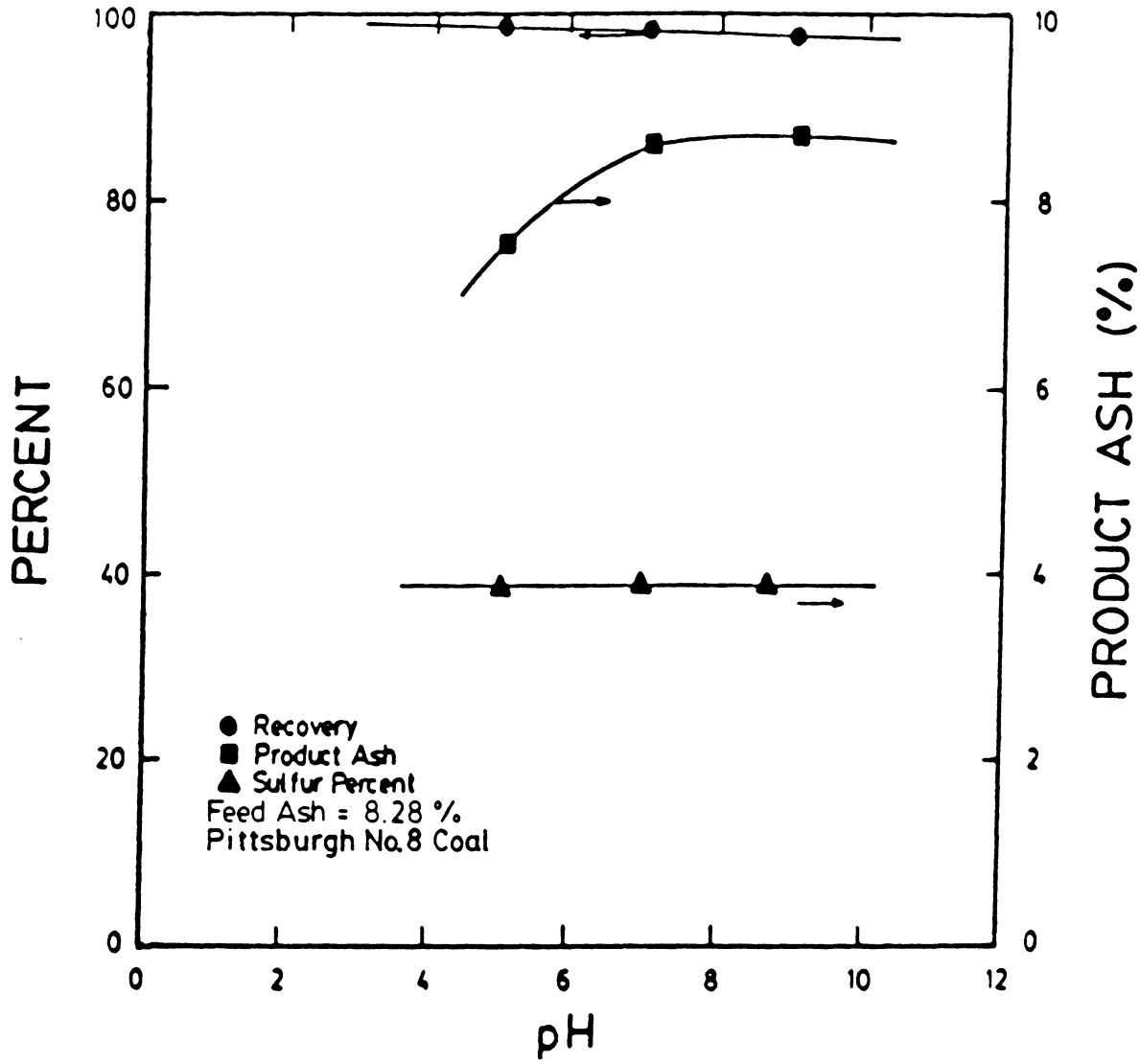

Figure 2.14 The effect of pH on coal recovery and product ash percent for the Pittsburgh No.8 coal seam containing 8.28% ash in tap water using 3 cleaning stages.

selectivity. The Pittsburgh No. 8 coal sample, which contained more than 2% pyritic sulfur, was a typical example (Figure 2.14). Figure 2.15 is a plot of separation efficiency versus pyritic sulfur content of the various non-oxidized feed coal samples studied. This plot shows a linear decrease in separation efficiency with an increase in the amount of pyritic sulfur present in the feed.

Coal recovery, product ash content, and separation efficiency results for the various coal seams studied are summarized in Table 2.2. In this case, separation efficiency is defined as coal recovery in the product minus ash recovery in the product.

2.3.2 Effect of Ions

When distilled water was used as the medium instead of tap water, the effective pH range was shifted toward the alkaline side, as shown in Figure 2.16. The upper pH limit, which existed due to a drop in recovery and an increased ash percent, remained at pH 9. Therefore, the optimum pH range for a medium of tap water and distilled water was found to be 7-9 and 8-9, respectively. However, the minimum product ash percent value and the corresponding coal recovery percent were approximately the same between

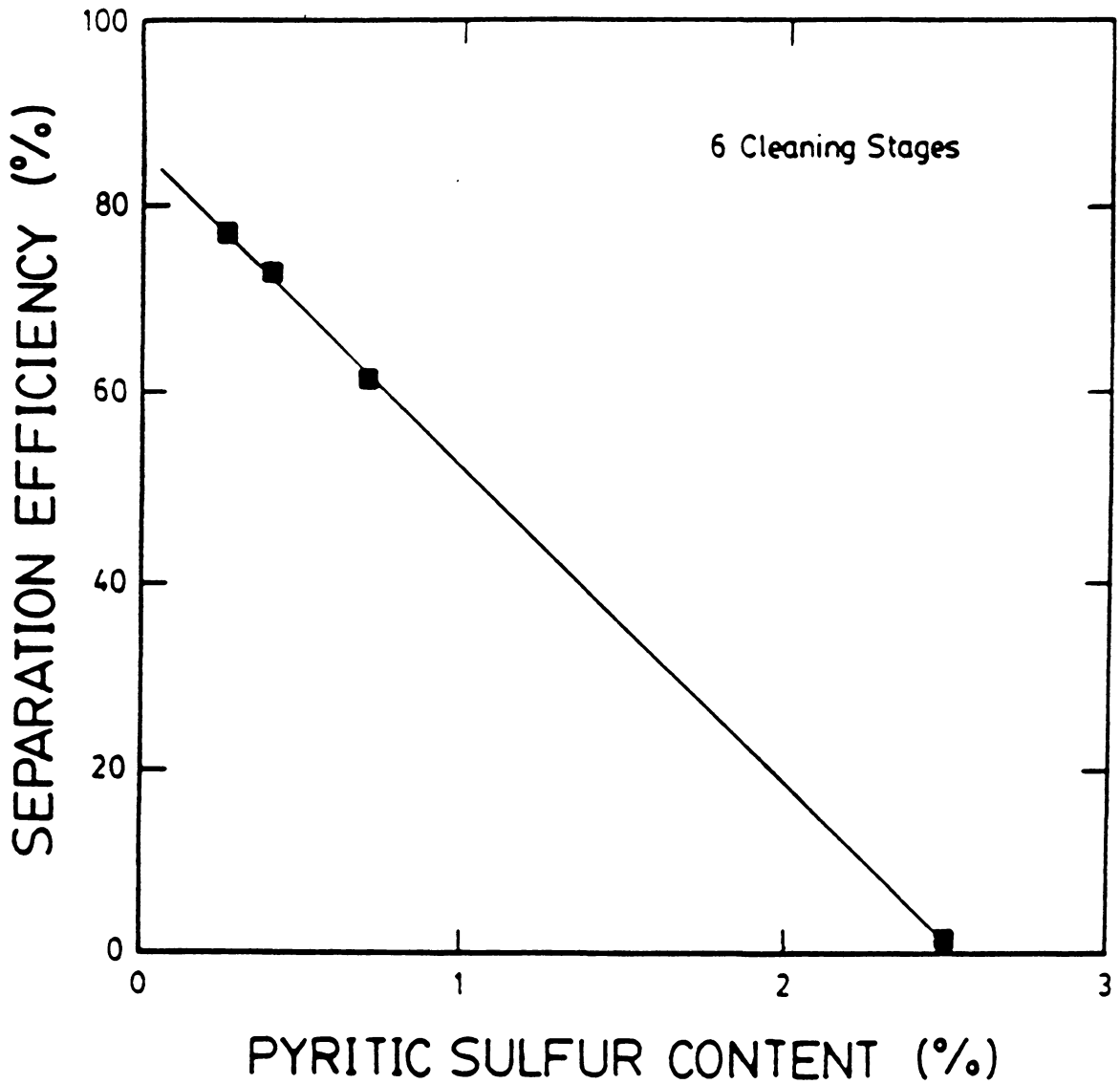

Figure 2.15 The effect of pyritic sulfur content in the feed coal sample on separation efficiency.

Table 2.2 : Tabulated Results for Various Coal Seam Samples

COAL SAMPLE	CLEANING STAGES	FEED ASH (%)	PRODUCT ASH (%)	COMBUSTIBLE RECOVERY (%)	SEPARATION EFFICIENCY (%)
Upper Cedar Grove	6	24.0	5.13	89.24	72.74
Upper Cedar Grove	8	12.0	2.45	91.08	72.53
Upper Cedar Grove	8	3.40	0.98	92.98	66.84
Lower Cedar Grove	4	1.44	0.36	79.07	59.53
Elkhorn No. 3	6	12.0	1.14	85.25	76.83
Elkhorn No. 3	6	6.00	1.34	93.91	70.41
Taggart	3	28.0	15.34	81.15	39.36
Splash Dam	3	3.50	2.07	99.11	39.22
Blair	3	40.0	36.9	96.79	11.68
Upper Freeport	4	22.2	7.50	82.89	59.26
Upper Freeport	3	13.8	13.0	95.93	6.33
Pittsburgh No. 8	6	8.28	8.20	98.21	1.11
RL - Consol	6	5.50	1.84	90.49	61.20

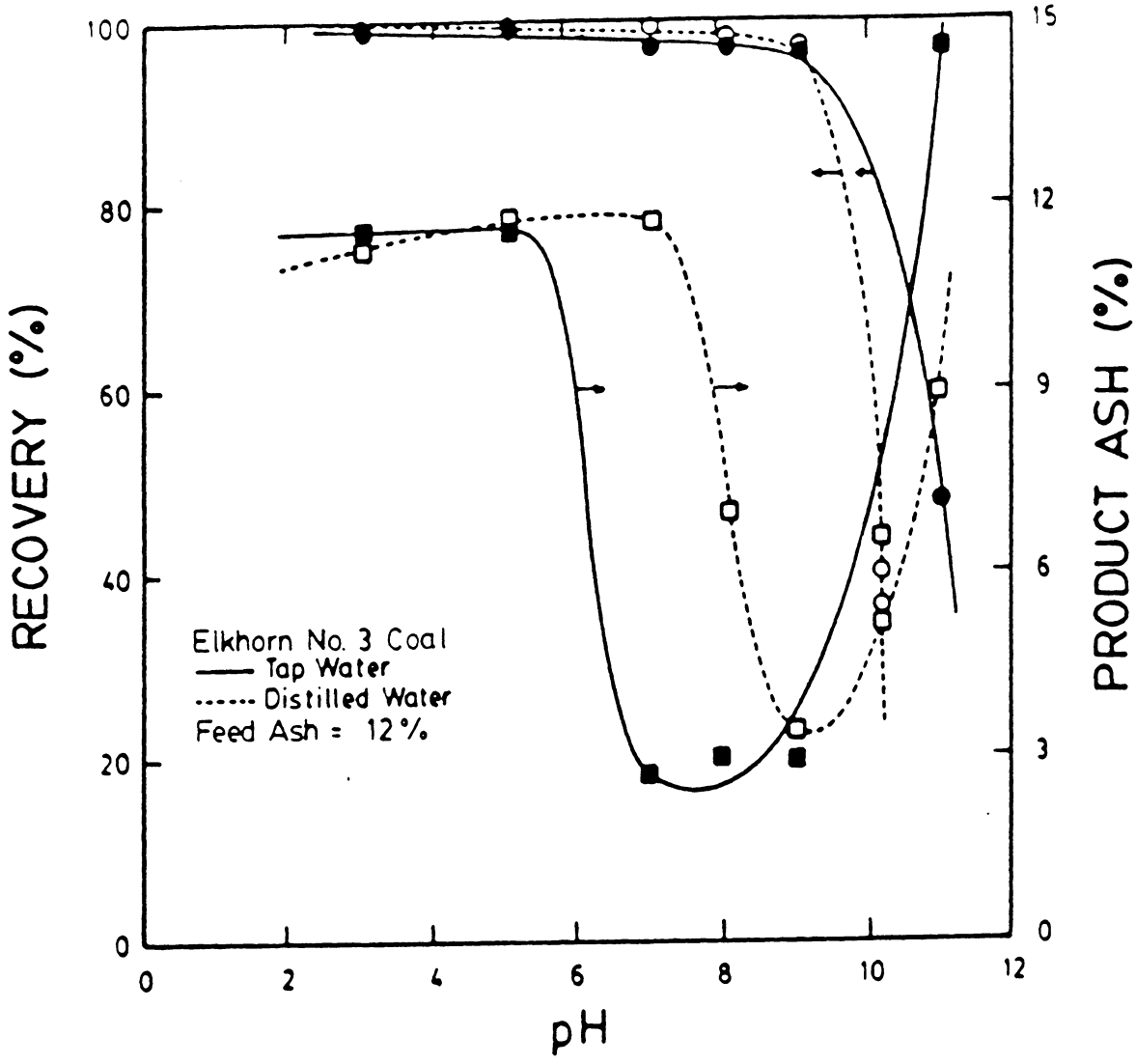

Figure 2.16 A comparison between using tap water and distilled water as the slurry medium over a range in pH for the Elkhorn No.3 coal seam using 3 cleaning stages.

the two medium types. The wider effective pH range discovered for tap water may have been caused by a stronger repulsive electrostatic charge between the coal and mineral matter particles at or near pH 7.

It was considered possible that the addition of hydrolizable cations could possibly improve the selective coagulation process due to a decrease in the zeta potential of the particulate system. Therefore, several experiments were conducted to determine the effect of hydrolizable cations in a distilled water medium. Each test consisted of 6 stages of treatment at pH 9. Approximately 10 ppm of each ion type were added to a slurry containing a micronized Cedar Grove coal sample (24% ash). The trivalent ions (i.e., aluminum and iron) improved coal recovery, but severely decreased selectivity, as indicated by the results shown in Table 2.3. There was little effect on recovery and product ash content as a result of the divalent ion (e.g., calcium, nickel, and zinc) concentration level employed.

Therefore, selective coagulation tests were conducted over a range of calcium additions. The results are shown in Figure 2.17. As shown, the critical Ca^{2+} concentration appeared to be around 25 ppm. In comparison, Schroeder and Rubin (1984) found that the critical concentration of Ca^{2+} for coal slurry stability was 8.5×10^{-4} M versus

Table 2.3 : Effect of Multivalent Cations

- Cedar Grove Seam Coal (24% ash)
- Distilled Water - 10 ppm of each ion - pH 9 - 6 stages of treatment.

MULTIVALENT ION	COMBUSTIBLE RECOVERY (%)	PRODUCT ASH (%)
Distilled Water	89.14	5.45
Calcium	89.25	5.88
Nickel	83.88	5.70
Zinc	87.20	6.18
Aluminium	94.93	16.09
Iron	95.69	14.37

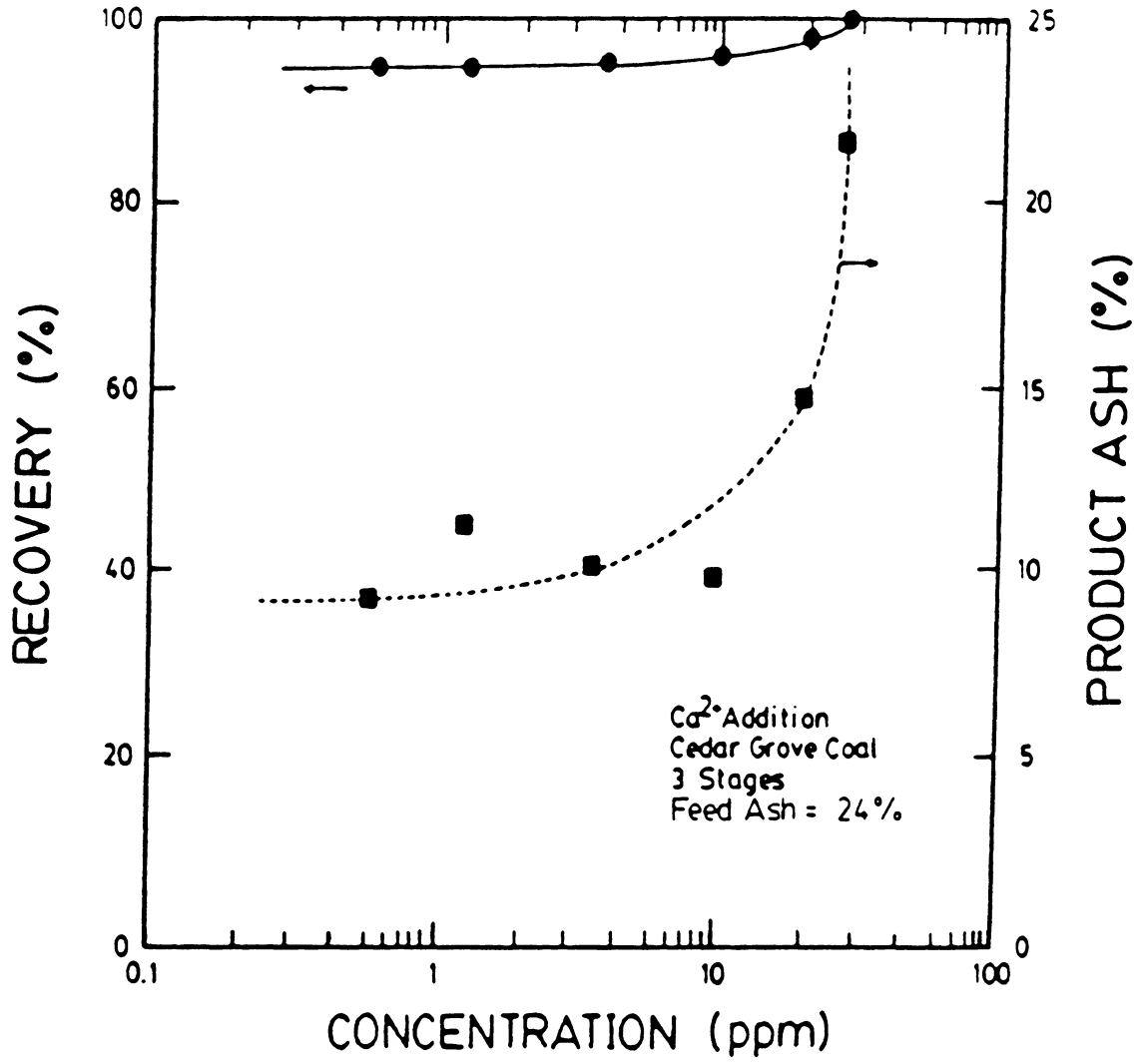

Figure 2.17 Effect of Ca^{2+} concentration on coal recovery and product ash percent using double distilled water at pH 9

6.5×10^{-4} M found in this investigation. Above this concentration, both the clean coal recovery and the product ash percent sharply increased. The increases were probably a result of homocoagulation and heterocoagulation between the coal and ash particles, due to a decrease in their surface potentials while in the presence of specifically adsorbing ions. Below the critical concentration, recovery and product ash remained relatively constant. Therefore, the presence of specifically adsorbing ions seemed to only hinder the process efficiency.

The results of experiments conducted to compare the effects of mediums having a low Ca^{2+} concentration with a pure distilled water medium are plotted in Figure 2.18. These results further showed that cation concentrations below the critical value have little effect on coal recovery and product ash percent.

2.3.3 Effect of the Grinding Environment

A major problem in mineral processing plants is the wear of the equipment due to abrasion and impact from the mineral, especially during grinding. The worn material contributes to the concentration of ash material in the feed slurry and cations, such as iron, in the medium.

Test results which illustrate the effect of grinding wear are shown in Figures 2.19-2.22 for a Cedar Grove coal

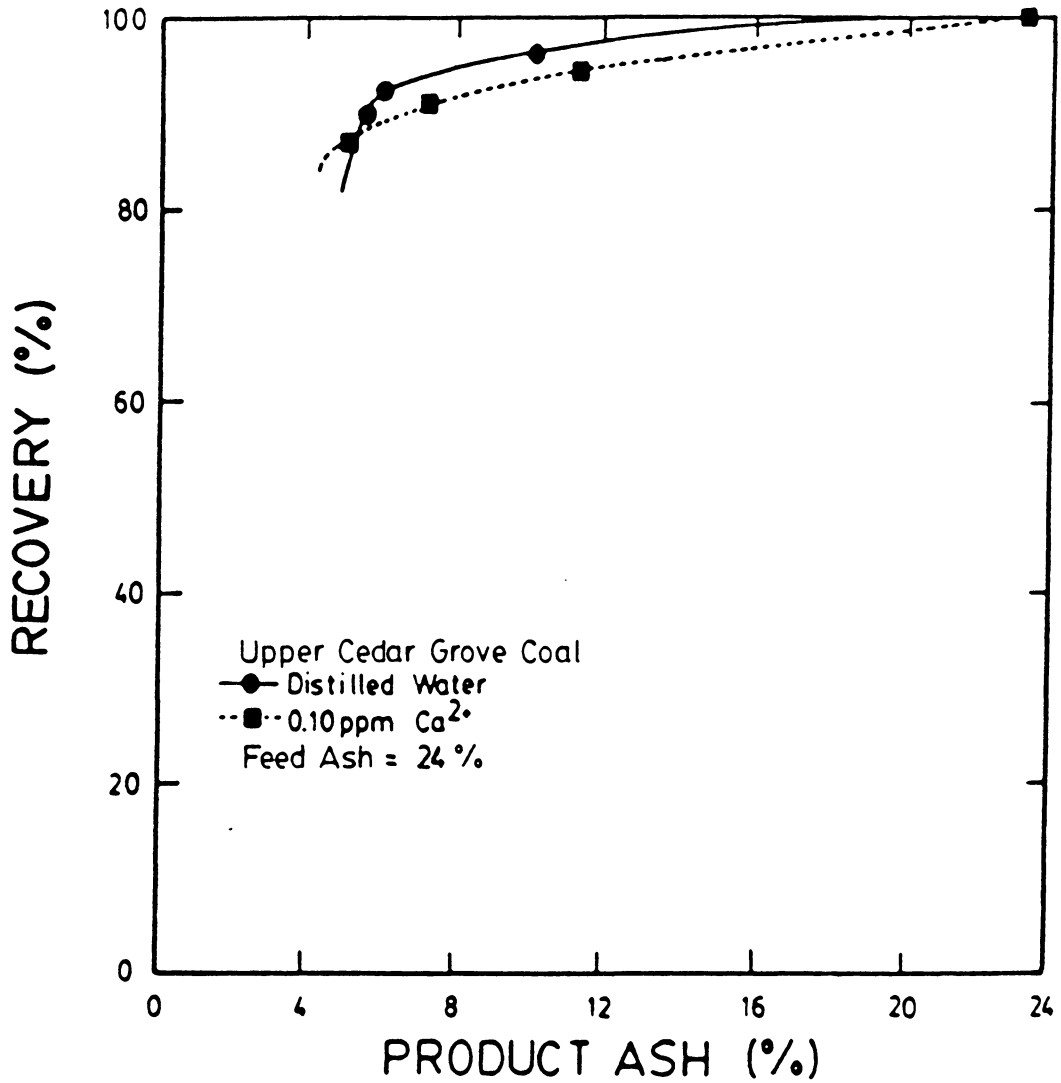

Figure 2.18 Effect of a small Ca^{2+} concentration on coal recovery and product ash percent.

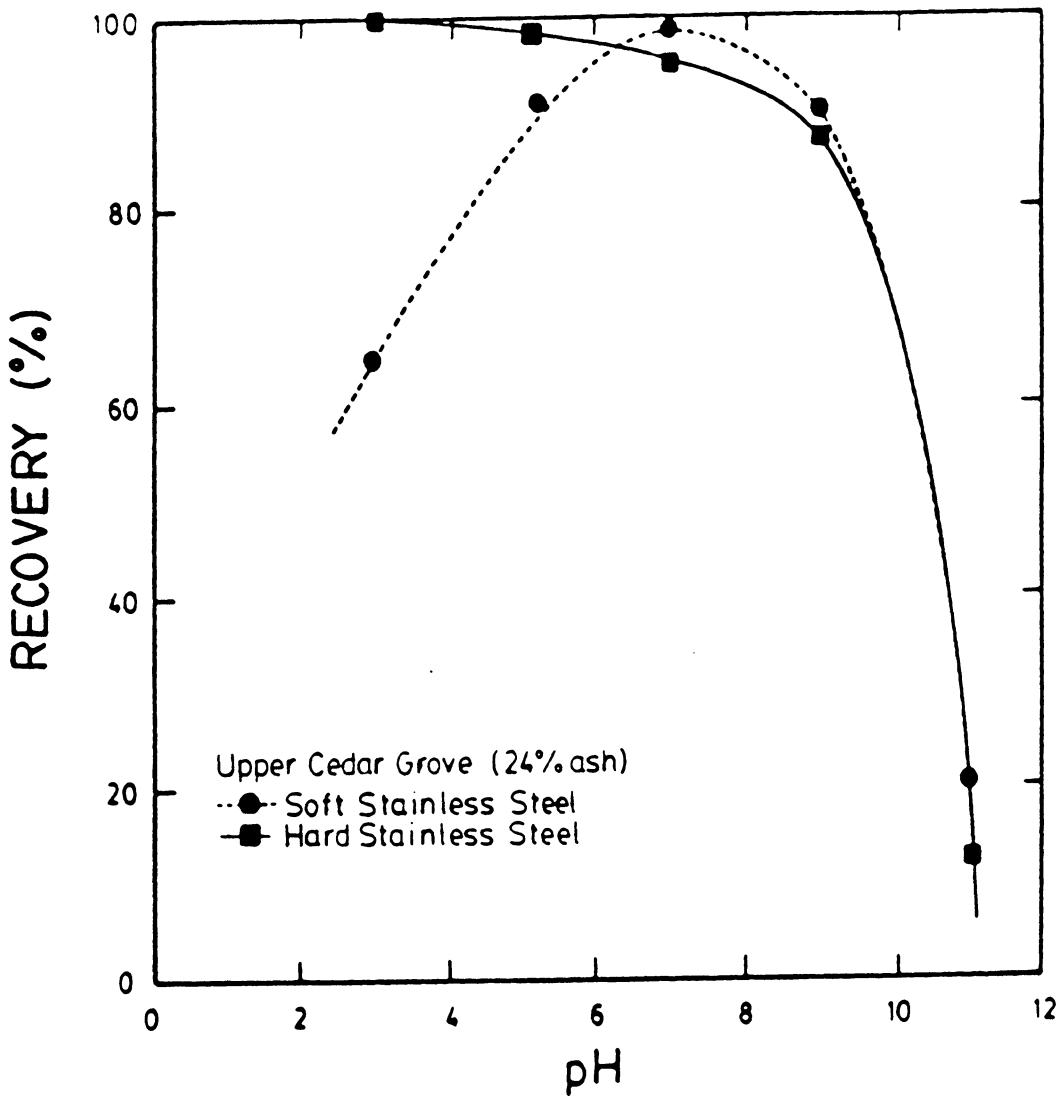

Figure 2.19 Effect of pH on coal recovery when using soft and hard grinding media.

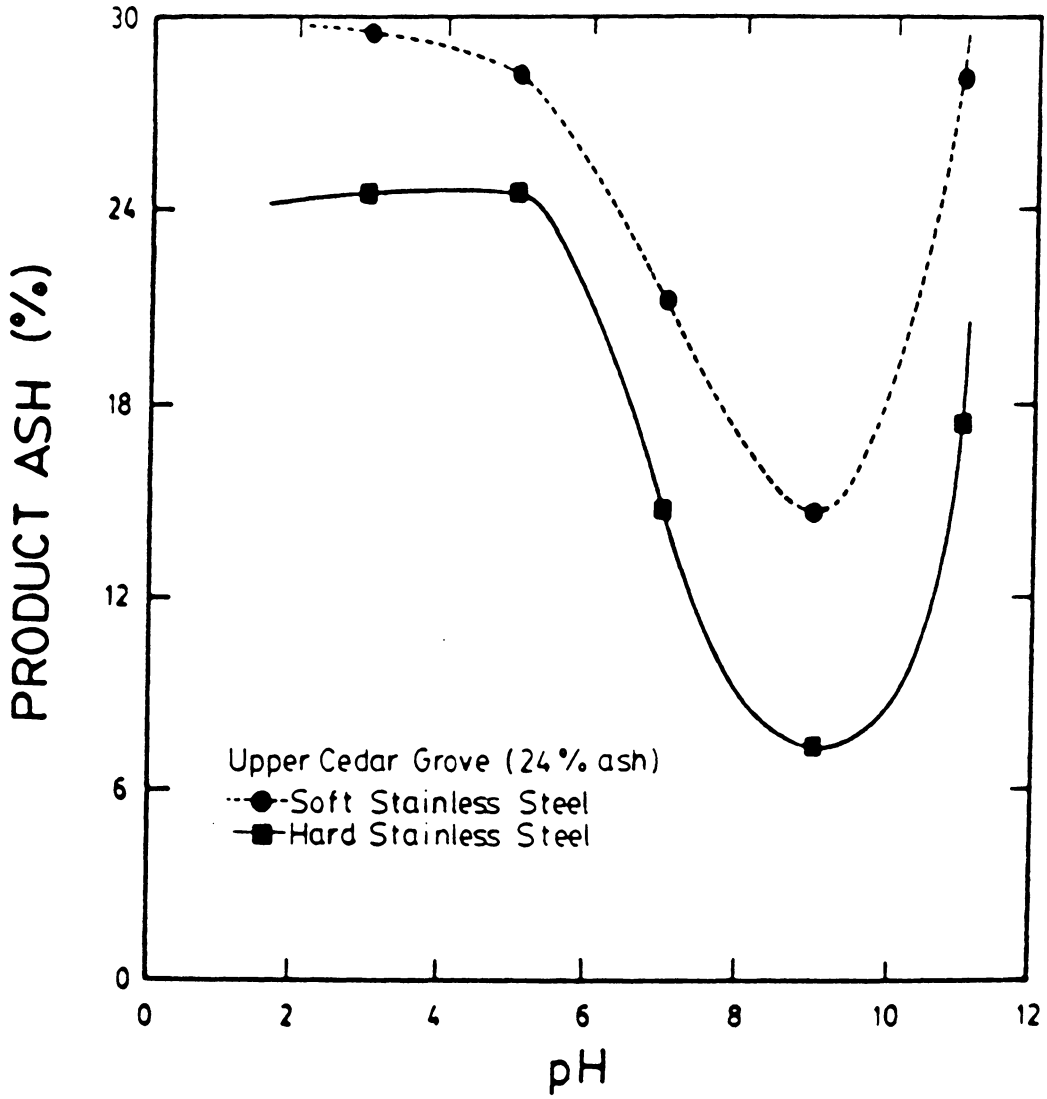

Figure 2.20 Effect of pH on product ash percent when using soft and hard grinding media.

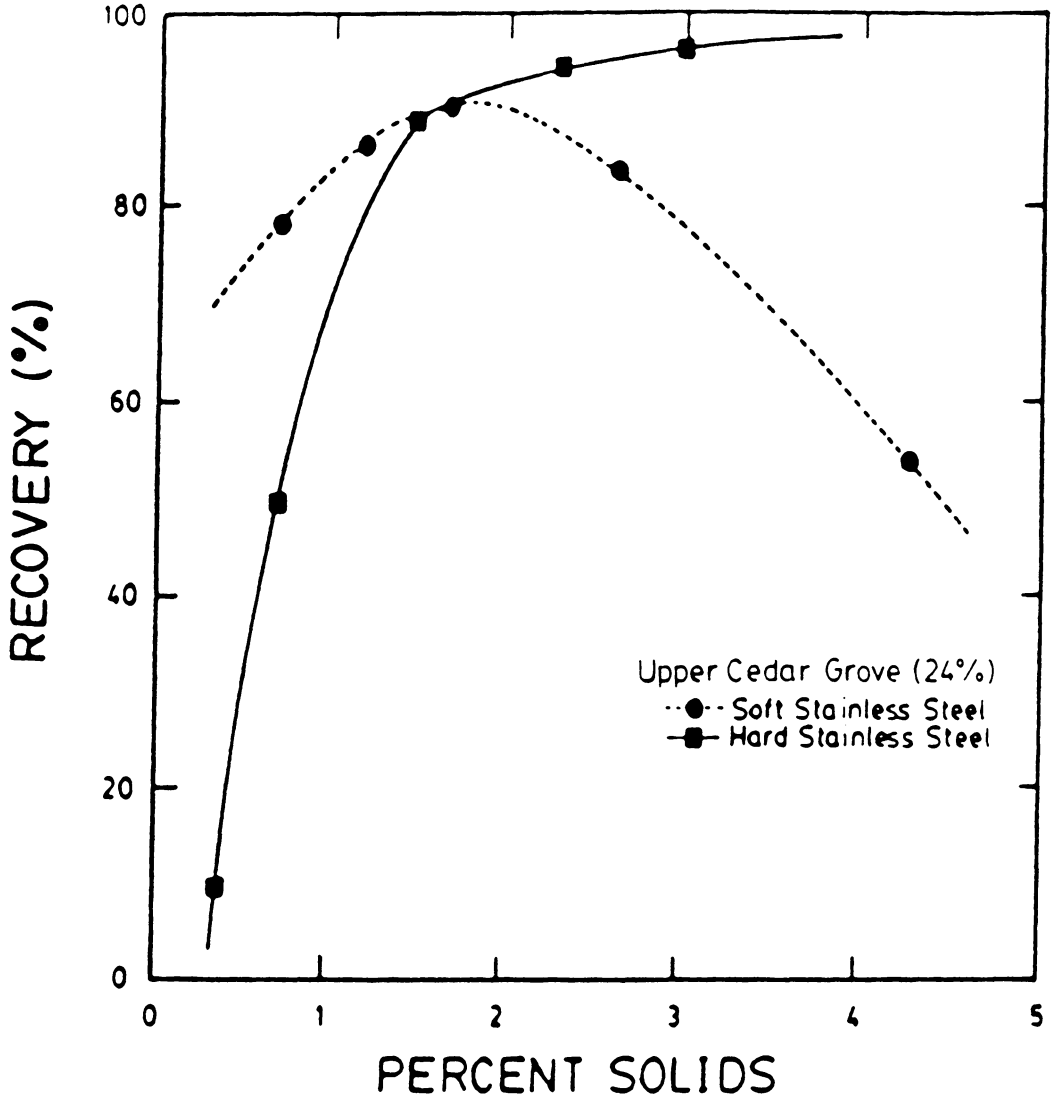

Figure 2.21 The effect of the grinding environment on recovery.

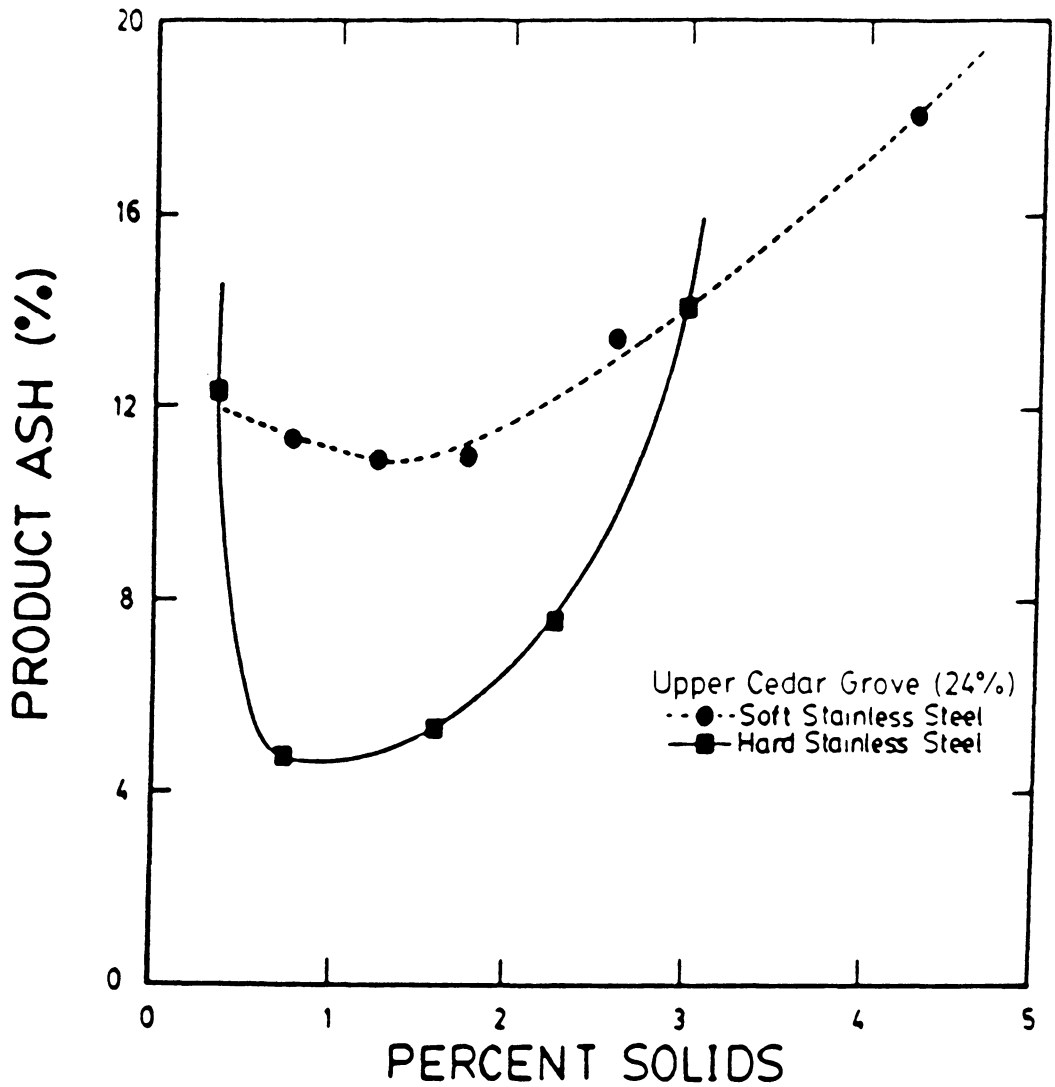

Figure 2.22 The effect of the grinding environment on product ash percent.

sample (24% ash). Results obtained using soft stainless steel media in a laboratory attrition mill were compared with those obtained using hard stainless steel in a smaller laboratory attrition mill. Figures 2.19 and 2.20 are plots showing the effect of pH on clean coal recovery and product ash percent using the different media. In the alkaline region, recovery remained unchanged. However, recovery significantly dropped in the acidic range. This could have been caused by a significant decrease in the surface charge of the particles containing mineral matter due to the adsorption of ferric or ferrous ions. Therefore, the heterocoagulation between the coal and mineral matter particles decreased, hence decreasing the coal recovery. Product ash percent followed the same trend throughout the pH range studied, although the mill containing the soft stainless steel had 6-7% more ash. Figures 2.21 and 2.22 depict a similar comparison using percent solids as the variable instead of pH. Similar trends were found between the two grinding environments, although the product ash percent was higher for the mill consisting of soft stainless steel. The increase in product ash percent in both cases was due to the increase in the feed ash percent caused by the worn material.

2.3.4 Effect of Kerosene Addition

For coal particles having a partially hydrophillic surface, the addition of a hydrocarbon may be needed to enhance the hydrophobicity of the surface. Figure 2.23 illustrates the effect of adding kerosene on clean coal recovery and product ash percent using an Elkhorn No. 3 coal sample (5.5% ash). A small kerosene addition of 3-5 lb/ton decreased the product ash from 2% to 1.25%. However, recovery also dropped from 92% to 81%. Additional amounts above 5 lb/ton showed no improvement in selectivity or coal recovery. The decreases in both recovery and product ash may have been caused by an increase in the electrostatic repulsion force between coal particles due to the oil coating (Hale, 1987). However, tests using an Upper Freeport coal sample found that lower ash values can be obtained at higher recoveries if a small amount of kerosene is used. This result is depicted in the plot shown in Figure 2.24, which compares the addition of 1 lb/ton to no addition using coal recovery/product ash curves. Therefore, the addition of small quantities of a fuel oil may be beneficial for improving the selective coagulation process, especially for partially oxidized coals.

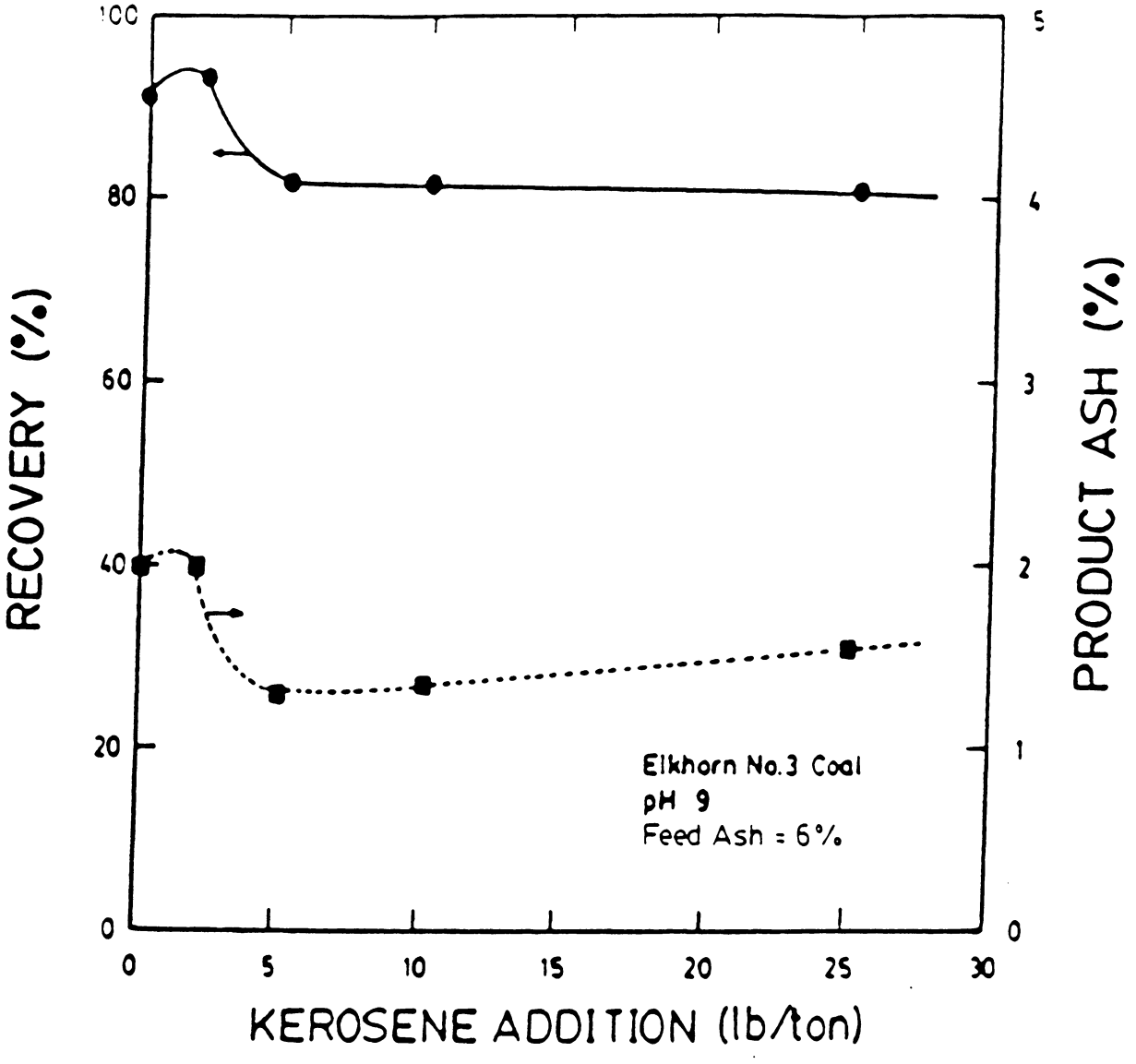

Figure 2.23 The effect of kerosene addition on coal recovery and product ash percent for the Elkhorn No.3 coal seam.

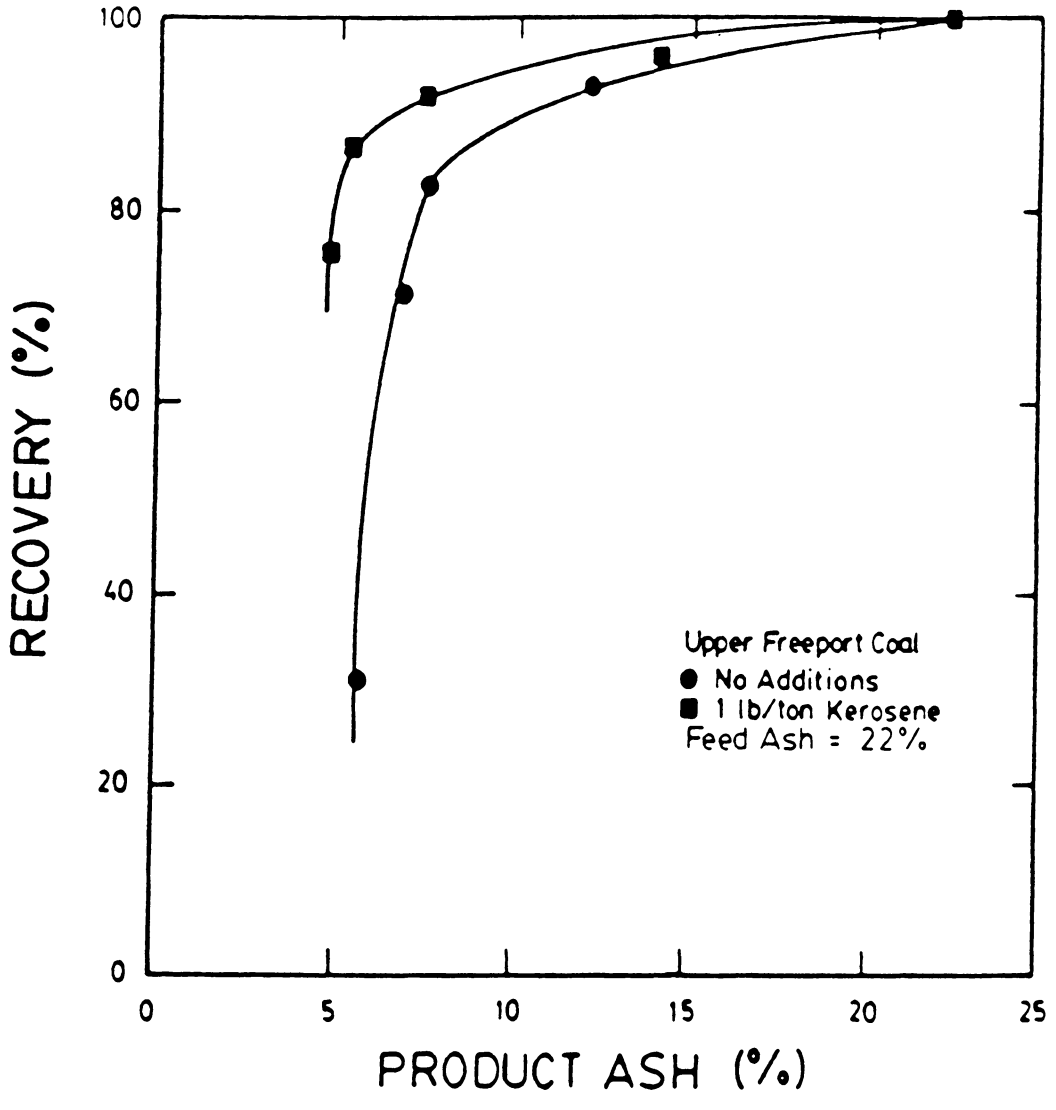

Figure 2.24 The effect of adding 1 lb/ton of kerosene on coal recovery and product ash percent for the Upper Freeport coal seam.

2.3.5 Electrokinetic Study on Coal

The zeta potentials of the Elkhorn No. 3 and Cedar Grove coal samples were determined as a function of pH in distilled water and plotted in Figures 2.25 and 2.26, respectively. The Elkhorn No. 3 clean coal particles exhibited an isoelectric point (iep) of 5.8. Above or below 5.8, the zeta potential increased fairly rapidly. The iep of the mineral matter appeared to be approaching 2. The charge of the mineral matter remained negative throughout the pH range studied. The zeta potential leveled out at approximately -40 mV in the alkaline pH range. The iep of the Cedar Grove clean coal was found to be at a pH of 7.2, whereas the iep of the mineral matter was determined to be around 2.8. The magnitude of the zeta potentials for this coal was larger than for the Elkhorn No. 3 coal, although similar trends were found for both the coal and ash curves.

Figure 2.27 is a plot of zeta potential versus pH for a Pittsburgh No. 8 seam coal which was taken from published literature (Arnold and Aplan, 1986). The results indicated an iep for the clean coal of around 5 in tap water. Below the iep, the increase in the potential of the coal particles was small. There was a very narrow difference found between the zeta potentials of the coal and ash particles.

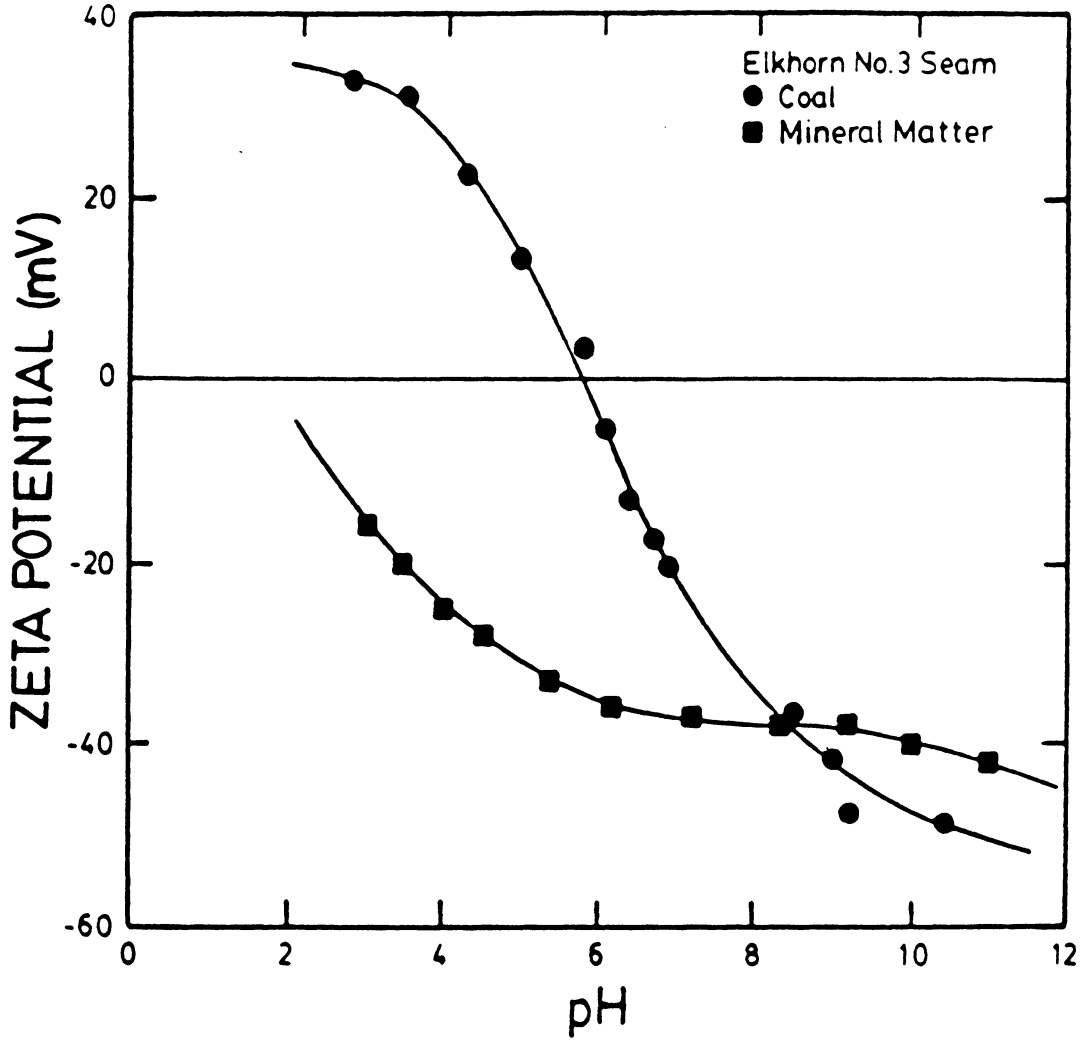

Figure 2.25 Zeta potential measurements over a range in pH for Elkhorn No.3 coal and mineral matter in distilled water.

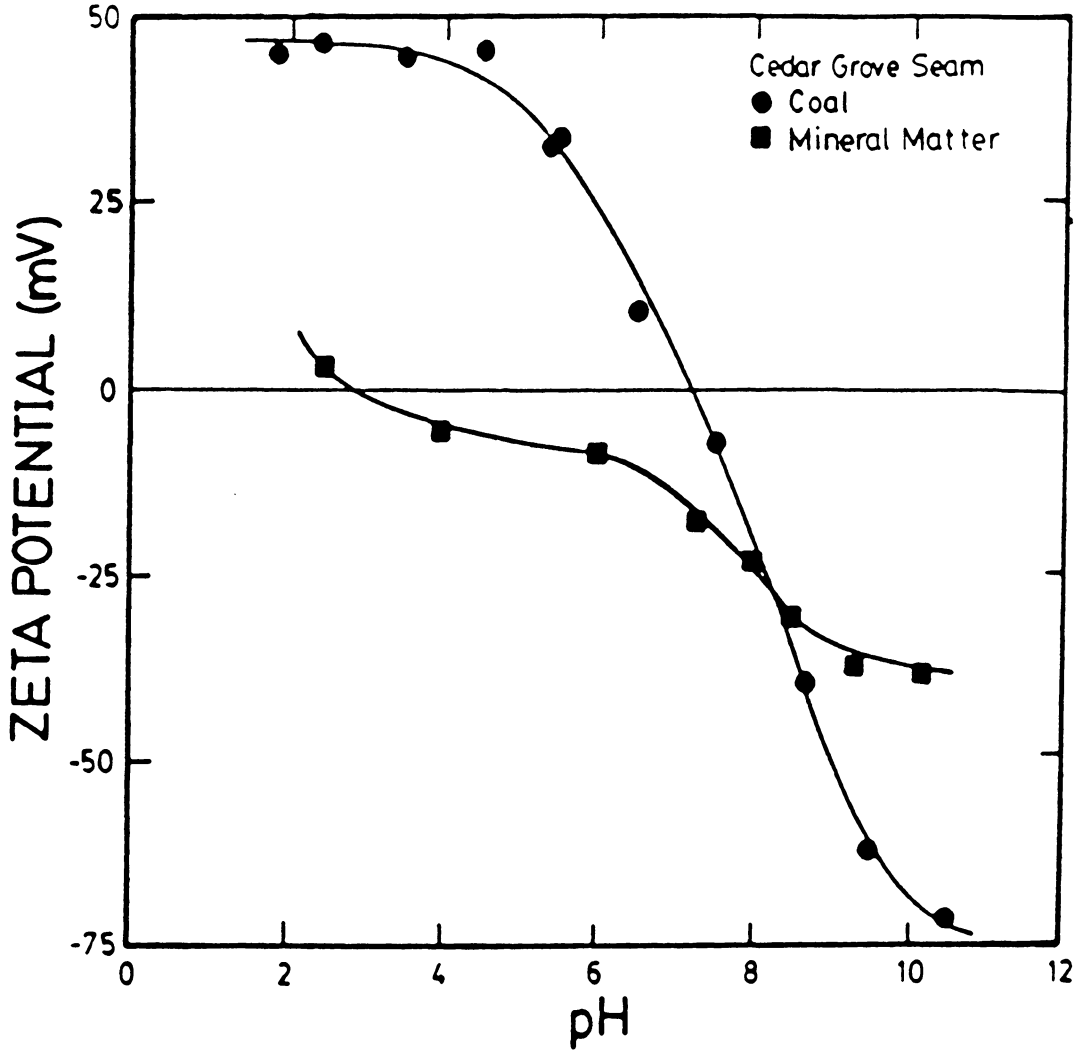

Figure 2.26 Zeta potential measurements over a range in pH for Upper Cedar Grove coal and mineral matter in distilled water.

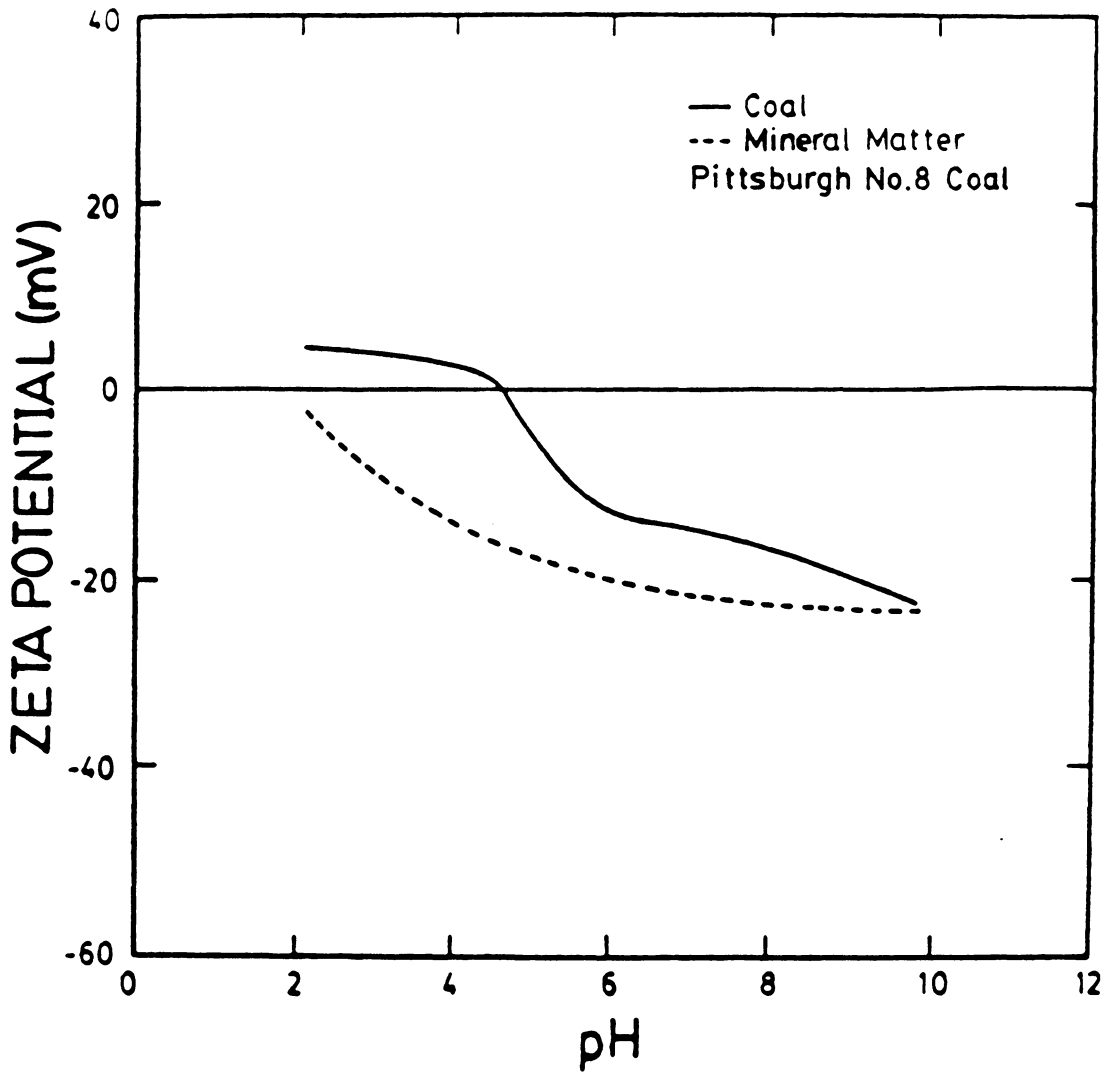

Figure 2.27 Zeta potential measurements over a range in pH for Pittsburgh No.8 coal and mineral matter in tap water.

Zeta potential measurements were also obtained for the Elkhorn No. 3 coal sample in the presence of tap water. Figure 2.28 shows the comparison between a coal suspension using tap water and distilled water as the media. The iep shifted from 5.8 for a distilled water system to 4.0 for a tap water system. Also, the magnitude of the zeta potentials was smaller for the tap water medium. This difference illustrated the effect of the specific adsorption of ions present in the tap water. The decrease in the iep and in the zeta potentials when using tap water was also found by Arnold and Aplan (1986). The zeta potentials of the ash particles also decreased in negativity for slurries consisting of tap water, especially in the alkaline pH region.

From Figure 2.29, calcium addition was found to decrease the negative charge of the coal particles above the iep and slightly increased the positive charge below the iep. Similar results were reported by Arnold and Aplan (1986). Calcium addition was also found to decrease the negative charge of the ash material, as shown in Figure 2.30.

2.4 Discussion

In the foregoing section, it was illustrated that coal can be efficiently cleaned using the selective-shear

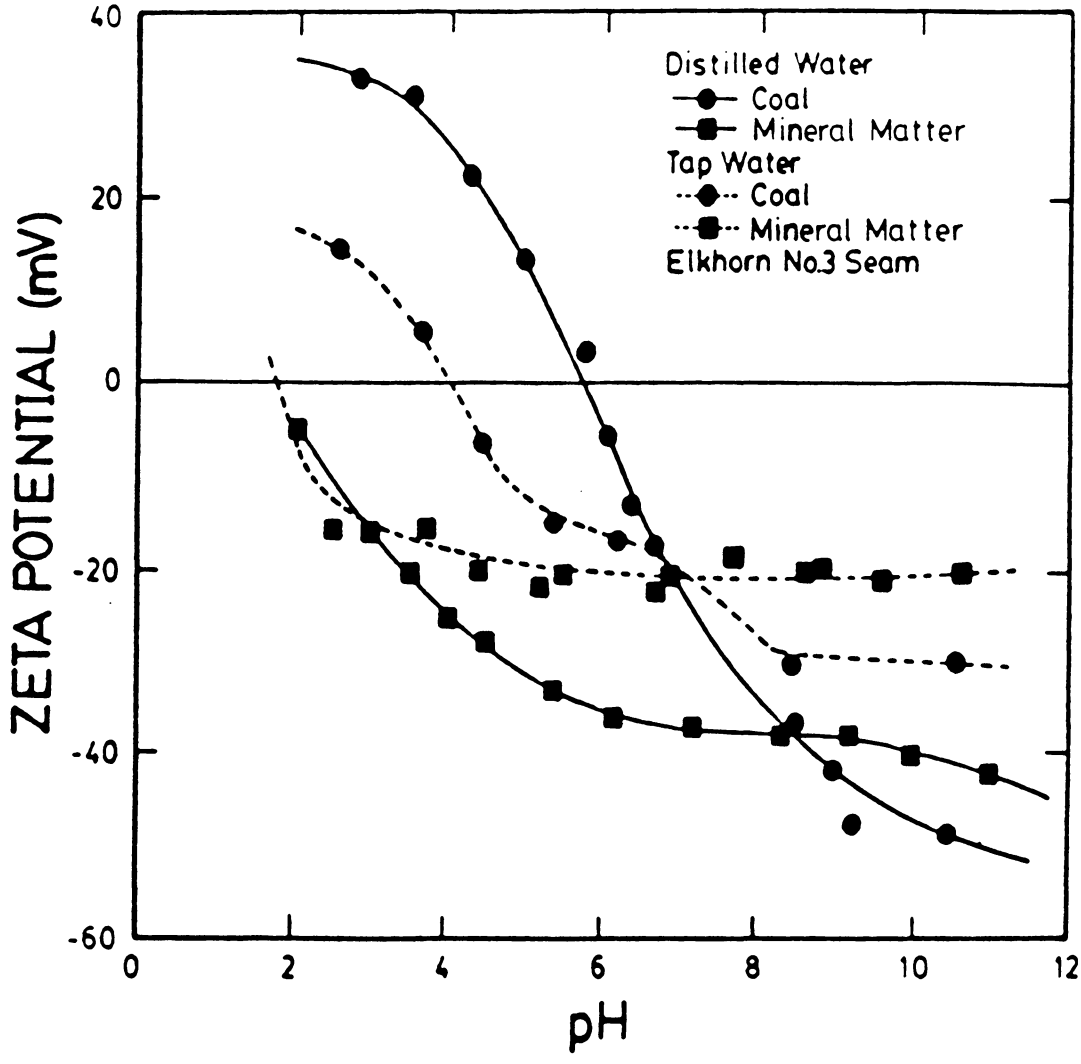

Figure 2.28 A comparison of zeta potential measurements over a range in pH between tap water and distilled water mediums.

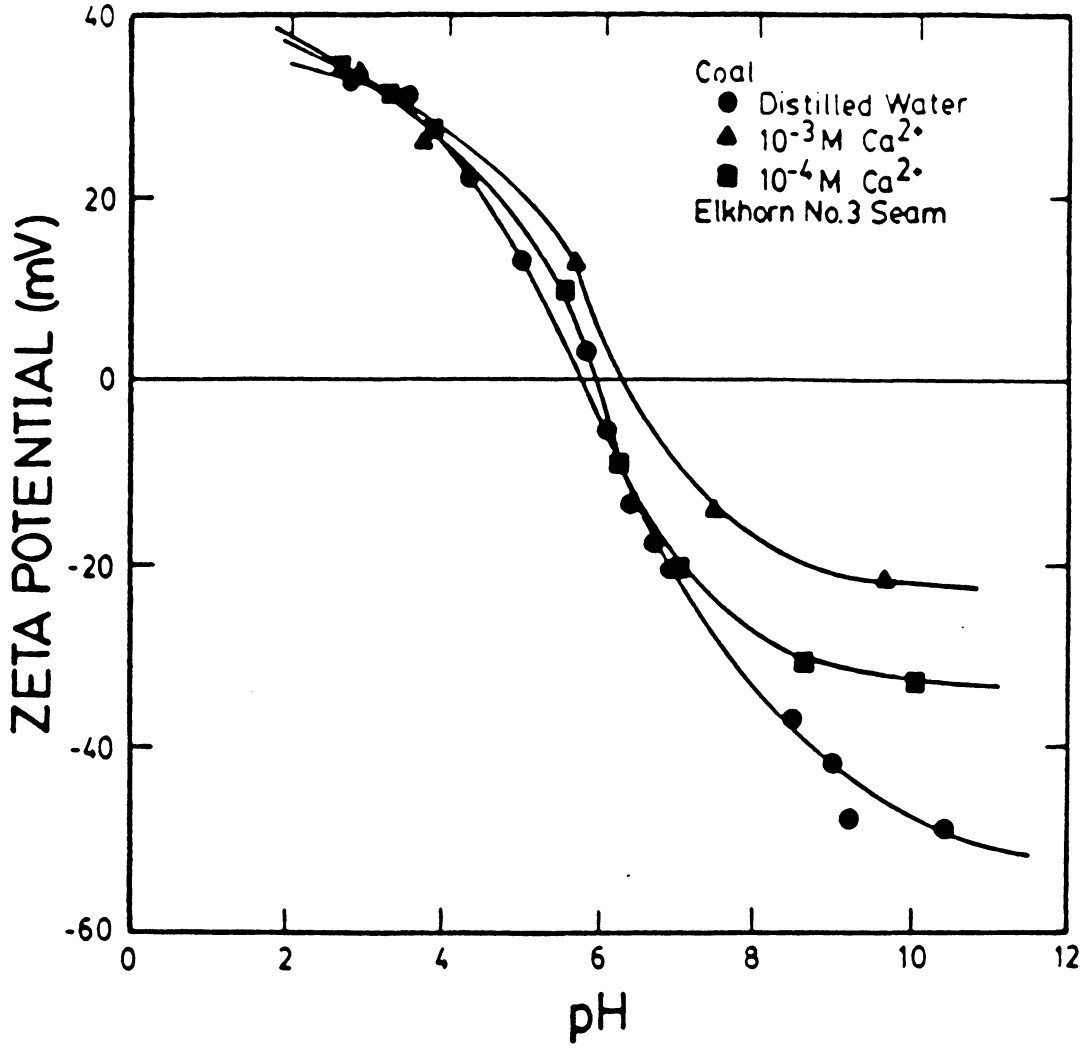

Figure 2.29 The effect of calcium additions on the zeta potentials of coal.

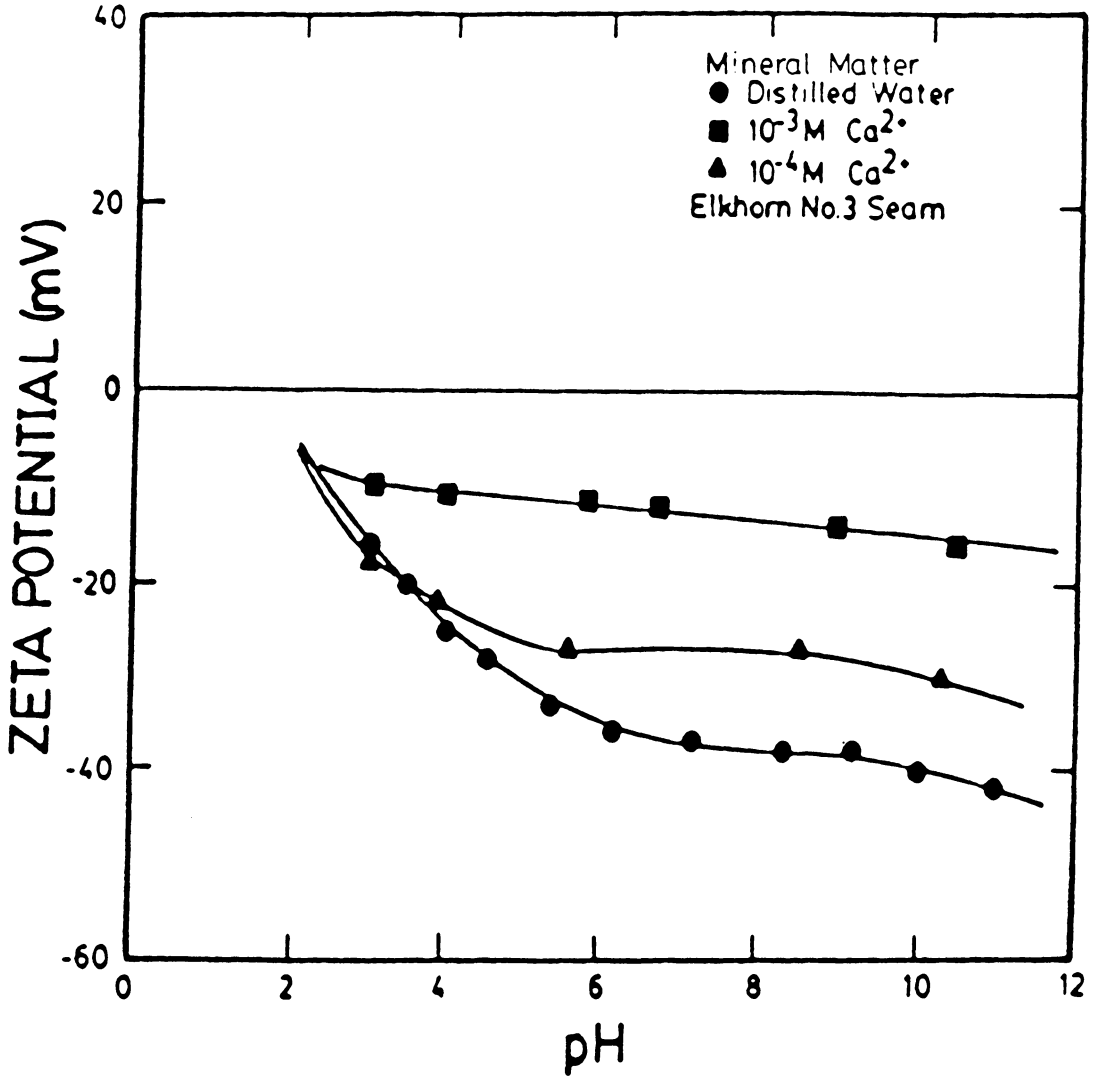

Figure 2.30 The effect of calcium additions on the zeta potentials of mineral matter.

coagulation (SSC) process. The selectivity of the process was accomplished by adjusting the surface potential of the coal and ash particles through pH control, and improving the hydrophobicity of the coal, if needed, using a fuel oil such as kerosene. The addition of specifically adsorbing ions, such as Ca^{2+}, to decrease the surface potential was found to decrease the selectivity of the process. Using distilled water instead of tap water as the slurry medium, decreased the pH range applicable for efficient separation of the coal and ash particles.

In order to understand the effect of pH and the basic principles of the process, zeta potential measurements were performed on the Elkhorn No. 3 seam coal (12% ash) using distilled water, as presented in the previous section (Figure 2.25). The results showing the effect of pH on recovery and selectivity (Figure 2.16) were combined with the zeta potential plot of Figure 2.25. The result was a zeta potential versus pH plot (Figure 2.31) divided into three zones of varying process performance.

The first zone represents high coal recovery and product ash percent and covers the pH range up to 8. This result was probably due to heterocoagulation and homocoagulation between the coal and ash particles. Below 5.8, heterocoagulation was due to the attracting surface charges between the coal and mineral matter particles.

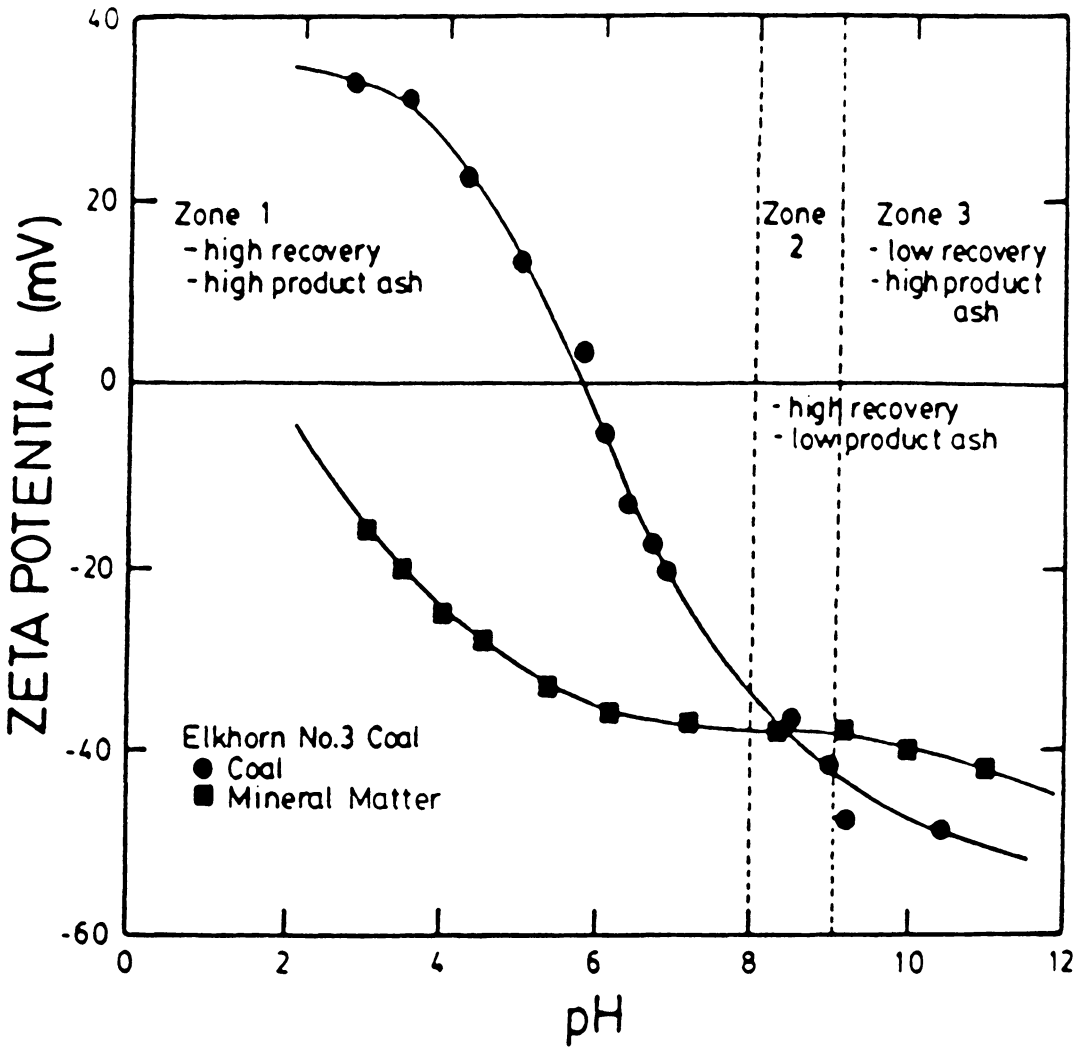

Figure 2.31 A comparison of process performance and zeta potential measurements over a range in pH - distilled water.

Homocoagulation of the coal particles ocurred due to their hydrophobic nature, whereas coagulation of the mineral matter was due to the attractive electrostatic force between the clay edges and the other mineral matter particles. However, between 5.8 and 8, the signs of the potentials were the same.

Derjaguin and his co-workers (Usui, 1984) found that for the case of two particles having the same surface potential sign but at different magnitudes, the force of interaction changes from repulsion to attraction after passing through a maximum. This is caused by an induced charge at a small separation distance on the particle having the lower surface potential, hence reversing the sign of the charge and forming an attractive electrostatic force between the two particles. Figure 2.32 is a plot of the electrostatic force component of the interaction energy between two particles of varying surface potentials versus twice the separation distance between the particles. A positive energy value represents a repulsive interaction and a negative value an attractive interaction. The plot depicts that as the difference between the surface potentials of two particles becomes smaller, the more repulsive or less attractive the electrostatic interaction energy becomes. This theoretically obtained plot was based on what is now known as the constant surface potential

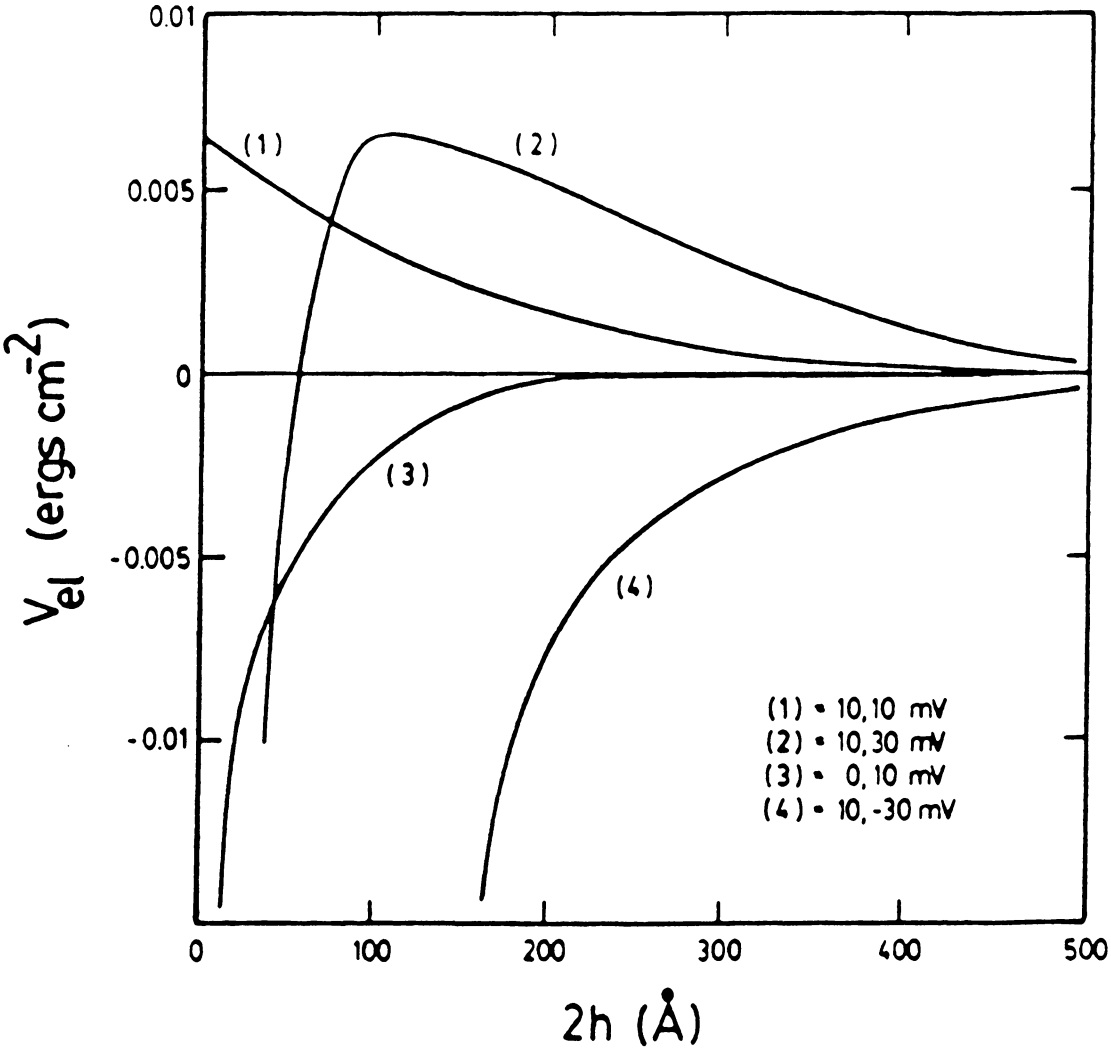

Figure 2.32 The electrostatic potential energy of interaction versus 2 times the particle-particle separation distance - c = 1 mmol/liter - 1-1 electrolyte (Usui, 1984).

model for the interaction of electrical double layers. The constant potential model, along with the constant surface charge model, represents idealized and extreme situations. However, Pugh (1973) reported a closer agreement with the constant potential model of colloid stability than with the constant surface charge model when modeling the selective coagulation of hematite/quartz and rutile/quartz suspensions. Chan et al. (1975, 1976) introduced the regulation model, which predicts similar results as presented in the above discussion (Usui, 1984).

Zone 2, which covers the pH range of 8 to 9, is characterized by high recovery and low product ash. The increase in selectivity appears to be due to an increase in the electrostatic repulsive force between the coal and ash particles. Based on the constant surface potential model, the increase in the repulsive force was caused by the near equality of the surface potentials, which is depicted in Figure 2.32. The zeta potential value for the coal particles in this zone was found to be approximately -40 mV, which is high for coagulation to occur according to the classical DLVO theory. Therefore, an attractive hydrophobic interaction force between the coal particles must exist in order for coagulation to occur.

The magnitude of the hydrophobic force has been reported to be 1-2 orders greater than the attractive van

der Waals forces (Warren, 1981; Rabinovich and Deryagin, 1988). Churaev and Derjaguin (1984) modified the DLVO theory to include hydrophobic interaction as a structural force. They found that the structural force is attractive for hydrophobic material and repulsive for hydrophilic material. Xu and Yoon (1988) described the hydrophobic force as an entropy-based interaction. Since the water around a hydrophobic surface is highly ordered, the attachment of two hydrophobic particles is favored by an increase in entropy. The entropy increase is caused by the removal of the ordered water at the hydrophobic surface to a disordered state in the medium. Around a hydrophilic surface, the water is very disordered. Therefore, the removal of the water from the hydrophilic surface is thermodynamically unfavorable.

In Zone 3, low coal recovery and high product ash percent coexisted. The drop in selectivity appeared to be due to the sharp decrease in coal recovery caused by the stabilization of the suspension of coal and mineral matter. The increase in the zeta potential of the coal particles (Figure 2.25) may be the reason the coal particles stopped coagulating. From Figure 2.32, it is shown that the zeta potentials of both the coal and ash particles did not change very significantly beyond pH 9. Although the drop in coal recovery may have been solely due to the small

increase in zeta potential, other possible explanations do exist.

One explanation may be that a complete OH^- monolayer adsorbed on the coal surface through hydrogen bonding, rendering the coal surface hydrophilic (Campbell and Sun, 1970; Schroeder and Rubin, 1984; Arnold and Aplan, 1986). However, according to Jessop and Stretton (1969), the adsorption of hydroxyl ions does not determine the potential of the coal particles. They concluded that the preferential orientation of the water dipoles at the water/hydrophobic surface controls the potential of the coal surface. Therefore, based on the dipole orientation conclusion, the reduction in coal coagulation cannot be attributed to OH^- adsorption.

Another possible explanation may be an adsorption combination of OH^- ions and highly hydrated cations, such as Na. Hydrophobic particles can be altered by the adsorption of hydrated ions so as to behave like hydrophilic material. As a result, the structural force, discussed earlier, is changed from attractive to repulsive. Several colloids, such as silica and polystyrene latices, are stable even at very high salt concentrations. This stability may be due to the surface adsorption of hydrated cations (Pashley, 1982). In explaining the reduction of the coagulation efficiency of the coal particles, it may be

the addition of sodium hydroxide to increase the pH, followed by adsorption of the hydrated Na cation, which induced the very strong hydration force that prevented the coal from coagulating. However, Celik and Somasundaran (1980) reported no difference in coal floatability in the presence of 10^{-2} M NaCl over a pH range of 1-13.

For the case of using tap water as the medium, the analysis is the same as in the above discussion. The difference is that the cations and anions contained in the tap water reduced the zeta potential values of both the coal and the particles of mineral matter. Therefore, the pH value corresponding to the near equality of the coal and ash zeta potentials was lower than for the distilled water medium, as shown in Figure 2.28. For this reason, the effective pH range for a tap water system was found to be 7-9, compared to 8-9 for a distilled water system.

The presence of multivalent cations depressed the negativity of both the coal and ash particles in the alkaline pH range. This observation is illustrated in Figures 2.29 and 2.30 for Ca^{2+} addition. The magnitude to which the zeta potential was depressed depended on the ionic concentration. Continued depression of the surface potentials resulted in an increase in coal recovery, although the selectivity of the process decreased. Therefore, it appears that the lower the multivalent cation

concentration, the more selective the coagulation process. This was proven by the batch test results plotted in Figure 2.17.

Celik and Somasundaran (1986) found that the calcium adsorption on coal in the alkaline pH range was due to $CaOH^+$ formation. In fact, the adsorption of other multivalent ions, such as Al^{3+}, Fe^{3+}, and Fe^{2+}, is based on their hydroxl formation, which induces coagulation of both the coal and ash particles. Also, Arnold and Aplan (1986) concluded that the presence of ions causes thinning of the hydration layer on the coal particles, hence, increasing the floatablity of the coal and enhancing coagulation of the coal particles. They also found that Ca^{2+} ions tie up some of the hydrophilic oxygen groups, such as the carboxyl sites on the coal surface, rendering them less hydrophilic. However, even though coal coagulation was enhanced, the agglomeration of the ash particles was also induced by the presence of specifically adsorbing ions.

As presented in the previous section, some coal samples have demonstrated either the inability to coagulate or the ability to coagulate non-selectively. In laboratory experiments, coals having a large sulfur content coagulated well, although the selectivity was poor. The separation efficiency of the process has been shown to decrease with an increase in the pyritic sulfur content of the feed coal

sample (Figure 2.15). Batch test results on the Pittsburgh No. 8 coal sample, which contained 4.0% sulfur of which 2.5% was pyritic sulfur, showed high coal recoveries and product ash percents over a range of pH values shown in Figure 2.14. Zeta potential data on this coal was obtained from the literature and is shown in Figure 2.27 (Arnold and Aplan, 1986). The excellent coagulation performance seemed to be a result of the low surface potential of both the coal and ash particles. For the same reason, heterocoagulation occurred, which resulted in poor selectivity.

Batch tests have also shown that oxidized coals tend to coagulate only around their respective iep values. However, the addition of a fuel oil, such as kerosene, has demonstrated an ability to enhance the hydrophobicity of the coal, hence improving the efficiency of the selective coagulation process, as depicted in Figures 2.23 and 2.24. The improvement in separation efficiency after the addition of the fuel oil demonstrates the strength of the hydrophobic interaction force. As reported by Hale (1987), the zeta potential of a coal sample increases significantly after the addition of fuel oil. Therefore, the electrostatic force between the oil-coated coal particles is larger than between the uncoated particles. Since the process efficiency improves, the incremental change in the

strength of the hydrophobic force (attributable to the fuel oil coating of the coal particles) must be much larger than the change in the strength of the electrostatic force.

Although this investigation did not include a study of the different coal ranks, it is the author's opinion that the coagulation of the coal particles will improve with increasing coal rank, except for anthracite. Anthracite has been reported to be less floatable than bituminous coal, hence, less hydrophobic. With the exception of anthracite, the reason that coal coagulation will improve is because the composition of the functional groups, such as carboxylic and hydroxylic groups, on the coal surface decreases with increasing rank (Fuerstenau et al., 1987). In other words, the hydrophobicity of the coal increases. However, the treatment of graphite by the selective coagulation process was found to be difficult due to the large hydrophobic force. This force induced coagulation and severe bridging between the graphite particles, which slowed the settling process and entrapped a large amount of the gangue material. According to zeta potentials reported by Wen and Sun (1977), the negative value of the coal decreases with increasing rank. Therefore, the selectivity of the process may decrease with an increase in rank.

2.5 Summary and Conclusions

1. The selective coagulation process has proven to be an efficient physical cleaning technique for treating fine coal slurries. Advantages pointed out in this chapter include:
   - the ability to treat ultrafine coal
   - high coal recovery and low product ash content
   - no reagent requirement
   - applicability to various coal seams.

2. Present studies on the effect of pH on the selective coagulation of coal have been explained through the forces associated with the DLVO theory (i.e. van der Waals and electrostatic) and structural forces (hydrophobic interactions and hydration). The strength of the hydrophobic interaction was found to be a controlling factor in the coagulation of coal particles. This attractive force was enhanced by the addition of kerosene. The magnitude of the repulsive electrostatic force controlled the selectivity of the process. For this reason, the slurry pH was determined to be a very important parameter. The optimum pH range for a coal slurry with distilled

water as the medium was found to be 8-9, whereas the range for a tap water system was 7-9.

3. The presence of multivalent cations in the coal slurry enhanced homocoagulation and heterocoagulation between the coal and ash particles. Therefore, the overall effect of multivalent cations on the selective coagulation process was high coal recoveries and product ash values. A critical ion concentration was found for Ca^{2+} to be around 20-25 ppm (5×10^{-4} M).

CHAPTER 3

THE EFFECT OF THE ASSOCIATED PHYSICAL PARAMETERS ON THE SELECTIVE COAGULATION OF COAL

3.1 Introduction

Coal beneficiation research in recent years has concentrated on the recovery of fine material, presently considered waste, and the production of superclean and ultraclean coals. In order to obtain superclean coal, which contains less than 2% ash, the mineral matter contained in the feed material must be liberated from the coal particles. In most cases, this requires grinding the material down to ultrafine sizes. Therefore, a new technique, called selective-shear coagulation, was developed at Virginia Tech. This technique has proven the ability to efficiently produce superclean coal using ultrafine material.

The selective coagulation process utilizes particle surface forces, such as electrostatic repulsion, van der Waals, and hydrophobic interaction, to induce the coagulation of the coal particles. The selectivity of the process requires a fairly strong electrostatic repulsive force between the coal and the ash particles, which prevents heterocoagulation. Coagulation of the coal particles occurs due to strong hydrophobic interactions

between the particles and the attractive van der Waals forces. Mechanical energy is required to overcome the DLVO energy barrier and to provide a sufficient amount of particle-particle collisions to allow coagulation to occur.

The coagulation rate is the multiplicative product of the collision rate and the probability of adhesion (Warren, 1977). Therefore, an increase in either of the two will increase the coagulation rate, hence increasing the recovery of the preferentially agglomerated material. The probability of adhesion is controlled by the magnitude of the DLVO energy barrier, the degree of hydrophobicity, and the van der Waals attractive forces of both the coal and mineral matter. Equations representing collision rate vary for different hydrodynamic conditions, such as turbulent, laminar, and quiescent. However, each equation depicts particle size, particle population, and applied energy as important parameters for determining the magnitude of the collision rate.

The purpose of this chapter is to present results illustrating the effect of physical parameters on the selective coagulation of coal. The list of parameters studied include particle size, percent solids, agitation time, rotational speed of the impeller, specific energy, and slurry medium type (i.e., distilled water or tap water). Also, since all agglomeration processes have a

problem with entrapment of gangue material in the agglomerates, the number of treatment stages required to sufficiently reject the mineral matter was studied.

3.2 Experimental

The coal samples used in the present work are listed in Table 3.1, along with their respective ash values. As soon as the samples were received, they were crushed to -1/4-inch using a laboratory jaw crusher. The coal was then riffled into representative lots of approximately 1000 grams each, placed into air-tight containers, and stored in a freezer at -20^{o}C to minimize oxidation.

Preparation of the coal slurry and the batch coagulation tests were conducted as described in Section 2.2.2 of the previous chapter. One exception is that the mixer used was a Heller HST20 series which provided precision speed control and torque measurement.

3.3 Results

3.3.1 Effect of Multi-Stage Treatment

A major problem for any agglomeration process used as a cleaning technique is entrapment of gangue material inside the agglomerates. Re-treatment, which includes the breaking-up and re-agglomeration of the selected material,

Table 3.1 : Various Coal Seam Samples Studied

COAL SAMPLE	TYPE	FEED ASH (%)
Upper Cedar Grove	ROM	24.0
Upper Cedar Grove	ROM	12.0
Upper Cedar Grove	Processed	3.40
RL-Consol	Processed	5.50
Elkhorn No.3	ROM	12.0
Elkhorn No.3	Processed	5.25

is normally used to minimize the entrapment problem. Figures 3.1-3.5 show the effect of increasing the number of treatment steps or stages for several coal samples using both tap and distilled water.

In Figure 3.1, Elkhorn No. 3 coal was used in distilled water at pH 9. The clean coal recovery decreased gradually from 100% to 76% as the number of stages increased from 0 to 10. Recovery dropped more during the later stages, which may have been due to a depletion in the concentration of the counter ions or surfactants released from the coal or oxidation of the coal during the retreatment stages. Product ash was found to decrease sharply from 12% to 4.6% over the first few stages. As the number of re-treatment steps was increased, the amount of entrained material decreased, hence decreasing the product ash percent which leveled off at 1.01% after 10 stages, where most, if not all, the unlocked ash particles were removed. This trend was the same for all of the coals tested. Along with the decrease in product ash percent, pyritic sulfur reduction was above 50% for every coal sample studied. In particular, the RL coal sample, shown in Figure 3.5, experienced a 60% reduction, which decreased the overall sulfur percent from 1.30 to 0.88. In this case, the selective-shear coagulation process converted a non-compliance coal into a compliance coal.

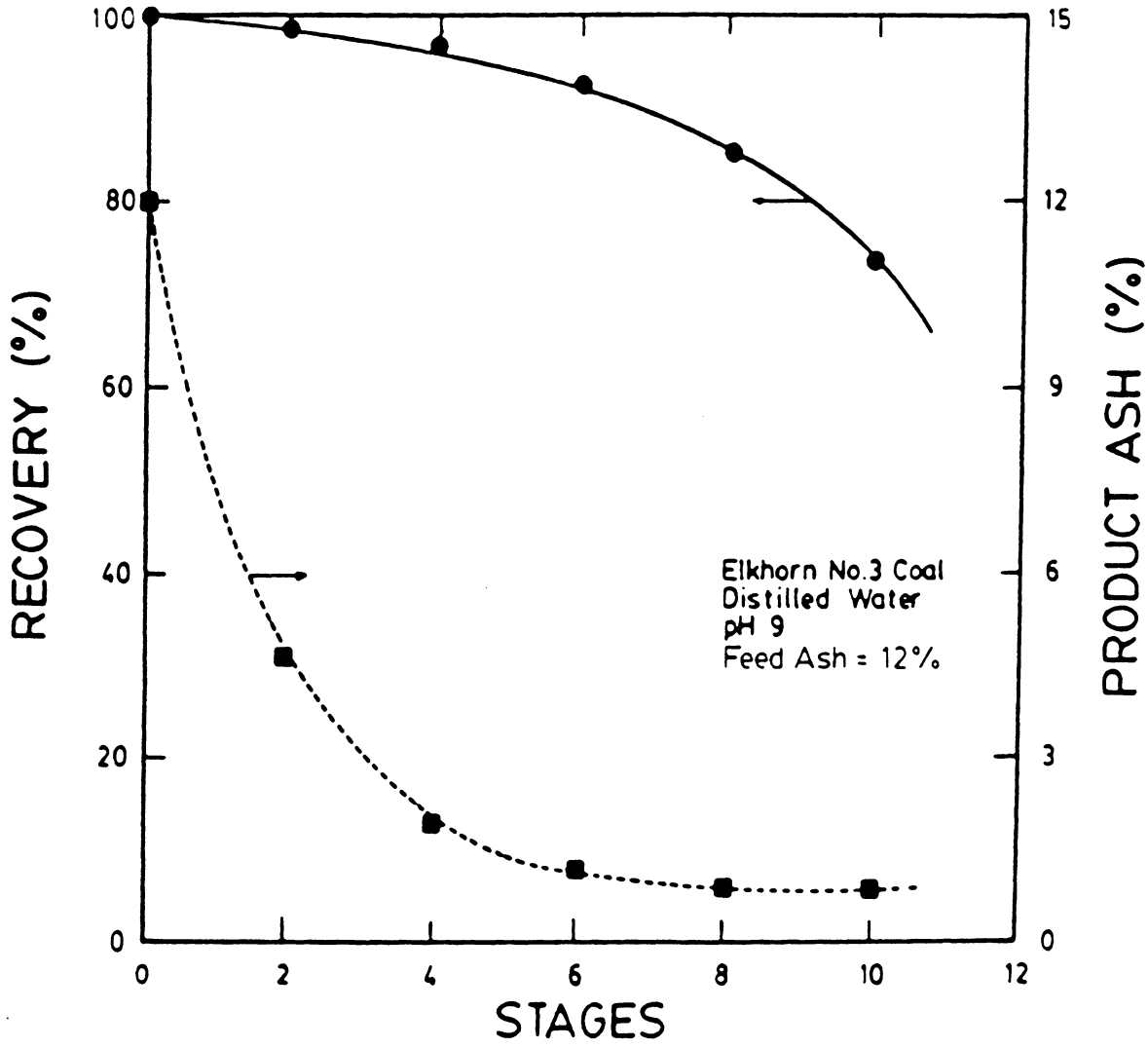

Figure 3.1 The effect of cleaning stages on recovery and product ash percent for the Elkhorn No.3 coal seam containing 12% ash.

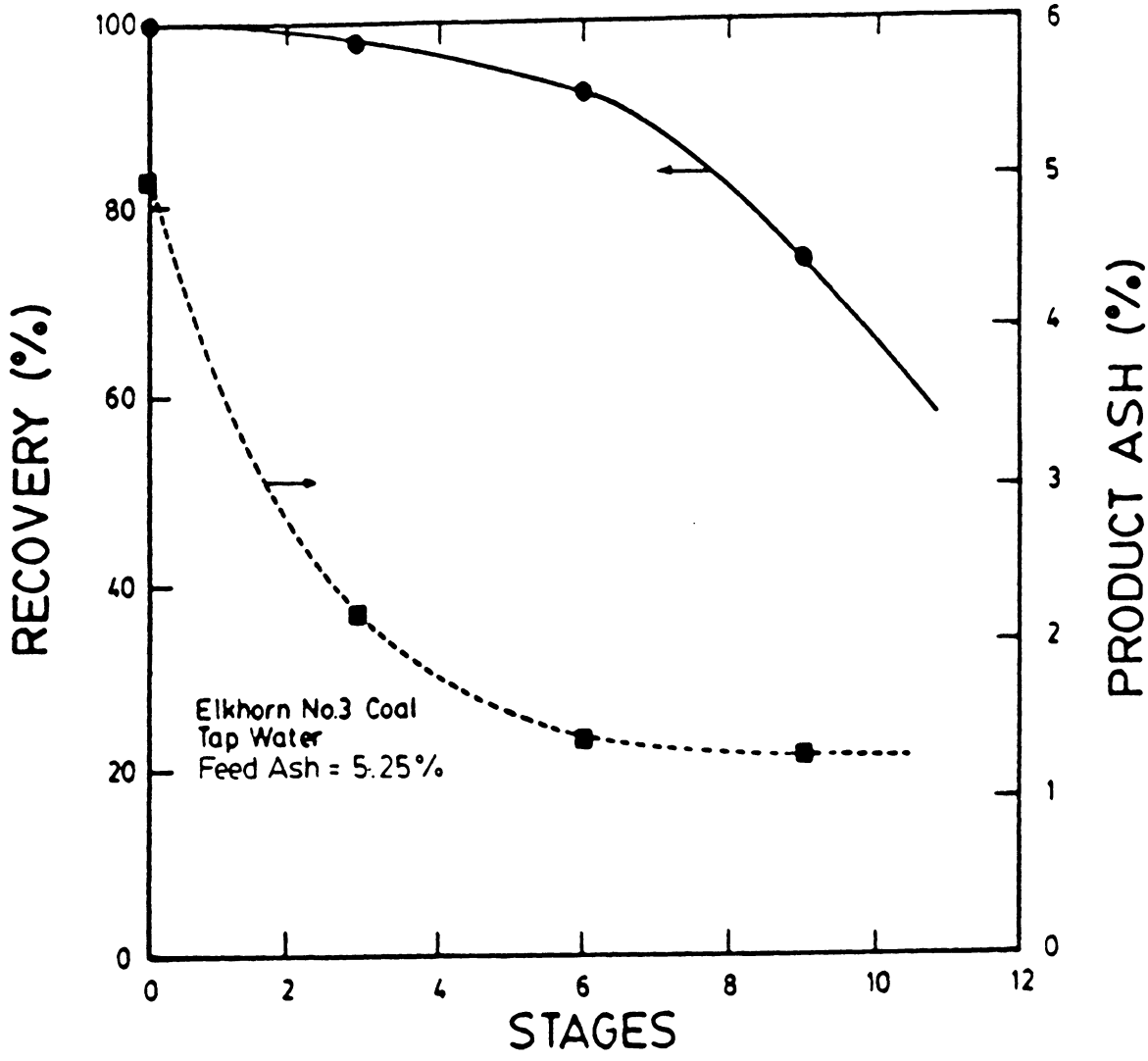

Figure 3.2 The effect of cleaning stages on recovery and product ash percent for the Elkhorn No.3 coal seam containing 5.25% ash.

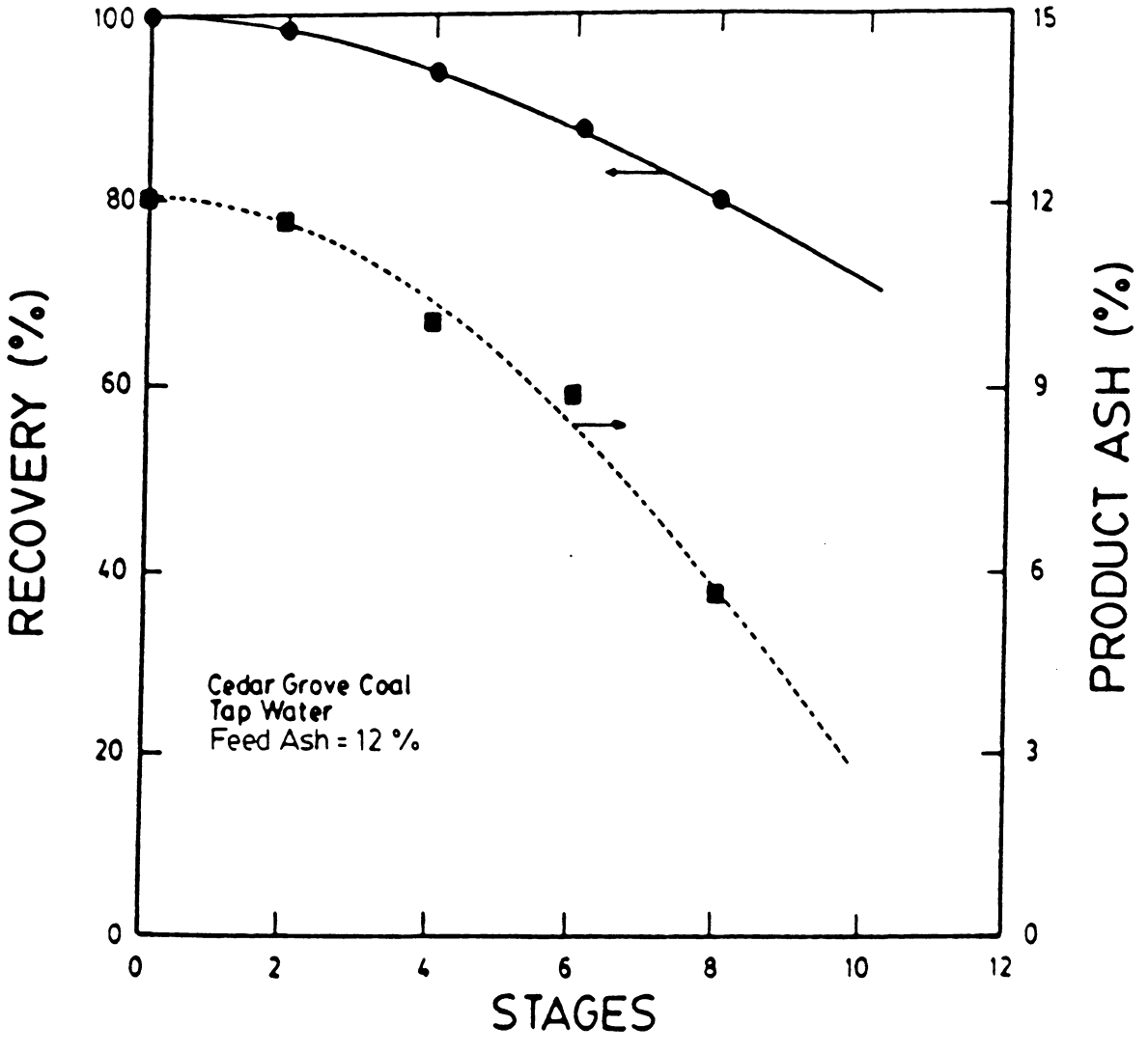

Figure 3.3 The effect of cleaning stages on recovery and product ash percent for the Upper Cedar Grove coal seam containing 12% ash.

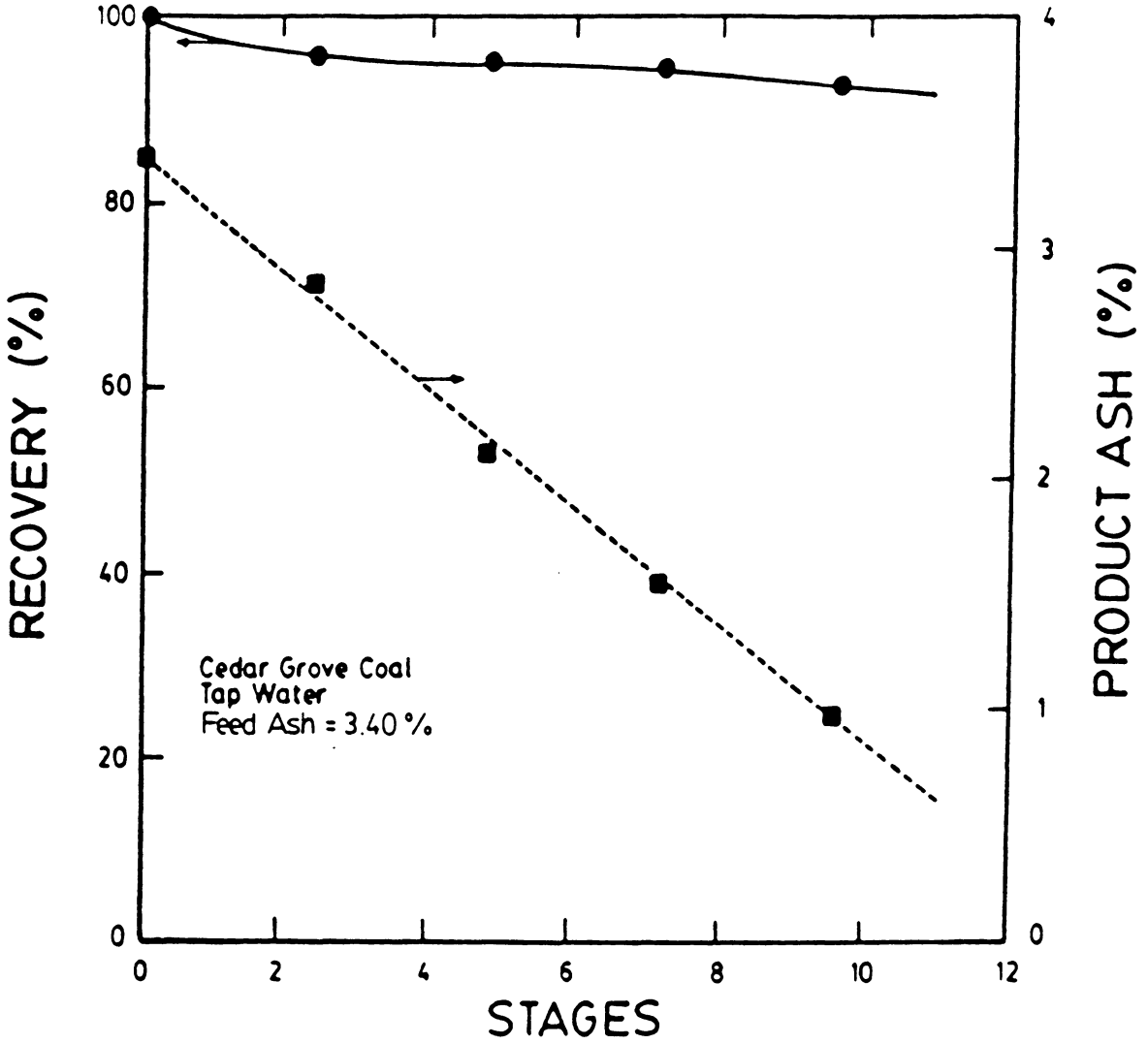

Figure 3.4 The effect of cleaning stages on recovery and product ash percent for the Upper Cedar Grove coal seam containing 3.4% ash.

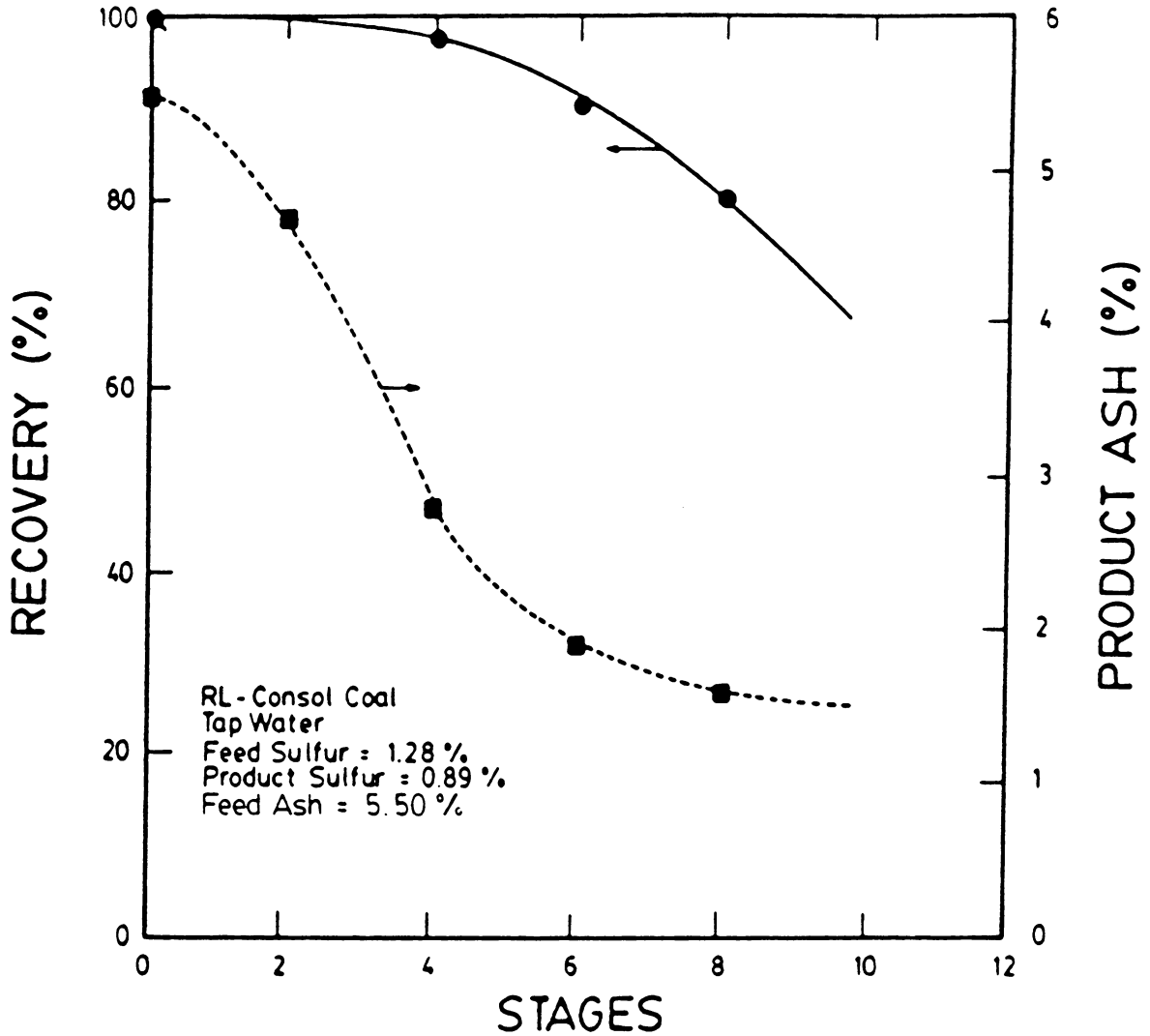

Figure 3.5 The effect of cleaning stages on recovery and product ash percent for the RL-Consol coal sample containing 5.5% ash.

3.3.2 Effect of Percent Solids

One method of increasing the throughput of a process involves increasing the percent solids of the feed material. Therefore, a series of tests were performed over a range of percent solids to determine the effect of percent solids on the selective coagulation of coal. The results are shown in Figures 3.6 and 3.7 for the Upper Cedar Grove (24% ash) and Elkhorn No. 3 (5.65% ash) coal samples, respectively. In Figure 3.6, clean coal recovery was a low 10% at a solids concentration of 0.40% and increased sharply to 88% at 1.6% solids. Beyond 1.6%, recovery increased gradually to 96% at 3% solids. The increase in recovery was probably due to an increase in the probability of collision between particles as the percent solids was increased. Product ash percent initially decreased sharply from 12.5% to 4.4% as the solids concentration was raised from 0.40% to 0.80%, which corresponds to the large recovery increase. Larger solids concentrations resulted in an increase in the product ash percent to 13.8% at 3% solids due to the settling and entrapment of ash material during a long, hindered settling process. The tests using Elkhorn No. 3 coal yielded similar results. Therefore, the lower values of percent solids were affected by the small population of particles per unit volume, which decreased the probability of two

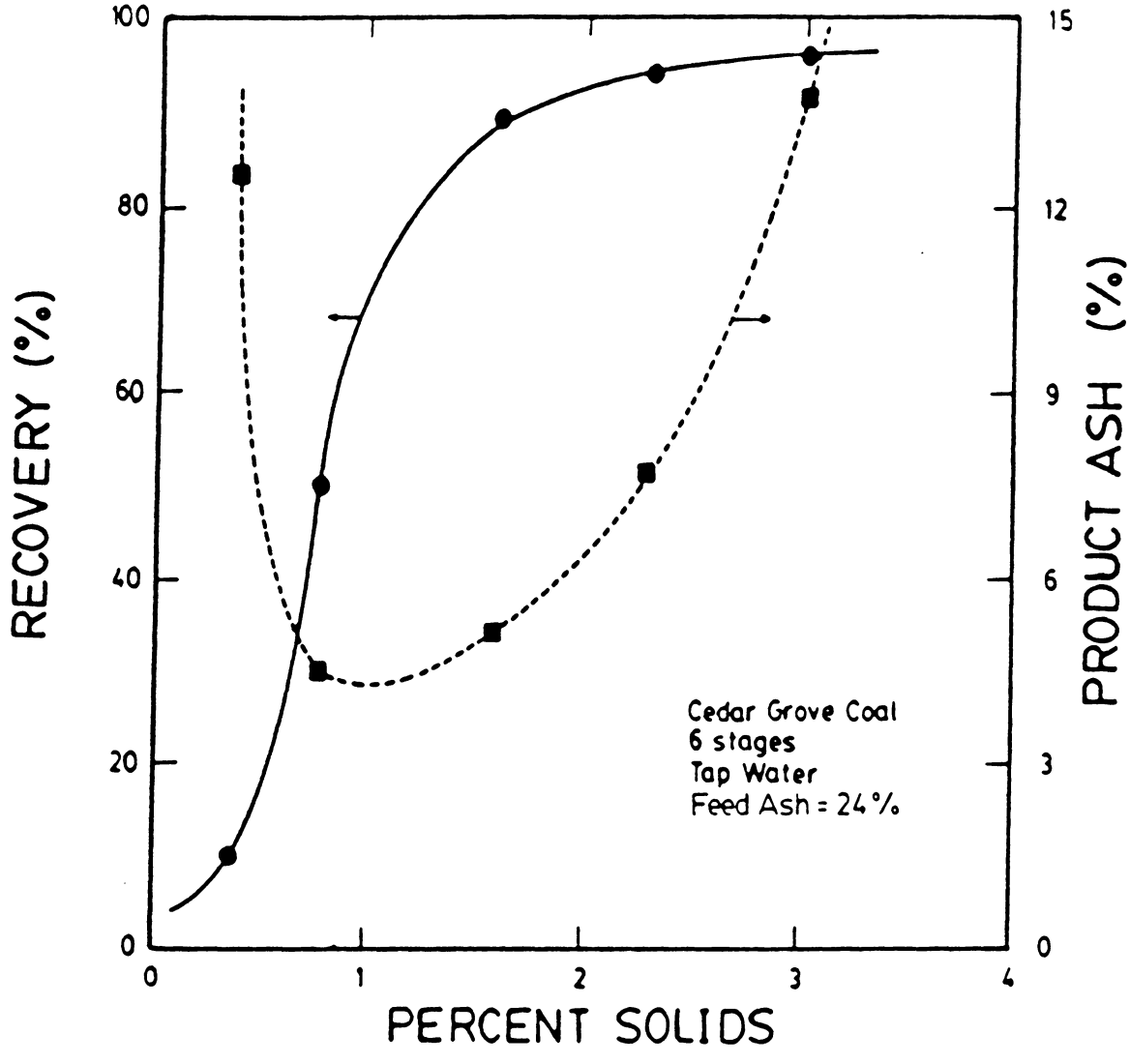

Figure 3.6 The effect of % solids on coal recovery product ash percent for the Upper Cedar Grove coal seam containing 24% ash.

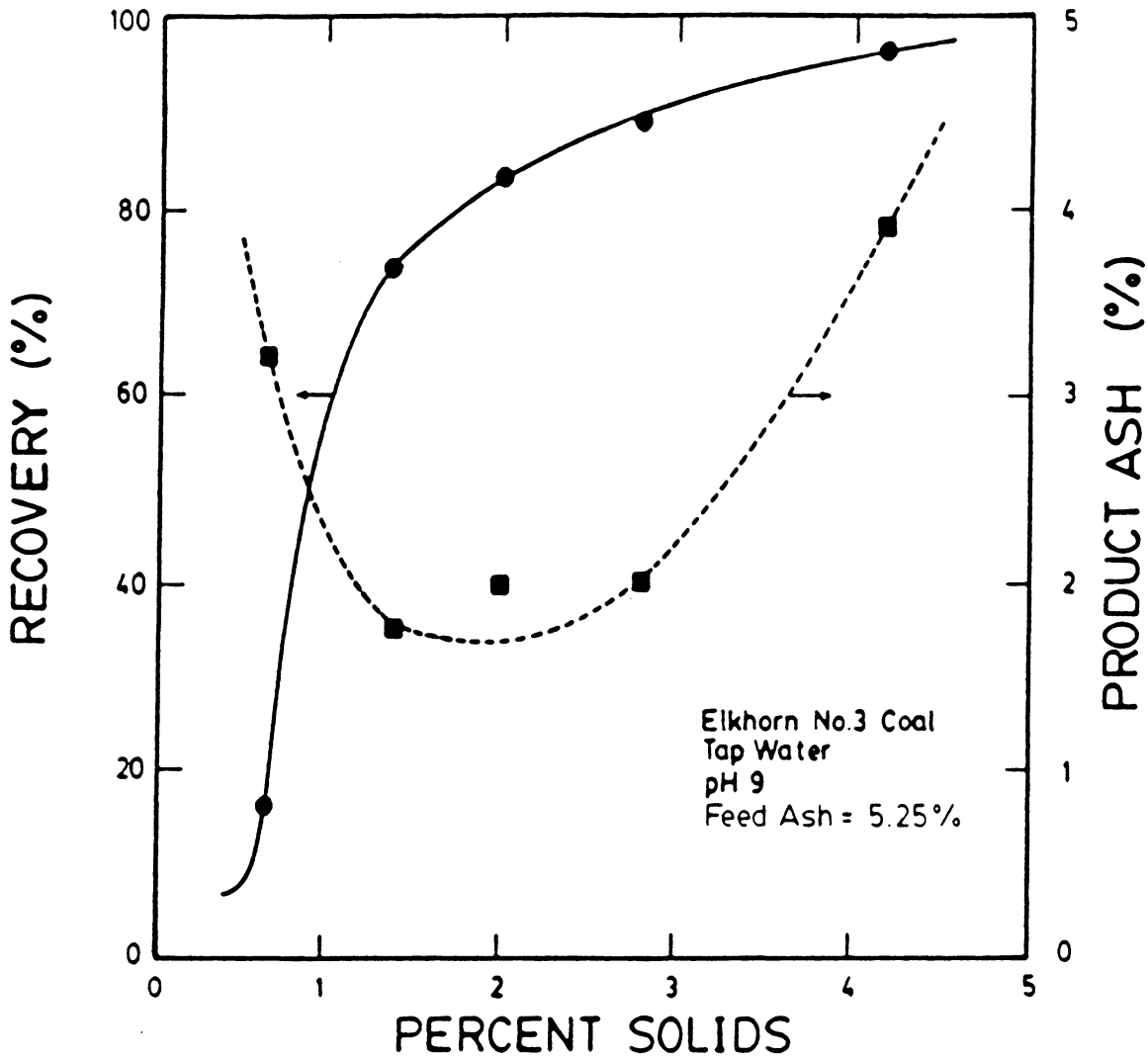

Figure 3.7 The effect of percent solids on coal recovery and product ash percent for the Elkhorn No.3 coal seam containing 5.25% ash.

particles colliding and coagulating. The increase in product ash percent in the upper percent solids range was due to an entrapment problem during settling, which may be minimized in a continuous process.

3.3.3 Effect of Particle Size

Since ultrafine grinding is normally needed to completely liberate the gangue material, tests were performed over a wide range of ultrafine particle sizes to determine the upper and lower particle size limits for the selective coagulation process. Figure 3.8 shows the effect of particle size on clean coal recovery, product ash percent, and percent sulfur reduction using the Elkhorn No. 3 coal sample (12% ash) after 6 stages of treatment. The results indicate a linear decrease in recovery from 95% at 4.4 microns to 73% at 14.5 microns. The product ash percent decreased from 5.1% at 14.5 microns to where it levels off at 1.66% at 6.1 microns. This was a combined result of decreasing ash liberation and increasing amounts of ash settling into the product as the particle size was increased. Sulfur reduction increased from 7% at 14.5 microns to 27% at 4.4 microns due to the continuing liberation of pyritic sulfur. The increase in sulfur reduction as particle size decreased indicates continued liberation of the coal pyrite.

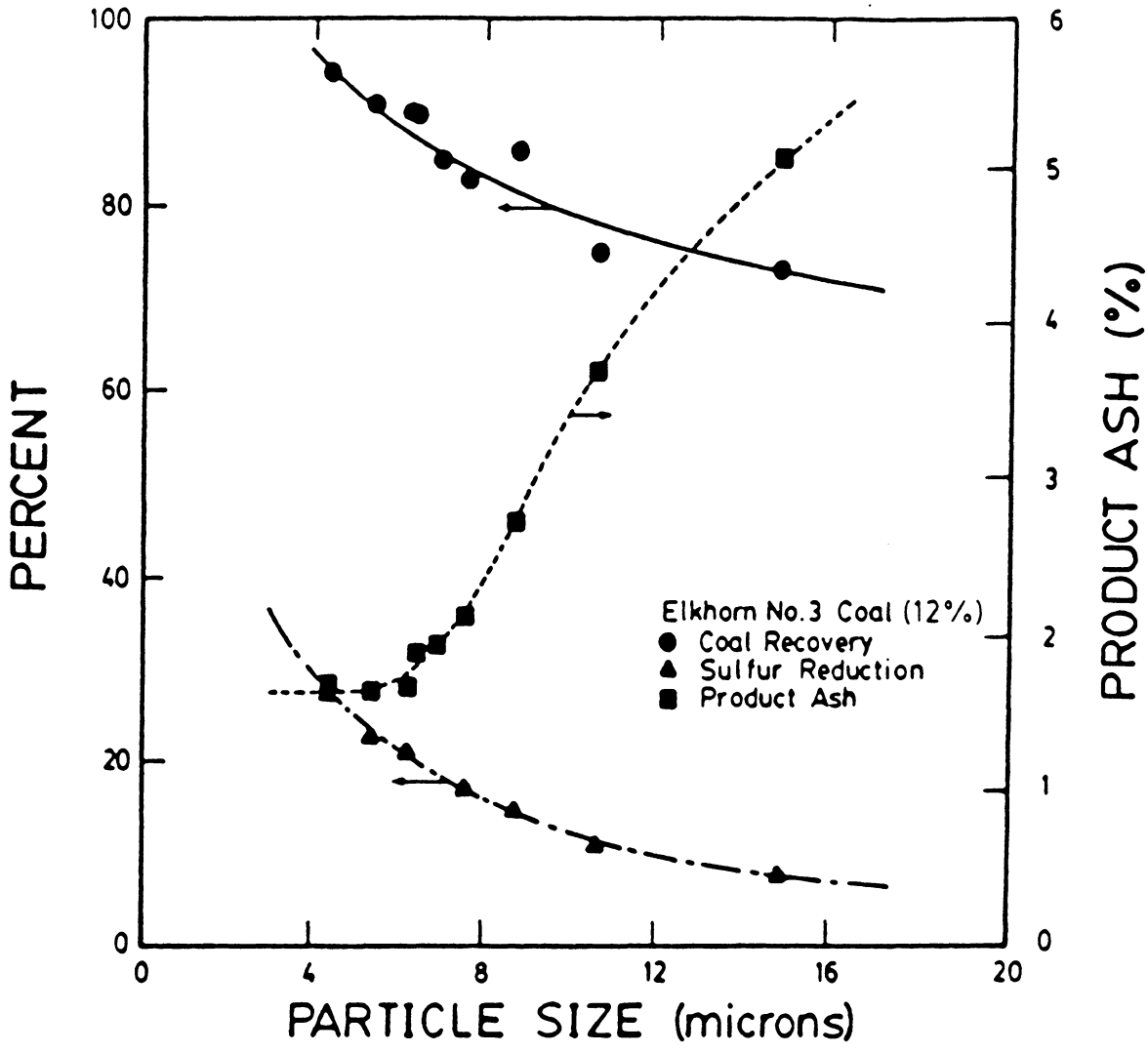

Figure 3.8 The effect of particle size on coal recovery, product ash percent, and sulfur reduction for the Elkhorn No.3 coal seam containing 12% ash.

Figure 3.9 demonstrates similar results as above using the Upper Cedar Grove coal sample (24% ash). The product ash content for the 3.7-micron particles leveled out at 5.5% compared to 17.0% for 75-micron material. This clearly illustrates the importance of ash liberation. Figure 3.10 is a plot of clean coal recovery versus product ash percent for 3 different particle sizes using an Elkhorn No. 3 coal sample (5.35% ash). It depicts that a higher recovery and lower product ash percent can be obtained for smaller particle sizes. Therefore, the results indicate that by decreasing the particle size, clean coal recovery and sulfur reduction are increased and product ash percent is decreased; hence, the process is more effective.

3.3.4 Effect of Energy Parameters

A series of experiments were performed to determine the effect of agitation time on recovery and product ash for the selective-shear coagulation process using an Elkhorn No. 3 coal sample (12% ash). As shown in Figure 3.11, recovery was a very low 38% after 30 seconds of agitation. However, as the agitation time was increased to 3 minutes, the recovery sharply increased to 94%. Beyond 3 minutes, recovery slightly decreased with an increase in agitation time to 86% after 30 minutes. The effect on selectivity is illustrated in Figure 3.12. Product ash content was found

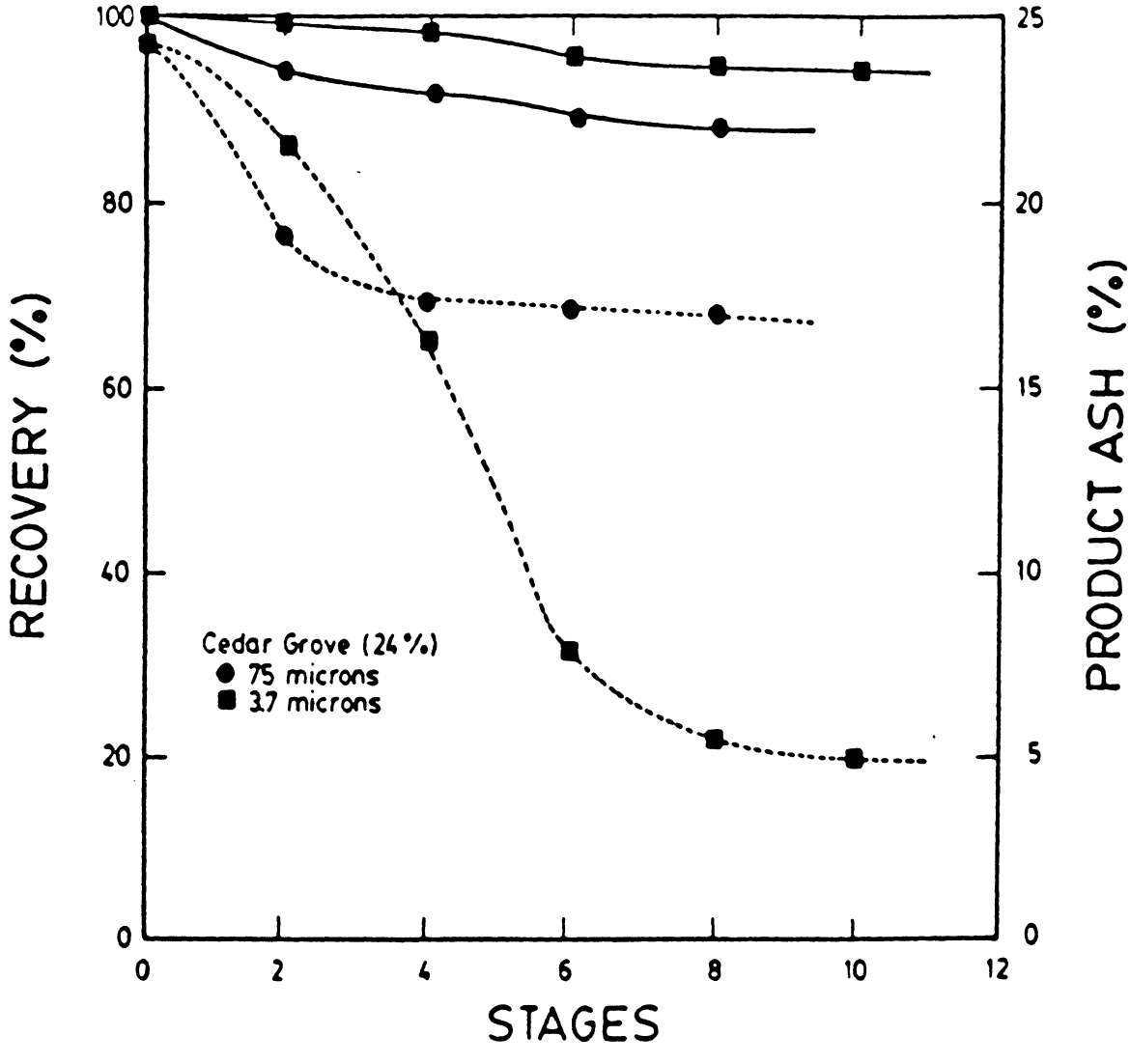

Figure 3.9 Coal recovery versus product ash percent curves for two particle sizes using the Upper Cedar Grove coal seam containing 24% ash.

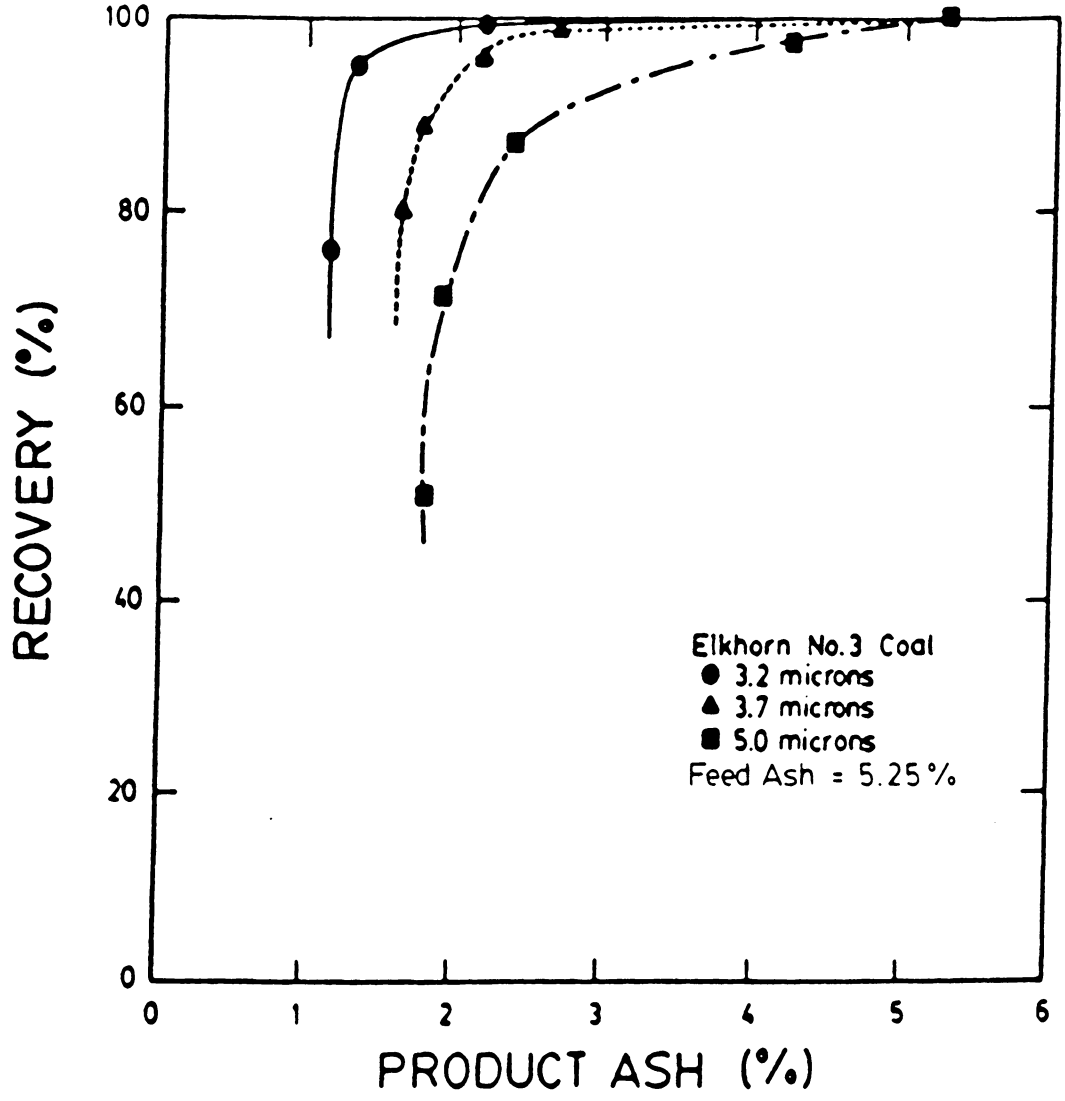

Figure 3.10 Coal recovery versus product ash percent curves for three particle sizes using an Elkhorn No.3 coal seam sample containing 5.25% ash.

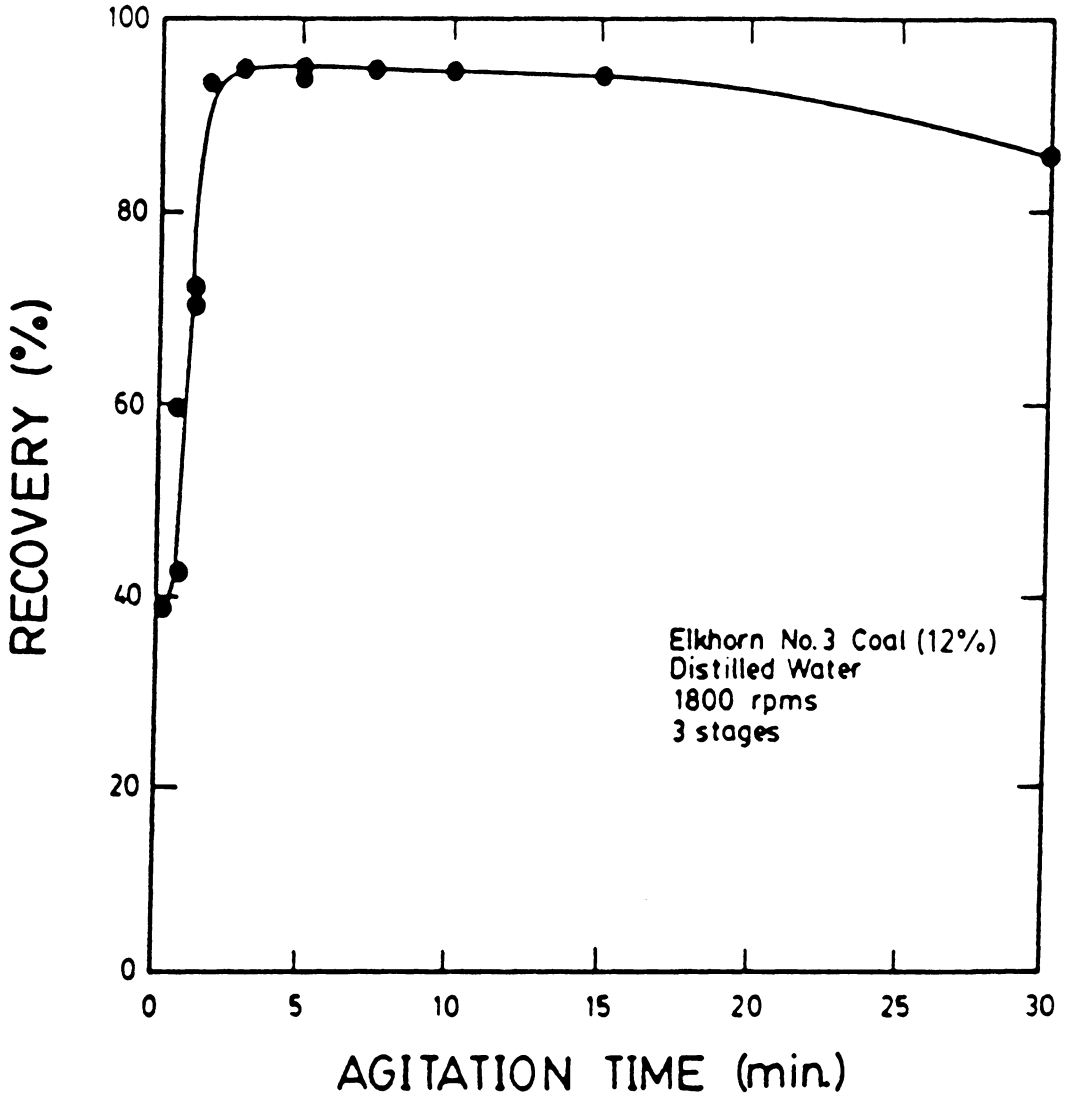

Figure 3.11 The effect of agitation time on coal recovery.

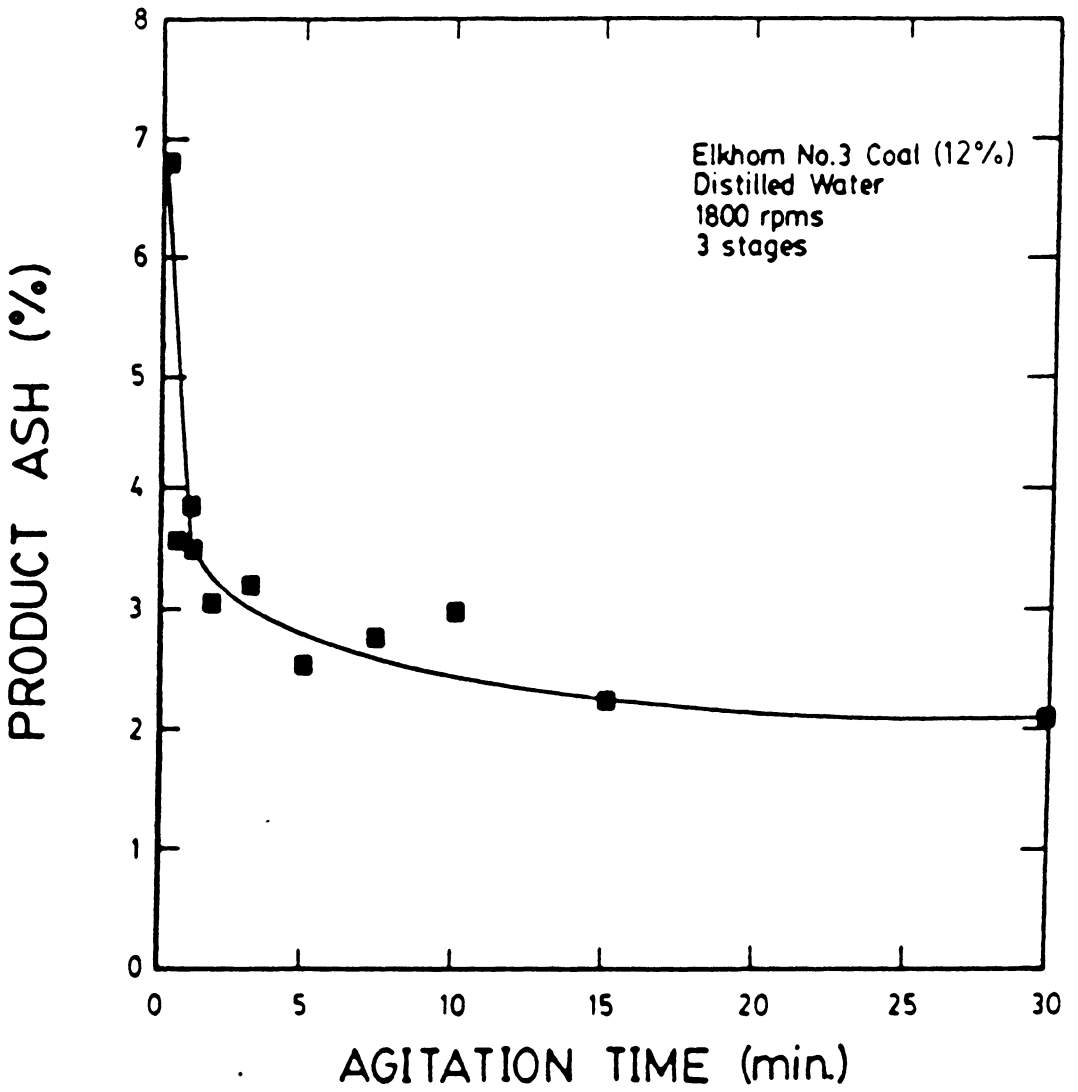

Figure 3.12 The effect of agitation time on product ash percent.

to sharply decrease from 6.8% after 30 seconds of agitation to 3.1% after 3 minutes. After 30 minutes of mixing, the product ash percent gradually decreased to 2.1%.

Rotational speed was also examined using the same coal sample for 5-, 10-, and 20-minute agitation times. The results are shown in Figure 3.13. Clean coal recovery was a low 20% at 250 rpms, utilizing 5 minutes of agitation, and sharply increased to 88% at 750 rpms, where the recovery remained constant through 2500 rpms. Using 10 minutes of mixing time, recovery was slightly higher at 30% for a rotational speed of 250 rpms and increased to 92% at 750 rpms, where recovery also levelled off. Recovery gradually decreased from 95% at 500 rpms to 92% at 2500 rpms when the slurry was mixed for 20 minutes. The results illustrating the effect on product ash percent are shown in Figure 3.14. As expected, less rpms were required to obtain sufficient selectivity using larger agitation times. Product ash content decreased from 11.5% at 250 rpms to 5% at 1000 rpms when using 5 minutes of mixing, whereas 10 minutes of agitation required only 750 rpms to reduce the product ash content to 4.7%. The ash percent remained fairly constant at 4.0-4.1% with 500-2500 rpms when using a mixing time of 20 minutes.

Tests were also conducted to determine the difference in required rotational speed when using distilled water at

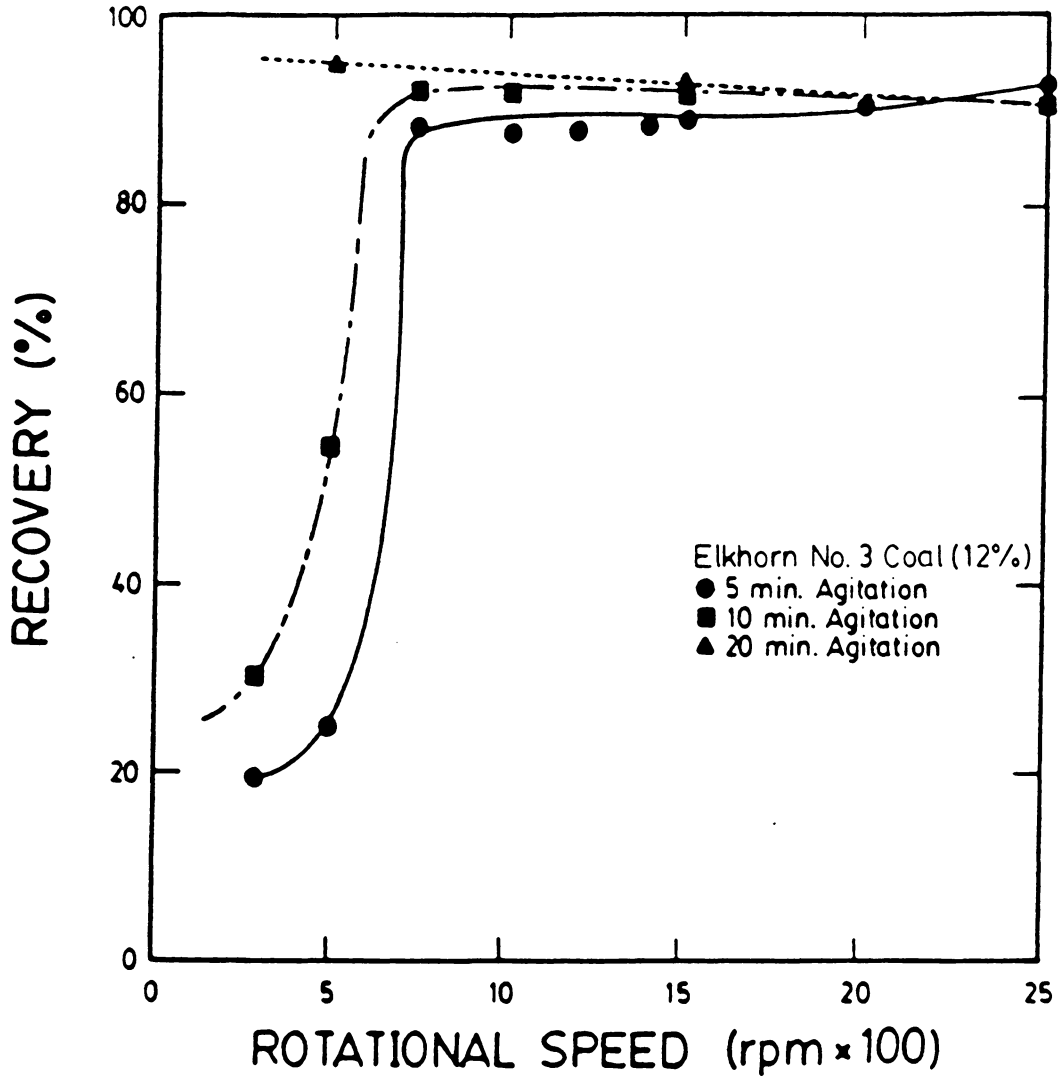

Figure 3.13 The effect of rotational speed on coal recovery for three agitation times.

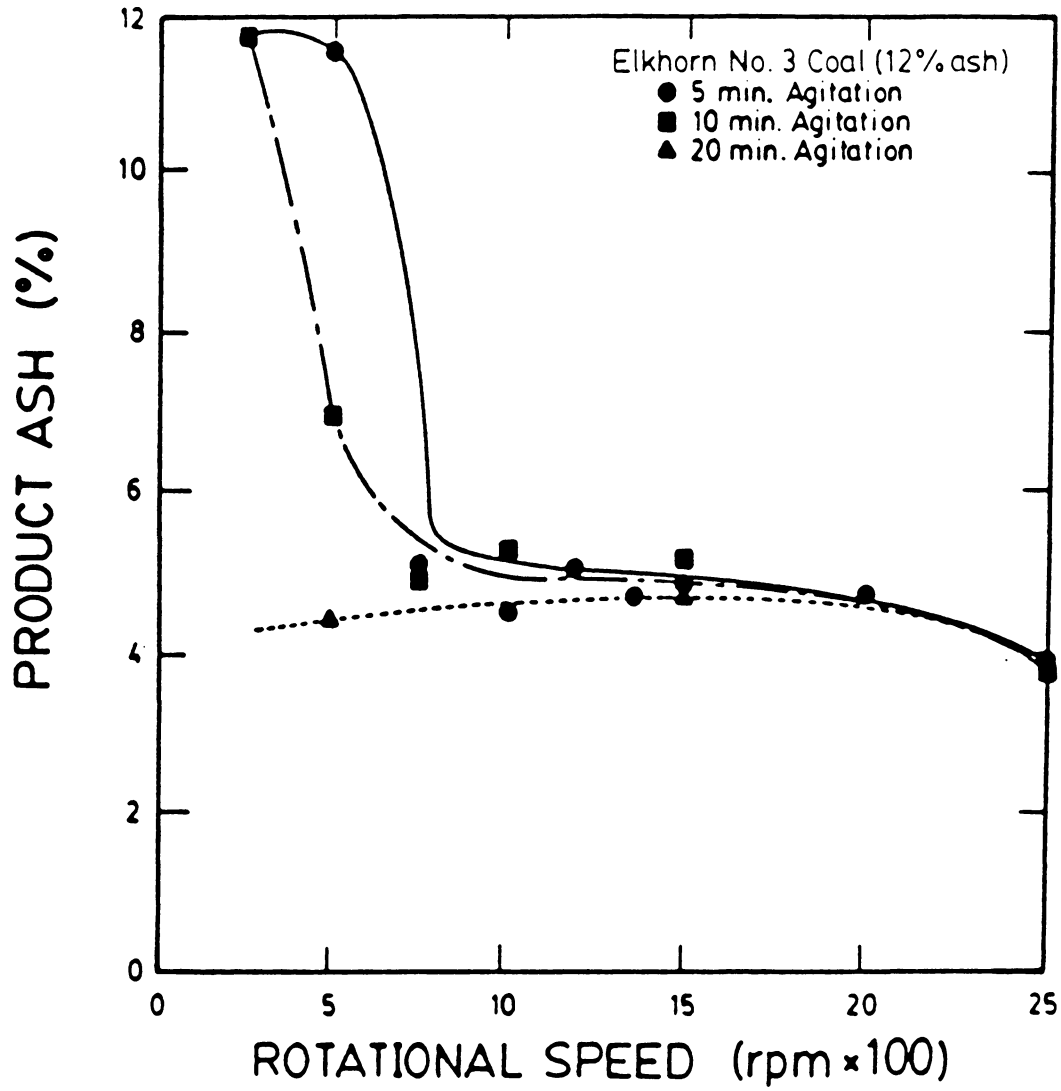

Figure 3.14 The effect of rotational speed on product ash percent for three agitation times.

pH 9, as in the previous results, and tap water at pH 7 and 9. The results for clean coal recovery and product ash percent are shown in Figures 3.15 and 3.16, respectively. In the case of distilled water, the effect on recovery as the agitation time was increased was the same as discussed earlier, where the recovery sharply increased and leveled off at around 750 rpms, whereas recovery was 90% and greater throughout the rpm range with both of the pH values used for tap water. A similar result was obtained for the product ash percent. Product ash decreased sharply, as reported earlier, to 5% at 750 rpms and gradually decreased with increasing rpms. In the case of tap water, the ash content was approximately 6.0% and 7.0% for the pH values of 9 and 7, respectively, and remained fairly constant over the range of rotational speeds studied.

In order to determine the energy consumption required for the efficient selective coagulation of coal, torque measurements, along with the agitation time and rotational speed results obtained using micronized Elkhorn No. 3 seam coal, were applied to the following specific energy equation (Brown, 1986):

$$E = 2.978 * 10^{-3} T t n / w, \qquad [3.1]$$

where E is the specific energy (kwh/ton), T is the torque (in*lb), t is time (sec), n is rotational velocity (rpm),

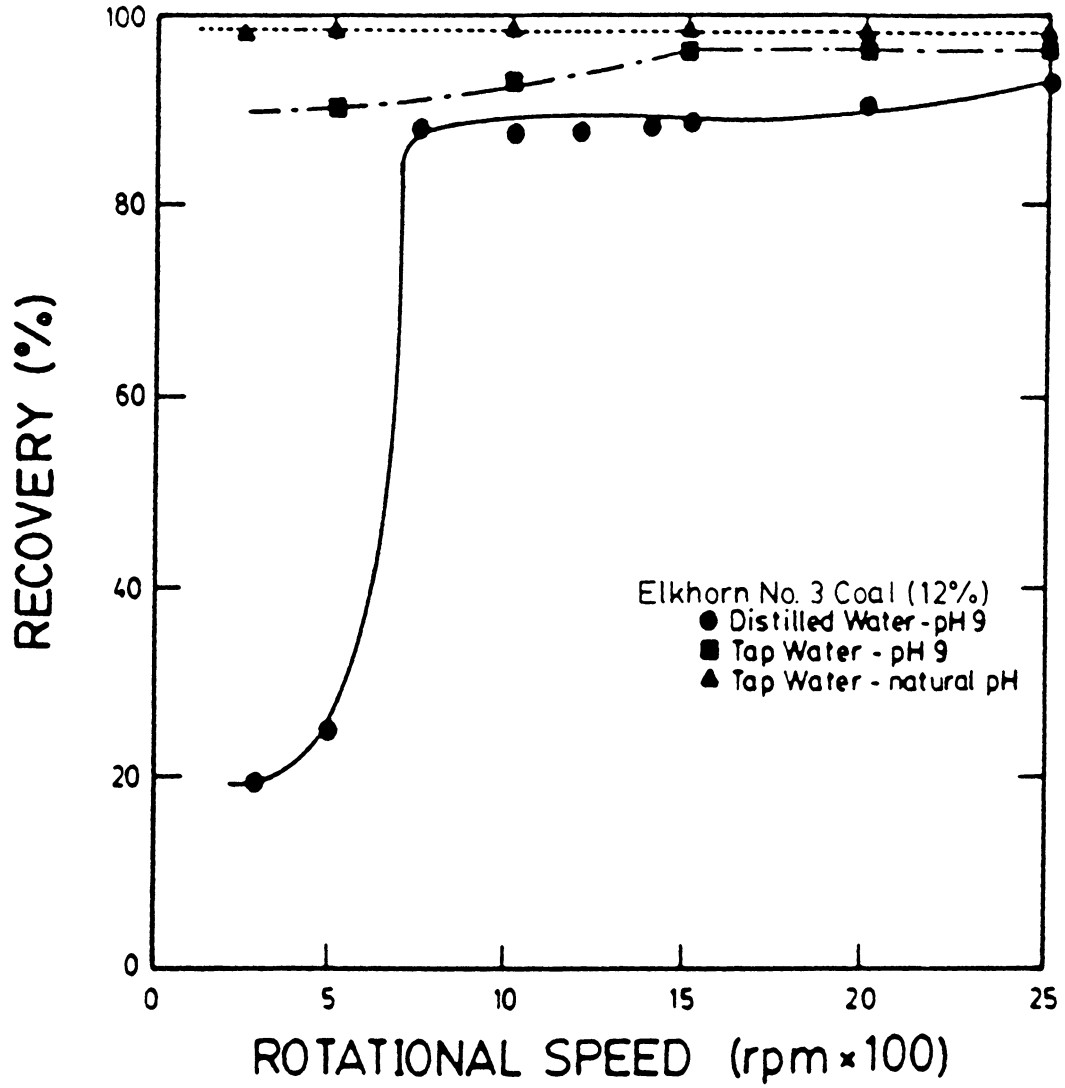

Figure 3.15 Coal recovery versus rotational speed curves for three different media conditions.

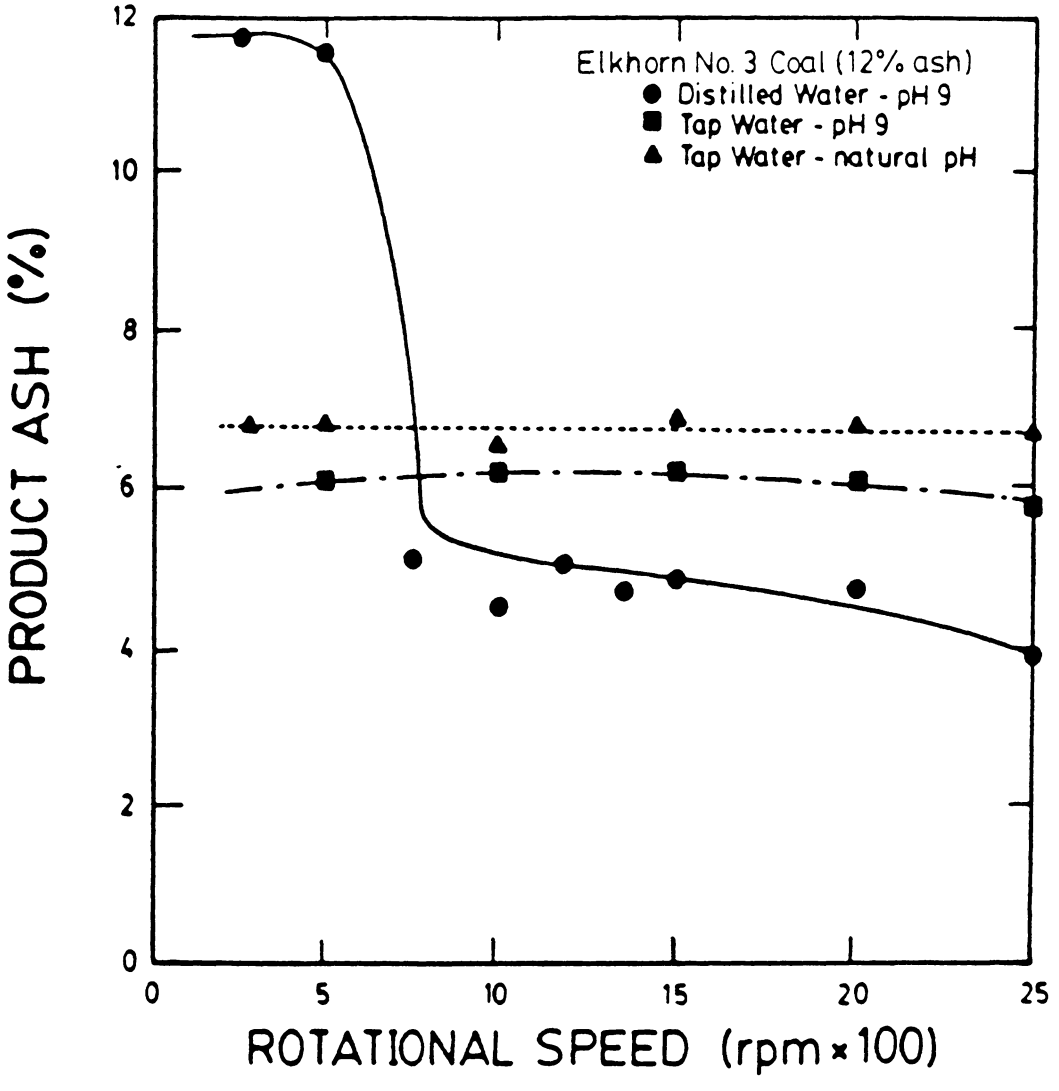

Figure 3.16 Product ash percent versus rotational speed curves for three different media conditions.

and w is the mass of the material (grams). Torque and rotational speed were measured using the Heller HST20 mixer.

Figure 3.17 shows clean coal recovery plotted versus specific energy, cumulated over 3 stages of treatment, using tap water at its natural pH and pH 9 and distilled water at pH 9. The recovery for tap water at its natural pH remained a constant 98% throughout the range of specific energy values studied, while tap water at pH 9 achieved a slight increase in recovery from 90% at 100 kwh/ton to 97% at 4500 kwh/ton. In the case of distilled water at pH 9, recovery rose sharply from 20% at 10 kwh/ton to 90% at 500 kwh/ton. Beyond 500 kwh/ton, the recovery steadily increased to 95% at 4500 kwh/ton. The differences in recovery between the three cases are more than likely due to the specific adsorption of ions present in the tap water which would decrease the electrostatic repulsive force between the coal particles. As a result, less energy is required to induce coagulation for tap water systems.

Figure 3.18 shows the effect that increasing energy input has on the selectivity of the process. The product ash percent, when using tap water at its natural pH, remained a relatively constant 7.0% throughout the specific energy range studied, whereas at pH 9, the product ash slightly decreased from 6.1% at 100 kwh/ton to 5.7% at 4500

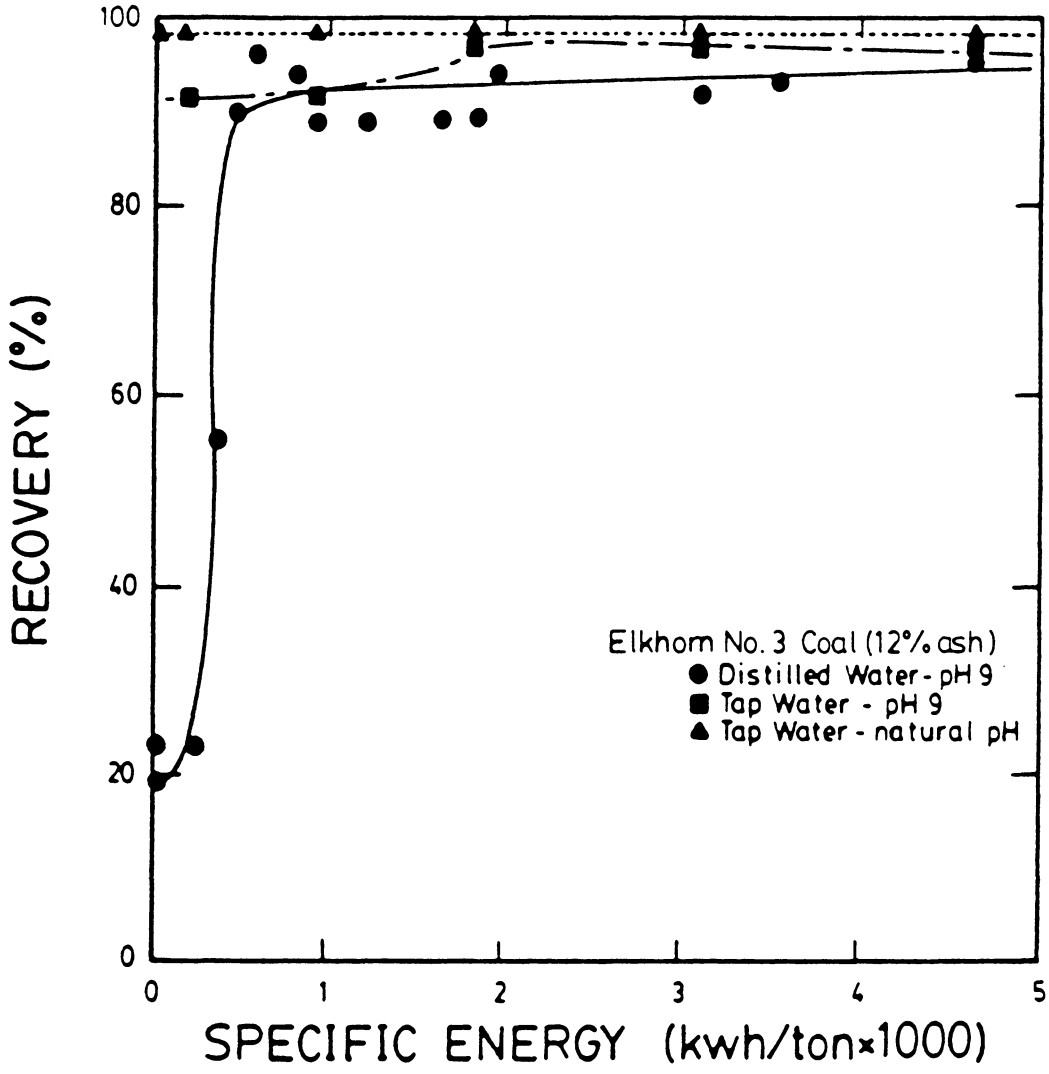

Figure 3.17 The effect of specific energy input on recovery for 3 media conditions; specific energy accumulated over 3 cleaning stages.

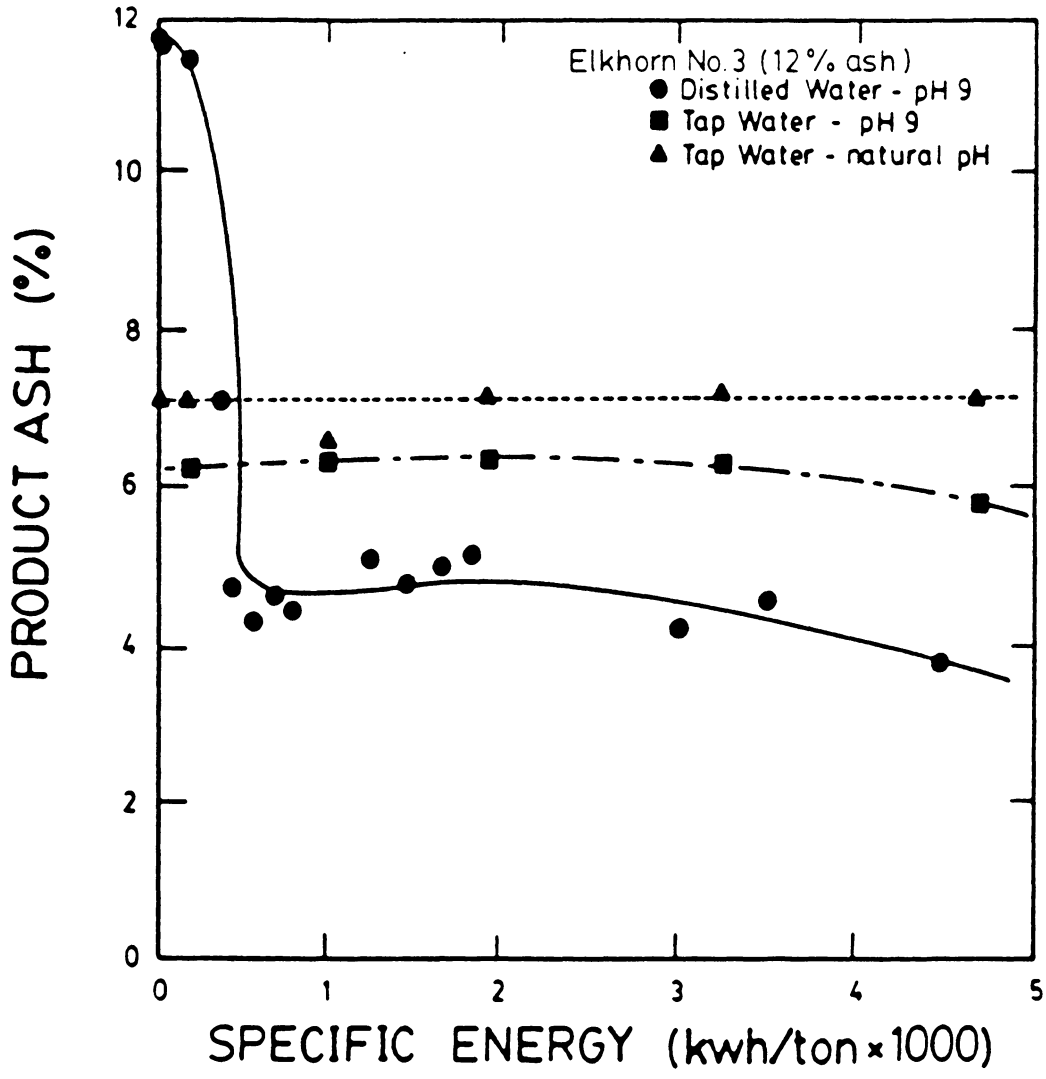

Figure 3.18 The effect of specific energy input on product ash percent for 3 media conditions; specific energy accumulated over 3 cleaning stages.

kwh/ton. In the case of distilled water, product ash decreased sharply from 11.8% at 10 kwh/ton to 4.5% at 500 kwh/ton, which corresponds to the large increase in recovery incurred at the same energy input. A plot showing separation efficiency versus specific energy in Figure 3.19 resembles the plot obtained for clean coal recovery. The lowest specific energy value obtained using distilled water, which resulted in a maximum separation efficiency value of approximately 55%, was 500 kwh/ton accumulated over 3 stages of treatment. However, present work involving the design and operation of a continuous selective-shear coagulation process for coal has found that only 25% of the above specific energy value is needed to produce similar results. In the case of tap water, energy applied during the grinding step appears to be sufficient enough to induce the selective coagulation of a coal slurry.

3.4 Discussion

The coagulation rate of particles in a slurry is a function of the collision rate or frequency and the number of collisions between particles which result in adhesion. Determining factors which dictate whether two particles will attach after collision are the magnitudes of the van der Waals, electrostatic repulsive, and hydrophobic

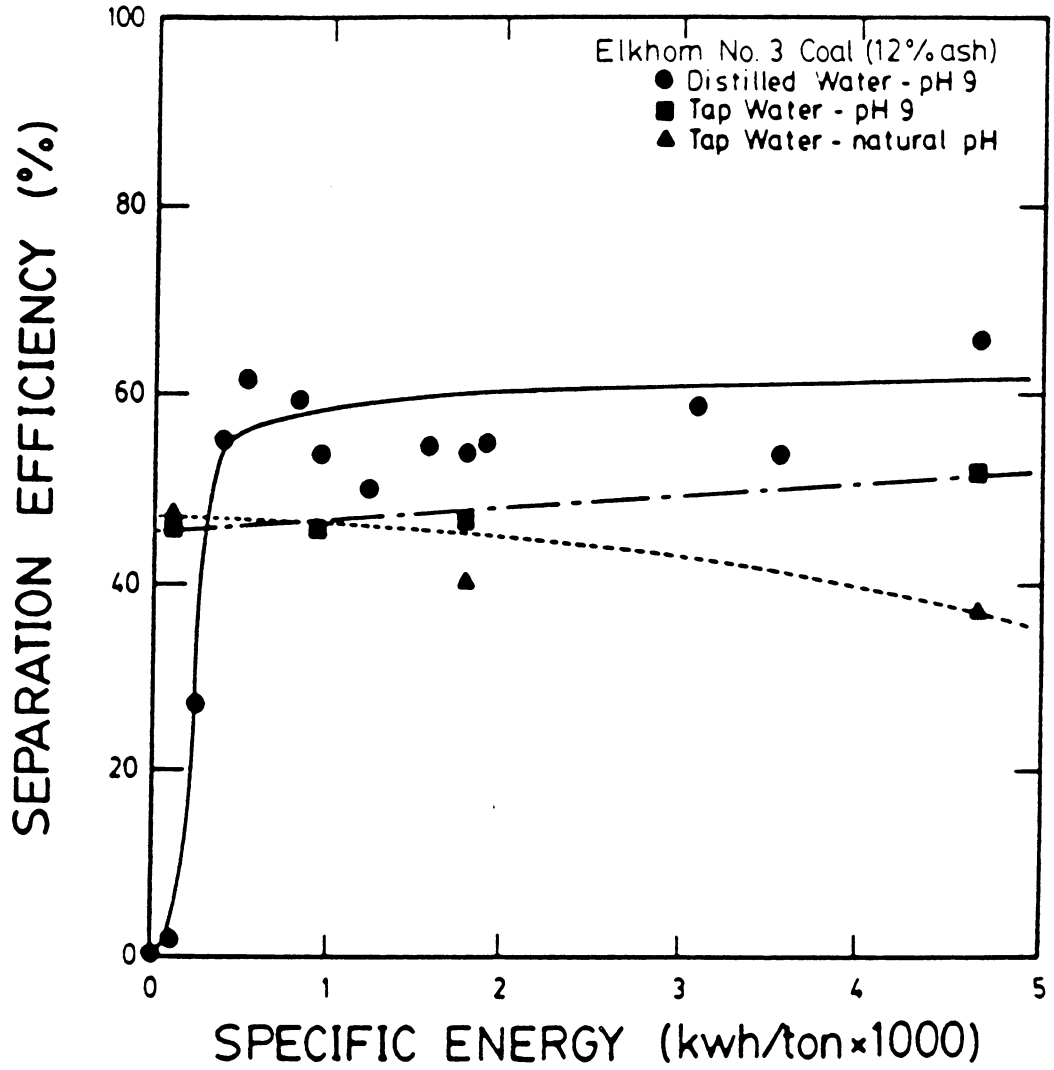

Figure 3.19 The effect of specific energy input on separation efficiency for 3 media conditions; specific energy accumulated over 3 cleaning stages.

interaction forces (Warren, 1977). The collision rate can be determined by using Levich's equation for turbulent conditions as follows:

$$J = 12 \pi r^3 n^2 (e/\eta)^{1/2}, \qquad [3.2]$$

where J is the turbulent collision rate, n is the initial number of particles per unit volume of slurry, r is the radius of a single particle, B is a constant, e is the energy loss per second per unit volume, and η is the kinematic viscosity (Warren, 1981). Analysis of Eq. [3.2] indicates that the collision rate can be improved by increasing the particle concentration, particle size, and shear rate.

The effect of increasing the percent solids or particle concentration determined experimentally is shown in Figures 3.6 for Cedar Grove coal and 3.7 for Elkhorn No. 3 coal. Both plots indicate an increase in clean coal recovery as the percent solids was increased. This result correlates well with predictions from Eq. [3.2], which indicates that an increase in percent solids increases the collision rate, hence increasing recovery.

By first appearance, Eq. [3.2] indictates that by increasing the particle size, the collision rate is increased. This would result in an increase in coal recovery. However, if the mass of the system was kept

constant and the particle size was increased, the number of particles per unit volume would be substantially decreased. For example, assuming spherical particles and maintaining the same percent solids, decreasing the particle size from 14 to 4 microns increases the collision rate by a factor of 43 (Appendix I). Therefore, Eq. [3.2] indicates a decrease, rather than an increase, in collision rate with an increase in particle size, hence decreasing coal recovery at a constant particle concentration. Also, inertia may be another force that may reduce recovery as the particle size is increased, especially under turbulent conditions.

Experimental results showing that coal recovery decreases with increasing particle size are shown in Figure 3.8. Recovery dropped from 94% at 4.4 microns to 73% at 14.5 microns for an Elkhorn No. 3 coal sample (12% ash). Since clean coal recovery improves with decreasing particle size, complete liberation of the mineral matter can be achieved, while at the same time increasing the efficiency of the process. Also, the recovery of the coarser material could possibly be improved by increasing the percent solids, which would increase the collision rate. In fact, a mixture of fine and coarse particles may be beneficial. Warren (1981) found that a slurry containing 1-micron and 20-micron scheelite particles aggregated much faster than a

pure 1-micron scheelite suspension. This observation suggests that small particles will more likely adhere to large than to small particles. In Figure 3.8, product ash percent dropped sharply with decreasing particle size until it levelled off at 1.6%, which corresponds to approximately 6 microns. At this particle size, it appears that most of the mineral matter was liberated, except for a small amount of finely disseminated pyrite particles. Therefore, since clean coal recovery, product ash percent, and sulfur reduction improves with decreasing particle size, the selective coagulation process seems to have an excellent ability to produce superclean (< 2% ash, < 0.80% sulfur) and ultraclean coal (< 1% ash).

Shear rate is another parameter which can be used to both increase the collision rate of particles and overcome the energy barrier provided by the electrostatic repulsive force, which would permit coagulation in the primary minimum. In Figure 3.20, the shear coagulation domain is established for 1-micron particles as a function of shear rate and zeta potential (Warren, 1982). The plot indicates that coagulation in the primary minimum, which is stable and irreversible, occurs at very low shear rates for low zeta potential values. However, as the zeta potential increases, the shear rate required for primary minimum coagulation increases as a result of the enlarging DLVO

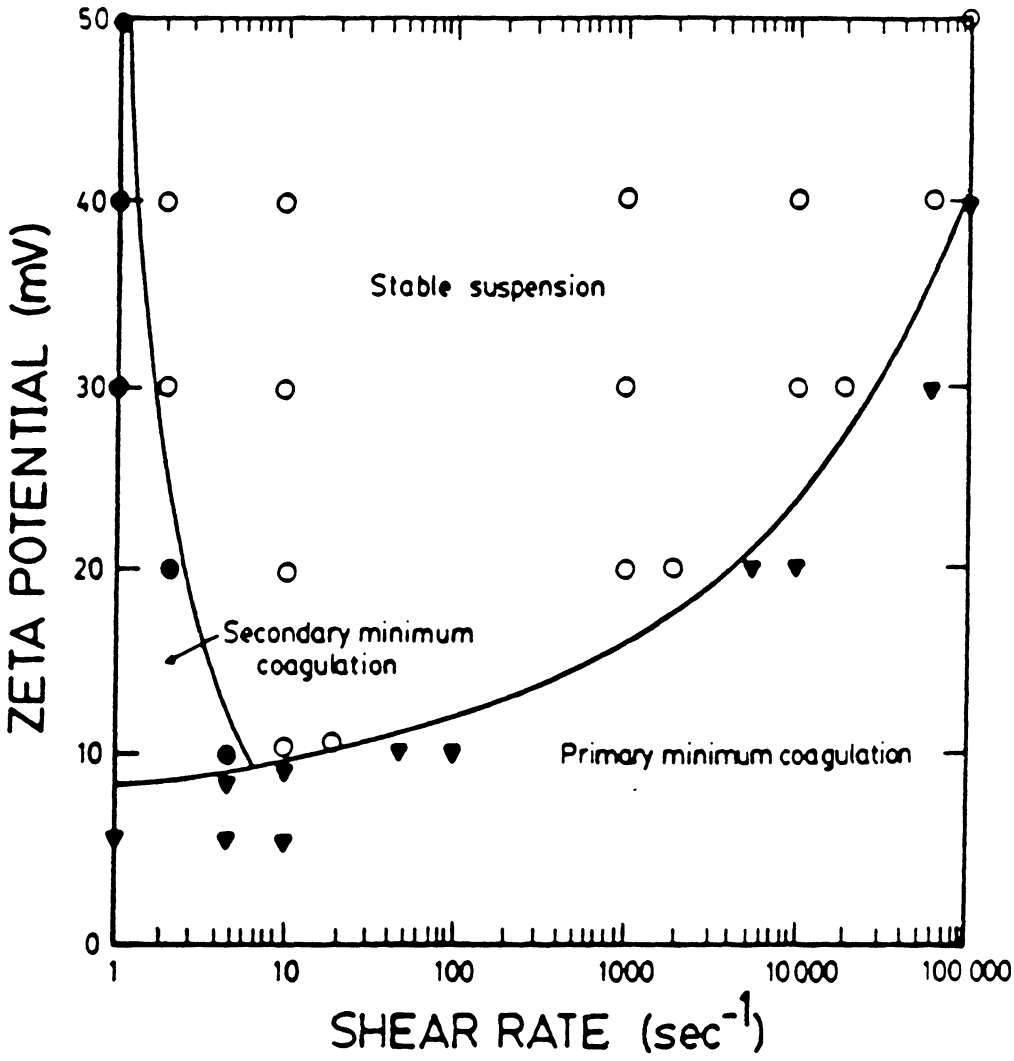

Figure 3.20 Shear coagulation domain for 1 micron particles as a function of shear rate and zeta potential (Warren, 1982).

energy barrier. Secondary minimum coagulation, which is reversible, occurs only at low shear rates due to the instability of the coagula. Van de Ven and Mason (1976) established that a colloidal suspension is unstable at very low shear rates due to aggregation in the secondary minimum, stable at intermediate shear rates because hydrodynamic forces are large enough to push the particles out of the shallow secondary minimum, and unstable at high shear rates because the hydrodynamic forces are more than large enough to overcome the DLVO energy barrier and allow the particles to coagulate in the primary minimum.

For the coal slurry system investigated, coagulation of the coal particles having a low surface potential was very non-selective due to the fairly low repulsive forces existing between the coal and ash particles, which inhibits heterocoagulation. Selectivity improved when the surface potential of the particles was increased. For this reason, high shear rates were required to overcome the DLVO energy barrier in order to selectively coagulate a coal/mineral matter slurry with distilled water as the medium. Figures 3.16 and 3.17 show that in the case of distilled water, 500 kwh/ton of energy is needed to obtain the results illustrated for 3 stages of treatment, or 167 kwh/ton to simply coagulate the coal slurry.

Using tap water instead of distilled water as the slurry medium found that little, if any, additional energy beyond that applied during grinding was needed for the initial stage of treatment (see Figures 3.17 through 3.19). Additional stages required a small amount of mechanical agitation to break up the coal coagula in order to release entrained material and to re-coagulate the suspension. The decrease in the specific energy requirement, when using tap water as the medium, was due to a decrease in the electrostatic repulsive force in the presence of specifically adsorbing ions, as indicated in Chapter 2 by a decrease in the zeta potential values. Figure 3.21 depicts the effect of a decrease in potential on the magnitude of the DLVO energy barrier for 1-micron particles (Wiese and Healy, 1970). The diagram is a plot of the total potential energy of interaction versus the distance between two sperical particles. Calculations were made using the classical DLVO theory and the constant potential assumption. The plot demonstrates that a decrease in surface potential decreases the magnitude of the DLVO energy barrier and, hence, the amount of mechanical energy required for primary minimum coagulation. Therefore, media containing counter ions require less mechanical energy for effective coagulation.

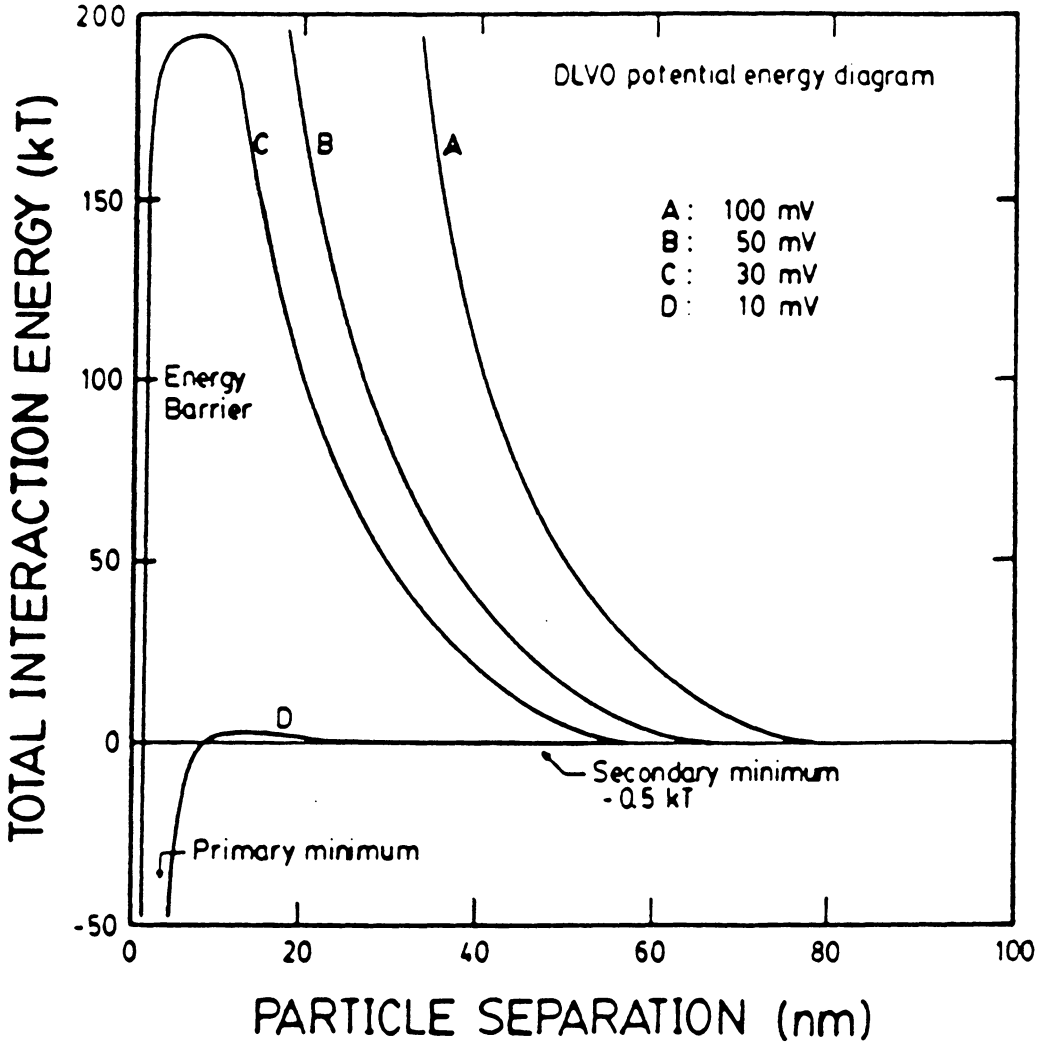

Figure 3.21 Total potential energy of interaction between particles of 1 micron diameter in 0.001 M electrolyte, as calculated by DLVO theory - constant potential assumption (Wiese and Healy, 1970).

3.5 Summary and Conclusions

1. The selective shear coagulation process appears to be an excellent technique for treating ultrafine coal. Results, presented over a particle size range of 4 - 15 microns, indicated that the process improved with decreasing particle size. Therefore, complete liberation of the mineral matter can be achieved without hindering the process efficiency. This makes the selective coagulation process very applicable in the production of superclean and ultraclean coals.

2. Entrapment is a major problem in every agglomeration and flotation process. The selective coagulation process is no exception. Multiple stages of treatment, normally around eight, were found to be needed in order to totally remove the liberated material from the clean coal product.

3. Hydrodynamic forces proved to be very important in controlling the collision rate (where collision rate determines coagulation rate) and, hence, the recovery of the agglomerated material. Increasing the particle population density or percent solids increased the coal recovery because of a rise in the

collision rate. The upper limit on percent solids was found to be controlled by hindered settling, which increased the problem of entrapment. The optimum value, where the product ash percent was lowest and the coal recovery was highest, was determined to be around 2%. Decreasing the slurry particle size was also found to increase the collision rate.

4. A fairly large amount of mechanical energy was required to selectively coagulate a coal slurry having a medium of distilled water. However, for a medium of tap water, the energy applied to the system during grinding was sufficient enough to induce coagulation.

CHAPTER 4

A CONTINUOUS ELUTRIATION COLUMN FOR THE SELECTIVE-SHEAR COAGULATION PROCESS

4.1 Introduction

The selective-shear coagulation process shows promise as an advanced physical beneficiation technique for mixtures of minerals which are too fine (< 10 microns) for conventional flotation (Trahar and Warren, 1976). An example of selective coagulation by pH control was reported by Maynard et al. (1969) where titanium particles selectively coagulated and settled out, leaving a purified bright clay suspension. Another slurry mixture treatable by the coagulation process is coal and mineral matter, the coagulation of which involves the selective agglomeration of the coal particles by hydrophobic interactions. Once the material is coagulated, separation of the valuable mineral and the gangue mineral must be accomplished. This separation must be done under conditions of low mixing or turbulence due to the weak strength of the coagula. A separation technique which operates under fairly quiescent conditions involves the use of an upward current of wash water.

Elutriation is a technique for sizing materials in the range of 10-110 microns. The particle size separation is

based on the terminal settling velocity of the particulates, which can be calculated using Stoke's equation. In this elutriation technique, the upward velocity of the water was adjusted so that it exceeded the settling velocity of the mineral matter but was lower than that of the coagula. The coal coagula settled to the bottom of the column as the product. A major problem in all agglomeration processes is entrapment of the dispersed material in the agglomerates. However, the elutriation technique minimizes entrapment by gently agitating the agglomerates by the rising flow of wash water.

There are several reports which describe the elutriation technique for the separation of selectively flocculated material from the dispersed material. Read (1971) reported an efficient upgrading of flocculated hematite by agitation in a rising stream of wash water using an elutriation column. Appleton et al. (1975) achieved similar results by using an elutriation column for a system consisting of selectively flocculated cassiterite and a quartz powder suspension. Friend et al. (1973) also used the technique when investigating the selective flocculation of a quartz/calcite mixture.

In the present work, an elutriation column has been constructed and studied for its application to the separation of selectively coagulated coal particles from a

coal/ash suspension. The effect of operational parameters such as feed rate, elutriation water rate, percent solids and cell dimensions have been studied in order to fully characterize and enhance understanding of the elutriation column.

4.2 Process Description

Figure 4.1 shows the flowsheet for the process, which consisted of grinding, selective coagulation, and the separation of coagulated coal from dispersed mineral matter in the elutriation column. Coal slurry, having a percent solids of 35%, was fed into an attrition mill, where the material was ground to a mean size of 3 microns, as determined by an Elzone 80-XY particle size analyzer. The ground slurry was sent to a holding sump, where the percent solids was adjusted to 2% by the addition of tap water. The system was operated at the natural pH of the slurry, which was approximately 7-8. The coal slurry was then pumped at a rate of 50 ml/min to a 6-inch diameter mixing vessel, which contained four 1/4-inch baffles placed vertically along the cell wall 90^{o} apart. The slurry was mixed to induce coagulation using a 3-inch diameter shear impeller at 1800 rpms. The slurry level in the mixing vessel was maintained at 1000 ml, which provided a retention time of 20 minutes. From the mixing stage, the

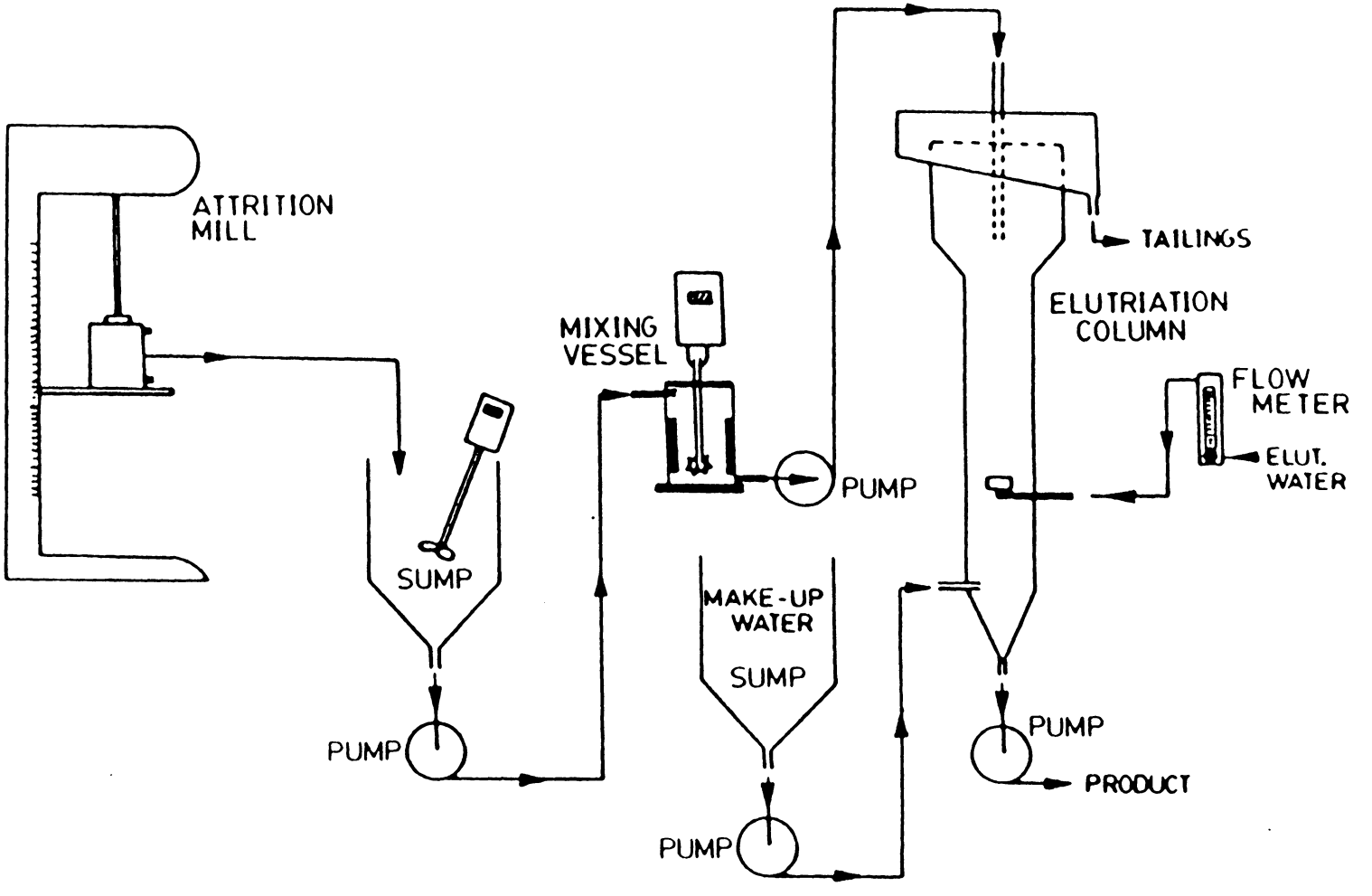

Figure 4.1 Flowsheet for the continuous selective coagulation/elutriation process.

selectively coagulated coal slurry was transported to the elutriation column, where the agglomerated coal particles were separated from the dispersed ash particles. The clean coal product from the column underflow and the tailings from the column overflow were sampled periodically in order to ensure that steady-state conditions were obtained.

Figure 4.2 shows the elutriation column designed for this investigation. The selectively coagulated slurry was fed into the column 9 inches from the top, where the column diameter increased from 4 to 8 inches. Feed rate was normally operated at 50 ml/min. The elutriation water was added 25 inches down from the feed point at a rate of 400 ml/min using a circular disperser resembling a sprinkler. The product was extracted from the bottom of the column at a rate equal to the addition of the make-up water. Hence, increasing or decreasing the rate of product extraction had no effect on the flow rates within the column. Tailings were allowed to naturally flow over the top of the column into a launder.

Increasing the column diameter in the upper section of the column decreased the velocity of the flow in that section, which allowed the coal coagula to settle, yielding a higher recovery. Therefore, higher elutriation water rates were applied, which increased the amount of agitation of the coagula. This resulted in a decrease in the amount

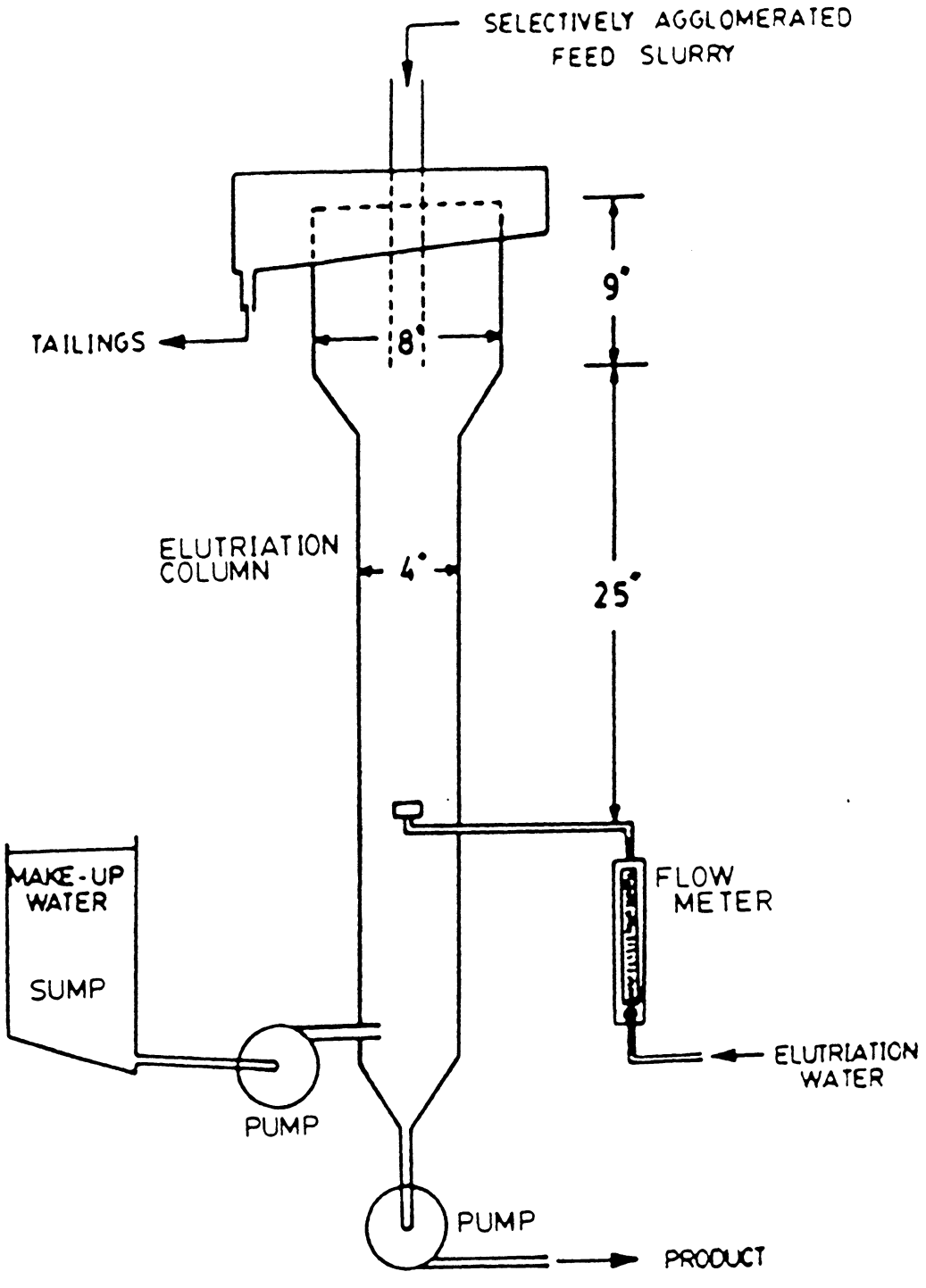

Figure 4.2 Diagram of the continuous elutriation column.

of ash being entrapped.

4.3 Experimental

The tests were performed using a run-of-mine Elkhorn No. 3 coal sample containing 12% ash and 0.81% total sulfur, of which 0.56% was organic sulfur. When the sample was received, the coal was crushed and screened at 100% passing 1/4-inch. Next, the sample was split into representative quantities of 1000 grams each by riffling, and stored in a freezer to prevent oxidation. Before each experiment, a sample was initially pulverized to a mean size of approximately 75 microns using a laboratory hammer mill. Following the hammer mill, the sample was finely ground in a stirred ball mill at 35% solids. The mean particle size, as determined by an Elzone 80-XY particle size analyzer, was 3.0 microns. The ground slurry was transferred to a sump, where the solids concentration was adjusted to 2% by the addition of tap water prior to the coagulation step. The selective coagulation of the coal slurry was achieved at the slurry's natural pH. Final samples were taken of both the product and the tailings after 120 minutes from the beginning of the experiment or after a parameter change. Each sample was analyzed for ash and sulfur content.

4.4 Results

4.4.1 Effect of Elutriation Water Rate

Figure 4.3 illustrates the effect of increasing the elutriation water rate on clean coal recovery, percent pyritic sulfur reduction, and product ash percent. After decreasing gradually with an increase in the elutriation water rate, recovery was found to drastically decrease from a value of 84% at a rate of 450 ml/min to 40% at 550 ml/min. Beyond 550 ml/min, recovery gradually approached zero as the elutriation water rate was increased. Product ash percent decreased from 7% at 100 ml/min to 4.9% at 450 ml/min, where the ash percent began increasing to 7.1% at 800 ml/min. Pyritic sulfur reduction in the product gradually increased from 20% at 100 ml/min to 30% at 450 ml/min. However, the reduction percentage sharply increased to 50% at 600 ml/min, which corresponds to the loss in coal recovery, indicating a liberation or entrapment problem. Therefore, for the cell design used and a feed rate of 50 ml/min, the optimum elutriation water rate was 450 ml/min, where the coal recovery was a high 84% and the product ash percent was the lowest at 4.90%. The corresponding pryritic sulfur reduction was 30%.

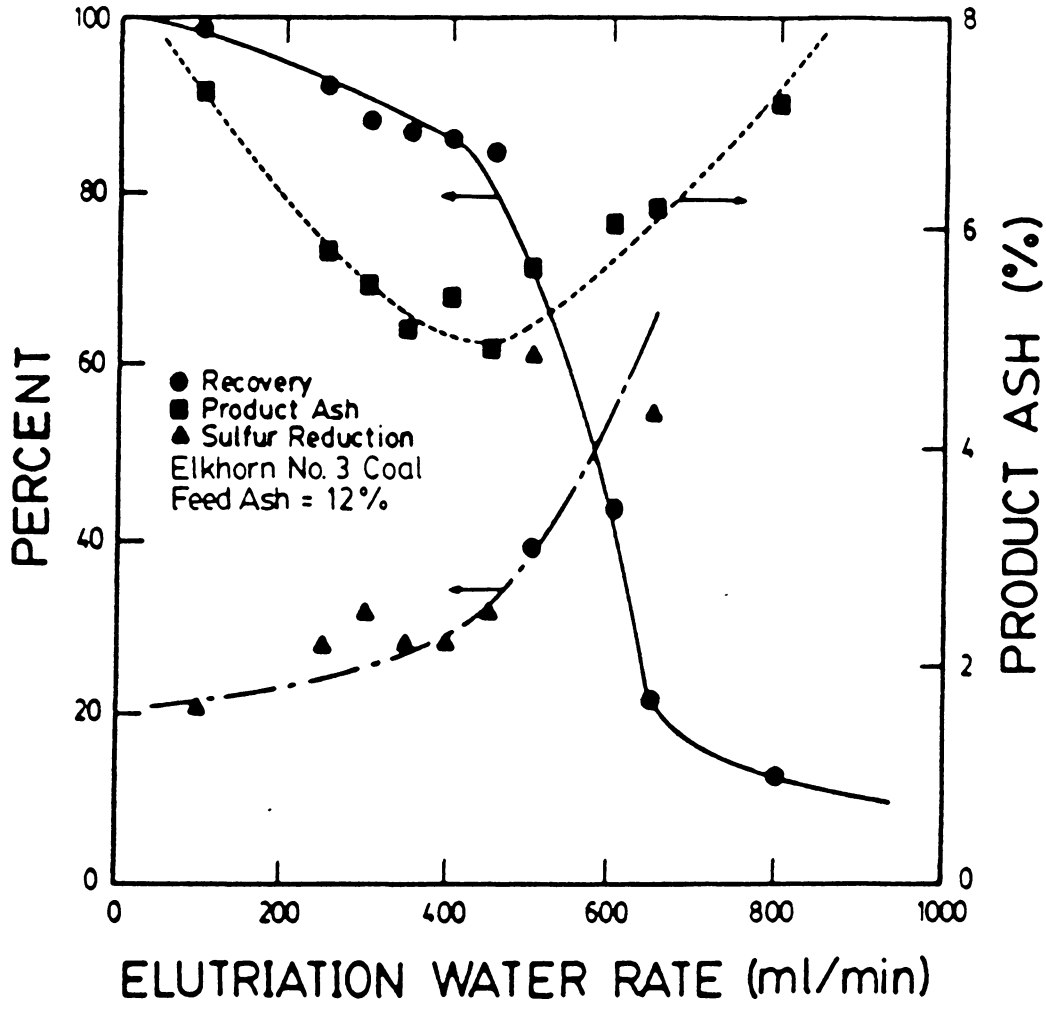

Figure 4.3 The effect of elutriation water rate on coal recovery, sulfur reduction, and product ash percent - feed rate = 50 ml/min.

4.4.2 Effect of Feed Rate

The effect of increasing the feed rate was investigated over a range of 25-150 ml/min, using an elutriation water rate of 400 ml/min. Figure 4.4 shows that as the feed rate was increased from 25 to 150 ml/min, recovery and pyritic sulfur reduction gradually decreased almost linearly from 82% to 56% and 36% to 22%, respectively. Product ash percent increased linearly from 4.8% to 7.0% over the same range of feed rates. The loss in recovery with an increase in feed rate appeared to be caused by an increase in the solids concentration within the column, hence increasing the effect of hindered settling. Also, the increase of the flow in the upper section may account for a portion of the recovery drop. The increase in product ash and sulfur content was a result of the loss in coal recovery.

Figures 4.5 and 4.6 show the changes in recovery and product ash percent at two different feed rates. Coal recovery was found to be higher for a feed rate of 50 ml/min when the elutriation water rate was between 300-500 ml/min and lower when the rate was beyond 500 ml/min. The minimum product ash values found for the feed rates of 50 and 100 ml/min were 4.90% and 5.50%, respectively. These values were obtained at wash water rates of 450 ml/min for a feed rate of 50 ml/min and 600 ml/min for a rate of 100

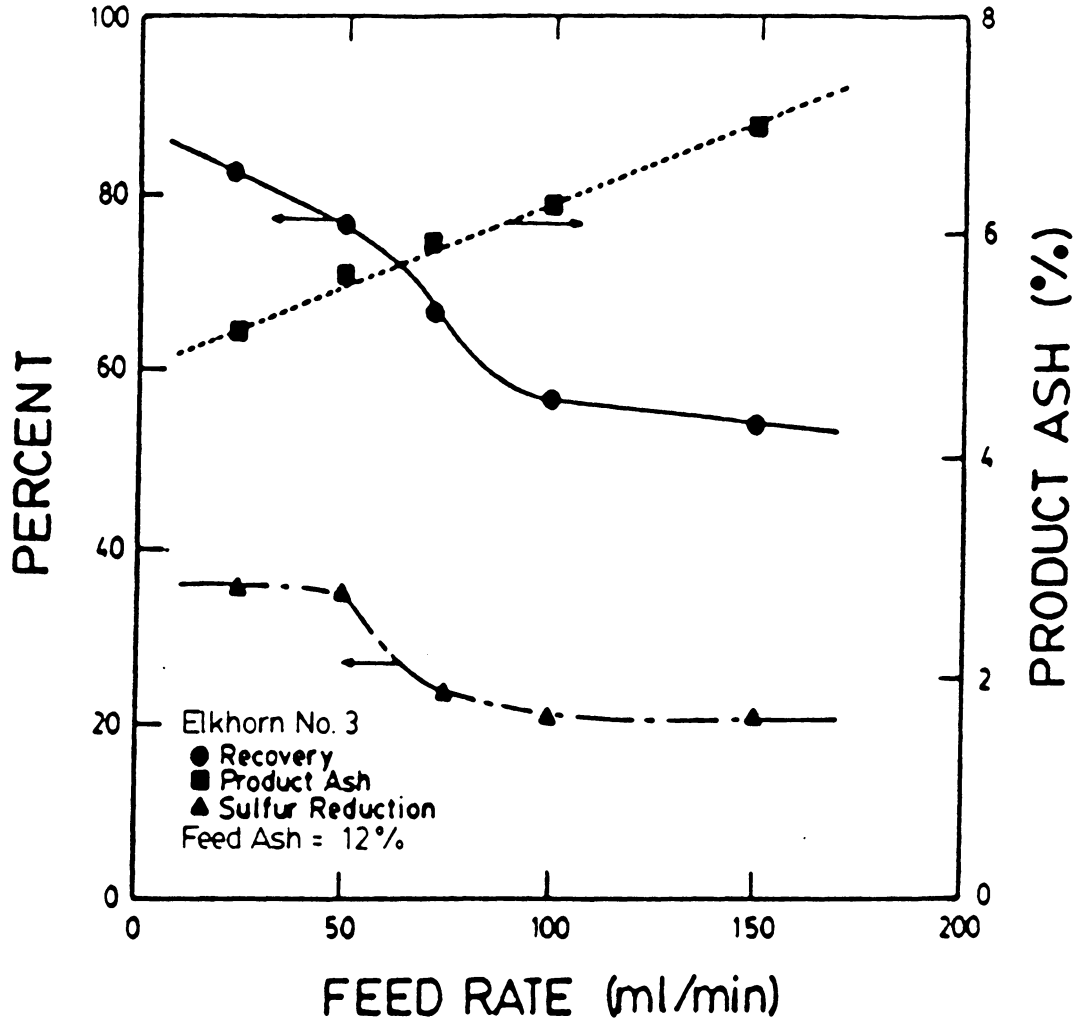

Figure 4.4 The effect of feed rate on coal recovery, sulfur reduction, and product ash percent - elutriation water rate = 400 ml/min.

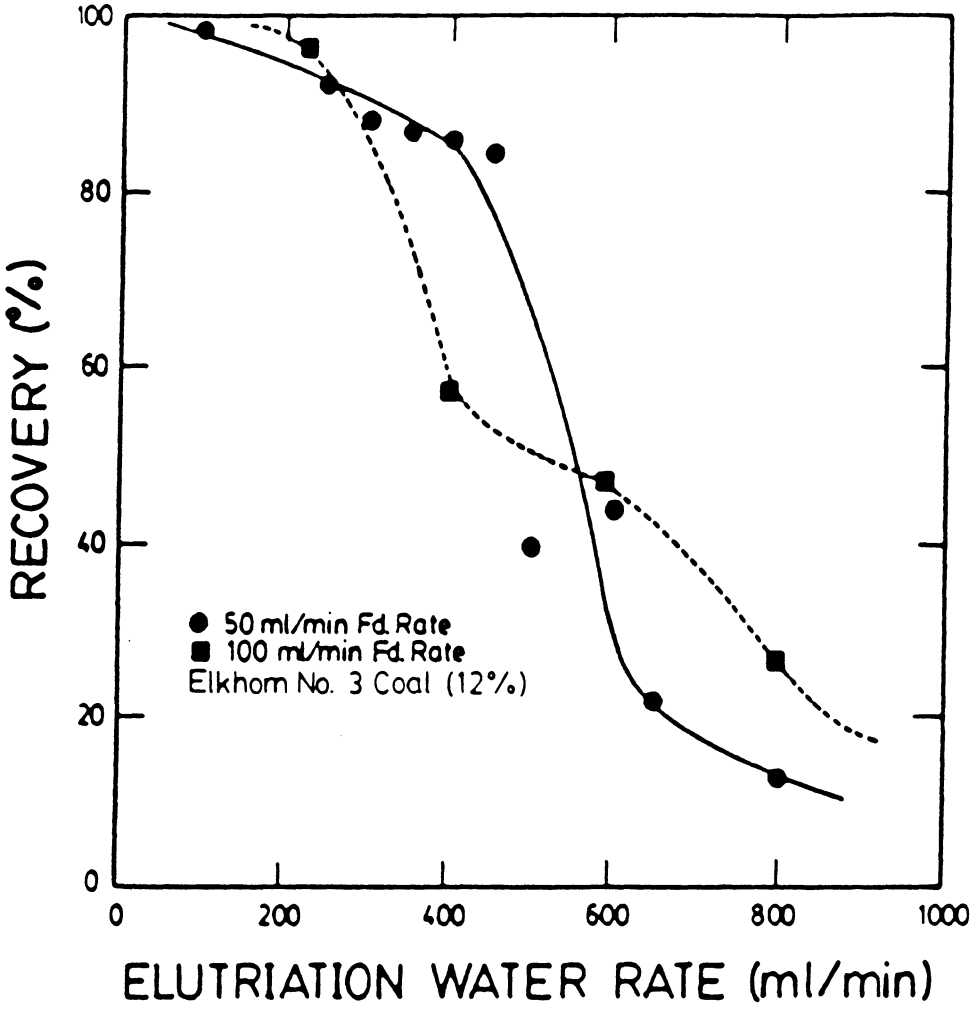

Figure 4.5 Coal recovery versus elutriation water rate curves for 2 feed rates.

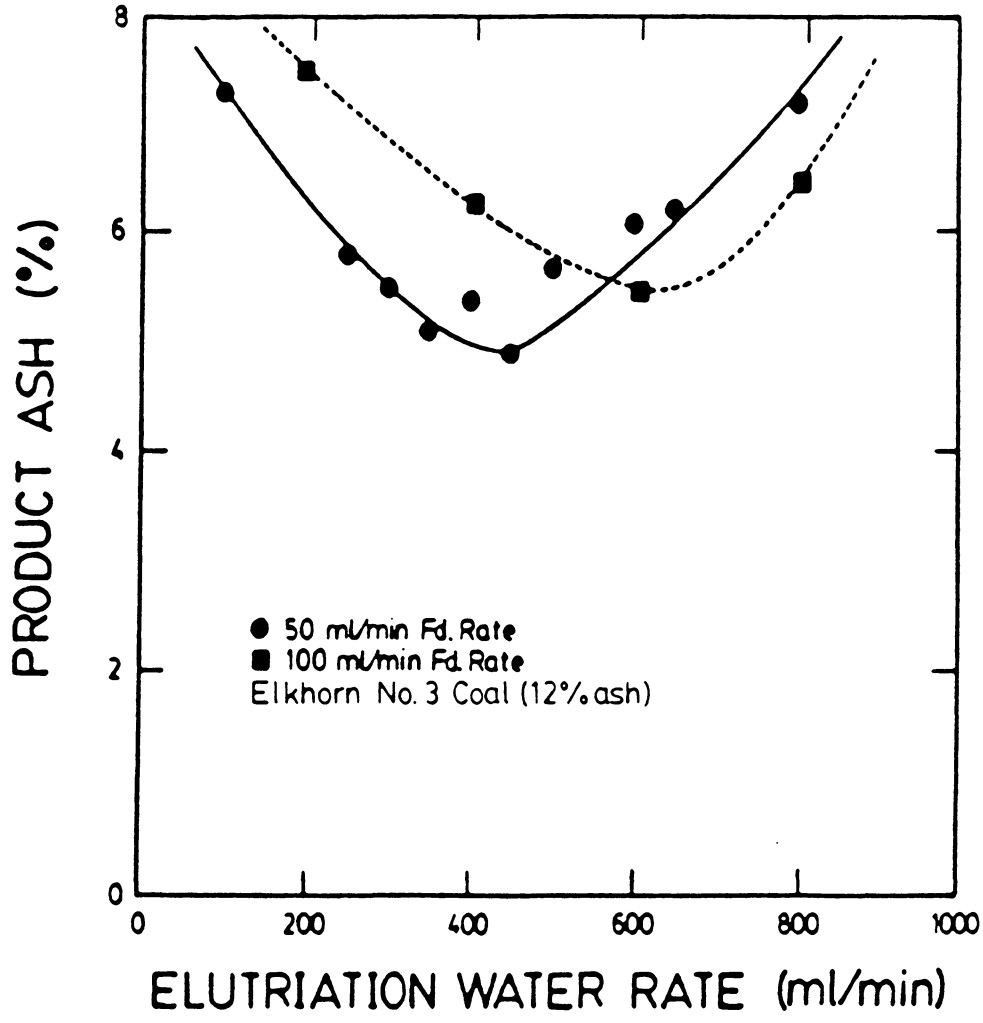

Figure 4.6 Product ash percent versus elutriation water rate curves for 2 feed rates.

ml/min. The corresponding recovery value for the 50 ml/min feed rate was higher at 85% than the value obtained for the rate of 100 ml/min, which was 47%. Therefore, the elutriation column's separation efficiency improved with a decrease in feed rate.

4.4.3 Effect of Feed Percent Solids

The effect of increasing percent solids in the feed was also examined by raising the solids content from 2% to 3%. The results, given in Figures 4.7 and 4.8 which show the changes in recovery and product ash with elutriation water rate for the two percent solids values, indicate that an increase in the feed percent solids from 2 to 3 had little effect on clean coal recovery and product ash percent.

4.4.4 Process Dynamics

A process dynamics study was undertaken by collecting product and tailing samples over a specific time interval. Recovery and product ash percent values were plotted versus cumulative time in order to determine the time interval required to reach steady-state. Figure 4.9 depicts the results using an Elkhorn No. 3 coal sample (12% ash). Clean coal recovery gradually increased from 85% at 30 minutes to 95% at 140 minutes from the time the test was started. Recovery seemed to be nearly steady-state after

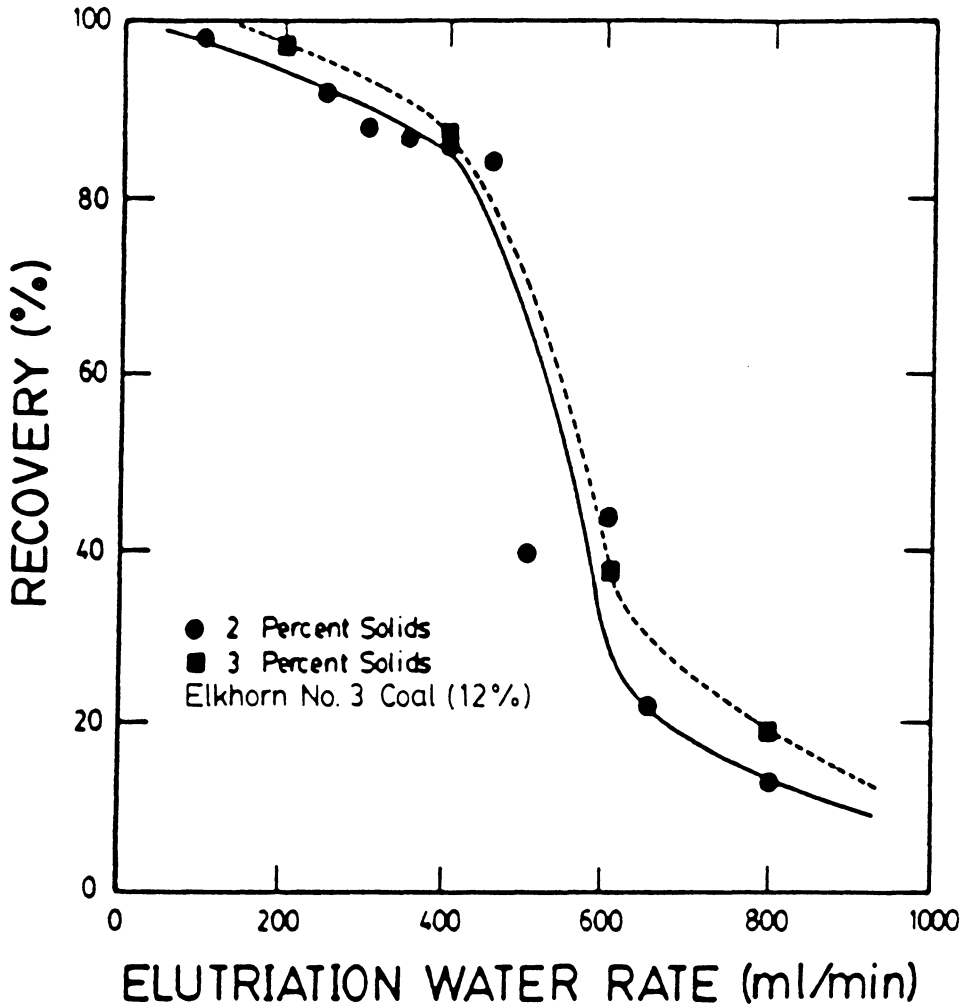

Figure 4.7 Coal recovery versus elutriation water rate curves for 2 percent solids.

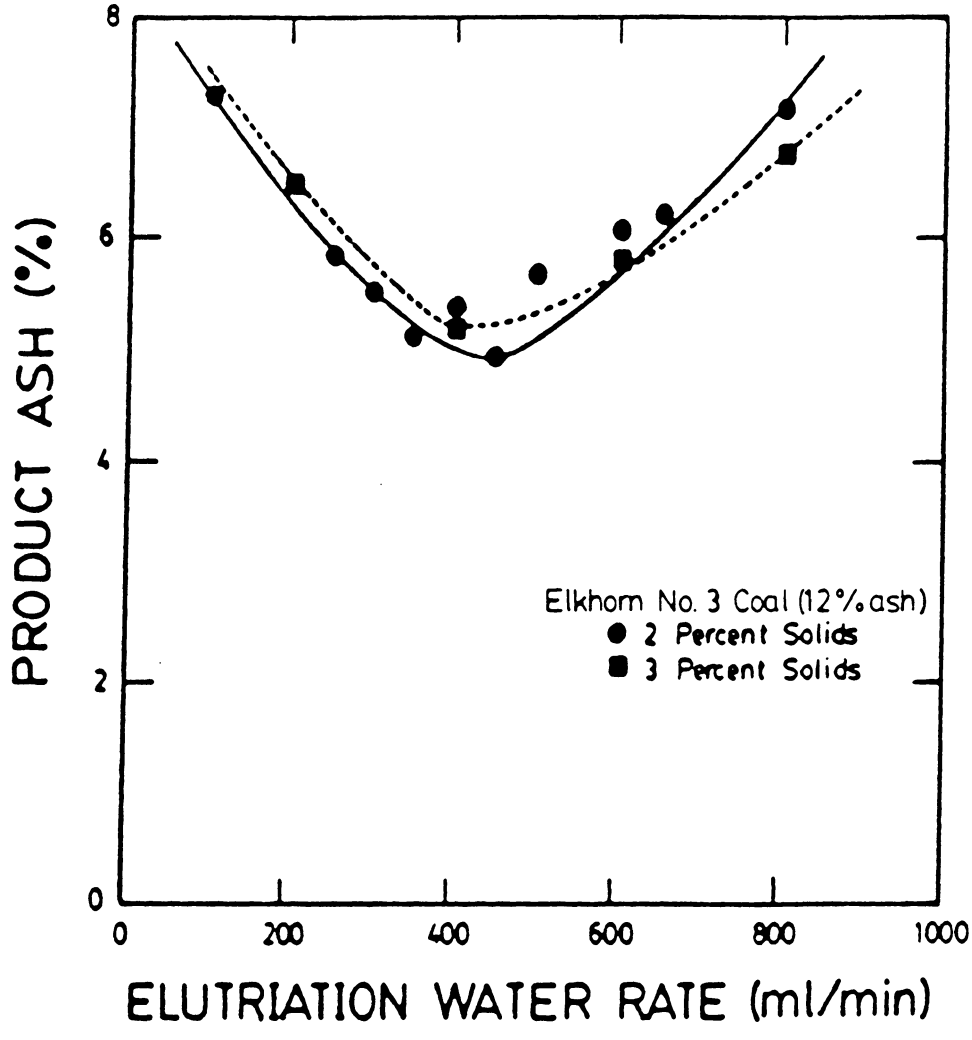

Figure 4.8 Product ash percent versus elutriation water rate curves for 2 percent solids.

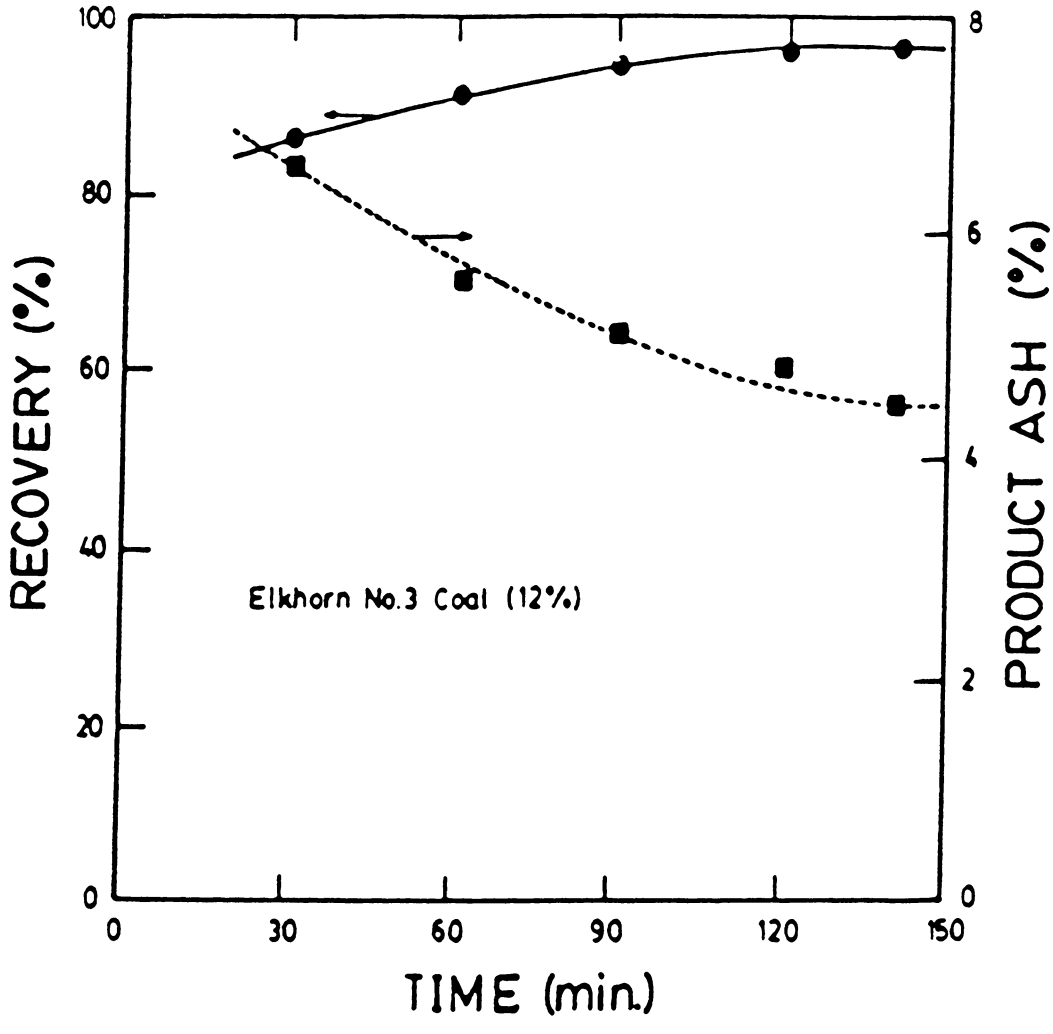

Figure 4.9 Coal recovery and product ash percent versus accumulated operation time for Elkhorn No.3 coal seam containing 12% ash.

140 minutes. Product ash decreased from 6.5% at 30 minutes to 4.5% at 140 minutes, which was probably due to the increase in recovery. Figure 4.10 shows similar results using an Elkhorn No. 3 seam coal sample, containing 1.6% ash. Recovery increased from 78% at 40 minutes to 79% at 90 minutes, where the recovery sharply rose to 94% at 160 minutes. Beyond 160 minutes, recovery remained steady at 94%. Product ash decreased slightly from 1.25% at 30 minutes to 1.0% at 220 minutes.

In Figure 4.11, clean coal recovery and product ash percent values were plotted versus mean residence time (t). The mean residence time was defined as the average time needed to fill a cell with a completely new volume. For a system containing micronized material, t represents the average time a particle spends within a cell. It was calculated by dividing the cell volume by the feed flow, which included any elutriation water used, as shown in the following equation:

$$t = V_c / (Q_e + Q_f), \qquad [4.1]$$

where t was the mean residence time (min), V_c was the cell volume (ml), Q_f was the feed flow rate (ml/min), and Q_e was the flow rate of the elutriation water (ml/min). This definition of mean residence time was used when dealing with micronized material, where the particles tend to follow the

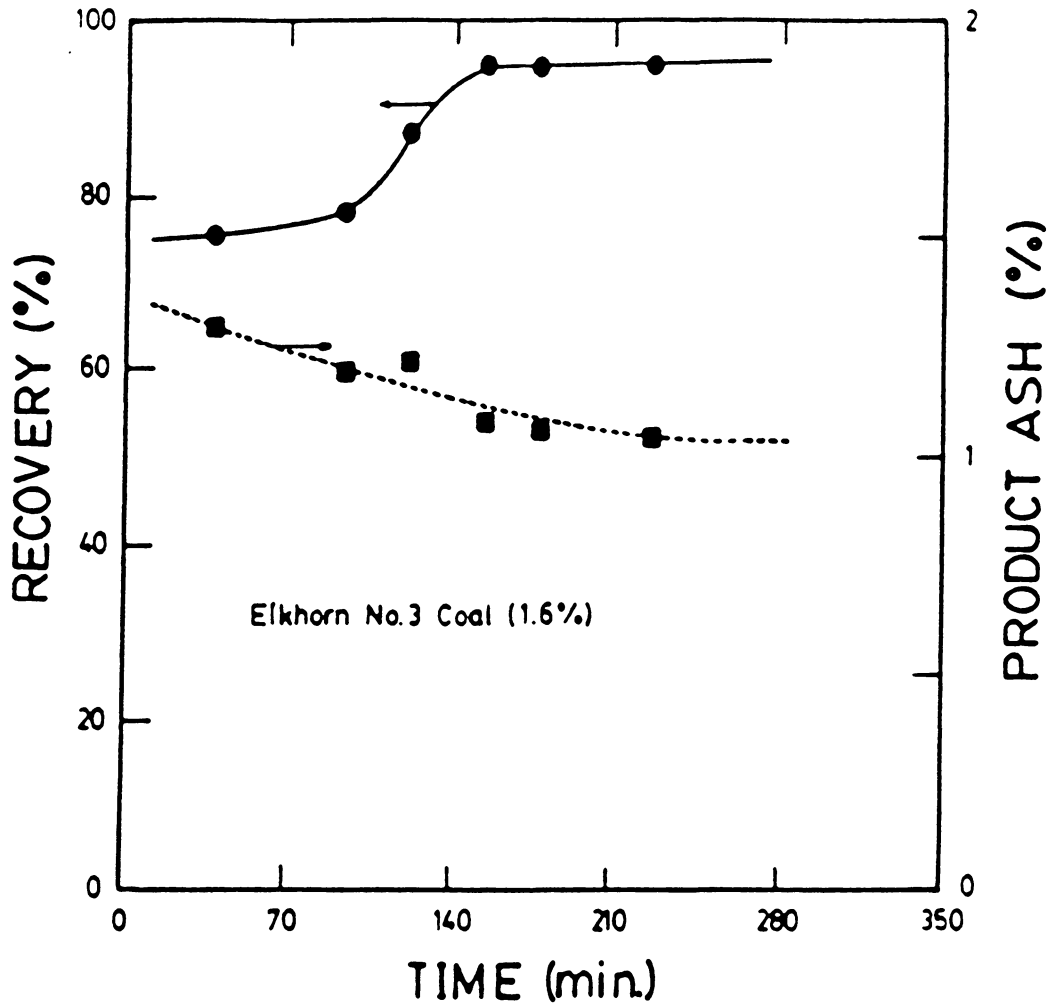

Figure 4.10 Coal recovery and product ash percent versus accumulated operation time for Elkhorn No.3 coal seam containing 1.6% ash.

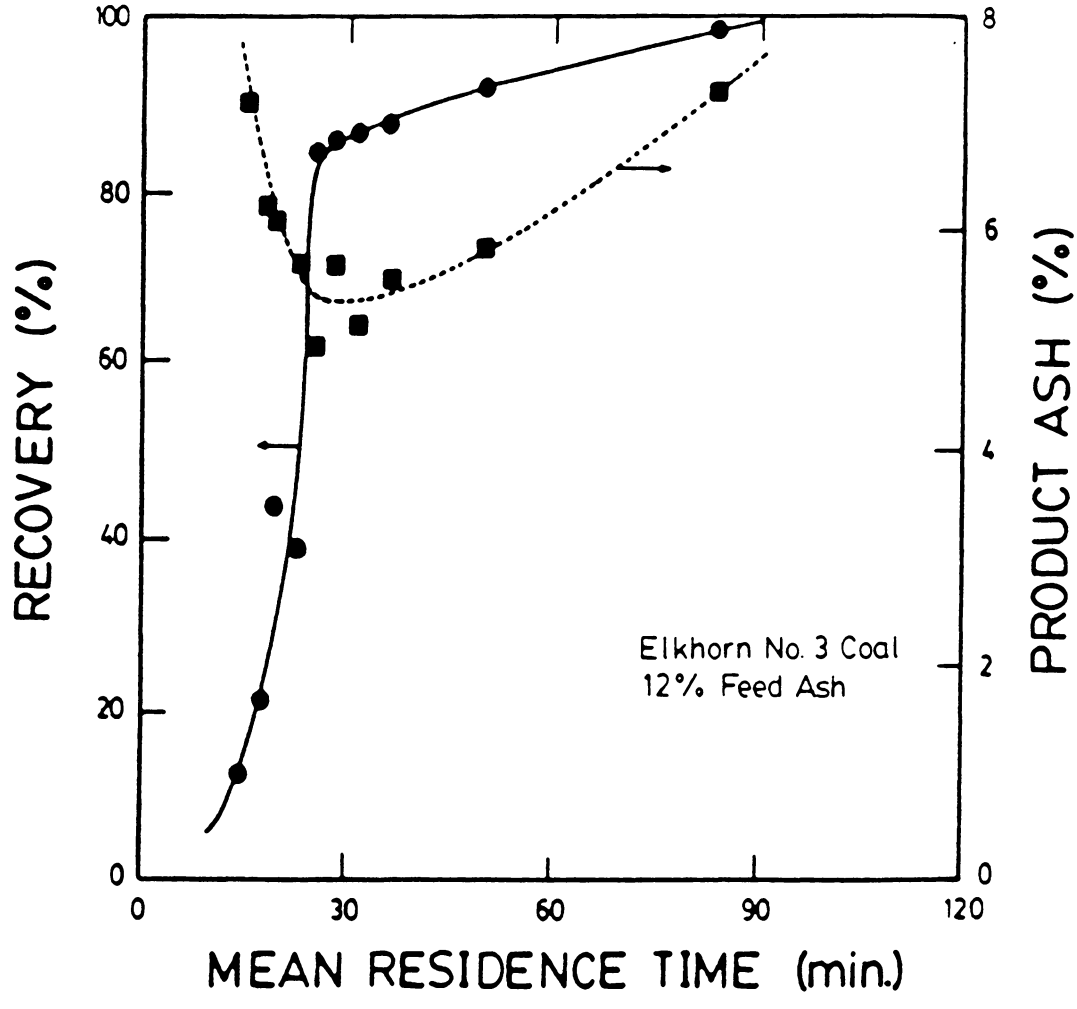

Figure 4.11 Coal recovery and product ash percent versus mean residence time in the column.

flow of the medium.

By applying Eq. [4.1] to the previous results, the mean residence time of the coal coagula was calculated and plotted against coal recovery as in Figure 4.11. As shown, recovery sharply increased from 12% at 15 minutes residence time to 84% at 28 minutes, which was followed by a gradual increase to 98% after 80 minutes. This indicates that the mean residence time for the coal coagula needed for sufficient recovery was approximately 28 minutes. The product ash initially decreased from 7.1% at 15 minutes to 4.9% at 28 minutes, resulting from an increase in coal recovery. Beyond 28 minutes, product ash gradually increased to 7.1% at 80 minutes. This result illustrated that as the mean residence time was increased, the particles had more time to settle, hence allowing both coal and ash material to settle out. Therefore, coal recovery and product ash percent increased with increasing residence time. The optimum mean residence time, which represents the minimum product ash of 4.9%, appeared to be around 28 to 30 minutes, where coal recovery was 85%.

Some of the results obtained using the selective-shear coagulation/elutriation column process are listed in Table 4.1. All of the results represent one stage of treatment. High coal recovery values and respectable ash reductions were found for each of the coal samples studied.

TABLE 4.1 : SELECTIVE COAGULATION/ELUTRIATION PROCESS RESULTS

Sample	Feed Ash (%)	Product Ash (%)	Ash Red. (%)	Coal Recovery
Elkhorn No.3	12.0	4.50	62.5	95
Elkhorn No.3	1.6	1.00	37.5	95
Elkhorn No.3	1.3	0.75	42.3	85

4.5 Discussion

4.5.1 Operational Parameters

Clean coal recovery was affected by both elutriation water rate and feed rate. The nature of the effect was a change in the superficial velocity within the column. As the upward velocity in the column was increased, recovery decreased. A change in the wash water rate was found to be more sensitive toward recovery due to the effect on the superficial velocity throughout the column. A change in feed rate affected the upward velocity above the feed point, thus influencing only the coal coagula in the upper portion of the cell.

The sudden drop in recovery experienced when the elutriation water rate was increased beyond a specific value can be explained by comparing the superficial velocity within the column to the settling velocity of the coal coagula. The settling velocity of a particle is a function of particle size and material density, as indicated by Stoke's equation:

$$v_t = d^2 g (\rho_s - \rho_f)/(18 \eta), \qquad [4.2]$$

where v_t is the particle terminal velocity, d is the particle diameter, g is the acceleration due to gravity, ρ_s and ρ_f are the density of the solid and medium,

respectively, and η is the medium viscosity. An analysis of Eq. [4.2] yielded the plot in Figure 4.12 of settling velocity versus particle diameter for various solid densities between 1.3 gm/cm^3 (typical for coal) and 2.3 gm/cm^3 (typical for coal mineral matter). The plot indicates that the effect of solid density effect is small for ultrafine particles (< 10 microns). As the particle diameter was increased, the solids density became increasingly important. The plot also shows the square power effect of particle diameter on settling velocity. The importance of the settling velosity is that if the settling rate of a coal coagulum is greater than the upward velocity of the wash water, the coagulum will settle to the underflow of the column (product). If the settling velocity is less, the coal coagulum will report to the overflow (tailings).

Another important parameter controlling the settling velocity of a particle is the solid concentration of the slurry. As the solid concentration is increased, a particle settling velocity will become more and more hindered by neighboring particles. An empirical equation was developed by Richardson and Zaki (1954), which corrects the settling velocity for hindered settling as shown below:

$$V_s = V_t (1 - C)^{3.65}, \qquad [4.3]$$

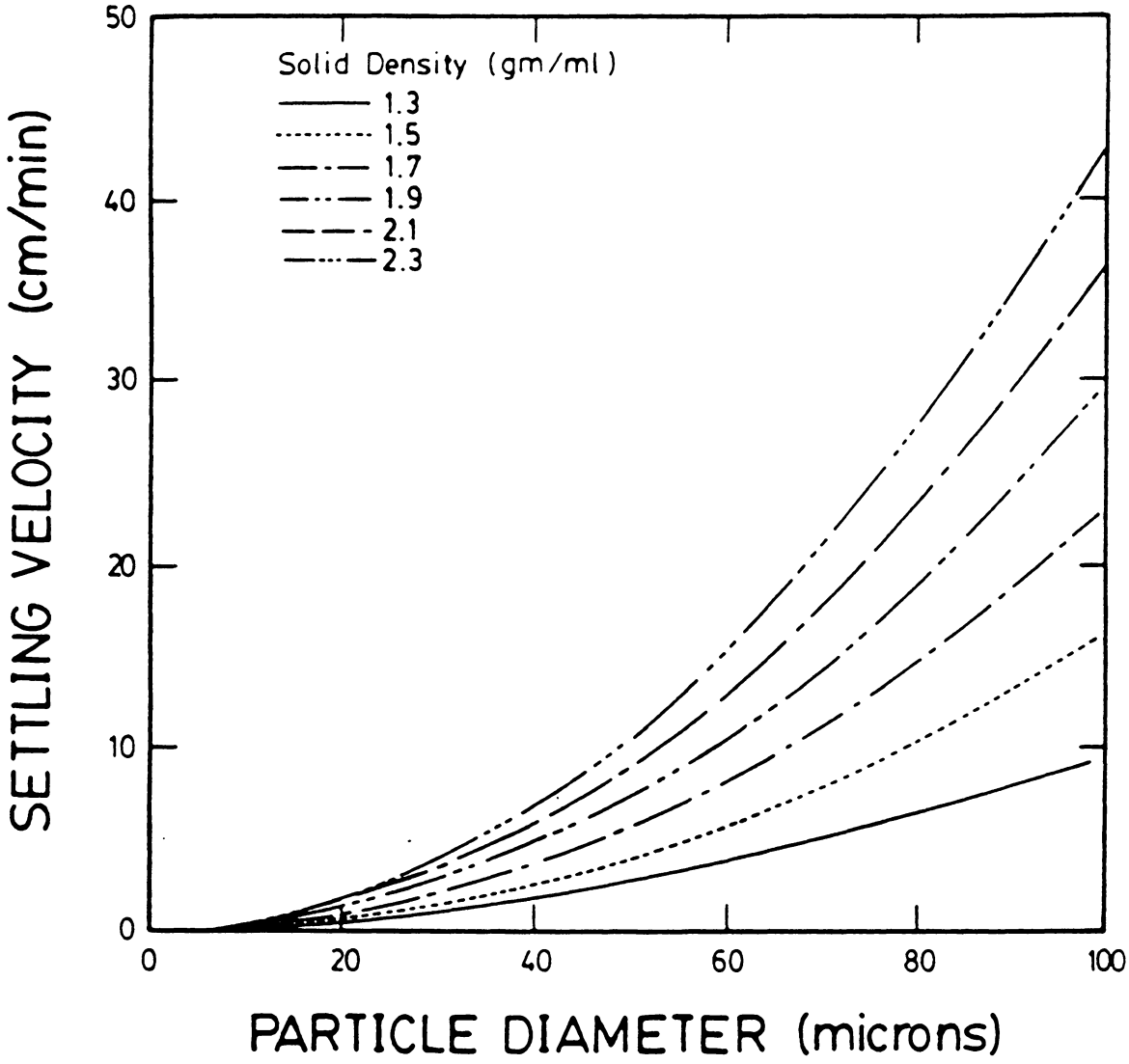

Figure 4.12 The effect of particle diameter and solid density on particle settling velocity according to Stoke's equation.

where V_s is the particle settling velocity after the hindered settling correction, V_t is the particle terminal settling velocity determined from Stoke's equation, and C is the volume concentration of solids.

The terminal settling velocity for a 75-micron coal coagulum was calculated as 5.5182 cm/min. The superficial velocity in a 4-inch section of column when using a 400-ml/min wash water rate was 4.9338 cm/min, which was less than the terminal settling velocity of the coagulum. Therefore, a high coal recovery was expected under the given conditions, which was found to be experimentally correct, as shown in Figure 4.3. Using 800 ml/min, the upflow velocity below the feed point was 9.86766 cm/min, which was much higher than the settling velocity of the coagulum. Hence, a low recovery of 10% was obtained experimentally when using 800 ml/min of wash water.

A simple analysis like the one above cannot solely explain the experimental results obtained for product ash percent. The terminal settling velocity for a 5-micron particle was 0.08166 cm/min. For a wash water flow rate of 400 ml/min, the resulting upflow velocity was 4.9338 cm/min, which was nearly two orders of magnitude greater than the settling velocity of the 5-micron particles of mineral matter. Even at an elutriation water rate of 100 ml/min, the upward velocity was still much greater at

1.2336 cm/min. As evident from Figure 4.12, an efficient separation of the coal coagula (75 microns, 1.3 gm/cm^3) and the particles of mineral matter (5 microns, 2.3 gm/cm^3) should be attainable by sedimentation without elutriation water. Therefore, the mineral matter particles were expected to be completely washed out of the overflow. However, complete removal of the ash material was not attained, as shown in Figures 4.3 and 4.4.

Two possible reasons for the product ash percent values obtained experimentally are the entrapment of particles consisting of mineral matter in the coal coagula, which is a common problem in all selective agglomeration processes, and the entrainment of the mineral matter in the water recovered in the product which would be a result of column mixing.

Another possible explanation is related to the velocity profile of the column. The superficial velocity calculated in the above discussion is actually the average velocity in the column. The largest velocity is found in the very center of the column and the lowest velocity is located around the inside circumference of the column. Depending on the magnitude of the lowest velocity, some particles of mineral matter could be settling into the product from around the sides of the elutriation column.

Product ash percent was found to decrease when the

elutriation water rate was increased from 0 to 450 ml/min (Figure 4.3). This trend may have been a result of the washing out of the coarse particles of mineral matter. For example, a 30-micron particle of mineral matter has a terminal settling velocity of 3.8280 cm/min. For an upflow rate of 300 ml/min, the superficial velocity in a 4-inch column is 3.7020 cm/min. Therefore, the 30-micron particles have a net downward velocity, especially around the sides of the column due to the velocity profile.

Another possible reason for the experimental product ash values is that the upward velocity of the wash water provides a scrubbing action which cleans the coal coagula of attached clay slimes and some of the entrapped mineral matter. An increase in the elutriation water rate would increase the intensity of the scrubbing action.

An increase in the elutriation water rate above the 450 ml/min rate yielded an increase in product ash percent (Figure 4.3). This result was likely due to the differnce in the terminal settling velocities of the clean coagula and the heavier coal coagula containing unliberated and entrapped mineral matter. As the wash water was increased, the cleaner coal coagula were washed out the overflow first due to their slower terminal settling velocities. The coal coagula containing mineral matter were recovered which yielded an increase in the product ash percent. The

increase in product ash percent obtained when the feed rate was increased, as shown in Figure 4.4, is believed to be a result of the gradual decrease in coal recovery.

Another important throughput controlling parameter is feed percent solids. The upper limit represents the concentration that induces hindered settling to a point where the particle settling velocity is less than the velocity of the upward flow of wash water. The magnitude of hindered settling can be illustrated using the Richardson and Zaki equation (Eq. [4.3]). At 2% solids, the settling velocity of a particle is decreased 5.5% due to hindered settling. At 10% solids, the settling rate is decreased 25.3%. However, the elutriation water added to the column dilutes the solids content, therefore, a higher feed percent solids can be used effectively. There was very little difference obtained experimentally between 2% and 3% solids content in the feed slurry, as illustrated by Figures 4.7 and 4.8. This result indicates that hindered settling has no effect at very low feed solids concentrations.

Pyritic sulfur reduction decreased with increasing elutriation water rate, as shown in Figure 4.3. This appeared to be a result of unliberated pyrite particles locked in the coal since pyritic reduction increased gradually when recovery was slightly decreasing and increased sharply when recovery dropped sharply. Pyritic

sulfur reduction was found to decrease slightly when feed rate was increased. Since the flow below the feed point was not affected by an increase in feed rate, pyrite particles entrapped or locked in the coal coagula remained in the lower section of the column. Slower settling coal coagula around the feed point tend to be washed out of the overflow when the feed rate is increased. Therefore, the percentage of pyrite in the product increased due to a decrease in coal recovery.

4.5.2 Mean Residence Time

As mentioned earlier, the mean residence time indicates the average time that a particle resides within a cell. If a cell operates perfectly plug flow, the mean residence time is exactly the residence time for the whole feed distribution. However, if the cell runs completely mixed, the mean residence time does not represent the entire feed distribution (Levenspiel, 1972).

From the experimental results shown in Figure 4.11, the mean residence time required for minimizing the product ash percent while maintaining a high recovery was approximately 30 minutes. Also, under the conditions of the experiment, the column appears to have operated fairly plug flow since theoretically attained settling data agreed with experimental results and coal recovery sharply

increased with respect to time (Figure 4.9). For an elutriation column, plug flow conditions are necessary for an efficient size classification.

A major problem with the selective coagulation/ elutriation process is slow dynamics or long retention times, which result in a low throughput. One method of increasing the kinetics is by increasing the settling velocity of the coagula, which can be achieved by enlarging the size of the coal agglomerates and/or by increasing their density. The addition of a heavy hydrocarbon oil, such as fuel oil No. 6 or bitumen, in small quantities may supply both the enlarged coagulum size and increased density. However, heavy oils have been found to be less selective for the oil agglomeration processes; hence, they may only be applicable for dewatering the clean coal product (Capes, 1979). Since the particle settling velocity, according to Stoke's equation, is mainly influenced by particle diameter rather than density, a light weight oil may be sufficient at low additions to increase the coagulum diameter. However, the size increase of the coagula must be large enough to overcome the change in density, otherwise the additon of fuel oil will not help (Figure 4.12). A large addition of the light weight fuel oil will decrease the density below 1 gm/ml and cause the coal to float. Another technique may involve replacing the

elutriation column with a lamella thickener designed to use elutriation water to reduce entrapment. This type of device would decrease settling distance and increase the surface area on which the particles can settle, therefore increasing the throughput of the process.

4.5.3 Steady-State

Steady-state represents the point in time, after a process has been initially started, where the product and tailings quality and quantity is constant. This point can be determined by obtaining product and tailing samples over several time intervals. After sample analysis, coal recovery and product ash percent values can be calculated and plotted versus time as illustrated in Figures 4.9 and 4.10. Steady-state is reached when both curves level out at a constant value.

In Figure 4.9, recovery and product ash percent were close to being constant after 140 minutes for a 12% ash feed material. When using a sample containing only 1.6% ash, the recovery levelled out at 95% after 150 minutes, where the product ash was fairly constant at 1.0%. Therefore, the steady-state time for the selective coagulation/elutriation column process under the given conditions was approximately 150 minutes.

The mean residence time did not correspond with the

time needed for steady-state to occur as described above. Although most of the coal coagula reported at or near the mean residence time, some remaining coal coagula smaller in size and/or containing less entrapped material settled slower. Hence, the time needed for a system to reach steady-state was 4 or 5 times the mean residence time.

Mean particulate residence time was also calculated, mainly to enhance understanding of the principles behind the operation of the elutriation column. The particulate residence time was calculated by using Stoke's equation to determine the particle settling velocity and subtracting the settling velocity from the superficial velocity. Multiplying the result by the settling distance (the distance between the feed point and the underflow) yielded the time needed for the particle to enter and leave the column. If the superficial velocity was greater than the settling velocity, the particles reported to the overflow. In this case, the residence time was determined by multiplying the rise velocity by the length from the feed point to the overflow.

Figure 4.13 is a plot showing mean particulate residence time versus column length (rising or settling length). An estimated coagulum size of 75 microns was used, which later proved to be fairly reasonable in Chapter 5 of this thesis. The particles of mineral matter were

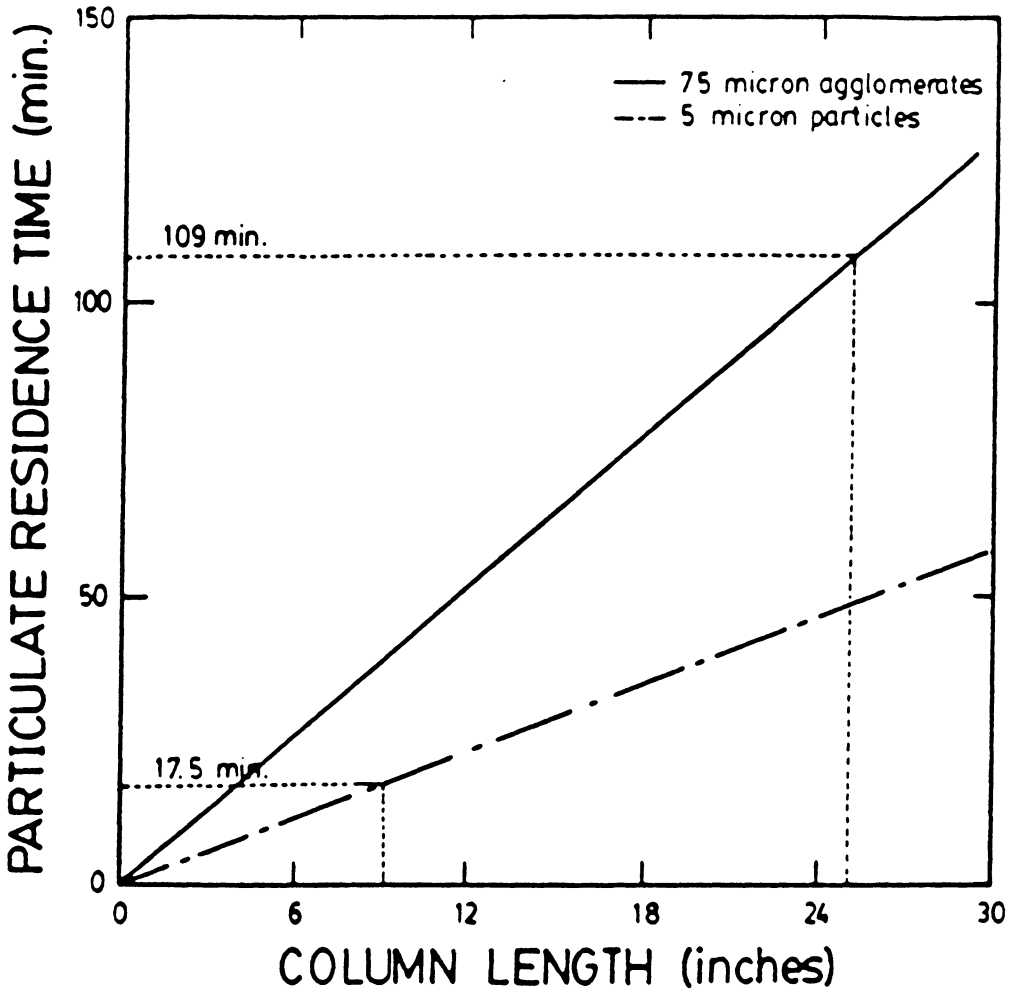

Figure 4.13 Particulate residence time versus column length for 75 micron agglomerates and 5 micron particles

assumed to have a size of 5 microns. The residence time increased linearly in both cases with increasing column length. However, the slope of the 75-micron line was larger than the 5-micron line, which illustrates the fact that the overall velocity of the 75-micron agglomerates was less than the overall velocity of the 5-micron ash particles. For the column dimensions used in the actual experiments, the particulate residence times for the coal coagula and the ash particles were 109 and 17.5 minutes, respectively.

The particulate residence time came close to predicting the steady-state time for coal recovery but not the product ash percent. This result may be due to the fact that micron-size particles tend to follow the fluid flow, whereas coarser particles act according to Stoke's law for settling.

4.6 Summary and Conclusions

1. An elutriation column has been investigated as the separation device for the selective-shear coagulation process. Promising results have been obtained which indicate the process' ability to produce superclean coal (< 2% ash, 0.80% sulfur) while maintaining a high recovery.

2. The mean residence time needed for optimum results was found to be around 30 minutes. Steady-state was reached in approximately 150 minutes.

3. An optimum elutriation water rate was determined to be near 400-450 ml/min (superficial velocity of 4.93-5.55 cm/min), which corresponds with the minimum product ash percent and a high coal recovery. This result correlated well with values obtained theoretically using Stoke's equation.

4. As the feed rate was increased, both the coal recovery and the selectivity of the process gradually decreased. This result was due to an increase in the superficial velocity above the feed point. The decrease in separation efficiency may also be attributed to an increase in mixing.

5. Changes in the feed percent solids was found to have little effect at low concentrations. However, theoretical calculations using the Richardson and Zaki (1954) hindered settling equation predicted a decrease in the particle settling velocity when the solids content became too concentrated. As a result, the coal recovery should decrease when using higher solids concentrations.

CHAPTER 5

A STEADY-STATE MODEL FOR AN ELUTRIATION COLUMN

5.1 Introduction

With the increasing demand for minerals and the continuously diminishing grades of ores, it is necessary to mine and process larger tonnages of ores. Consequently, more fines are being produced. This has led research scientists toward development of new physical and chemical processes which have the ability to treat material too fine for conventional flotation. As a result, the selective flocculation and coagulation processes have been introduced as an effective means of separating ultrafine mineral mixtures. Both processes selectively agglomerate the desired mineral while leaving the remaining minerals in suspension. The flocculation process achieves agglomeration through the use of polymers while the coagulation process utilizes strong attractive surface forces to induce agglomeration.

A problem with selective agglomeration processes involves the entrapment of the non-agglomerated material. This problem has been minimized for the selective flocculation process by applying gentle agitation to the flocs during the separation process. Researchers found

that much of the entrapped, non-flocculated material can be released by supplying mechanical agitation (Yarar and Kitchener, 1970) or by inducing a countercurrent flow of wash water for agitation (Read, 1971). Read (1971) reported an efficient upgrading of flocculated mineral when using an elutriation column, which utilized an upflow of wash water. Friend et al. (1973) developed a trapezoidal device using countercurrent wash water to concentrate flocculated mineral.

The elutriation column separates particles based on their settling velocity. If the velocity of the upflow of water is greater than the settling velocity of a particle, the particle will report to the overflow of the cell. A particle with a greater settling velocity will report to the underflow. The settling velocity of a particle is a function of its particle diameter and density as dictated by Stoke's equation. Another parameter controlling the settling velocity of a particle is the solids concentration. As the percent solids is increased, particle settling velocity decreases due to the crowding effect of neighboring particles, which is known as hindered settling.

In order to study the effect of the various operating parameters and to provide scale-up information, a steady-state population balance model based solely on fundamental

principles was developed for an elutriation column. Laboratory experiments were conducted in order to validate the model.

5.2 Process Description

The elutriation column is a sedimentation technique for the sizing of material that is dispersed in a fluid and allowed to settle against a rising fluid velocity. If the rising fluid velocity is less than the particle's terminal velocity, the particle will report to the overflow. If the particle's terminal velocity is greater, the particle will settle out into the underflow. Under quiescent conditions, which corresponds to a Reynold's number less than 2, a particle's terminal velocity can be determined using Stoke's equation, as given previously in Eq. [4.2]. As indicated by this equation, particle size has a greater effect than density when determining the terminal velocity of a particle. For this reason, coarser but lighter material can be separated from dense material having a small particle size (Figure 4.12).

As the concentration of particles in the column increases, the system behaves more and more like a heavy liquid whose density is that of the pulp rather than that of the liquid. This is a condition where the settling of particles is hindered by the flow of neighboring particles;

hence, it is called hindered settling. An equation was developed by Richardson and Zaki (1954) which represents both free and hindered settling based on the volume concentration of solid material in the suspension. The equation was given previously in Eq. [4.3]. Both Eq. [4.2] and Eq. [4.3] were used in the model to predict the settling velocity of the particles.

An illustration of a typical elutriation column is shown is Figure 5.1. The selectively agglomerated feed enters in the middle of the column at a desired height. Elutriation water is fed in at the bottom of the cell through a porous plate. The agglomerated mineral is concentrated and collected directly above the porous plate, while the non-agglomerated mineral is removed out of the cell overflow.

5.3 Model Development

The model was developed by first dividing the column into 5 different zones, as shown in Figure 5.2. From top to bottom, the zones are as follows: overflow zone, upper intermediate zone, feed zone, lower intermediate zone, and product zone. Due to the user's ability to change the feed height, the above zones apply to a general case when the feed point is placed in the middle of the cell. A mass balance of particles entering and exiting each zone either

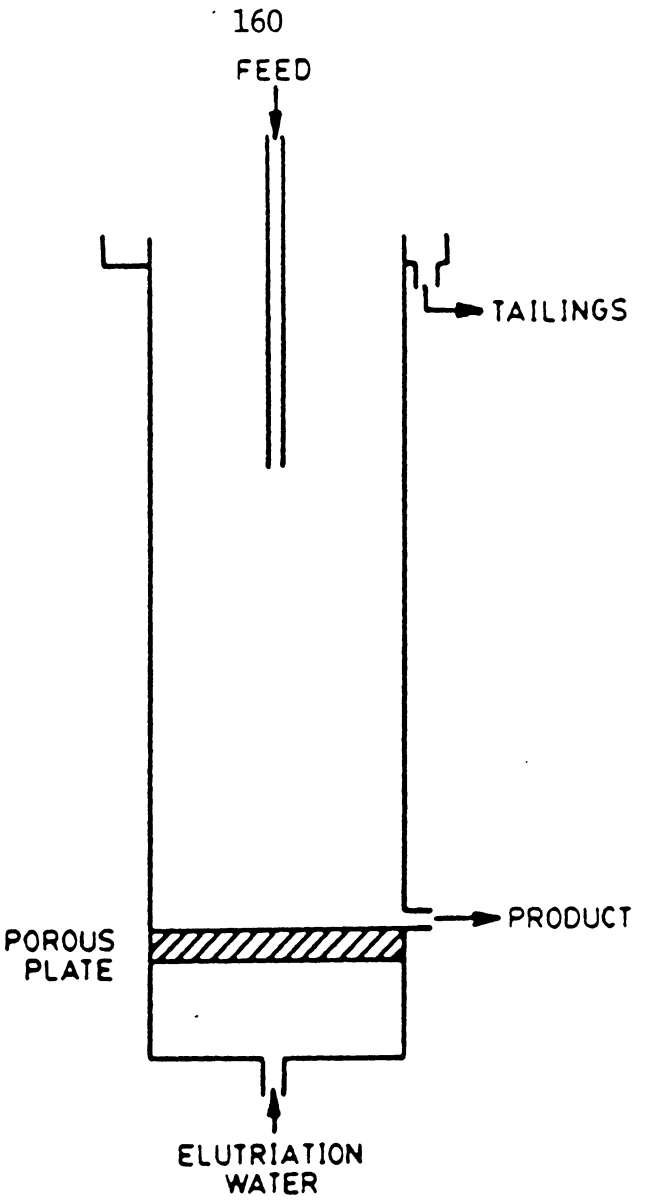

ELUTRIATION COLUMN

Figure 5.1 Schematic of a simple elutriation column.

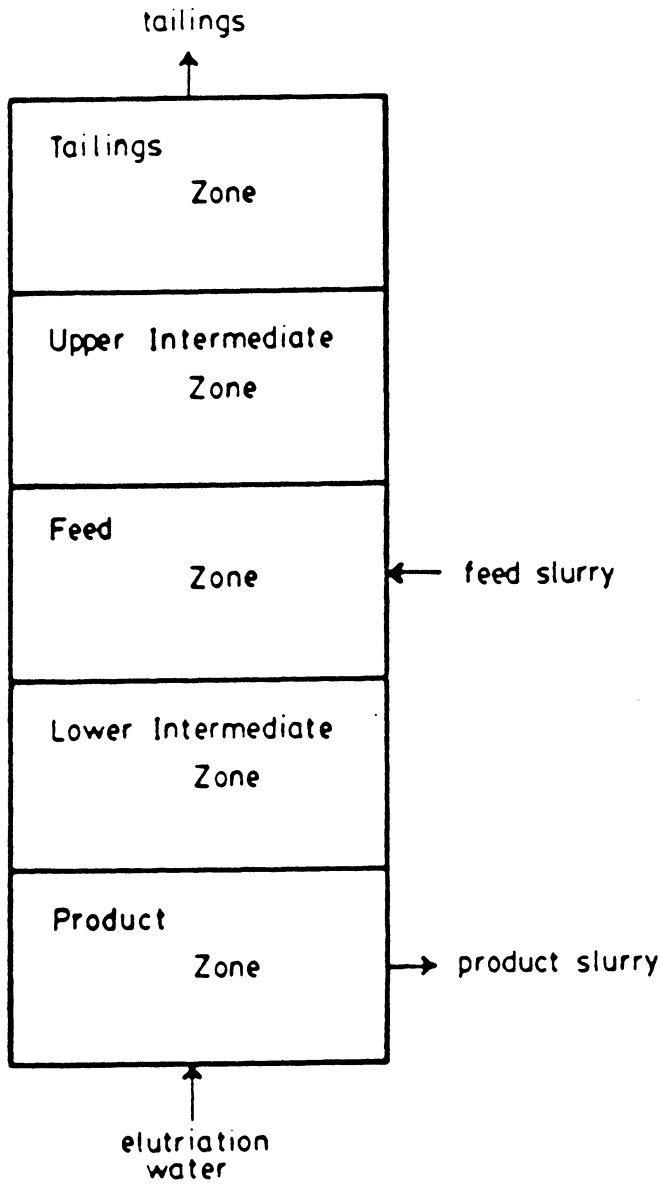

Figure 5.2 Schematic representation of the sections in an elutriation column.

by being carried by the liquid or by settling was performed. A flow balance was also done for each zone and is shown along with the mass balance in Figure 5.3. For convenience, a complete list of parameter nomenclature is given in Table 5.1. A kinetic equation representing mass per unit time was derived for each zone by summing the amount of material entering and subtracting the amount of material leaving. For example, the product zone had particles entering due to settling from the zone above, and their mass per unit time was the product of the particle settling velocity, V_s, the cross-sectional area of the zone above, A(J+1), and the concentration of the above zone, C(J+1). The mass of particles leaving the zone due to the upward flow of wash water was represented by the product of the net flow rate in the bottom section, Q_b, and the concentration of the zone, C(J). Q_b was set equal to the elutriation water flow rate minus the product flow rate. Also, particles leaving through the product stream were considered and the amount was calculated by multiplying the product flow rate, Q_p, and the zone concentration, C(J). Therefore, the kinetic equation for the product zone was written as follows:

$$dm(J)/dt = [V_s(J+1)*A(J+1)*C(J+1)] - [Q_b*C(J)] - [Q_p*C(J)]. \quad [5.1]$$

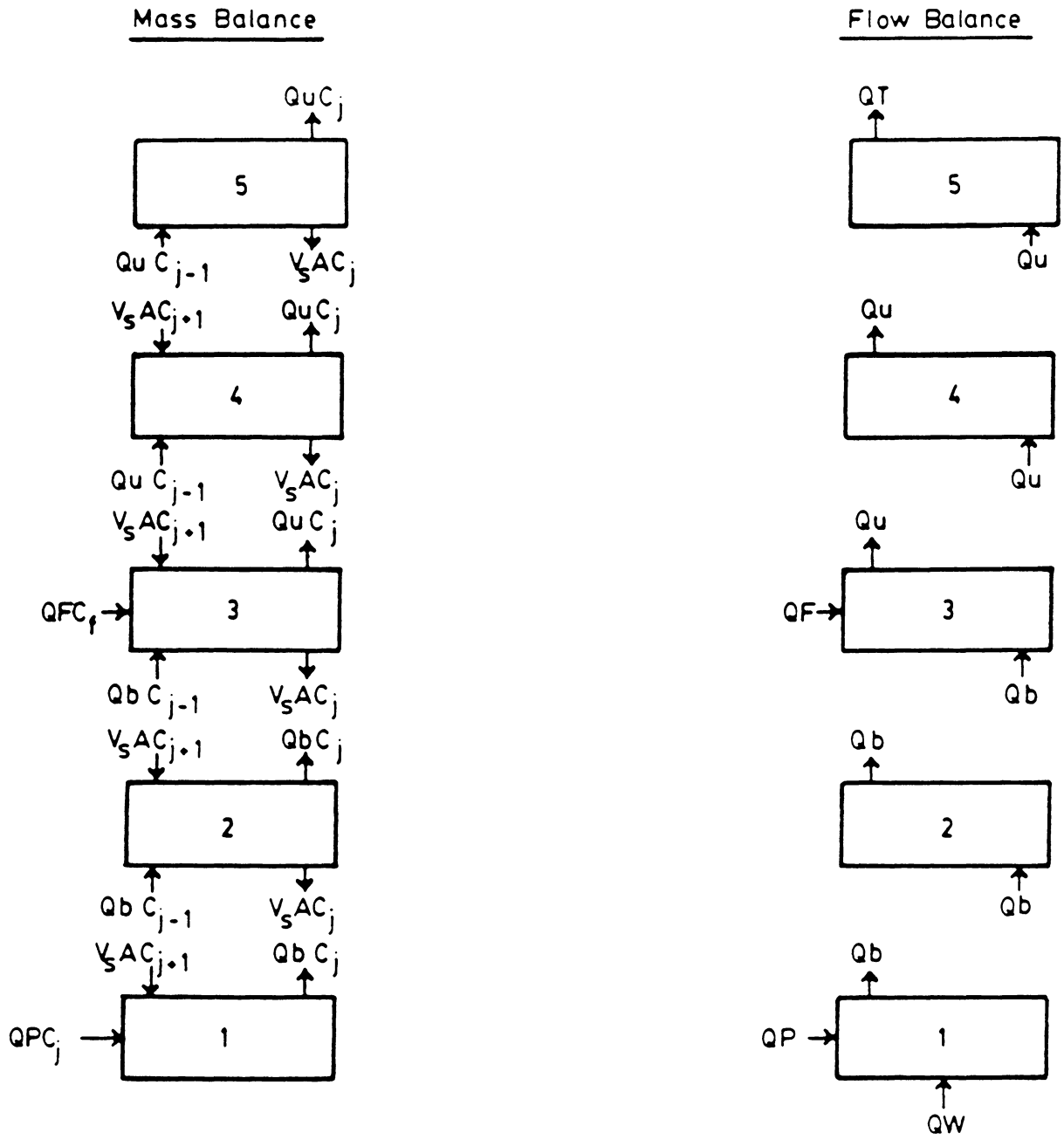

Figure 5.3 Schematic representation of the mass and volumetric flow balances for the column.

Table 5.1 : Nomenclature

$V_t(J)$ = a particle's terminal settling velocity in zone J (cm/sec).

$V_s(J)$ = a particle's hindered settling velocity in zone J (cm/sec).

d = coagulum or particle diameter (cm).

G = gravitation acceleration (981 cm/sec^2).

D_s = density of solid (gm/ml).

D_f = density of the medium (gm/ml).

N = medium viscosity (0.01 dyne sec/cm^2).

C(J) = solids concentration of zone J (gr/ml).

m(J) = mass of solids in zone J (grams).

t = time (sec).

A(J) = cross-sectional area of the column in zone J (cm^2).

QF = flow rate of feed slurry entering the column (ml/sec).

QW = flow rate of elutriation water (ml/sec).

QP = flow rate of product stream (ml/sec).

z = zone height (cm).

hgt = column height (cm).

This equation can be simplified to the following form:

$$dm(J)/dt = [V_s(J+1)*A(J+1)*C(J+1)] - [Q_w*C(J)]. \qquad [5.2]$$

The equations for the other zones were derived using the same principles illustrated above and are shown below:

Lower Intermediate Zone:

$$dm(J)/dt = [V_s(J+1)*A(J+1)*C(J+1)] - [V_s(J)*A(J)*C(J)] + [Q_b*(C(J-1) - C(J))]. \qquad [5.3]$$

Feed Zone:

$$dm(J)/dt = [V_s(J+1)*A(J+1)*C(J+1)] - [V_s(J)*A(J)*C(J)] - [Q_u*C(J)] + [Q_b*C(J-1)] + [QF*C(FEED)]. \qquad [5.4]$$

Upper Intermediate Zone:

$$dm(J)/dt = [V_s(J+1)+A(J+1)*C(J+1)] - [V_s(J)*A(J)*C(J)] - [Q_u*C(J)] + [Q_u*C(J-1)]. \qquad [5.5]$$

Overflow Zone:

$$dm(J)/dt = - [V_s(J)*A(J)*C(J)] + [Q_u*C(J-1)] - [Q_u*C(J)]. \qquad [5.6]$$

where

$$Q_b = QW - QP \qquad [5.7]$$

and

$$Q_u = QW + QF - QP. \qquad [5.8]$$

Eqs. [5.2]-[5.6] were divided by their respective zone volumes to convert to concentration. This modification allowed the model to be dependent on the column height.

The model was designed to give a steady-state solution. A steady-state solution is the value reached over a period of time where the value remains constant with respect to time. In this case, the concentration equations were evaluated with respect to time in order to find the steady-state values for the elutriation column under specified conditions. This was represented by the following expression:

$$dC / dt = 0. \qquad [5.9]$$

Therefore, in order to obtain a steady-state solution, Eqs. [5.2]-[5.6] were set equal to zero. This resulted in five non-linear equations and five unknowns which were solved simultaneously using an iterative technique which is based on Newton's method.

During the development of the model, several important basic assumptions were made which need to be recognized. They are:

i) The elutriation column is completely mixed along the cross-sectional area of the column.

ii) The column operates plug-flow along the height of the column.

iii) The column maintains laminar flow conditions: Re < 2. Therefore, Stoke's equation can be used to determine particle terminal settling velocities.

iv) Particle size does not change within the column.

v) The size distribution of the coal and ash particles entering the column is very narrow. Therefore, a monosize can be used for each.

vi) Perfect liberation occurs (no locked particles).

vii) There are no discrete appearance or disappearance terms. This means that the coal coagula do not grow or break up in the column.

5.4 Program Capabilities

The program and samples of the simulation input and output information are shown in Appendix II. The input data required to run a simulation include:

i) Feed solids concentration.

ii) Feed non-agglomerate (ash) percent.

iii) Slurry, elutriation, and product (underflow) rates.

iv) Agglomerate (coal) and non-agglomerate (ash) density.

v) Agglomerate (coal) terminal settling velocity.

vi) Non-agglomerate (ash) mean particle size.

vii) Agglomerate and non-agglomerate settling constant (normally 3.65).

viii) Cell dimensions.

ix) Feed point height.

By allowing the agglomerate settling velocity to be entered as input, the user has the choice of conducting sedimentation experiments or using Stoke's equation to determine the velocity. The output consists of concentrations for both the agglomerated (coal) and non-agglomerated (ash) material for each zone, agglomerate recovery (coal), percent non-agglomerate material in underflow, and separation efficiency.

The program offers the ability to simulate a straight up-and-down column or a column having a step-up or step-down in diameter size. This was accomplished by using the feed height entered by the user to determine which zone the feed point lies in. The bottom of the feed zone was set as the point where the upper cell diameter begins. This

option can be used to study the effect of changing the column diameter on grade and recovery. Being able to change the cell dimensions also allows the user to predict scale-up information based on throughputs, grades, and recoveries.

5.5 Experimental

Validation of the model was performed by selectively coagulating a coal slurry and physically concentrating the coal coagula using a continuous, laboratory-scale elutriation column. A schematic representation of the plexiglass column with appropriate dimensions was previously shown in Figure 4.2. Tests were performed using an Elkhorn No. 3 coal sample (12% ash), which was finely pulverized in a stirred ball mill at 35% solids. The mean particle size determined by an Elzone 80-XY particle size analyzer was 3.0 microns. The ground slurry was transferred to a sump, where the percent solids was adjusted to 2%. The pH of the slurry was maintained between 7 and 9. The slurry and elutriation water were fed at 50 ml/min and 400 ml/min, respectively, unless otherwise noted.

Other standard information and assumptions used for the simulations include the following:

Solid Concentration = 0.02 gm/ml

Coal Density = 1.3 gm/ml

Ash Density = 2.3 gm/ml

Mean Agglomerate Size = 75 microns

Hindered Settling Constant = 3.65

5.6 Results

5.6.1 Model Predictions

Simulations were run to determine the effect of elutriation water rate and coagulum size on the recovery of coagulated coal. The results are shown in Figure 5.4. Clean coal recovery was found to be very high at low wash water rates. However, as the elutriation water rate was increased, recovery experienced a large decrease. The wash water rate corresponding to the sharp drop in recovery was found to be a function of coagulum size. Using 75-micron coagula, recovery decreased gradually from 100% to 88% when the wash water rate was increased from 0 to 400 ml/min. At 400 ml/min, the recovery dropped drastically from 88% to 25% at 700 ml/min. Using 100-micron coagula, recovery gradually decreased to 82% at 700 ml/min, and sharply dropped from 82% to 40% at 1000 ml/min.

The model was designed on the basis of the assumption that the flow of the feed slurry entering the cell only adds to the flow in the upper portion of the column. The

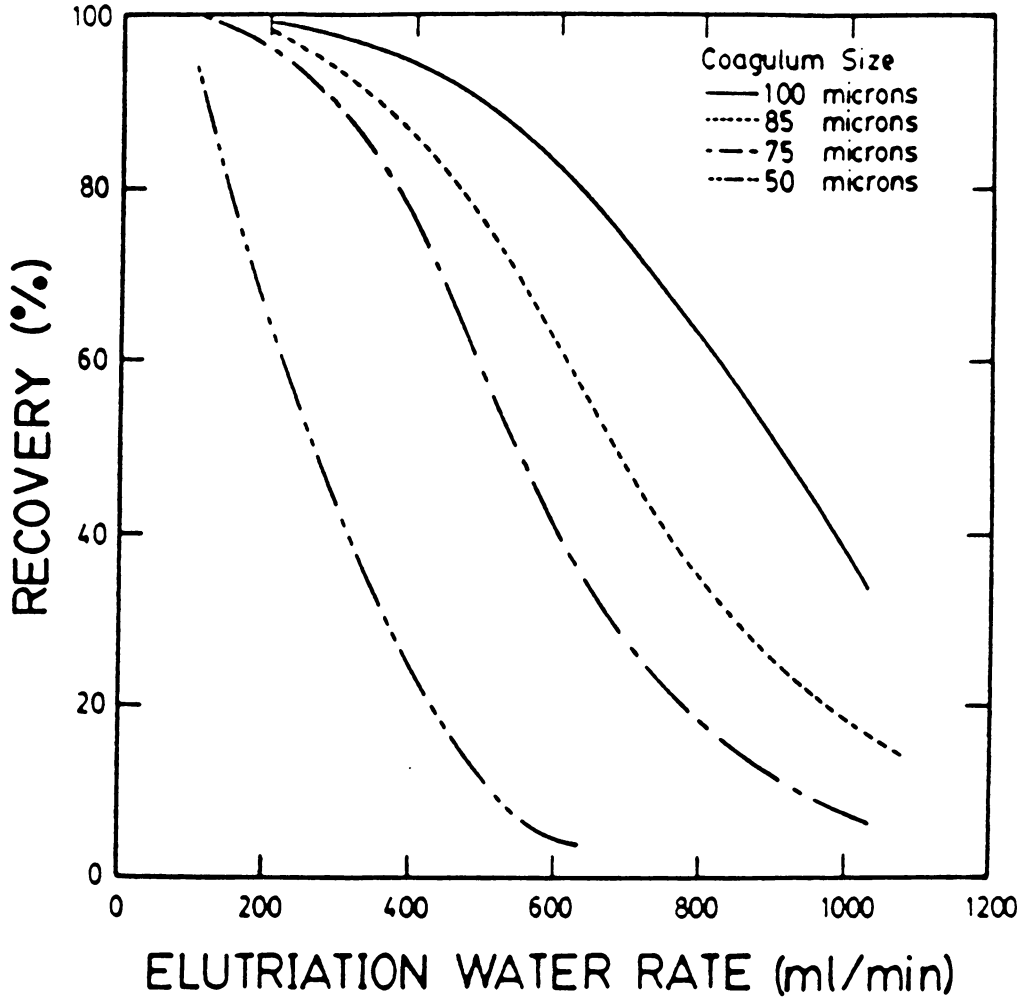

Figure 5.4 Model predictions on the effect of elutriation water rate on coal recovery over a range of coagulum sizes.

affected material would be the portion above the feed point due to increased upward velocity. Hence, an increase in feed rate should have little or no effect on recovery. This was the result found by simulating a wide range of feed rates for various coagula sizes. The results were plotted as clean coal recovery versus feed rate in Figure 5.5. As expected, recovery decreased very little as feed rate was increased. Using 75-micron coagula, recovery decreased from 80% at a feed rate of 25 ml/min to 65% at 200 ml/min. The slopes of the lines for each of the coagulum sizes are almost identical to one another, although, the 75-micron material has a slightly larger slope because of the proximity of the elutriation water velocity to the coagulum settling velocity. The large difference in recovery between the different agglomerate sizes was due to the effect of setting the elutriation water rate at 400 ml/min.

In order to determine the maximum feed concentration at which the column can efficiently operate, simulations were conducted over a wide range of feed concentrations at a feed rate of 50 ml/min. Coagulum recovery was found to gradually decrease from 75% at 0.02 gm/ml to 66% at 0.2 gm/ml, as shown by Figure 5.6. Beyond 0.02 gm/ml, recovery sharply decreased to 22% at 0.60 gm/ml, where it began to level off to a gradual decrease. The coal recovery was

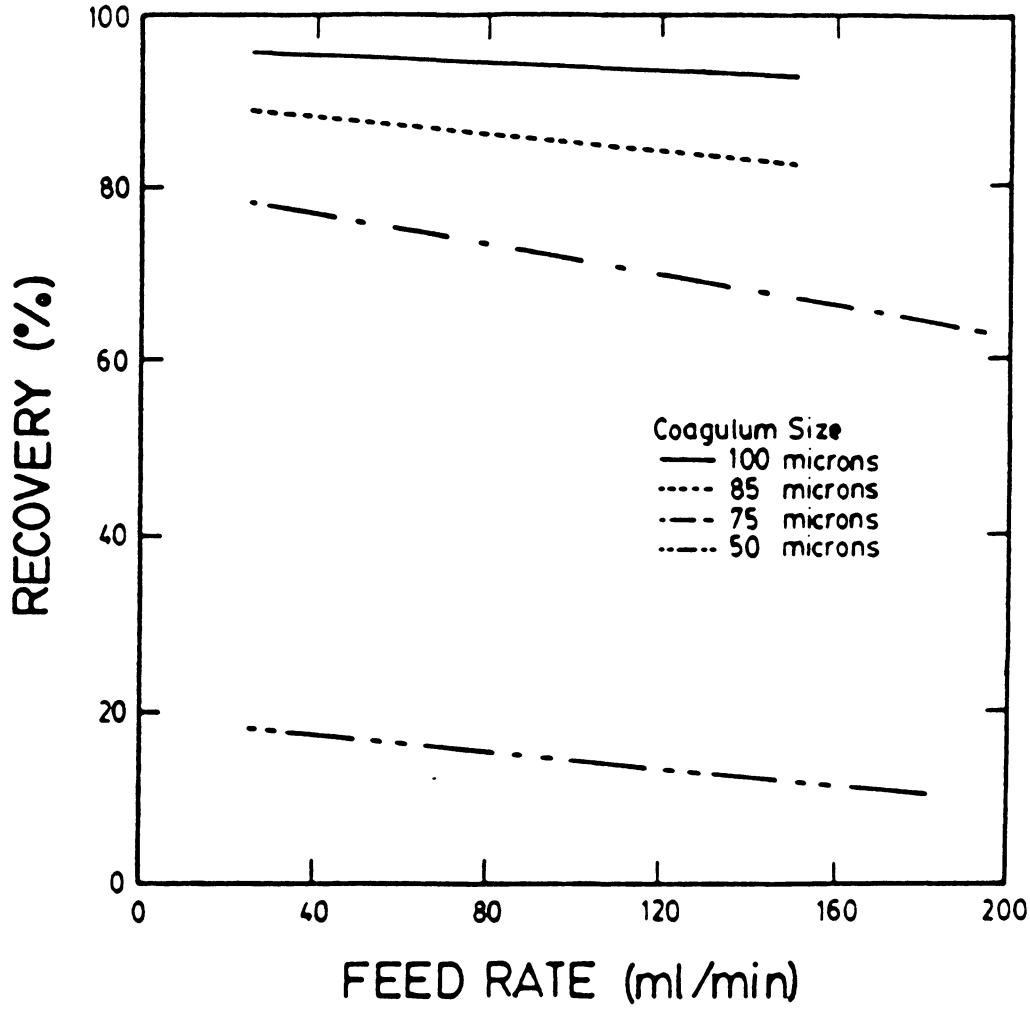

Figure 5.5 Model predictions on the effect of feed rate on coal recovery over a range of coagulum sizes.

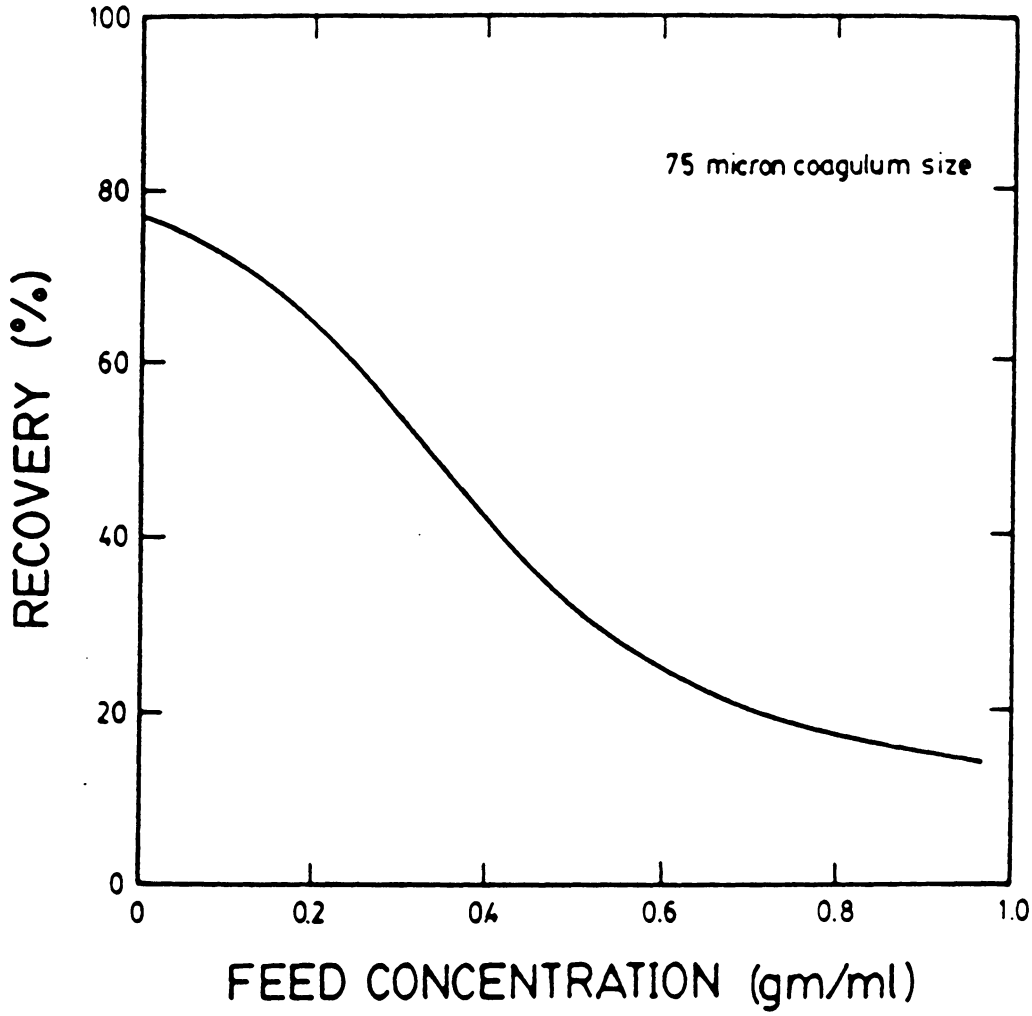

Figure 5.6 Model predictions on the effect of feed solids concentration on coal recovery.

approximately 12% at 1 gm/ml. Figure 5.7 is a plot of clean coal recovery versus elutriation water rate for various amounts of percent solids. At very low solids concentrations (0.02- 0.05 g/ml), recovery was affected very little. However, as the feed solids concentration was increased to 0.5 g/ml, the upper limit on the elutriation water rate decreased as a result of an increase in the effect of hindered settling.

Feed point within the column was found to be very important. Figure 5.8 is a plot showing coal recovery versus elutriation water rate for two feed heights. By placing the feed point 43 cm instead of 63 cm from the bottom of the column, the recovery was increased by approximately 20% when using an elutriation water rate of 400 ml/min. The recovery curve representing a feed height of 63-cm was lower than the 43-cm curve. However, both feed heights resulted in near 100% recovery at low elutriation water rates and decreased to near zero at high wash water rates. The increased recovery found for a decrease in feed height was a result of a decrease in the settling distance for the coagula.

The effect of increasing and decreasing upper and lower cell diameters was examined using a number of simulations. The results were plotted and are shown in Figures 5.9 and 5.10. Figure 5.9 illustrates the effect of increasing the

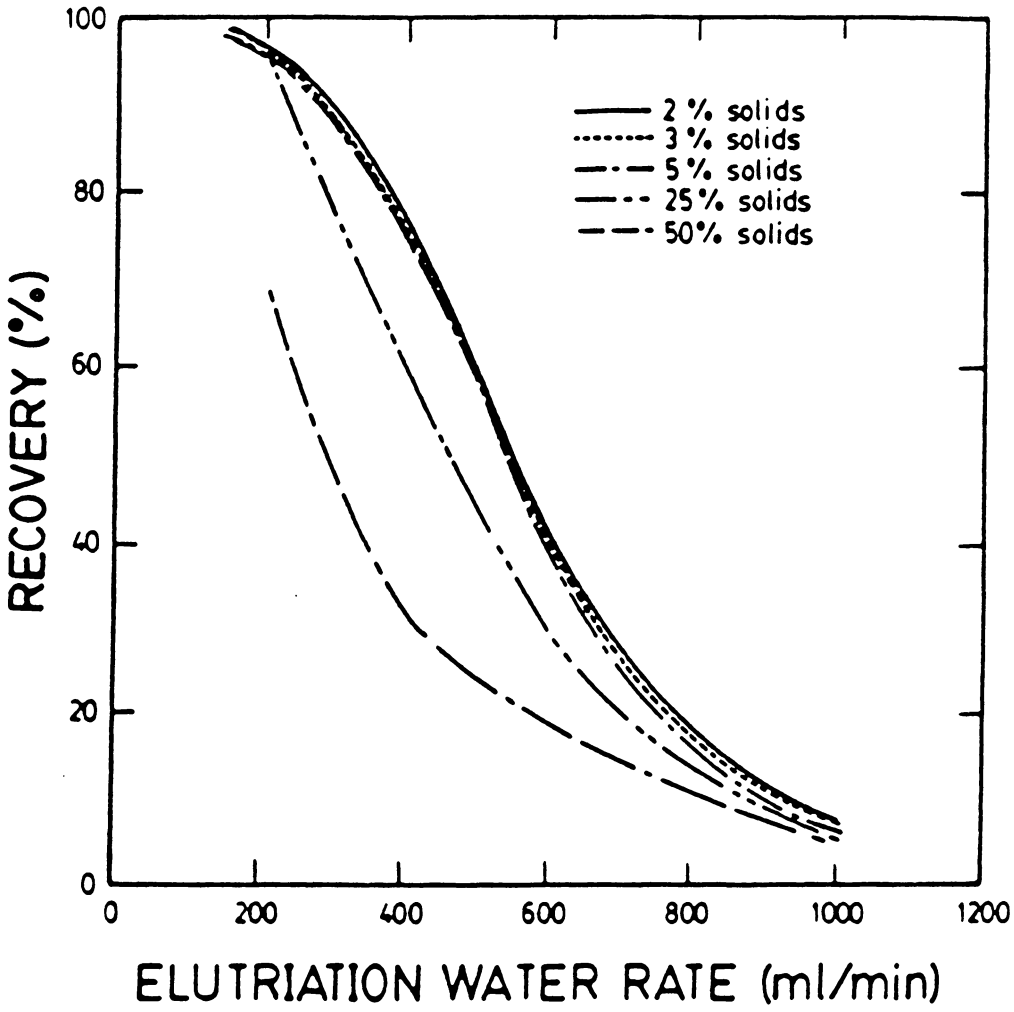

Figure 5.7 Model predictions showing coal recovery versus elutriation water rate for various feed percent solids values.

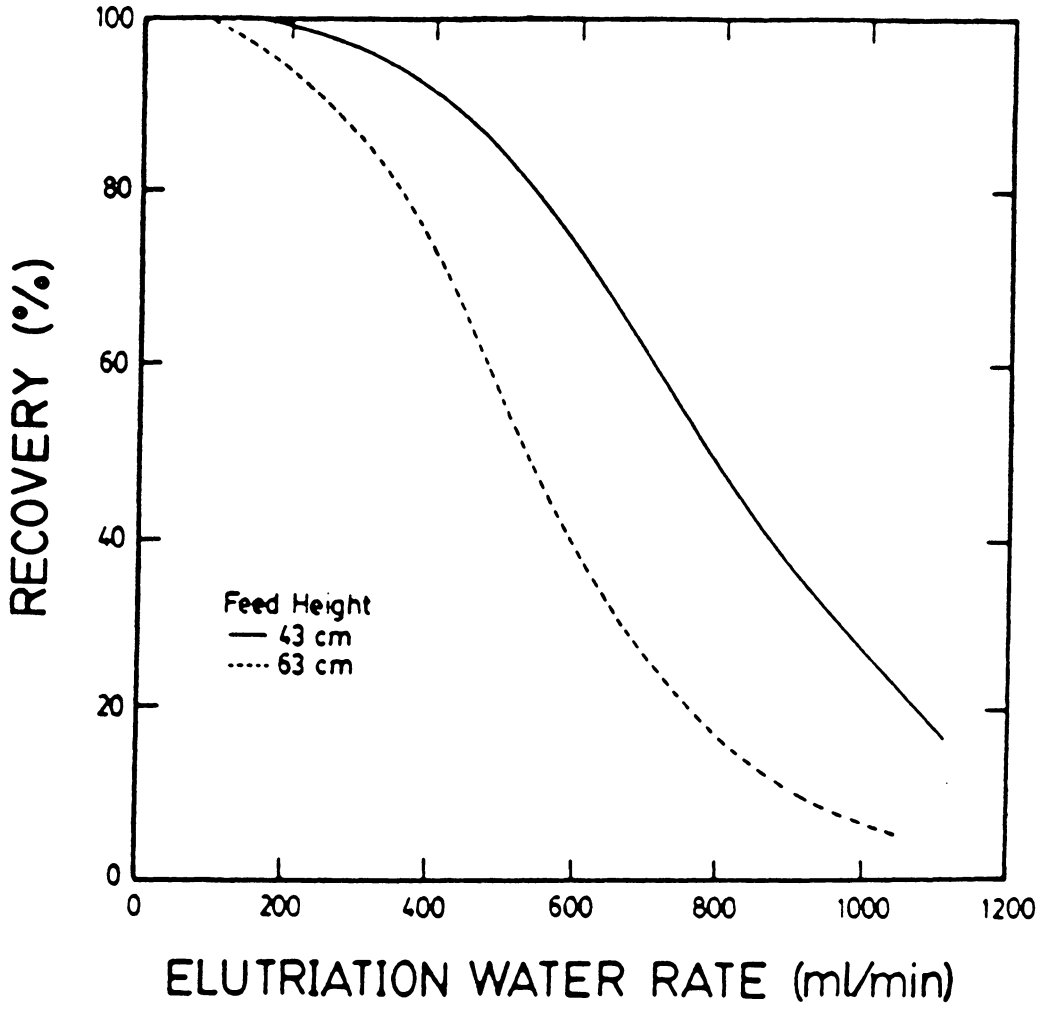

Figure 5.8 Model predictions showing the effect of feed height on coal recovery over a range of elutriation water rates.

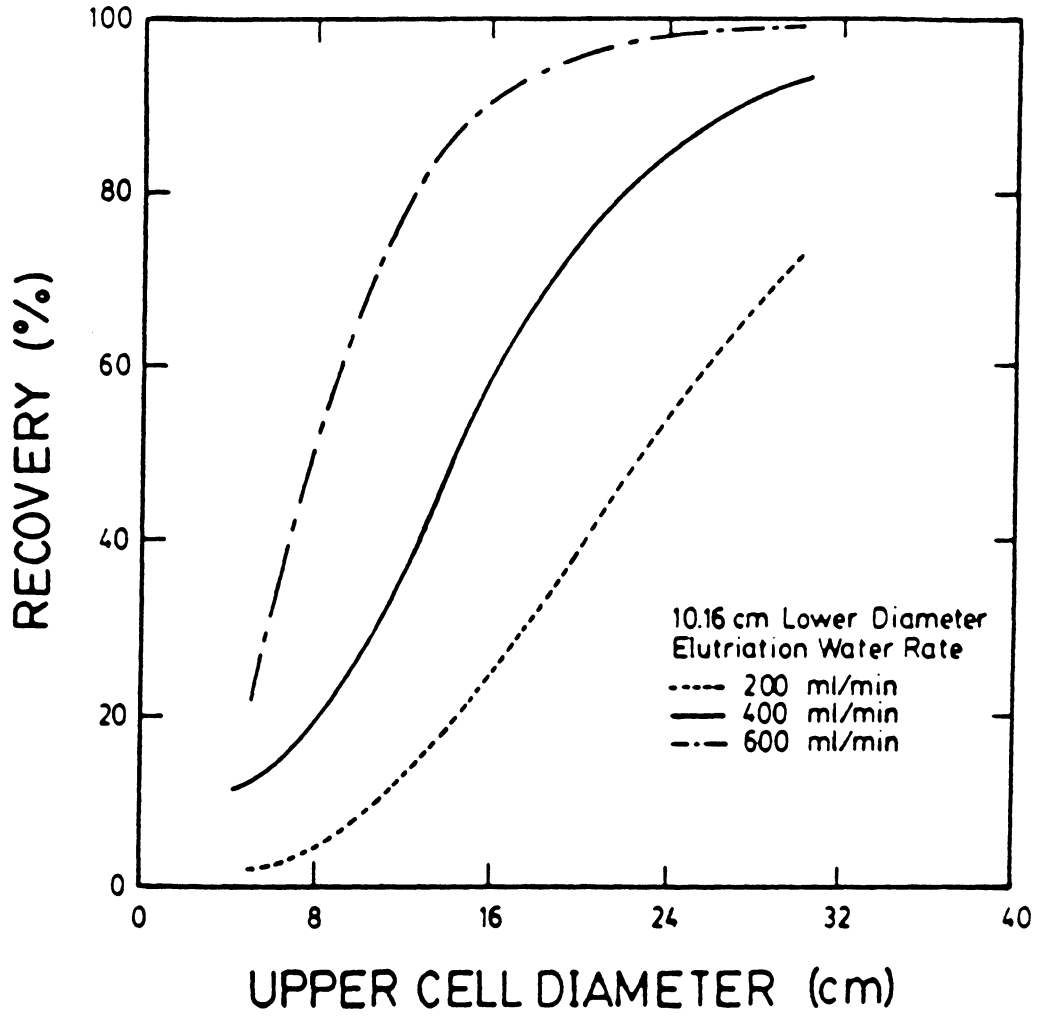

Figure 5.9 Model predictions showing the effect of upper cell diameter on coal recovery for three elutriation water rates.

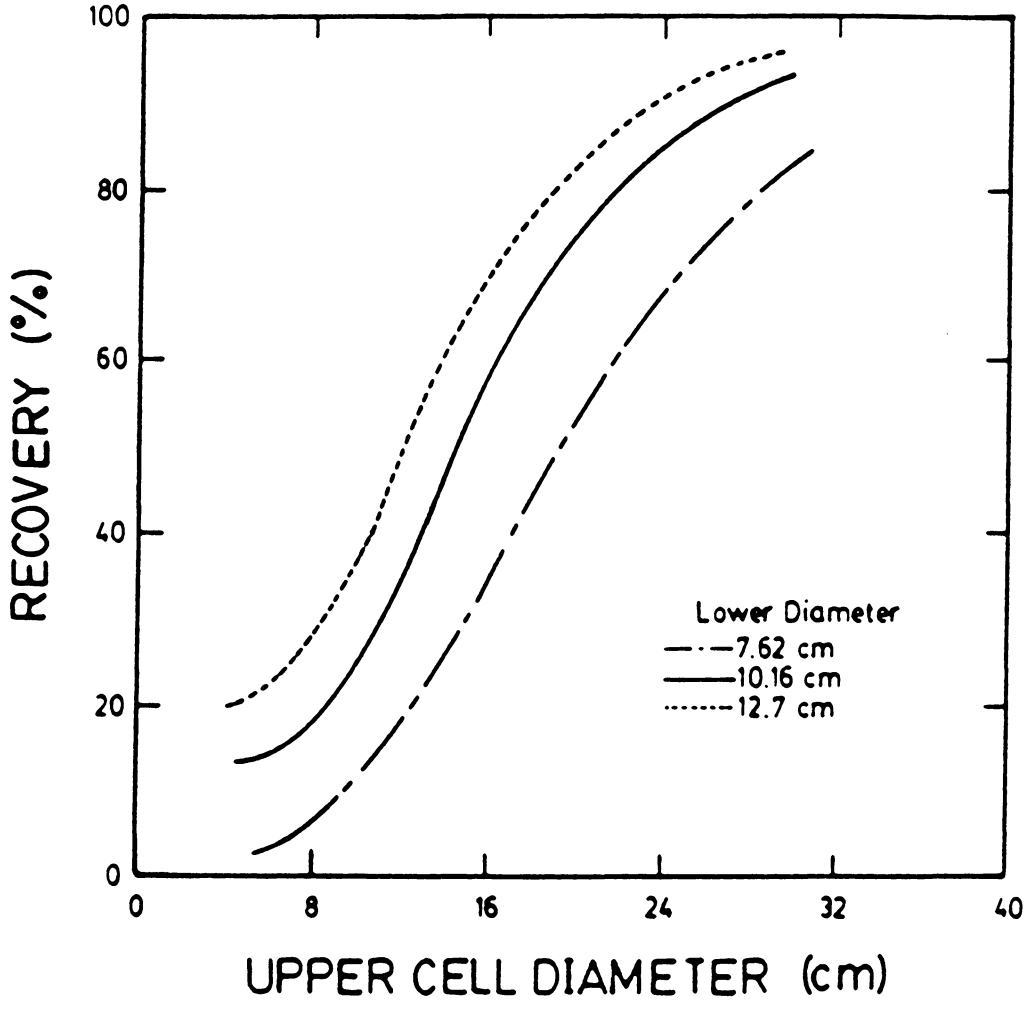

Figure 5.10 Model predictions showing the effect of both the upper and lower cell diameters on coal recovery.

upper cell diameter using three different elutriation water rates while maintaining the lower diameter at 10.16 cm (4 inches). At all wash water rates, recovery increased sharply with an increase in upper cell diameter. This was due to the fact that increasing the diameter while maintaining a constant column flow rate decreased the wash water velocity, hence allowing more material to be recovered. A similar result is shown in Figure 5.10. This figure demonstrates the effect of changing both the lower and upper cell diameter. Increasing the diameter of the two sections resulted in an increase in recovery.

5.6.2 Comparison of Experimental Data and Model Predictions

After characterizing the elutriation column using the model, previously obtained experimental data were plotted and compared with the model predictions. Figure 5.11 shows both the simulated (solid line) and experimental (points) recoveries of coal as a function of elutriation water rate. The predictions from the simulator correlate very well with the experimental results. However, the simulator's predictions indicate a perfect separation, or zero percent ash in the product (underflow), whereas the experimental results show a less perfect separation, as depicted in Figure 5.12. The experimental results show an optimum elutriation water rate around 400 ml/min, where the product

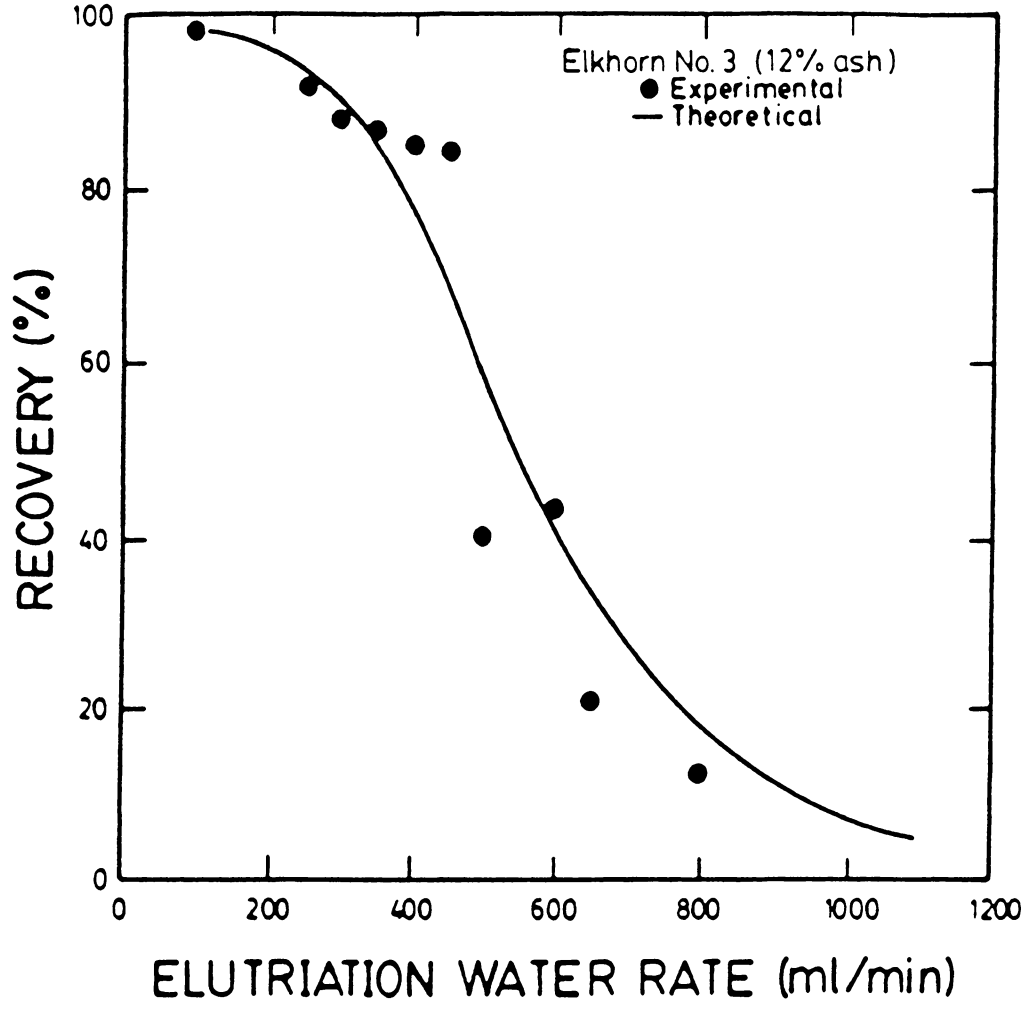

Figure 5.11 A comparison between model predictions and experimental results showing the effect of elutriation water rate on coal recovery.

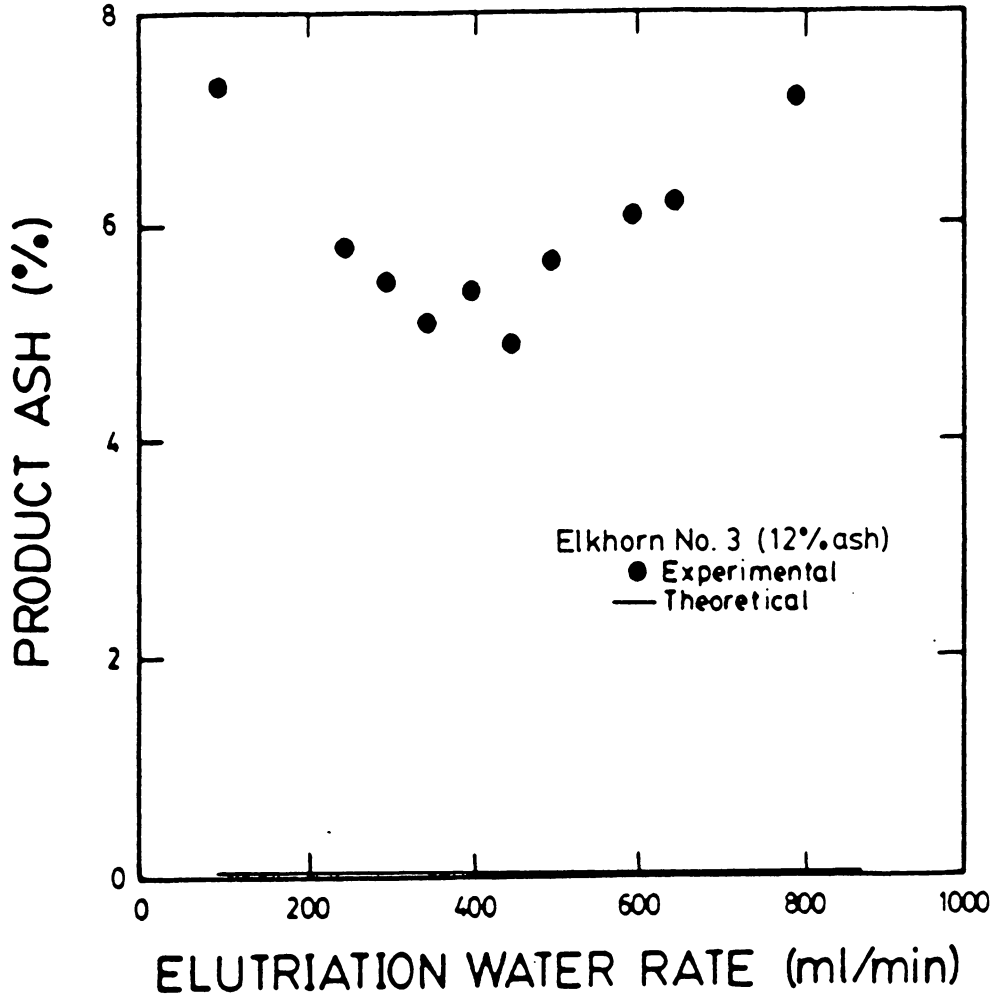

Figure 5.12 A comparison between model predictions and experimental results showing the effect of elutriation water rate on product ash percent.

ash was minimized at 4.9%. The difference between the simulated and experimental values was a result of the entrapment of fine ash particles in the coal coagula, which was not incorporated into the model, the presence of inherent ash locked in the coal, and possibly mixing.

Simulated recovery values showing the effect of feed rate were also compared with experimentally obtained values. The plot showing the comparison is given in Figure 5.13. The simulator results are in reasonable agreement with the experimental results, although the experimental recovery dropped off slightly at the higher feed rates. The decrease may have been due to an increase in mixing around the feed point as a result of the downward injection of the feed, which would result in the breakage of the coal coagula. Also, an increase in the superficial velocity in the upper section of the column may have caused the coal coagula above the feed point to be washed out the overflow. The simulator predicted a perfect separation for the underflow, as shown in Figure 5.14. The actual experimental product ash values began at 5.0%, using a feed rate of 25 ml/min, and increased with increasing feed rate to 6.8% at 150 ml/min. This may also be due to mixing in the column.

Simulator results illustrating the effect of feed solids concentration were compared with experimental

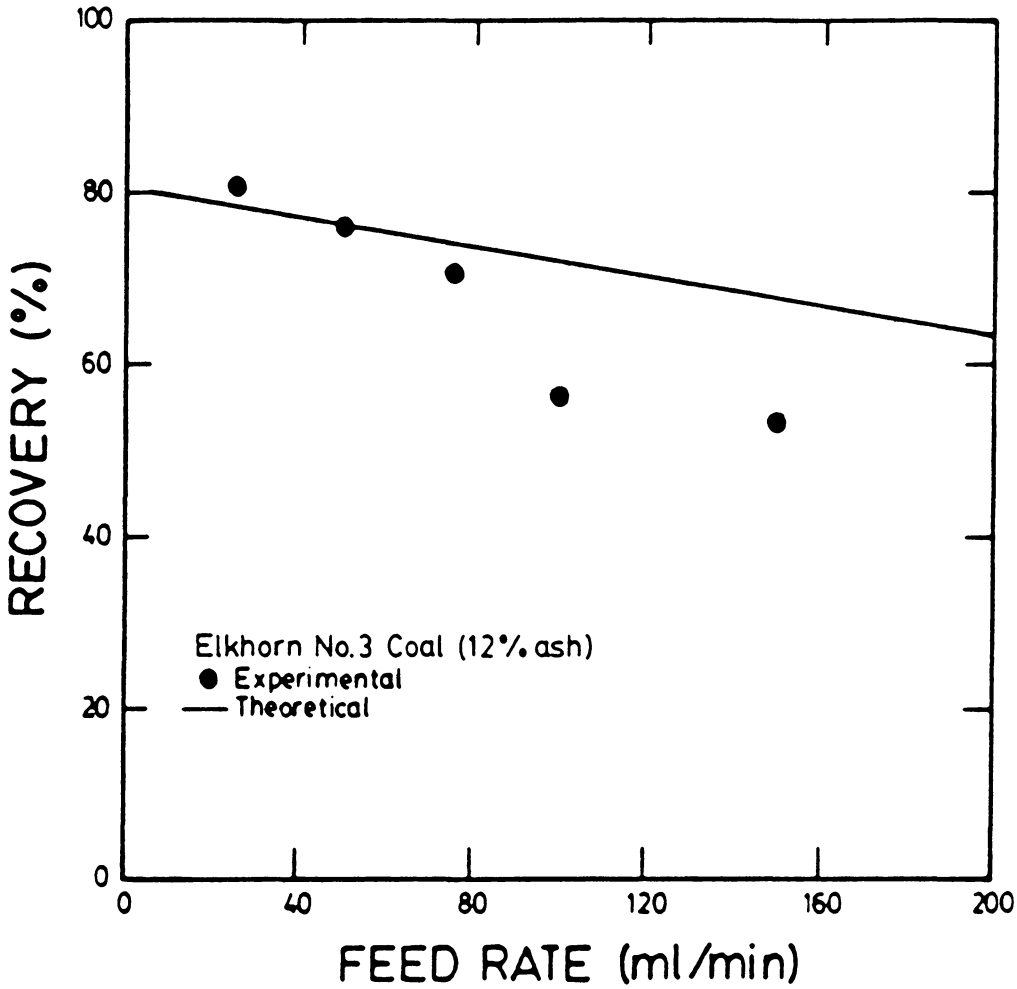

Figure 5.13 A comparison between model predictions and experimental results showing the effect of feed rate on coal recovery.

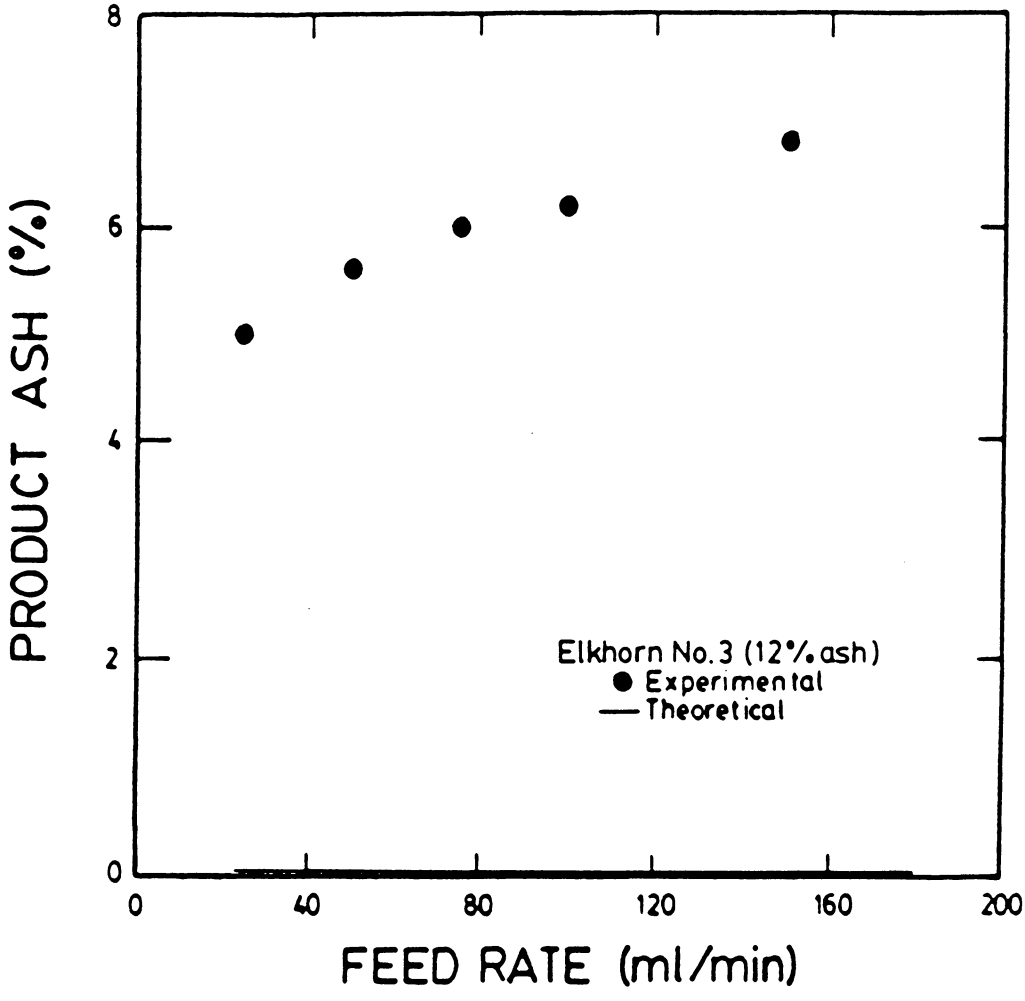

Figure 5.14 A comparison between model predictions and experimental results showing the effect of feed rate on product ash percent.

results in Figure 5.15. The model predictions correlated very well with the experimental values. Both sets of data depicted a decrease in recovery as the elutriation water was increased and no effect on recovery when the feed solids concentration was increased from 0.02 to 0.05 gm/ml.

5.7 Discussion

An elutriation column is based on an upflow of wash water whose velocity can be adjusted so that particles can be separated due to a difference in settling velocity. This principle was illustrated in Figure 5.4, where a range of elutriation water rates was simulated to determine the effect on coal recovery. Generally, recovery initially decreased gradually with an increase in the wash water rate. Beyond a specific flow rate, recovery began to drop sharply as a result of exceeding the settling velocity of the coagula. The upper limit for the wash water rate was found to be higher for the larger agglomerate sizes. Figure 5.11 illustrates the close similarity between experimental and predicted results.

An investigation of the size of the coal coagula has not yet been conducted. Therefore, the coagula size is not known. However, a comparison of the simulator predictions in Figure 5.4 and the experimental data resulted in the conclusion that the effective mean size was around 75

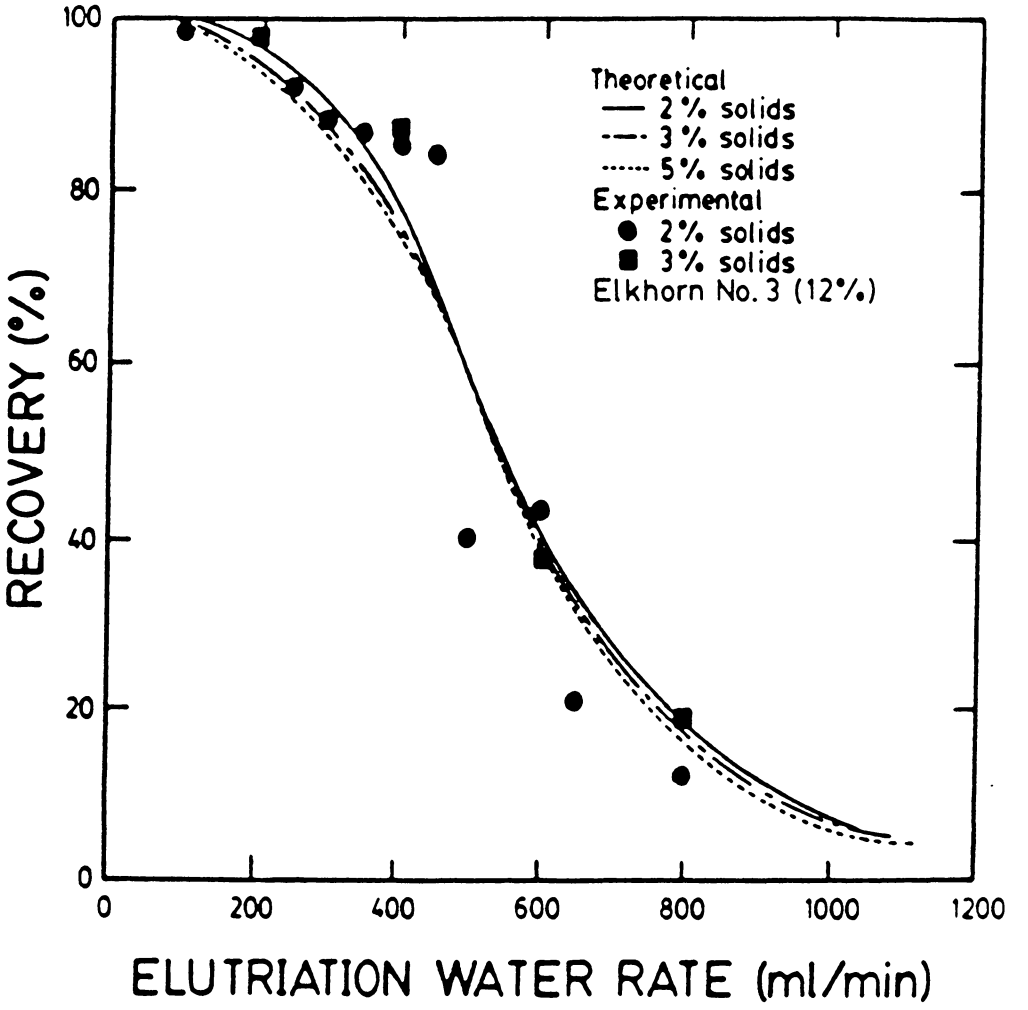

Figure 5.15 A comparison between model predictions and experimental results showing the effect of feed percent solids on coal recovery over a range of elutriation water rates.

microns, as depicted in Figure 5.11. The actual mean size of the coagula could be larger due to porosity.

The sharp drop in recovery experienced when the elutriation water rate was increased can be explained by using Stoke's equation to determine the settling rates of the coagula. The terminal settling velocity for a 75-micron coagulum was calculated to be 5.5182 cm/min, whereas the settling velocity for a 5-micron size mineral matter particle was found to be 0.0840 cm/min. The velocity of the upward stream of wash water in the bottom section of the column (4-inch diameter) at 400 ml/min was 4.9320 cm/min. Therefore, the result was high coal recovery and ash rejection, as shown in Figure 5.11. By utilizing 600 ml/min of elutriation water, the wash water velocity was 7.3980 cm/min, which resulted in a 50% loss in coal recovery. Since the terminal velocity of the coal coagula was less than the wash water velocity, an even lower recovery was expected. However, the portion of the cell above the feed point had a diameter twice that of the lower portion of the column. This resulted in a decrease of the upflow velocity in the upper region, hence allowing material to settle back into the lower section. Simulator results shown in Figure 5.10, indicated that using a straight up-and-down column having a diameter of 4 inches yielded less than 10% recovery when operated at a 600-

ml/min elutriation water rate. A column having an 8-inch diameter upper section and a 4-inch diameter lower section achieved 50% coal recovery.

Friend et al. (1973) expressed concern over the use of an elutriation column as a separation device due to the turbulence or mixing that occurs in large columns, especially when separating dense mineral flocs. Excessive turbulence leads to floc breakage and a poor separation efficiency. However, since the model does not include mixing terms and the experimental results and model predictions compared reasonably well, as shown in Figures 5.11 and 5.13, any mixing which may have occurred during the continuous operation of the column did not affect the separation efficiency. This result was due to the low density of the coal coagula and the small agglomerate size, which reduced the amount of elutriation water needed. Therefore, the elutriation column can be efficiently used for separations in size classification, selective flocculation, or selective coagulation processes when the settling velocity of the material involved is low enough so as to not require high elutriation water rates.

Increasing the feed rate was not found to affect coal recovery very drastically, although a gradual decrease was incurred. The decrease in recovery was a result of an increase in the velocity of the upward current of water.

Figure 5.13 compares the experimental results with the model predictions over a range of feed rates. The experimental results initially agree with the gradual decline of the predicted recovery values. However, experimentally determined recovery values dropped 15% lower than the predicted values beyond a feed rate of 80 ml/min. This difference may be due to the increase in mixing incurred in the feed tube causing coal coagulum breakage prior to entering the elutriation column.

The feed solids concentration was found to affect the separation efficiency of the elutriation column only when the particle concentration within the column impeded the settling of the particles. The model represented hindered settling by using the Richardson and Zaki (1954) equation (Eq. [4.3]). This equation indicates that as the concentration increases, the particle settling velocity decreases. The model predictions in Figure 5.6 illustrate the effect of hindered settling described above over a wide range of feed solids concentrations. At low feed solids concentrations, recovery was high due to the negligible effect of hindered settling. Figure 5.15 also illustrates this fact by comparing experimental and predicted results at low solids concentrations of 0.02, 0.03, and 0.05 gm/ml. Both sets of data show no change in recovery when the feed solids content was increased. However, according to Figure

5.6, as the concentration was increased, hindered settling became more and more a factor, resulting in a decrease in recovery. Recovery continued to decrease with an increase in feed solids concentration until the concentration within the column became fairly uniform, which caused a levelling off of recovery at approximately 15%.

5.8 Summary and Conclusions

1. A population balance model has been developed which allows predictions to be made with regard to the influence of operational parameters and column design on the separation efficiency.

2. A comparison of model predictions and experimental results showed a reasonable agreement for the coal coagula. However, the model predicted a complete rejection of the particles of mineral matter, whereas experimental results proved differently. This difference was decidedly caused by entrapment, unlocked particles of mineral matter and mixing factors, which were not accounted for in the model.

3. An elutriation column provided an efficient technique for the separation of coagulated coal particles from dispersed ash particles.

4. The model developed is based on first principles of particle settling behavior. As a result, the model is well suited for scale-up and process optimization.

5. The parameters investigated include feed rate, feed solids concentration, coagulum size, elutriation water rate, feed point, and cell dimensions. An increase in feed rate and feed solids concentration was found to gradually decrease coal recovery and increase product ash percent. The most sensitive parameter was the elutriation water rate. An optimum rate was found where the product ash percent was minimal and the recovery was high.

Chapter 6

SUMMARY AND RECOMMENDATIONS FOR FUTURE WORK

6.1 Summary

The results of the present investigation may be summarized as follows:

1. The selective-shear coagulation process has proven to be a very efficient physical cleaning technique for ultrafine coal. Its ability to treat various coal samples has been demonstrated. Of special importance, the process produced superclean and ultraclean coals while maintaining very high recovery values. Therefore, its high cleaning efficiency, combined with a low chemical requirement, makes the process' product very attractive for use in coal-water mixtures.

2. The pH of the coal slurry was found to be an important variable in controlling the selectivity of the process. Coal recovery, product ash percent, and zeta potential values obtained over a range of pH values indicated that the low selectivity below pH 7 was due to heterocoagulation and homocoagulation between the coal and mineral matter. Above pH 7, the electrostatic repulsion force between the two particle types

increased, which caused the heterocoagulation to stop. Hence, selectivity increased beyond pH 7 for a slurry having a tap water medium. For a suspension with a distilled water medium, selectivity did not improve until pH 8 due to a larger electrostatic repulsion force.

3. Hydrophobic interaction was believed to be the main attractive force contributing to the coagulation of the coal particles. Between pH 7 and 9, coal recovery and selectivity was high while the zeta potential of the coal was measured to be approximately -40 mV. The resulting force was too high for coagulation to be explained by van der Waals forces alone. Above pH 9, the coal stopped coagulating due to an increase in zeta potential.

4. The presence of multivalent cations increased coal recovery but decreased selectivity. This occurrence was due to a decrease in the negative surface charge of both the coal and the mineral matter as the cation concentration increased. A critical concentration was found for Ca^{2+} which corresponded with a sharp increase in product ash percent. This result was due to the heterocoagulation caused by the lowered surface potential of the particulate system.

5. The major problem found was the entrapment of gangue material in the coal coagula. Therefore, the process may require multi-stage cleaning in order to achieve the desired product quality.

6. Test results showed that the separation efficiency of the process increased with decreasing particle size. This was attributed to an increase in particle population, which increased the number of particle-particle collisions, and a decrease in the effect of inertial forces.

7. It was found from experimental results that as percent solids was increased, coal recovery increased, while the product ash percent initially decreased to a minimum and then increased. The enhanced recovery was due to an increase in the number of particle-particle collisions. The high product ash percent for low percent solids was concluded to be the result of the low coal recovery. At a high percent solids, the product ash percent was found to be high due to an entrapment problem.

8. Using distilled water as the medium for a coal slurry required an additional amount of energy beyond that applied during grinding to induce the coagulation of

the coal. A tap water medium did not require extra energy, except to break up the coagula and release the entrapped gangue after every stage. The additional energy for the distilled water system was apparently needed to overcome a larger energy barrier. The main advantage of increasing the specific energy applied was found to be an improvement in the selectivity of the process.

9. The effect of agitation time and speed was found to be the same as the trends found for specific energy input.

10. An elutriation column has been designed and investigated as the separation device for the selective-shear coagulation process. The results obtained were promising and illustrated the capability of the column to produce superclean coal. The elutriation water rate was optimized and found to be an important variable for controlling product quality. Test results indicated that an increase in feed rate caused a gradual decrease in coal recovery and selectivity. The mean residence time for the process was calculated to be approximately 30 minutes, whereas steady-state was reached after approximately 150 minutes.

11. A steady-state population balance model of the elutriation column has been developed. The model allowed predictions to be made in regard to the influence of the operational parameters and column design on separation efficiency. A comparison of the parameter effects between the model predictions and the experimental results showed remarkable agreement.

6.2 Recommendations for Future Work

From the information gathered in the present investigation, further research into the following areas is recommended:

1. A more thorough investigation needs to be conducted in order to determine the reason or reasons why some coal samples were not effectively cleaned using the selective-shear coagulation process. Since the addition of fuel oil enhances the hydrophobicity of the coal surface, it would be interesting to study coal samples varying in degrees of hydrophobicity over a range of fuel oil additions.

2. Since the hydrophobic interaction force is entropy-driven, the coagulation of the coal particles should improve with increasing temperature. Therefore, the effect of temperature should be studied, which may also

give an indication of the relative strength of the entropic force.

3. The present investigation concluded that the separation efficiency of the process decreased with increasing particle size. This result was due to a decrease in the collision rate between particles. However, by increasing the particulate concentration for the larger particle sizes, it may be found that the process can effectively treat particle sizes larger than the present results indicate. Also, the use of a mixture of coarse and fine coal particles may also increase the collision rate.

4. An investigation aimed at defining a method to quantify the amount of entrapped gangue in coal coagula needs to be conducted. Whether empirical or theoretical, the result could be implemented into the elutriation column model presented in this investigation, which would allow scale-up information to be based on both coal recovery and product ash percent. Another application includes the modelling of the flotation process, where entrapment of the gangue due to coagulation of the coal particles is a problem.

5. Before the process can be efficiently scaled up to a continuous process, coagulum size distributions need to be obtained and optimized for various operating conditions, such as agitation time, shear rate, feed particle size, feed percent solids, and slurry pH. Also, coagulum stability is another important factor which needs to be investigated.

6. The elutriation column needs further characterization in order to determine the upper limit of feed rate and percent solids. Recycling of a portion of the product in order to obtain an improved product quality needs to be investigated. Also, water treatment of both the product and tailing slurries needs to be studied.

7. The elutriation column in the present investigation illustrated very slow dynamics. Therefore, a study is needed to find a continuous separation device which would yield higher throughputs. Typical devices may include hydrocyclones, lamella thickeners, and continuous centrifuges.

REFERENCES

Anfruns, J.P. and Kitchener, J.A., 1977. "The Rate of Capture of Small Particles in Flotation," Transactions IMM, 86, Section C, p. C9.

Appleton, E.A., Clauss, C.R.A., and Vink, J.J., 1975. "Selective Flocculation of Cassiterite," Journal of the South African Institute of Mining and Metallurgy, pp. 117-119.

Arnold, B.J. and Aplan, F.F., 1986. "The Effect of Clay Slimes on Coal Flotation, Part II: The Role of Water Quality," International Journal of Mineral Processing, 17, pp. 243-260.

Attia, Y.A., Krishnan, S.V., and Deason, 1983. "Selective Flocculation Technology Group Program," Final Report, Battelle Columbus Division, Columbus, Ohio.

Attia, Y.A., Conkle, H.N., and Krishnan, S.V., 1984. "Selective Flocculation Coal Cleaning for Coal Slurry Preparation," Proceedings of the 6th International Symposium on Coal Slurry Combustion and Technology, pp. 571-581, Orlando, Florida.

Bagster, D.F. and McIlvenny, J.D., 1985. "Studies in the Selective Flocculation of Hematite from Gangue Using High Molecular Weight Polymers. Part 1: Chemical Factors," International Journal of Mineral Processing, 14, pp. 1-20.

Bagster, D.F., 1985. "Studies in the Selective Flocculation of Hematite from Gangue Using High Molecular Weight Polymers. Part 2: Physical Factors," International Journal of Mineral Processing, 14, pp. 21-32.

Banks, A.F., 1979. "Selective Flocculation-Flotation of Slimes from a Sylvinite Ore," in Beneficiation of Mineral Fines, (P. Somasundaran, ed.).

Bethell, P.J. and Sell, F.R., 1983. "The Availability of Very Low Ash Coal for Coal-Based Fuels," Proceedings, Fifth International Symposium on Coal Slurry Combustion and Technology, Tampa, Florida, April, p. 238.

Boron, D.J. and Kollrack, R., 1983. "Prospects for Chemical Coal Cleaning," Proceedings, 1983 Society of Mining Engineers Fall Meeting, Salt Lake City, Utah, October.

Brown, M.D., 1986. "An Investigation of Fine Coal Grinding Kinetics," M.S. Thesis, Department of Mining and Minerals Engineering, Virginia Polytechnic Institute and State University, Blacksburg, Virginia.

Campbell, J.A.L. and Sun, S.C., 1970. "Bituminous Coal Electrokinetics," Transactions AIME, 247, pp. 111-114.

Capes, C.E., 1979. "Agglomeration," in Coal Preparation, 4th Edition, (J.W. Leonard, ed.), p. 10-105.

Celik, M.S. and Somasundaran P., 1980. "Effect of Pretreatments on Flotation and Electrokinetic Properties of Coal," Colloids and Surfaces, 1, pp. 121-124.

Celik, M.S. and Somasundaran, 1986. "The Effect of Multivalent Ions on the Flotation of Coal," Separation Science and Technology, 21(4), pp. 393-402.

Churaev, N.V. and Derjaguin, B.V., 1985. "Inclusion of Structural Forces in the Theory of Stability of Colloids and Films," Journal of Colloid and Interface Science, 103(2), pp. 542-553.

Collins, G.L. and Jameson, G.J., 1976. "Experiments on the Flotation of Fine Particles - The Influence of Particle Size and Charge," Chemical Engineering Science, 31, p. 985.

Conkle, H.N., Krishnan, S.V., and Chauhan, S.P., 1986. "Scale-up of the Battelle-Developed Process for Ultracleaning of Coal by Selective Flocculation to One Ton/Day Scale," on-going research project, Battelle Columbus Division, Columbus, Ohio.

Flint, L.R. and Howarth, W.J., 1971. "The Collision Efficiency of Small Particles with Spherical Air Bubbles," Chemical Engineering Science, 26, p. 1155.

Friend, J.P., Iskra, J., and Kitchener, J.A., 1973. "Cleaning a Selectivily Flocculated Mineral Slurry," Transactions Institute of Mining and Metallurgy, 82, pp. C235-C236.

Friend, J.P. and Kitchener, J.A., 1973. "Some Physico-Chemical Aspects of the Separation of Finely-Divided Minerals by Selective Flocculation," Chemical Engineering Science, 28, pp. 1071-1080.

Fuerstenau, D.W., Yang, G.C.C., and Laskowski, J.S., 1987. "Oxidation Phenomena in Flotation Part I. Correlation Between Oxygen Functional Group Concentration, Immersion Wettability and Salt Flotation Response," Coal Preparation, 4, pp. 161-182.

Hale, W.M., 1987. "Surface Chemical Aspects of Microbubble Flotation," M.S. Thesis, Department of Mining and Minerals Engineering, Virginia Polytechnic Institute and State University, Blacksburg, Virginia.

Hucko, R., 1977. "Beneficiation of Coal by Selective Flocculation, A Laboratory Study," USBM, R.I. 8234.

Hutton, C.A. and Gould, R.N., 1982. Cleaning Up Coal: A Study of Coal Cleaning and the Use of Cleaned Coal, Ballinger Publishing Co., Cambridge, Mass..

Ishizuka, T., Hotta, H., and Nishimura, Y., 1984. "Coal-Deashing Process," U.S. Patent #4,437,861.

Jessop, R.R. and Stretton, J.L., 1969. "Electrokinetic Measurements on Coal and a Criterion for Its Hydrophobicity," Fuel Science, 48, pp. 317-320.

Kneller, W.A. and Maxwell, G.P., 1985. "Size, Shape, and Distribution of Microscopic Pyrite in Selected Ohio Coals," in Processing and Utilization of High Sulfur Coals, (Coal Science and Technology 9, Y.A. Attia, ed.), p. 41.

Krishnan, S.V. and Attia, Y.A., 1985. "Flocculation Characteristics in Selective Flocculation of Fine Particles," Proceedings of Engineering Foundation Conference on Flocculation, Sedimentation, and Consolidation, Sea Island, Georgia.

Krishnan, S.V. and Attia, Y.A., 1986. "Polymeric Flocculants," in Reagents in Mineral Industry, New York: Marcel and Decker.

Krishnan, S.V., 1987. "Selective Flocculation of Fine Coal," in Fine Coal Processing, (S.K. Mishra and R.R. Klimpel, eds.), p. 160.

Levenspiel, O., 1972. Chemical Reaction Engineering, An Introduction to the Design of Chemical Reactors, (John Wiley and Sons, New York), p. 242.

Luttrell, G.H., Weber, A.T., Adel, G.T., and Yoon, R.H., 1988. "Microbubble Flotation of Fine Coal," Proceedings, 1988 Annual AIME Meeting, Phoenix, Arizona, January.

Mathieu, G.I. and Mainwaring, P.R., 1986. "Mineralogy and Deep-Cleaning of Canadian High-Sulfur Coals," Proceedings, AIME-TSM Annual Meeting, New Orleans, Louisianna, March.

Maynard, R.N., Millman, N., and Iannicelli, J., 1969. Proceedings, National Conference on Clays and Clay Minerals, 17, p. 59.

McCartney, J.T., O'Donnell, H.J., and Ergun, S., 1969. "Pyrite Size Distribution and Coal-Pyrite Particle Association in Steam Coals," USBM, R.I. 7231.

Mehrotra, V.P., Sastry, K.V.S., and Morey, B.W., 1983. "Review of Oil Agglomeration Techniques for Processing of Fine Coals," International Journal of Mineral Processing, 11, pp. 175-201.

Mezey, E.J., Hayes, T.D., Mayer, R., and Dunn, D., 1985. "Application of Oil Agglomeration for Effluent Control from Coal Cleaning Plants," U.S. EPA Report No. EPA/600/7-85/042, December.

Parshley, R.M., 1982. "Hydration Forces between Mica Surfaces in Electrolyte Solutions," Advances in Colloidand Interface Science, 16, pp. 57-61.

Pugh, R.J. and Kitchener, J.A., 1971. "Theory of Selective Coagulation in Mixed Colloidal Suspensions," Journal ofColloid and Interface Science, 35(4), pp. 656-664.

Pugh, R.J. and Kitchener, J.A., 1972. "Experimental Confirmation of Selective Coagulation in Mixed Colloidal Suspensions," Journal of Colloid and Interface Science, 38(3), pp. 656-657.

Pugh, R.J., 1973. "Selective Coagulation in Quartz-hematite and Quartz-rutile Suspensions," Colloid and Polymer Science, 252(5), pp. 400-406.

Rabinovich, Y.I. and Deryagin, B.V., 1988. "Direct Measurement of Forces of Attraction of Hydrophobized Quartz Fibers in Aqueous KCl Solutions," Colloid Journal of USSR, (Translated from Kolloidnyi Zhurnal), 49(4), pp. 682-687.

Read, A.D., 1971. "Selective Flocculation Separations Involving Hematite," Transactions/Section C Mineral Processing and Extractive Metallurgy, 80, pp. C24-C31.

Reay, D. and Ratcliff, G.A., 1973. "Removal of Fine Particles from Water by Dispersed Air Flotation," Canada Journal of Chemical Engineering, 51, p.178.

Richardson, J.F. and Zaki, W.N., 1954. "Sedimentation and Fluidisation: Part I," Transactions to the International Society of Chemical Engineers, 32, pp. 35-53.

Schroeder, P.R. and Rubin, A.J., 1984. "Aggregation and Colloidal Stability of Fine-Particle Coal Suspensions," Environmental Science Technology, 18(4), pp. 264-271.

Steedman, W.G. and Krishnan, S.V., 1987. "Oil Agglomeration Process for the Treatment of Fine Coal," in Fine Coal Processing, (S.K. Mishra and R.R. Klimpel, eds.), p. 179.

Trahar, W.J. and Warren, L.J., 1976. "The Floatability of Very Fine Particles - - A Review," International Journal of Mineral Processing, 3, p. 103.

Usui, S., 1984. "Interaction of Electrical Double Layers and Colloid Stabilty" in Electrical Phenomena at Interfaces, (A. Kitahara and A. Watanabe, eds.), p. 47.

Van de Ven, T.G.M. and Mason, S.G., 1976. "The Microrheology of Colloidal Dispersions. IV. Pairs of Interacting Spheres in Shear Flow," Journal of Colloid andInterface Science, 57, pp. 505-516.

Van de Ven, T.G.M. and Mason, S.G., 1977. "The Microrheology of Colloidal Dispersions. VII. Orthokinetic Doublet Formation of Spheres," Colloid Polymer Science, 225, pp. 468-479.

Villar, J.W. and Dawe, G.A., 1975. "The Tilden Mine - A New Processing Technique for Iron Ore," Mining Congress Journal, 61(10), pp. 40-48.

Warren, L.J., 1975. "Shear-flocculation of Ultrafine Scheelite in Sodium Oleate Solutions," Journal of Colloid and Interface Science, 50, pp. 307-318.

Warren, L.J., 1977. "The Stability of Suspensions, A Guide for Beginners," Chemistry in Australia, 44(12), pp. 315-318.

Warren, L.J., 1981. "Selective Flocculation," Chemtech, pp. 180-185.

Warren, L.J., 1982. "Flocculation of Dispersed Suspensions of Cassiterite and Tourmaline," Colloid Surface, 5, pp. 301-319.

Warren, L.J., 1984. "Ultrafine Particles in Flotation," in Principles of Mineral Flotation, The Wark Symposiu, (M.H. Jones and J.T. Woodcock, eds.), Australia Institute of Mining and Metallurgy, Symp. Series No. 40, Victoria, Australia, pp. 185-213.

Wen, W.W. and Sun, S.C., 1977. "An Electrokinetic Study on the Amine Flotation of Oxidixed Coal," Transactions AIME, 262, pp. 174-180.

Wiese, G.R. and Healy, T.W., 1975. "Effect of Particle Size on Colloid Stabilty," Transactions of the Faraday Society, 66(2), pp. 490-499.

Wright, A.C., 1985. "Collectin Fines for New Markets," Coal Age, January, p. 57.

Yarar, B. and Kitchener, J.A., 1970."Selective Flocculation of Minerals: 1-Basic Principles 2-Experimental Investigation of Quartz, Calcite, and Galena," Transactions Institute of Mining and Metallurgy, pp. C23-C33.

Yoon, R.H., 1982. "Flotation of Coal Using Micro-Bubbles and Inorganic Salts," Mining Congress Journal, December.

Yoon, R.H., Adel, G.T., and Luttrell, G.H., 1987. "Development of the Microbubble Column Flotation Process," Processing and Utilization of High Sulfur Coals, (Y.P. Chugh and R.D. Caudle, eds.), pp. 533-543.

Xu, Z. and Yoon, R.H., 1988. "Modeling of Hydrophobic Interactions," Presentation, 62nd Colloid and Surface Science Symposium, University Park, Pennsylvania, June.

APPENDIX I

Effect of Particle Size on Turbulent Collision Rate

Levich's equation for turbulent collision rate:

$$J = 12 \pi B r^3 n^2 (e/\eta)^{1/2},$$

where J is the turbulent collision rate, B is a constant, r is the radius of a single particle, n is the initial number of particles per unit volume of slurry, e is the energy loss per second per unit volume, and η is the kinematic viscosity.

In order to determine the effect of a decrease in particle size from r_1 to r_2, a collision rate ratio was determined as follows:

$$J_2/J_1 = r_2^3 n_2^2 / r_1^3 n_1^2,$$

where e and v were considered constant.

The number of particles per unit volume of size 2 per size 1 was found by dividing the spherical volume of size 2 into the spherical volume of size 1. The result after the cancellation of common terms was:

$$n_2 = r_1^3 / r_2^3.$$

Therefore,

$$J_2/J_1 = r_2^3 (r_1^3/r_2^3)^2 / r_1^3 (1) = r_1^3 / r_2^3.$$

The effect of decreasing the particle size from 14 microns to 4 microns on the turbulent collision rate is:

$$J_2 / J_1 = 7^3 / 2^3 = 43.$$

Therefore, a decrease in particle size from 14 microns to 4 microns would increase the turbulent collision rate by a factor of 43 for a system of constant mass.

APPENDIX II

Elutriation Column Program and Example Simulations

```
 REAL PAR(20), X(20), FNORM, WK(225), CONSLD, PCTASH,QF,QW,QP,
$    DIAM(2), UPDIAM, BOTDIA, HGT, FDHGT, G, VISC, DENSFL, ZONE,
$    C(2,5)
 INTEGER N, NSIG, ITMAX, IER
 EXTERNAL FCN
 WRITE (*,*) '*****************************************************'
 WRITE (*,*) '****                CONCENTRATIONS                ****'
 WRITE (*,*) '*****************************************************'
 WRITE (*,*)
 WRITE (*,*) 'FEED SOLIDS CONCENTRATION (gm/ml)              = ? '
 READ  (*,*) CONSLD
 WRITE (*,*) 'PERCENT ASH OF FEED                            = ? '
 READ  (*,*) PCTASH
 WRITE (*,*)
 WRITE (*,*)
 WRITE (*,*) '*****************************************************'
 WRITE (*,*) '****                 COLUMN FLOWS                 ****'
 WRITE (*,*) '*****************************************************'
 WRITE (*,*)
 WRITE (*,*) 'FEED RATE OF SLURRY (ml/min)                   = ? '
 READ  (*,*) QF
 WRITE (*,*) 'RATE OF ELUTRIATION WATER (ml/min)             = ? '
 READ  (*,*) QW
 WRITE (*,*) 'RATE OF PRODUCT REMOVAL (ml/min)               = ? '
 READ  (*,*) QP
```

```
WRITE (*,*)
WRITE (*,*)
WRITE (*,*) '*****************************************************'
WRITE (*,*) '****          SOLID  CHARACTERISTICS           ****'
WRITE (*,*) '*****************************************************'
WRITE (*,*)
WRITE (*,*) 'COAL DENSITY (gm/cc)                              = ? '
READ  (*,*) PAR(15)
WRITE (*,*) 'ASH DENSITY (gm/cc)                               = ? '
READ  (*,*) PAR(16)
WRITE (*,*) 'FREE SETTLING RATE OF THE COAL FLOCCS (cm/sec)= ? '
READ  (*,*) PAR(5)
WRITE (*,*) 'MEAN ASH PARTICLE DIAMETER (cm)                   = ? '
READ  (*,*) DIAM(2)
WRITE (*,*) 'COEFFICIENT OF SETTLING FOR THE COAL FLOCCS   = ? '
READ  (*,*) PAR(1)
WRITE (*,*) 'COEFFICIENT OF SETTLING FOR THE ASH PARTICLES = ? '
READ  (*,*) PAR(2)
WRITE (*,*)
WRITE (*,*)
WRITE (*,*) '*****************************************************'
WRITE (*,*) '****              CELL  DIMENSIONS             ****'
WRITE (*,*) '*****************************************************'
WRITE (*,*)
WRITE (*,*) 'UPPER CELL DIAMETER (cm)                          = ? '
READ  (*,*) UPDIAM
WRITE (*,*) 'BOTTOM CELL DIAMETER (cm)                         = ? '
READ  (*,*) BOTDIA
WRITE (*,*) 'COLUMN HEIGHT (cm)                                = ? '
READ  (*,*) HGT
```

```
      WRITE (*,*) 'FEED POINT FROM BOTTOM OF CELL                    = ? '
      READ  (*,*) FDHGT
      WRITE (*,*)
      X(1) = .0070
      X(2) = .006
      X(3) = .0010
      X(4) = .0010
      X(5) = .0010
      X(6) = .00001
      X(7) = .00010
      X(8) = .00001
      X(9) = .00010
      X(10) = .00010
      PAR(10) = QF/60
      PAR(11) = QP/60
      PAR(12) = QW/60
      PAR(9)  = PAR(12) - PAR(11)
      PAR(13) = HGT/5
      G = 981.
      VISC = .01
      DENSFL = 1.
C       DETERMINING FEED CONCENTRATION
      PAR(7) = CONSLD * (1 - (PCTASH/100))
      PAR(8) = CONSLD * (PCTASH/100)
      PAR(6) = ((DIAM(2)**2)*G*(PAR(16) - DENSFL))/(18*VISC)
C                    DETERMINING THE FEED ZONE
      ZONE = 0
      DO 200 I = 1,5
             ZONE = ZONE + PAR(13)
             IF (ZONE .GE. FDHGT) GO TO 300
200   CONTINUE
300   PAR(14) = I
      PAR(3) = (3.1416*BOTDIA**2)/4
      PAR(4) = (3.1416*UPDIAM**2)/4
```

```
      N = 10
      NSIG = 7
      ITMAX = 200
      CALL ZSPOW(FCN, NSIG, N, ITMAX, PAR, X, FNORM, WK, IER)
      DO 4000 J = 1,5
               C(1,J) = X(J)
4000  CONTINUE
      WRITE (*,*)
      DO 5000 J= 6,10
               C(2,J-5) = X(J)
5000  CONTINUE
      TLSCON = (C(1,5) + C(2,5))
      PRDCON = C(1,1) + C(2,1)
      TOTMAS = (TLSCON * (QW+QF-QP)) + (PRDCON*(QP))
      FDMASS = CONSLD * QF
      ASHPRD = (C(2,1)/(C(2,1) + C(1,1)))*100
      ASHTLS = (C(2,5)/(C(2,5) + C(1,5)))*100
      RECOV  = ((C(1,1)*QP)/(FDMASS*(1-(PCTASH/100))))*100
      ASHREC = ((C(2,1)*QP)/(FDMASS*(PCTASH/100)))*100
      SPNEFF = RECOV - ASHREC
      WRITE (*,10) RECOV, ASHREC
10    FORMAT(3X,'CLEAN COAL RECOVERY  =',1X,F6.2,3X,'ASH RECOVERY  =',
     $1X,F6.2)
      WRITE (*,20) ASHPRD,ASHTLS
20    FORMAT(3X,'PRODUCT ASH PERCENT  =',1X,F6.2,3X,'TAILINGS ASH  =',
     $1X,F6.2)
      WRITE (*,30) SPNEFF
30    FORMAT(3X,'SEPARATION EFFICIENCY  =',1X,F6.2)
      WRITE (*,*)'
      WRITE (*,50)
50    FORMAT(1X,'COAL CONCENTRATION (gm/ml)',5X,'ASH CONCENTRATION
     $ (gm/ml)')
```

```
      DO 6000 I = 1,5
      WRITE (*,40) I, C(1,I), C(2,I)
40    FORMAT (1X,I1,3X,F6.5,30X,F6.5)
6000  CONTINUE
      END
C
      SUBROUTINE FCN(X, F, N, PAR)
      INTEGER N,I,J,K,L,M,P,S
      REAL X(N), F(N), PAR(20)
      L = 3
      I = 1
      J = 1
600   F(J) = ((PAR(I+4)*((1 - (X(2)/PAR(15) + X(7)/PAR(16)))**PAR(I)
     $     ))*X(J+1))/PAR(13) - (PAR(12)*X(J))/(PAR(13)*PAR(L))
      IF (J .EQ. 6) GO TO 700
      J = J + 5
      I = 2
      GO TO 600
700   I = 1
      DO 900  J = 2,9
      M = J + 6
      K = J + 5
      IF (J .LT. 5) GO TO 800
      M = J + 1
      K = J
      I = 2
      IF (J .EQ. 5) GO TO 900
      IF (J .EQ. 6) GO TO 900
800   F(J) = ((PAR(I+4)*((1 - X(M-5)/PAR(15) - X(M)/PAR(16))
     $ **PAR(I))*X(J+1))/PAR(13)) - ((PAR(I+4)*((1 - X(K-5)/PAR(15)
     $ - X(K)/PAR(16))**PAR(I))*X(J))/PAR(13)) + ((PAR(9)*(X(J-1)
     $ - X(J)))/(PAR(13)*PAR(L)))
C
```

```
900   CONTINUE
      I = 1
      J = 5
1100  F(J) = (-1*((PAR(I+4)*((1 - X(5)/PAR(15) - X(10)/PAR(16))**PAR(I))
     $  *X(J))/PAR(13))) + ((PAR(9)*(X(J-1) - X(J)))/(PAR(13)*PAR(L+1)))
     $ + ((PAR(10)*(X(J-1)-X(J)))/(PAR(13)*PAR(L+1)))
      IF (J .EQ. 10) GO TO 1200
      I = 2
      J = 10
      GO TO 1100
1200  I = 1
      A = PAR(14)
      B = A
1300  F(INT(A)) = (PAR(10)*((PAR(I+6)/(PAR(13)*PAR(L+1)))
     $ - (X(INT(A))/(PAR(13)*PAR(L+1)))))
     $ + ((PAR(9)*(X(INT(A)-1)/PAR(L+1) - X(INT(A))/PAR(L+1)))/PAR(13))
     $ + ((PAR(I+4)*((1 - X(INT(B)+1)/PAR(15) - X(INT(B)+6)/PAR(16))
     $ **PAR(I))*X(INT(A)+1))/PAR(13)) - ((PAR(I+4)*((1 - X(INT(B))
     $ /PAR(15) - X(INT(B)+5)/PAR(16))**PAR(I))*X(INT(A))*PAR(L))/
     $ (PAR(13)*PAR(L)))
      F(INT(A)-1) = ((PAR(I+4)*((1 - X(INT(B))/PAR(15) - X(INT(B)+5)
     $ /PAR(16))**PAR(I))*X(INT(A))*PAR(L+1))/(PAR(13)*PAR(L)))
     $ - ((PAR(I+4)*((1 - X(INT(B)-1)/PAR(15) - X(INT(B+4))/PAR(16))
     $ **PAR(I))*X(INT(A)-1))/PAR(13)) + ((PAR(9)*(X(INT(A)-2)
     $ - X(INT((A)-1))))/(PAR(13)*PAR(L)))
      IF (I .EQ. 2) GO TO 1400
      I = 2
      A = PAR(14) + 5
      GO TO 1300
1400  I = 1
      P = 1
1700  DO 1500 J = INT(PAR(14))+1,4
      S = J
```

```
      IF (P .EQ. 1) GO TO 1600
      S = J + 5
1600  F(S) = (PAR(10)*(X(S-1) - X(S))/(PAR(13)*PAR(L+1)))
     $ + ((PAR(9)*X(S-1))/(PAR(13)*PAR(L+1)))
     $ - ((X(S)*PAR(9))/(PAR(13)*PAR(L+1)))
     $ + ((PAR(P+4)*((1 - X(J+1)/PAR(15) - X(J+6)/PAR(16))**PAR(P))
     $ *X(S+1))/PAR(13)) - ((PAR(P+4)*((1 - X(J)/PAR(15) - X(J+5)
     $ /PAR(16))**PAR(P))*X(S))/PAR(13))
1500  CONTINUE
      IF (P .EQ. 2) GO TO 1800
      P = 2
      GO TO 1700
1800  RETURN
      END
```

```
**************************************************
****                CONCENTRATIONS                ****
**************************************************

FEED SOLIDS CONCENTRATION (gm/ml)                 = ?
.02
PERCENT ASH OF FEED                               = ?
12


**************************************************
****                 COLUMN FLOWS                 ****
**************************************************

FEED RATE OF SLURRY (ml/min)                      = ?
50
RATE OF ELUTRIATION WATER (ml/min)                = ?
500
RATE OF PRODUCT REMOVAL (ml/min)                  = ?
100
```

```
**************************************************
****          SOLID  CHARACTERISTICS            ****
**************************************************

COAL DENSITY (gm/cc)                              = ?
1.3
ASH DENSITY (gm/cc)                               = ?
2.3
FREE SETTLING RATE OF THE COAL FLOCCS (cm/sec)= ?
.1635
MEAN ASH PARTICLE DIAMETER (cm)                   = ?
.0005
COEFFICIENT OF SETTLING FOR THE COAL FLOCCS   = ?
3.65
COEFFICIENT OF SETTLING FOR THE ASH PARTICLES = ?
3.65


**************************************************
****              CELL  DIMENSIONS              ****
**************************************************

UPPER CELL DIAMETER (cm)                          = ?
20.32
BOTTOM CELL DIAMETER (cm)                         = ?
10.16
COLUMN HEIGHT (cm)                                = ?
86
FEED POINT FROM BOTTOM OF CELL                    = ?
63
```

CLEAN COAL RECOVERY	= 95.30	ASH RECOVERY	= .00
PRODUCT ASH PERCENT	= .00	TAILINGS ASH	= 74.36
SEPARATION EFFICIENCY	= 95.30		

	COAL CONCENTRATION (gm/ml)	ASH CONCENTRATION (gm/ml)
1	.00839	.00000
2	.00535	.00000
3	.00379	.00002
4	.00074	.00029
5	.00009	.00027

```
**************************************************
****                CONCENTRATIONS                ****
**************************************************

FEED SOLIDS CONCENTRATION (gm/ml)                 = ?
.02
PERCENT ASH OF FEED                               = ?
12


**************************************************
****                 COLUMN FLOWS                 ****
**************************************************

FEED RATE OF SLURRY (ml/min)                      = ?
100
RATE OF ELUTRIATION WATER (ml/min)                = ?
500
RATE OF PRODUCT REMOVAL (ml/min)                  = ?
100
```

```
**************************************************
****          SOLID  CHARACTERISTICS            ****
**************************************************

COAL DENSITY (gm/cc)                              = ?
1.3
ASH DENSITY (gm/cc)                               = ?
2.3
FREE SETTLING RATE OF THE COAL FLOCCS (cm/sec)= ?
.1635
MEAN ASH PARTICLE DIAMETER (cm)                   = ?
.0005
COEFFICIENT OF SETTLING FOR THE COAL FLOCCS    = ?
3.65
COEFFICIENT OF SETTLING FOR THE ASH PARTICLES = ?
3.65


**************************************************
****              CELL  DIMENSIONS              ****
**************************************************

UPPER CELL DIAMETER (cm)                          = ?
20.32
BOTTOM CELL DIAMETER (cm)                         = ?
10.16
COLUMN HEIGHT (cm)                                = ?
86
FEED POINT FROM BOTTOM OF CELL                    = ?
63
```

CLEAN COAL RECOVERY	= 94.24	ASH RECOVERY	= .00
PRODUCT ASH PERCENT	= .00	TAILINGS ASH	= 70.30
SEPARATION EFFICIENCY	= 94.24		

	COAL CONCENTRATION (gm/ml)	ASH CONCENTRATION (gm/ml)
1	.01659	.00000
2	.01075	.00000
3	.00765	.00004
4	.00149	.00051
5	.00020	.00048

The vita has been removed from the scanned document